Electrophilic Activation of Carbon-Carbon Bond Unsaturation by Au(I) and Pt(II): Experimental and Theoretical Considerations

Ryan J. Felix

A dissertation submitted to the faculty of the University of North Carolina at Chapel Hill in partial fulfillment of the requirements for the degree of Doctor of Philosophy in the Department of Chemistry.

Chapel Hill
2013

Approved By:

Dr. Michel R. Gagné

Dr. Jeffrey Johnson

Dr. Marcey Waters

Dr. David Nicewicz

Dr. David Lawrence

Abstract

RYAN J. FELIX: Electrophilic Activation of Carbon-Carbon Bond Unsaturation by Au(I) and Pt(II): Experimental and Theoretical Considerations
(Under the direction of Michel R. Gagné)

In an attempt to replicate the selectivity demonstrated by enzymes in the cascade cyclization of linear polyenes, the Gagné group has developed Pt(II)-catalyzed systems capable of efficiently creating bi- and tricyclic compounds in a single step. While investigating methylenecyclopropane substrates in an attempt to overcome a steric limitation of these Pt(II) systems, which prevents the use of trisubstituted alkenes, a Au(I)-catalyzed Cope rearrangement was discovered. This system was developed into the first example of an asymmetric Cope rearrangement starting from achiral 1,5-dienes and adds to the relatively young, but rapidly expanding, field of enantioselective gold catalysis. This reaction could be applied to alkyl, aryl, and oxygen- and nitrogen-containing substrates to provide the rearranged products in generally high yields and enantioselectivities. The thermodynamic driving force for this reaction, which takes place at low temperature and provides products with less substituted olefins than are present in the starting material, is relief of ring strain from the cyclopropylidene moiety. Density functional theory calculations, carried out in collaboration with the research group of Dean Tantillo (UC-Davis), provide theoretical and mechanistic insight into this system.

In a follow up investigation, the Au(I)-catalyzed Cope rearrangement was applied to cyclic methylenecyclopropane substrates with a pendant alkene in hopes of developing a methodology that would allow the facile synthesis of medium-sized rings. Instead of the anticipated medium-sized rings, tricyclic compounds were produced with a unique bicyclo[4.2.0]octene core, a structural motif

present in a number of natural products. While the substrate scope proved to be limited, this study further developed our understanding of the Au(I)-catalyzed reactivity of methylenecyclopropanes.

A theoretical framework was developed for the ring closure selectivity observed in the Gagné Pt(II)-mediated cyclization systems. The basis of this new framework is viewing the transition state of the initial cyclization event as a nonclassical-carbocation-like structure with a large degree of bicyclic character. The different possible bicyclic species contain varying amounts of ring strain, which leads to the exclusive observation of 6-*endo* ring closure in 1,5-dienes. A collaboration with the Tantillo group provided supporting computational data for this analysis.

In loving memory of Jeffrey M. Felix

Acknowledgements

I would like to thank first and foremost Professor Michel R. Gagné for giving me the opportunity to study and work in his laboratory. Without his guidance through the years I don't honestly know where I would be today. I have deeply appreciated having the freedom to pursue my own ideas. At the same time, Mike always had suggestions ready when I hit a wall and helped me keep up my morale through a few long, long years of unsuccessful project after unsuccessful project. Thank you Dr. Gagné.

I also could not have made it through graduate school without the support of my family, Anthony, Dolores, and Sheila Felix. Always there for me when I needed it most, it has been a blessing to have a family so supportive of my goals and choices, even when they take me halfway across the country.

Dr. Colleen Munro-Leighton has been an invaluable friend and mentor to me while I have pursued my academic and career goals. Colleen helped me get started in Mike's lab and was always ready and willing to lend a hand in setting up an experiment, jerry-rigging some lab equipment, or just thinking about my chemistry and troubleshooting the problem of the day. Remaining a friend throughout the years since she has left the lab, she has always been a voice of encouragement and wisdom; she is truly wise beyond her (considerable) years. Most recently she has helped me prepare for the next step of my academic career, providing insights and feedback on my innumerable questions and concerns, for which I do not think I can adequately express in words how grateful I am. In fact, I am so grateful I considered taking out the (not so) subtle jab at her (old, old) age. In all honesty though, thank you Colleen.

I would like to thank my coworkers in the Gagné lab for making it such an enjoyable place to work. Joe Sokol and Nikki Cochrane have been right there with me through the long haul of graduate

school and have proven to be valuable assets for the sharing of ideas, resources, and misery. Laura Adduci has been a rock in an (at times) sea of madness, always ready to help out anyone in the lab with logistics or brainstorming, and eager to fix any problem that comes to her attention, no matter how busy she may already be. She can also be convinced to walk with me while I get an early morning or mid-afternoon snack, for which I appreciate the company. Michael Bertucci has also been a fantastic person to work with and know, getting me back into sports and exercise in general, as well as being a great friend whom I am glad to have met. His endless amounts of energy and dedication are inspiring. I am also grateful for having someone in lab that is just as enthusiastic about teaching as I am. I would like to thank Dr. Dieter Weber for getting me started in the field of gold catalysis, which led to my first real success in graduate school. Allison Hulchanski has been a good friend and colleague, in addition to providing me with snacks for my ever-aching sweet tooth. Michael Geier, Ha Nguyen, Marshall Nisbeth, Dr. Stephen Andrews, and Dr. Mee-Kyung Chung have been instrumental in creating the unique environment of the Gagné lab that I have enjoyed so much over my five years at UNC.

I would also like to acknowledge the great teachers that I have had over the course of my academic career who have guided and inspired me along the way: Dr. Albert Matlin (Oberlin College), Dr. Matthew Elrod (Oberlin College), Dr. Catherine Oertel (Oberlin College), Dr. Michael Nee (Oberlin College), and Dr. Jeffrey Johnson (UNC). My mentors and professors from Oberlin have remained a source of information and guidance to this day, for which I am deeply grateful.

Finally, I would like to thank Dr. Osvaldo Gutierrez and Dr. Dean J. Tantillo (UC-Davis) for being such helpful and efficient collaborators on my research projects in the last two years. Their contributions have been vital to the continued development and elaboration of the Au(I)-catalyzed reactivity of methylenecyclopropanes.

Table of Contents

List of Tables

List of Schemes

List of Figures

List of Abbreviations and Symbols

˚C	Degrees, in Celsius
α	Alpha – Position bound to a metal center
A	Electron affinity
aq	Aqueous
β	Beta – position adjacent to a bound metal center
BINAP	2,2'-Bis(diphenylphosphino)-1,1'-binaphthyl,
Bn	Benzyl
ca	Circa, approximately
COD	1,5-cyclooctadiene
d	Doublet
$d^{\#}$	*d*-orbital electron configuration of a transition metal
δ	Delta – change from a standard value
DCE	1,2-dichloroethane
DCM	dichloromethane
dd	Doublet of doublets
DFT	Density functional theory
dppe	1,2-bis(diphenylphosphino)ethane
dr	Diastereomeric ratio
E	Entgegen, opposite
ee	Enantiomeric excess
Endo	Endocyclic
Et_2O	Diethyl ether
$EtNO_2$	Nitroethane
η	eta, binding mode of a ligand to a metal center

η_{LS}	Absolute hardness
EtOAC	Ethyl acetate
eq	equivalents
eV	Electronvolts
Exo	Exocyclic
g	Gram
GC	Gas chromatography
h	Hours
$HNTf_2$	Bis-trifluoromethanesulfonimide, triflimide
HOMO	Highest occupied molecular orbital
HR	High resolution
HSAB	Hard and soft acids and bases
I	Ionization potential
KHMDS	Potassium bis(trimethylsilyl)amide
KO^tBu	Potassium tertiary-butoxide
L	Any ligand
LBA	Lewis acid assisted chiral Brønsted acid
LUMO	Lowest unoccupied molecular orbital
M	Any metal
m	Multiplet
M+	Molecular ion
mcp	Methylenecyclopropane, cyclopropylidene
mCPBA	*meta*-chloroperoxybenzoic acid
Me	Methyl
$MeNO_2$	Nitromethane

mg	milligrams
MHz	Megahertz
Min	Minutes
mmol	millimoles
mol%	Mole percent
MS	Mass spectroscopy
m/z	Mass-to-charge ratio
$NaIO_4$	Sodium periodate
NHC	N-heterocyclic carbene
NMR	Nuclear magnetic resonance
OAc	Acetate
OMe	Methoxy
OTf	Trifluoromethanesulfonate, triflate
PHANEPHOS	4,12-Bis(diphenylphosphino)-[2.2]-paracyclophane
Ph	Phenyl
PMB	*Para*-methoxybenzyl ether
PNP	2,6-bis((diphenylphopshino)methyl)pyridine
ppm	Parts per million
PPP	Triphos, bis(diphenylphosphinoethyl)phenylphosphine
π	Pi – electrons involved in carbon-carbon multiple bonds
π^*	Antibonding pi orbital
R	Any alkyl substituent
rac	Racemic
rt	Room temperature
s	Singlet
SE	Strain energy

SEGPHOS	5,5’-bis(diphenylphosphino)-4,4’-1,3-benzodioxole
s-BuLi	Secondary-butyl lithium
σ	Sigma – electrons involved in carbon-carbon single bonds
t	Triplet
TBD	1,5,7-triazabicyclo[4.4.0]dec-5-ene
TDA-1	tris[2-(2-methoxyethoxy)ethyl]amine
TFA	Trifluoroacetate
THF	Tetrahydrofuran
Tr^+	Triphenylmethyl cation, trityl cation
Xylyl	3,5-dimethylphenyl
Z	Zusammen, together

Chapter 1 - Introduction

Electrophilic Activation – Lewis Acids

Electrophilic activation is the resultant increase in reactivity in a chemical moiety due to the interaction of a lone pair of electrons or a π-bond with an electrophile. This interaction is the donation of a pair of electrons into either a reactive vacant orbital, or an energetically accessible lowest unoccupied molecular orbital on the electrophile. The result is a thermodynamically favorable interaction that increases the polarity of the donor functional group, with a concomitant increase in reactivity toward nucleophiles. The electron donor in these interactions is referred to as a "Lewis base" while the electron acceptor is referred to as a "Lewis Acid."[1] Figure 1.1 shows an example of a Lewis acid-Lewis base interaction in which the carbonyl group is acting as the Lewis base, donating electrons to the positively charged Lewis acid. The reactivity enhancement is easily visualized by the right hand resonance structure in which a full positive charge now rests on the carbonyl carbon.

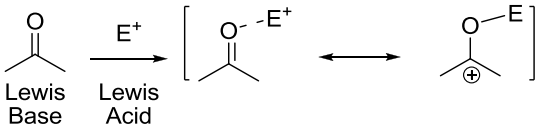

Figure 1.1. Lewis acid-Lewis base interaction.

This broad definition of a Lewis acid means that every chemical species carrying a net positive charge can function as an electrophile, and therefore includes all metal cations and cationic metal complexes.[2] A positive charge is not necessary for a compound to exhibit Lewis acidic properties, however, as demonstrated by the efficacy of neutral boron species for electrophilic activation. This simple and intuitive formulation has proven to be an extremely powerful concept in

[1] Lewis, G. N. *Valence and the Structure of Atoms and Molecules*; The Chemical Catalog Co.: New York, N.Y., 1923.
[2] Fürstner, A.; Davies, P. W. *Angew. Chem. Int. Ed.* **2007**, *46*, 3410.

chemistry, leading to the development of a multitude of stoichiometric and, recently, catalytic reactions enabled by Lewis acids. In addition to the extensive use of alkali metals, alkaline earth metals, and Group 13 elements in Lewis acid applications, recent research has led to the development of organocatalytic Lewis acids and an increasing focus on transition metals as potent sources of electrophilic activation.

One application of Lewis acids is to increase the acidity of hydrogen atoms α to the electron donating moiety. The positive, or partial positive, charge created upon complexation to a Lewis acid inductively activates the α-hydrogen, resulting in more facile deprotonation. This concept was employed by Kessar to deprotonate tertiary amines for use in the synthesis of alkaloid compounds (Scheme 1.1).[3] Upon reacting compound **1** with *s*-BuLi deprotonation occurs exclusively at C4, which forms products **2a** when trapped with an electrophile. Treating **1** with the Lewis acid BF_3-etherate prior to deprotonation, however, results in a complete reversal of regioselectivity. The activated complex **1-BF_3** undergoes deprotonation at C1 due to the inductive stabilization of the negative charge by the adjacent positively charged nitrogen. This protocol led to the synthesis of the alkaloid cordrastine, **2b**, in 47% yield with no C4 substitution products being observed.

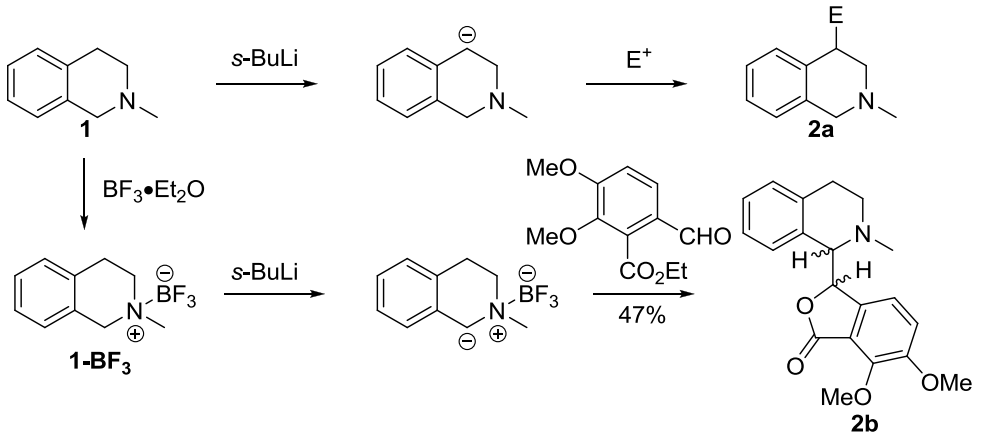

Scheme 1.1. Control of deprotonation regioselectivity provided by electrophilic activation.

[3] a) Kol, M.; Rozen, S. *Chem. Soc., Chem. Commun.* **1991**, 567. b) Kessar, S. V.; Singh, P. *Chem. Rev.* **1997**, *97*, 721.

Lewis acids have also been employed extensively in enhancing the reactivity of allylic tin compounds.[4] The primary method by which these reactions are promoted involves interaction of the Lewis acid with the nucleophilic compound by coordination (see Figure 1.1) to increase polarity. This effect has been studied extensively for allylic tin compounds and the employment of Lewis acids was found to have important implications for both the enhancement of the reaction rate and the stereoselectivity of the products (Figure 1.2). Allylic tin reagents are much less reactive than the analogous alkali and alkaline earth metal compounds but will react with carbonyl compounds under appropriate reaction conditions. For instance, when employing tin in crotylation reactions, the Lewis acidic properties of Sn play a large role and the reaction is known to proceed through the chair-like transition state **3a** (Figure 1.2a). When a Lewis acid additive is present, however, the reaction is made more facile and proceeds through the acyclic, antiperiplanar transition state **3b**.

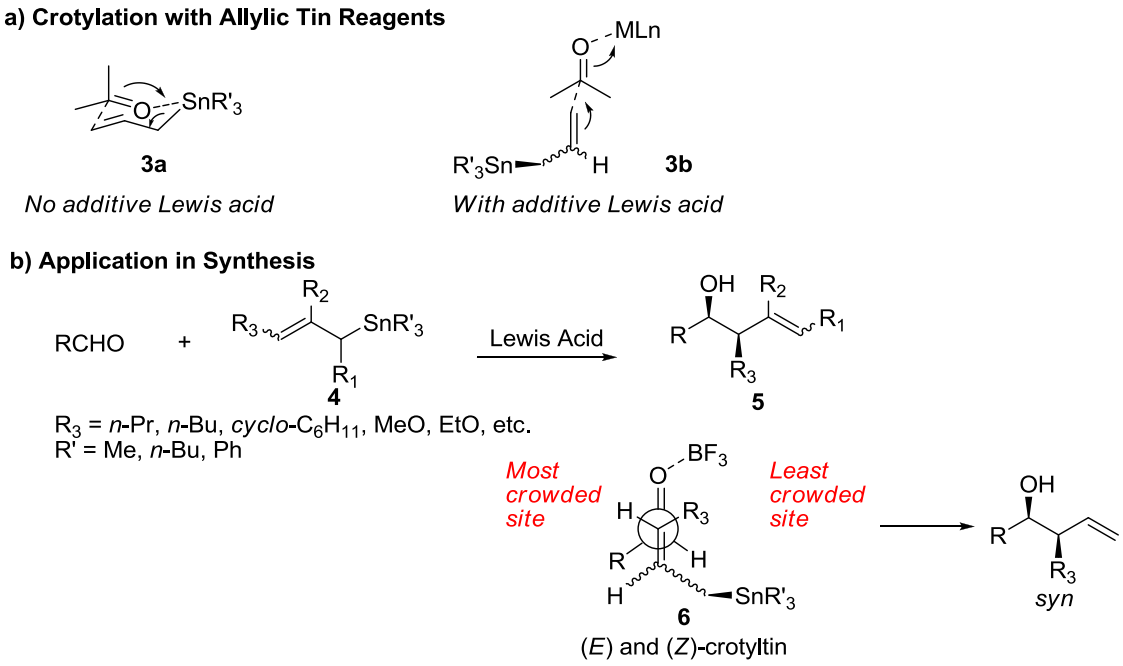

Figure 1.2. Lewis acid promoted allylic tin crotylations.

[4] Nishigaichi, Y.; Takuwa, A.; Naruta, Y.; Maruyama, K. *Tetrahedron* **1993**, *49*, 7395.

When the appropriate Lewis acid is employed, a variety of allylic tin compounds, **4**, can be transformed into the *syn* product isomers, **5**, with excellent selectivity.[5] This selectivity is generated by alignment of the crotyl reagent, in the acyclic transition state, to reduce steric interactions between the aldehyde R fragment and the R_3 substituent (see compound **6**, Figure 1.2b). This leads to both (*E*)- and (*Z*)-crotyltin compounds giving *syn* products. These reactions have been employed in natural product synthesis.[6]

In recent years an increasing amount of focus has been placed on "green" chemistry, which is defined in part by low waste, highly atom economic transformations with minimal environmental impact. With this increasing focus on the use of environmentally benign reagents, the commonly employed and well-studied, but harmful and corrosive, Lewis acids (e.g. $AlCl_3$, BF_3) are being discouraged from use in large-scale preparations. Metal trifluoromethanesulfonates (triflates, $M(OTf)_n$) are a promising class of Lewis acids that have been applied to a large variety of organic transformations.[7] Many of these Lewis acidic compounds can be used catalytically, recovered, and recycled in subsequent reactions. Showing particular promise for potential large-scale preparations is the Lewis acid $Ga(OTf)_3$.[8]

In addition to being water-tolerant, $Ga(OTf)_3$ demonstrates high efficiency at low catalyst loadings and is capable of driving a range of reactions such as Friedel-Craft alkylations, hydroxyalkylations and acylations. In many cases excellent yields and chemoselectivity are observed and the catalyst is recyclable. Of particular interest in the pharmaceutical industry is the efficacy $Ga(OTf)_3$ demonstrates in the Friedel-Craft acylation of heteroaromatics (Scheme 1.2).[9]

---

[5] a) Keck, G. E.; Abbott, D. E.; Boden, E. P.; Enholm, E. J. *Tetrahedron Lett.* **1984**, *25*, 3927. b) Matsubara, S.; Wakamatsu, K.; Morizawa, Y.; Tsuboniwa, N.; Oshima, K.; Nozaki, H. *Bull. Chem. Soc. Jpn.* **1985**, *58*, 1196.
6 a) Koreeda, M.; Tanaka, Y. Tetrahedron Lett. 1987, 28, 143. b) Paquette, L. A.; Doherty, A. M.; Rayner, C. M. J. Am. Chem. Soc. 1992, 114, 3910.
[7] a) Kobayashi, S. *Synlett* **1994**, 689. b) Kobayashi, S.; Manabe, K. *Acc. Chem. Res.* **2002**, *35*, 209. c) Tschumimoto, T.; Tobita, K.; Hiyama, T.; Fukuzawa, S. *J. Org. Chem.* **1997**, *62*, 6997. d) Kawada, A.; Mitamura, S.; Kobayashi, S. *Chem. Commun.* **1996**, 183. e) Ma, Y.; Qian, C. *Tetrahedron Lett.* **2000**, *41*, 945.
[8] a) Prakash, G. K. S.; Mathew, T.; Olah, G. A. *Acc. Chem. Res.* **2012**, *45*, 565. b) Prakash, G. K. S.; Yan, P.; Béla Török, P. Y.; Bucsi, I.; Tanaka, M.; Olah, G. A. *Catal. Lett.* **2003**, *85*, 1.
[9] Komoto, I.; Matsuo, J.; Kobayashi, S. *Top. Catal.* **2002**, *19*, 43.

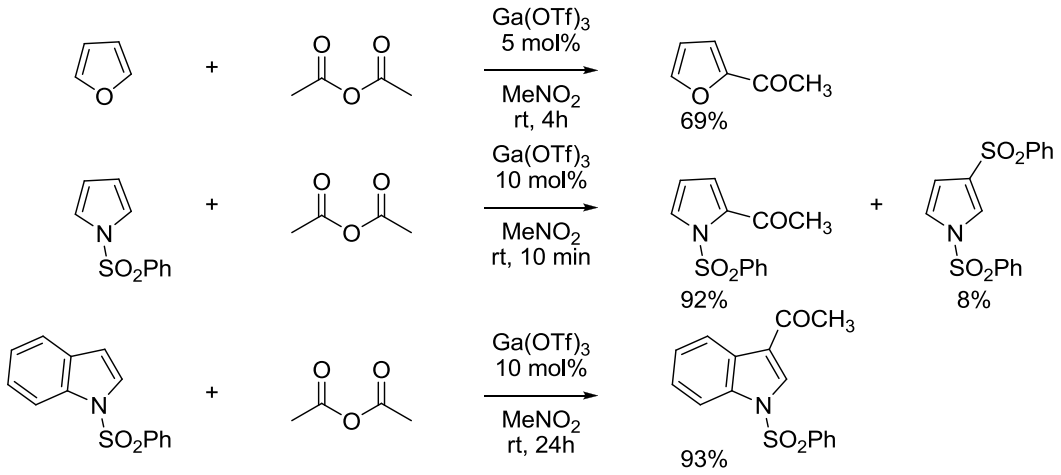

Scheme 1.2. $Ga(OTf)_3$ catalyzed Friedel-Craft acylation of heteroaromatics.

Lewis acids can also be utilized in asymmetric catalysis. A recent development employs a Lewis acid and an *N*-heterocyclic carbene (NHC) Lewis base in "cooperative catalysis" for the highly stereoselective construction of γ-lactams (Scheme 1.3).[10] Using the inorganic base 1,5,7-triazabicyclo[4.4.0]dec-5-ene (TBD) to deprotonate the imidazolium tetrafluoroborate salt, *N*-acyl hydrazones (**7**) could be treated with a wide range of homoenolate equivalents, **8**, to produce the lactam products (**9**) in good yields and high diastereo- and enantioselectivity.

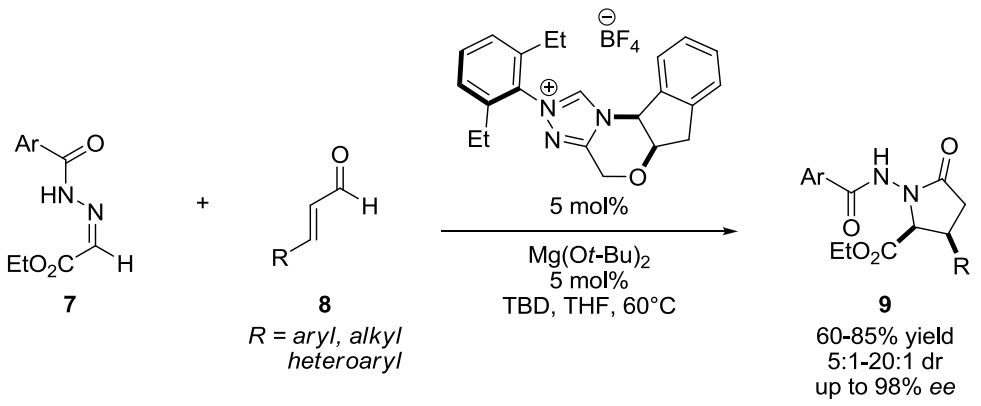

Scheme 1.3. Lewis acid catalyzed homoenolate annulation for stereoselective construction of γ-lactams.

The cooperative nature of this catalytic system comes from the tandem activation of the homoenolate equivalents by the NHC and the electrophilic activation of the *N*-acyl hydrazine by the Lewis acid (Figure 1.3). The catalytic transformation is initiated by addition of the NHC to **8**,

[10] a) Raup, D. E. A.; Cardinal-David, B.; Holte, D.; Scheidt, K. A. *Nature Chem.* **2010**, *2*, 766. b) Cohen, D. T.; Scheidt, K. A. *Chem. Sci.* **2012**, *3*, 53-57.

followed by H-migration to produce reactive intermediate **A**. Intermediate **A** then undergoes homoenolate addition with intermediate **B**, formed from the complexation of the magnesium alkoxide species to **7**, to generate the addition intermediate **C**. In this system formation of adduct **A** raises the energy of the highest occupied molecular orbital (HOMO) of the compound, allowing a more favorable donor interaction with the electrophile (structure **B**). Due to the presence of the Lewis acid, the electrophile undergoes a complementary reactivity increase. Formation of complex **B** lowers the energy of the lowest unoccupied molecular orbital (LUMO) of the electrophile. The efficiency of the reaction is attributed to this favorable HOMO-LUMO interaction in forming **C**, which comes from the cooperative catalysis of the Lewis acid and Lewis base. After tautomerization and dissociation of the Mg species from intermediate **C**, acylation can occur to form the final product with simultaneous release of the NHC. Electrophilic activation of **7** to form intermediate **B**, with its enhanced electrophilicity, is crucial to the effectiveness of the reaction. When the Lewis acid was omitted incomplete conversions and lower selectivities were observed, demonstrating the necessity for the presence of both the Lewis acid and Lewis base in the transformation, despite the enhanced nucleophilicity of intermediate **A**.

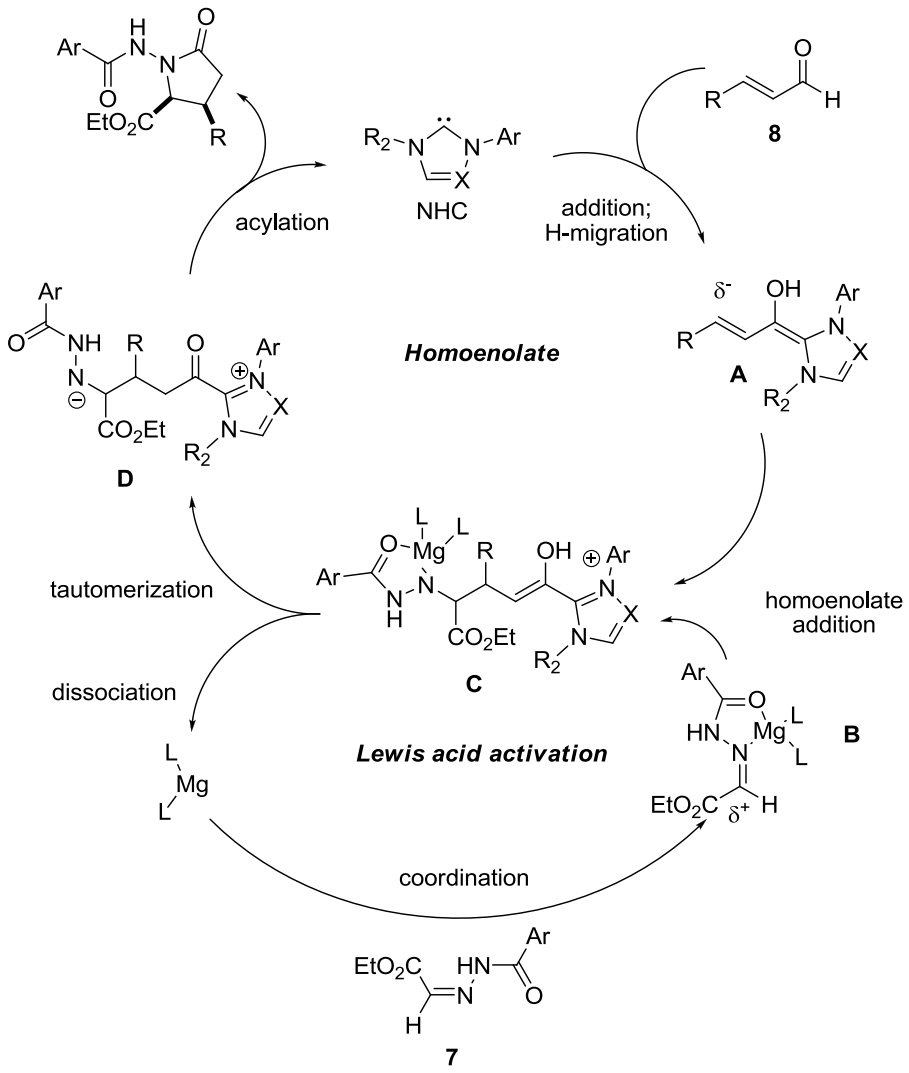

Figure 1.3. Cooperative catalysis in the formation of γ-lactams.

Another area of asymmetric catalysis where Lewis acids have been effectively employed is organocatalysis. Quaternary ammonium and phosphonium salts are well-known Lewis acidic organocatalysts, most commonly utilized in phase-transfer reactions. While the interactions for ammonium salts are purely electrostatic, quaternary phosphonium salts are capable of expanding their coordination sphere to assume hypervalent bonding configurations. Chiral backbone structures allow these compounds to form chiral ion pairs with Lewis bases and thereby influence the trajectory of approaching nucleophiles. Highly enantio- and diastereoselective transformations have been reported

using these types of Lewis acids.[11] In 2002, Maruoka used quaternary ammonium salt **9** to synthesize optically active β-hydroxy-α-amino acids (compounds **10**, Scheme 1.4). These protocols have the advantage of being experimentally simple and proceeding under mild conditions but examples of enantioselective applications are still limited compared to other areas of asymmetric catalysis.

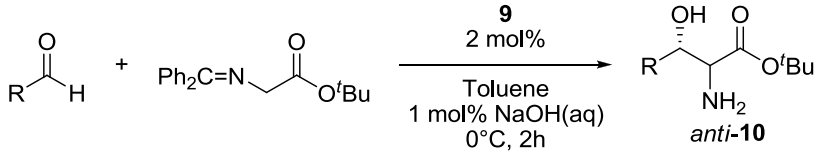

Entry	R	Yield (%)	*anti/syn*	*ee* (%)
1	$PhCH_2CH_2$	76	3.3:1	91
2	$CH_2=CHCH_2CH_2$	71	2.4:1	90
3	CH_3	58	2.3:1	92
4	*c*-C_6H_{11}	40	2.8:1	95

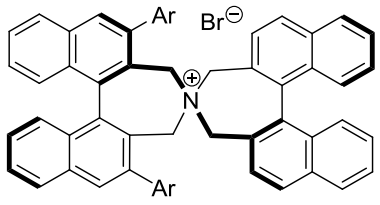

9
Ar = 3,5-$CF_3C_6H_3$

Scheme 1.4. **Phase-transfer catalyzed synthesis of β-hydroxy-α-amino acids**.

Transition metals, both early and late, have demonstrated profound capabilities for electrophilic activation. The variety of electronic configurations and reactivity profiles present in the *d*-block elements allows for a tremendous number of transformations to be mediated. Different oxidation states of the same element can fundamentally change the pathway of a chemical reaction. The ability to bind ligands, most notably organophosphorous compounds, can allow for the fine-tuning of product distributions and selectivities. These ligands impact both the electronic and steric environment of the metal center and provide the potential for asymmetric transformations. This is especially relevant for the late transition metals Pd(II), Pt(II) and Au(I).

The Lewis acidic properties of early transition metals have been known and employed in synthetic chemistry for decades. Variations of the classic Friedel-Craft alkylations catalyzed by $FeCl_3$ are still a point of ongoing research (Scheme 1.5).[12] Iron(III) is capable of many additional electrophilic activation processes, including alkyne activation and couplings and Prins-type

[11] a) Ooi, T.; Taniguchi, M.; Kameda, M.; Maruoka, K. *Angew. Chem. Int. Ed.* **2002**, *41*, 4542. b) Moss, T. A.; Fenwick, D. R.; Dixon, D. J. *J. Am. Chem. Soc.* **2008**, *130*, 10076. c) Werner, T. *Adv. Synth. Catal.* **2009**, *351*, 1469. d) Giacalone, F.; Gruttadauria, M.; Agrigento, P.; Noto, R. *Chem. Soc. Rev.* **2012**, *41*, 2406-2447.
[12] Womack, G. B.; Angeles, J. G.; Fanelli, V. E.; Heyer, C. A. *J. Org. Chem.* **2007**, *72*, 7046.

cyclizations.[13] It also has the advantages of being relatively cheap and environmentally friendly, but has demonstrated limited scope in some systems compared to analogous gold-catalyzed systems.[14]

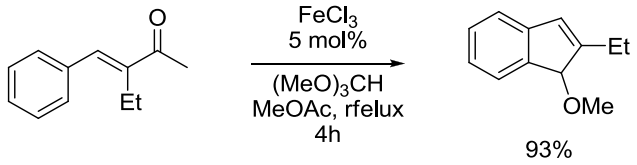

Scheme 1.5. $FeCl_3$ catalyzed intramolecular Friedel-Craft reaction.

The ability to activate alkynes is a characteristic shared by many transition metals including Pd(II), Ru(II), Rh(I), Ir(I), Pt(II), Au(I), Cu(I) and Ag(I).[15] The cycloisomerization of 1,*n*-enynes is a common reaction employed for the construction of carbocyclic frameworks, but most transition metals mediate these reactions through simultaneous activation of both the alkyne and alkene, then proceeding through metallacyclic intermediates. Electrophilic activation of an alkyne to render it susceptible to attack by a nucleophile is possible, however, as demonstrated by the work of Murai and co-workers (Scheme 1.6).[16] This system was found to be applicable to a wide range of enynes and provided the product compounds in good yields (Scheme 1.6a). The mechanistic pathway is postulated to start with coordination of Pt(II) to the alkyne to form η^2 complex **13** (Scheme 1.6b). Nucleophilic attack of the alkene could then proceed through transition state **14** to give bicyclic intermediate **15**. From here a ring expansion to a bicyclo[3.2.0] intermediate, followed by alkyl and/or hydride shifts would give the observed products.

[13] Plietker, B.; Padrón, J. I.; Martín, V. In *Iron Catalysis*; Springer Berlin Heidelberg, 2011; Vol. 33; pp 1-26.
[14] Nieto-Oberhuber, C.; Paz Munoz, M.; Lopez, S.; Jimenez-Nunez, E.; Nevado, C.; Herrero-Gomez, E.; Raducan, M.; Echavarren, A. M. *Chem. Eur. J.* **2006**, *12*, 1677.
[15] Michelet, V.; Toullec, P. Y.; Genet, J.-P. *Angew. Chem. Int. Ed.* **2008**, *47*, 4268.
[16] a) Chatani, N.; Morimoto, T.; Muto, T.; Murai, S. *Organometallics* **1996**, *15*, 901. b) Martín-Matute, B.; Cárdenas, D. J.; Echavarren, A. M. *Angew. Chem. Int. Ed.* **2001**, *40*, 4754.

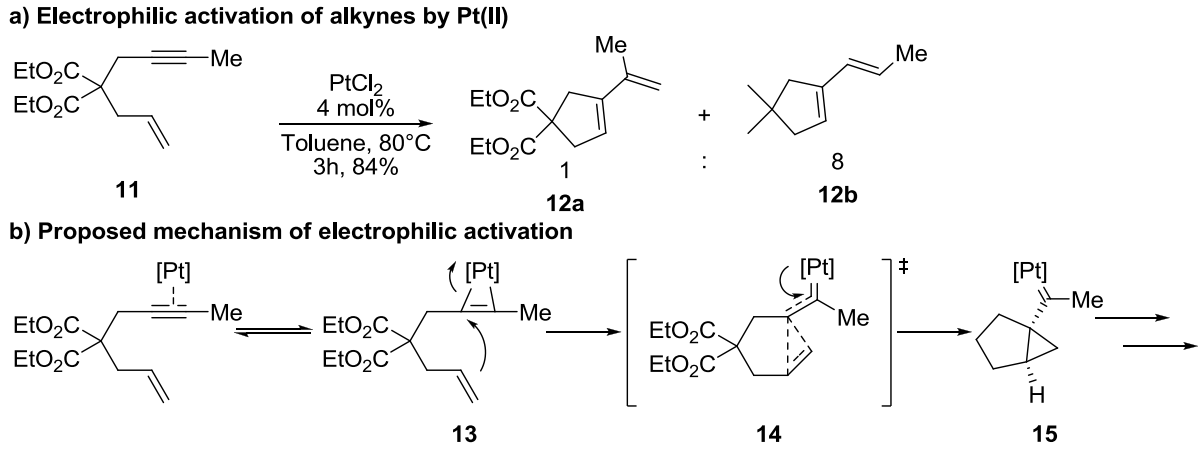

Scheme 1.6. Electrophilic activation and cyclization of alkynes by Pt(II).

Much less prevalent in the literature are examples of electrophilic alkene activation. Protocols have been developed using Rh(I) and Ir(I)[17] catalysts, but the most studied systems involve the use of Pd(II) and Pt(II) catalysts. In 1980 Overman utilized bis(benzonitrile)palladium(II) chloride to catalyze the Cope rearrangement of 1,5-dienes (Scheme 1.7).[18] The reaction is believed to be initiated by complexation of Pd(II) to the less substituted double bond, inducing polarization of the alkene and attack by the more substituted olefin (see structure **16**, Scheme 1.7). Overman proposed that the reaction proceeds stepwise through a tertiary carbocation intermediate such as **17**, but there has been debate as to whether these types of reactions are concerted or stepwise. A recent computational study has indicated that the reaction may in fact be concerted, especially when the structure lacks cation-stabilizing groups on the more substituted double bond.[19] Whether stepwise or concerted, the product is the thermodynamically more stable diene, and these Pd(II)-catalyzed Cope rearrangements proceed efficiently at room temperature in high yields.

[17] Yadav, J. S.; Antony, A.; Rao, T. S.; Subba Reddy, B. V. *J. Organomet. Chem.* **2011**, *696*, 16.
[18] Overman, L. E.; Knoll, F. M. *J. Am. Chem. Soc.* **1980**, *102*, 865.
[19] Siebert, M. R.; Tantillo, D. J. *J. Am. Chem. Soc.* **2007**, *129*, 8686.

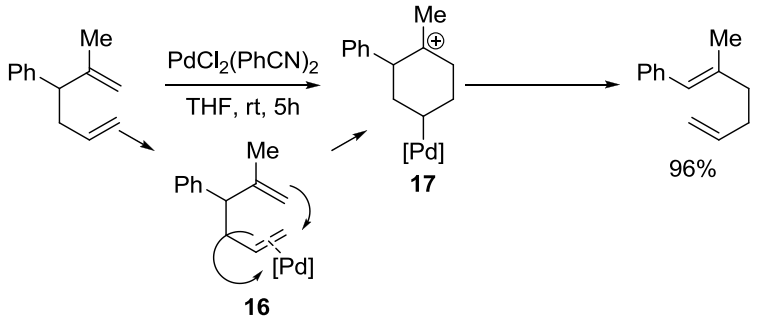

Scheme 1.7. Palladium(II) catalyzed Cope rearrangement.

Evolving from this early work the late transition metals have been employed to electrophilically activate alkenes for a variety of transformations. Prominent use of these systems include hydrofunctionalization of alkenes, which is the addition of H-X across a double bond (X = N, O, C; see Figure 1.4) and polyene cascade cyclizations.[20] These reactions efficiently generate molecular complexity and many examples of asymmetric pathways have been demonstrated.

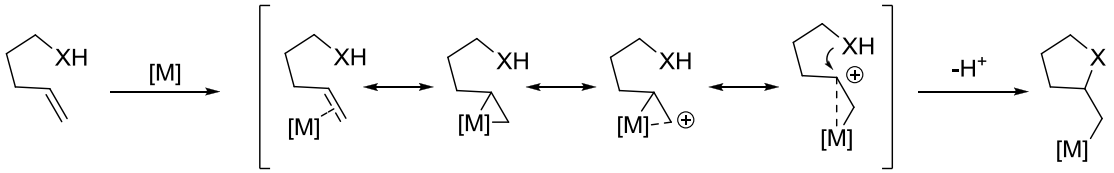

Figure 1.4. Hydrofunctionalization of alkenes catalyzed by late transition metals.

With so many different Lewis acids and Lewis bases, a system for rationalizing experimental observations and predicting reactivity is necessary. One of the most useful conceptualizations for explaining the behavior of Lewis acids and bases is that of the "hard and soft acids and bases" (HSAB) principle.[21] This concept explains the chemical reactivity of Lewis acids and bases primarily based on polarizability and electronegativity. Understanding this principle provides insight into the chemoselectivity of a large variety of Lewis acids and can lead to accurate predictions of new chemical phenomena. The next section is focused on the examination of this important concept.

[20] a) Liu, C.; Bender, C. F.; Han, X.; Widenhoefer, R. A. *Chem. Commun.* **2007**, 3607. b) Chianese, A. R.; Lee, S. J.; Gagné, M. R. *Angew. Chem. Int. Ed.* **2007**, *46*, 4042.
[21] Pearson, R. G. *J. Am. Chem. Soc.* **1963**, *85*, 3533.

Hard and Soft Acid and Base Theory

The concept of hard and soft Lewis acids and bases was formalized in 1963 by Pearson, building from contributions to the field by Edwards, Ahrland, Chatt, Davies, and Schwarzenbach.[22] Originally conceptualized as a classification system for Lewis acids and bases based on their reactivity profiles, the hard and soft acid and base (HSAB) theory has become an intuitive way to understand reactivity trends in electrophilic and nucleophilic systems. Hard acids and bases were originally defined as being small, nonpolarizable species with a high charge concentration. Soft acids and bases were characterized by being large, polarizable species with a low charge concentration. Polarizability is a measure of how easily the electron cloud is distorted within an atom or molecule. The HSAB principle postulated that soft acids will interact more strongly with soft bases while hard acids will interact more strongly with hard bases. Within this framework the relative hardness of a large number of Lewis acids and bases was determined by analyzing nucleophilic displacement reactions of the type represented in equation 1. Here N is a nucleophilic reagent (a Lewis base) and S-D is a substrate (S, Lewis acid) with a displaceable group (D, also a Lewis base). Keeping the reference base (D) constant allowed the equilibrium constants for the displacement reactions to be compared, giving a qualitative assessment of hardness for a series of Lewis bases (N) and Lewis acids (S).

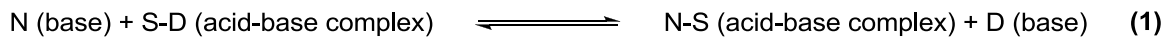

This formulation of the HSAB principle was more qualitative than quantitative as it provided information about which of two competing reactions will have the larger equilibrium constant, but did not provide data about the absolute value of that constant. Nevertheless, the principle was and continues to be a powerful tool for understanding chemical reactions. It should be noted that there is no absolute cutoff for a "hard" acid versus a "soft" acid and intermediate cases do occur, but dividing chemical species into the two classes can be quite useful. There is also no correlation between soft

[22] Pearson, R. G. *J. Am. Chem. Soc.* **1963**, *85*, 3533 and references therein.

Lewis bases and weak Brønsted bases, for instance the soft Lewis base RS^- binds strongly to H^+, but hard Lewis bases will also bind H^+ strongly.

Useful generalizations can be made though, especially about metal ions. Hard metal ions will form their most stable complexes with the first ligand atom of each periodic table group (e.g. N > P), while soft metal ions will form their most stable complexes with the second or a subsequent member of each group. For a typical soft metal ion decreasing complex stability for ligand atoms generally follows the order C~S > I > Br > Cl~N > O > F, which follows the increase in electronegativity. Hardness also increases with increasing oxidation state of the metal. For instance Fe^{3+} is harder than Fe^{2+} and Pt^{4+} is harder than Pt^{2+}. The hardness or softness of an element is also affected by the bound ligands. Any group which transfers negative charge density to the Lewis acid center will decrease the hardness.

Also discussed in Pearson's 1963 report was the π-bonding theory of Lewis acids, which applied mainly to metallic complexes. Soft Lewis acids were considered to have loosely held d-orbital electrons which could form π-bonds with suitable ligands, those having relatively low energy empty d-orbitals such as P, As, S, and I, or unsaturated ligands such as CO and isonitriles. In the latter cases the orbitals employed on the ligands would be antibonding molecular orbitals. Increasing the oxidation state of the metal would lead to the electrons available for this back-donation being lower in energy (more tightly bound to the metal center), and therefore lead to a less favorable π-bonding interaction. Hard Lewis acids, on the other hand, would have relatively tightly bound outer electrons but low energy acceptor orbitals. In this case harder ligands such as O and F, in addition to the σ-interactions, could form π-bonding interactions by donation of electrons into the acceptor orbitals on the metal. The concept of electron back-donation from the metal center to the ligand and its importance to the chemistry of Pt(II) and Au(I) will be discussed further in conjunction with carbophilic activation.

The basis for the favorability of hard-hard and soft-soft Lewis acid-base interactions was explained as hard species, with their small size and large charge density, tending to favor strong ionic

bonding while softer species, with their larger size and polarizability, would favor more covalency in their bonding interactions. For hard species this would mean that the interactions are mostly electrostatic in nature; electrostatic interactions rapidly decrease in strength with increasing charge separation. Smaller sized, hard Lewis acids and bases would allow the charge centers to approach closer, enhancing electrostatic interactions. For soft species, typically bearing smaller charge density, the approach needs to be close enough to allow favorable overlap of molecular orbitals. This leads to polarizability, the ability to distort electron clouds and begin forming chemical bonds at greater distances, being a highly important characteristic.

Table 1.1. Hardness parameters, η_{LS}, for select Lewis acids.

Acid	η_{LS} (eV)
Li^+	35.1
Na^+	21.1
Ag^+	6.9
Au^+	5.7
Sc^{3+}	24.6
Al^{3+}	45.8
$AlCl_3$	5.9
I_2	3.4

In subsequent studies, to address at least in part the qualitative nature of the HSAB theory, Parr and Pearson introduced the concept of absolute hardness, η_{LS}, defined as $\eta_{LS} = \frac{1}{2}(I - A)$ where I is the ionization potential and A is the electron affinity, measured in electronvolts (eV).[23] The term η_{LS} is used here with LS representing a Lewis species to avoid confusion with η used for defining the coordination mode of a metal-ligand interaction. Using this equation and tabulated data they were able to calculate the hardness for a variety of Lewis acids and bases (Table 1.1). It should be noted that the values shown for the ions in Table 1.1 should be considered hypothetical upper limits for

[23] a) Parr, R. G.; Pearson, R. G. *J. Am. Chem. Soc.* **1983**, *105*, 7512. b) Pearson, R. G. *J. Chem. Educ.* **1987**, *64*, 561.

hardness as they are values for *isolated* ions. For instance the coordination chemistry of Al^{3+} in aqueous solution will actually involve $Al(H_2O)_n^{3+}$, and therefore have attenuated hardness. The results do show the significant impact that ligands have on hardness, however, as the calculated value for $AlCl_3$ is a fraction of that for Al^{3+}.

This work does provide a way to relate HSAB theory to molecular orbital theory in that it mathematically relates hardness to the HOMO and LUMO energies of molecules and ions. The HOMO of hard species will be low in energy with high energy LUMOs, leading to a large HOMO-LUMO gap. In contrast soft species will have a small HOMO-LUMO gap resulting from relatively high energy HOMOs and low energy LUMOs (Figure 1.5).[24] Strong chemical bonds result from the interaction of orbitals close in energy. Donation from the high energy HOMO of a soft Lewis base to the low energy LUMO of a soft Lewis acid will result in a strong bond with a high degree of covalency. The large HOMO-LUMO energy gaps of hard species, however, will reduce the effectiveness of these types of bonding interactions, explaining why the bonding is mostly electrostatic in nature.

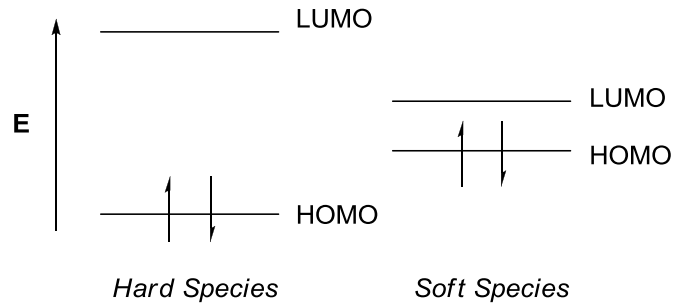

Figure 1.5. Relative HOMO and LUMO energies of hard and soft Lewis acidic and basic species.

Hard Lewis species can now be characterized by small size, low polarizability, and a large HOMO-LUMO gap. Hard Lewis acids prefer to form complexes with highly electronegative elements of the second row of the periodic table and are most commonly used in synthetic chemistry for oxophilic activation (see Figure 1.1, Scheme 1.3). Soft Lewis species are those characterized by

[24] Carey, F. A.; Sundberg, R. J. *Advanced Organic Chemistry*; 4th ed.; Spring: New York, N.Y., 2000.

large size, high polarizability, and a small HOMO-LUMO gap. Some of these compounds can be utilized for carbophilic activations in order to mediate synthetically useful transformations involving carbon-carbon π-bonds under mild conditions. Development of highly efficient, selective systems for these types of reactions is an important area of chemistry and the focus of this thesis.

Carbophilic Activation

Carbophilic activation is an increase in reactivity of a carbon-carbon π-bond caused by a soft Lewis acid depriving the π-bond of electron density, inducing a partial positive charge on the unsaturated Lewis base. The most successful Lewis acids employed in carbophilic activation chemistry are the late transition metals Pd(II), Pt(II), and Au(I).[2,15,20b] A useful model for considering the bonding situation in complexes between transition metals and alkenes or alkynes is the Dewar-Chatt-Duncanson model, which treats the bond as a donor-acceptor interaction between two closed-shell fragments.[25]

Within this framework a σ-bond is formed from electron donation by the π-system of the ligand into an empty orbital of appropriate symmetry on the metal. A π-bond can also be formed from electron back-donation from the metal center into an antibonding π* orbital on the ligand (Figure 1.6).[2] For an alkyne ligand additional interactions are possible through the perpendicular, out-of-plane π-orbitals (bonding and antibonding) and suitable orbitals on the metal center.

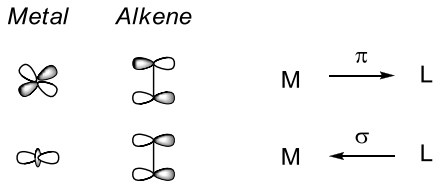

Figure 1.6. Orbital diagram of possible interactions between transition metals and alkene ligands.

To quantify the strength of these different interactions, density functional theory (DFT) calculations were carried out on the Au^+-acetylene complex $[Au^+(C_2H_2)]$ to determine the

[25] a) Chatt, J.; Duncanson, L. A. *J. Chem. Soc.* **1953**, 2939. b) Dewar, M. J. S. *Bull. Soc. Chim. Fr.* **1951**, *18*, C71. c) Frenking, G.; Fröhlich, N. *Chem. Rev.* **2000**, *100*, 717. d) Dedieu, A. *Chem. Rev.* **2000**, *100*, 543.

contribution of each bonding interaction to the overall complexation energy.[26] It was found that the σ interaction accounted for ca. 65% of the total bonding energy, with the in-plane back donation accounting for ca. 27%. The interaction of the out-of-plane π-bond with the metal center accounted for another 7%, while the back donation from the metal to the out-of-plane π* orbital made up only 1% of the bonding energy. It was concluded that alkynes and alkenes are strong two-electron σ-donors to Au(I) and Pt(II), but relatively weak π-acceptors.

These bonding interactions have important effects on the geometry of the unsaturated ligand. Both the σ-interaction and the π-backbonding interaction with the metal complex act to weaken the π-bond of the unsaturated ligand. This can lead to significant deviations from the ideal bond angles of the uncomplexed ligand, as seen in the Pt(0) complex with diphenylacetylene (**18**) in which the bound ligand's bond angles, θ, deviate from linearity by 60˚ (Figure 1.7a).[2] It was noted above that Pt(II) demonstrates weak back-bonding interactions. Pt(0), however, is able to strongly back-donate electron density into the π* orbital of the alkyne due to its lower oxidation state. It is a characteristic of all transition metals that lower oxidation states lead to stronger the π-backbonding interactions due to population of higher energy donor orbitals on the metal center.[27] This causes metals in higher oxidation states, such as Pt(II), to be stronger carbophilic activators than their lower oxidation state analogs. Lower π-backbonding leads to an increased relative electrophilicity of the carbon-carbon multiple bond.

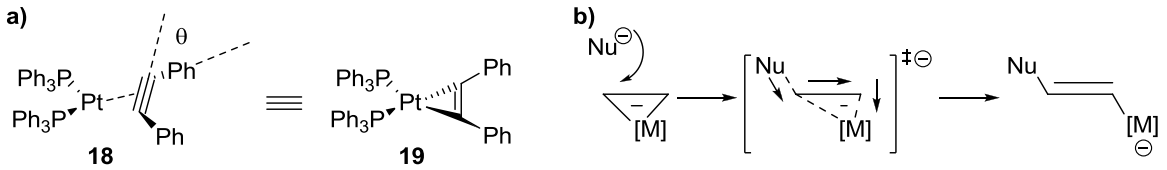

Figure 1.7. Effects of π-backbonding on bond angles and schematic representation of slippage.

While it is valid to consider the ground state complexation of transition metals and alkenes/alkynes as η^2 complexes similar to **19**, it is now commonly believed that the transition state

[26] Nechaev, M. S.; Rayón, V. M.; Frenking, G. *J. Phys. Chem. A* **2004**, *108*, 3134.
[27] Hahn, C. *Chem. Eur. J.* **2004**, *10*, 5888.

for nucleophilic addition to the bound ligand involves slippage of the metal center to an η^1 binding mode (see Figure 1.4, Figure 1.7b). Partial slippage can occur in the ground state of the complex as well, imparting electrophilicity to the ligand. Slippage also enables electron redistribution throughout the compound as the nucleophile transfers charge through the ligand and onto the metal center, a stabilizing effect when the metal is cationic.

While the utility of oxophilic activations is indisputable in synthetic chemistry, there are entire classes of natural products that can be accessed only by carbophilic activation, foremost among them the natural products derived from terpenes. Terpenes are natural products composed of isoprene units (**20**), produced biosynthetically from isopentenyl pyrophosphate (**21**) and dimethylallyl pyrophosphate (**22**, see Figure 1.8).

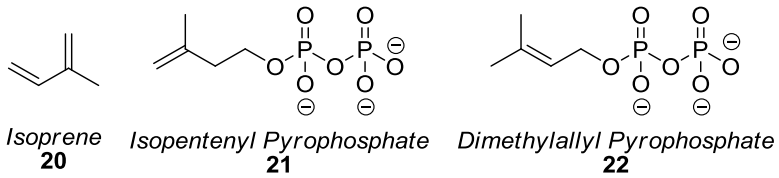

Figure 1.8. Synthetic building blocks of terpene biosynthesis.

Enzymes catalyze the reactions that stitch these components into linear forms that are classified based on the number of isoprene units the compound contains. For example, monoterpenes such as geranyl diphosphate (**23**) are synthesized from one unit of **21** and one unit of **22**, for a total of 2 isoprene units (Figure 1.9). Sesquiterpenes such as **24** contain 3 units and so forth through sesterterpenes (**25**, 5 isoprene units) and triterpenes such as squalene (**26**, 6 isoprene units) up to tetraterpenes, which contain 8 isoprene units. Larger terpenes are typically referred to as polyterpenes. These acyclic compounds in turn serve as the basis for a huge range of natural products, including all the hopanoids and steroids such as cholesterol, estrogen, and progesterone. Due to their complex molecular structures and important biological relevance these compounds have

served as attractive research targets for decades, driving innovation in synthetic and computational chemistry.[28-29]

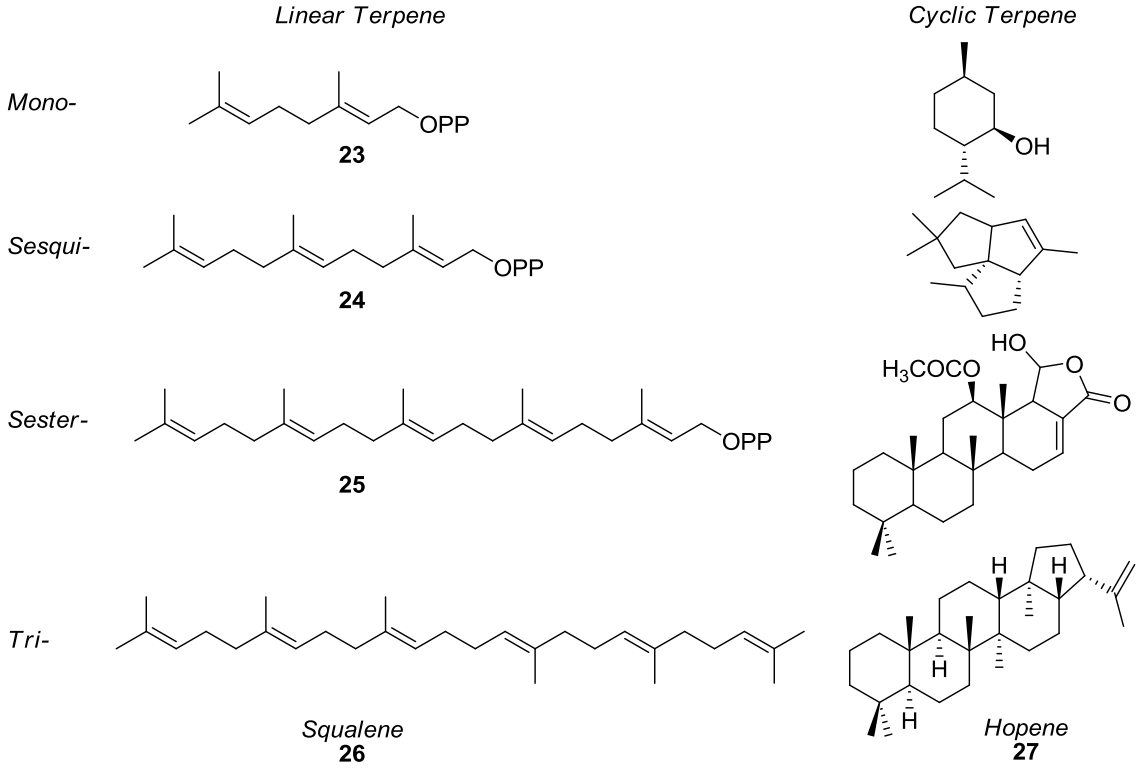

Figure 1.9. Linear and cyclic examples of various classes of terpenes.

Enzymes are capable of catalyzing the transformation of these linear polyene species into complex cyclic compounds with remarkable control of product stereoselectivity.[30] In the case of squalene (**26**), squalene-hopene cyclase catalyzes the conversion into hopene (**27**) setting 9 stereocenters in a single reaction (Scheme 1.8a). The cyclization is initated by protonation at C3 by an enzyme-based carboxylic acid moiety. Enzyme-labeling and computational studies have led to the proposal of a hydrogen bonding network within the active site of the cyclase enzyme that increases the acidity of the carboxylic acid sufficiently to allow initial protonation of the terpene (Scheme 1.8b). Cyclization of the ABC rings are believed to be concerted, but proceeds with initial formation

[28] a) Razzak, M.; De Brabander, J. K. *Nat. Chem. Biol.* **2011**, *7*, 865 and references therein. b) Yoder, R. A.; Johnston, J. N. *Chem. Rev.* **2005**, *105*, 4730.
[29] a) Tantillo, D. J. *Nat. Prod. Rep.* **2011**, *28*, 1035. b) Tantillo, D. J. *J. Phys. Org. Chem.* **2008**, *21*, 561. c) Matsuda, S. P. T.; Wilson, W. K.; Xiong, Q. *Org. Biomol. Chem*. **2006**, *4*, 530.
[30] a) Wendt, K. U.; Schulz, G. E.; Corey, E. J.; Liu, D. R. *Angew. Chem. Int. Ed.* **2000**, *39*, 2812. b) Christianson, D. W. *Chem. Rev.* **2006**, *106*, 3412 and references therein.

of a 5-membered C-ring to avoid formation of a secondary carbocation intermediate (Scheme 1.8a).[31] Ring expansion to the 6-membered C ring seems to be concerted, but highly asynchronous, with formation of the D ring.

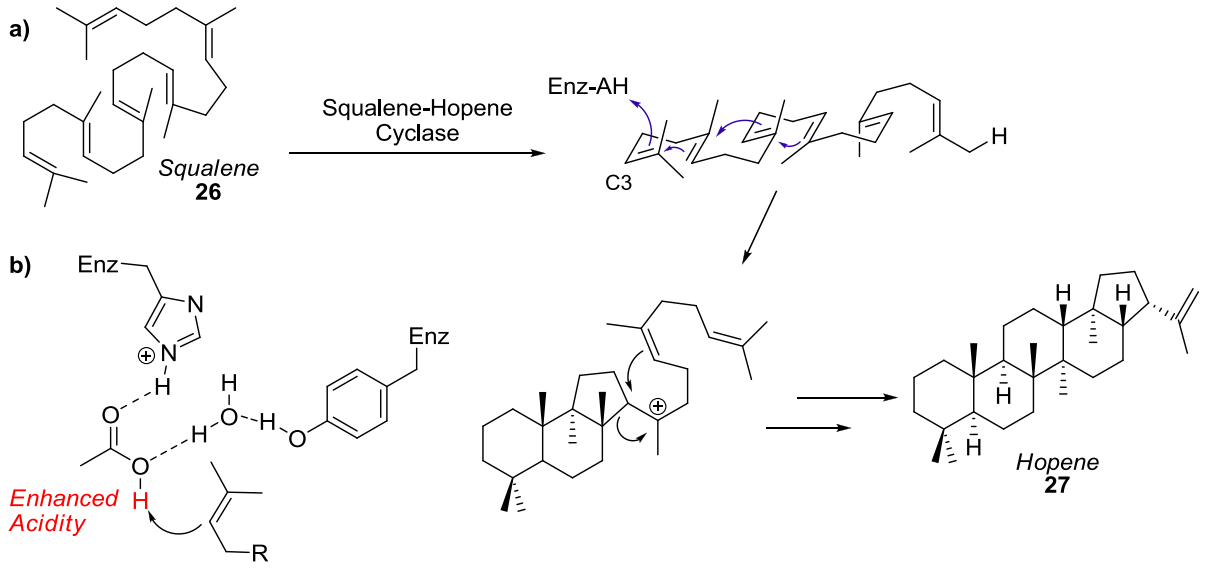

Scheme 1.8. Enzyme catalyzed polyene cascade cyclizations.

A similar pathway is believed to be followed by the D and E ring closures to avoid formation of secondary carbocations. Indeed, a large amount of research has indicated that secondary carbocation intermediates are avoided by complex hydride and alkyl shifts in terpene biosynthesis.[29a,31-32] The carbocationic intermediates in these cyclizations are stabilized by aromatic residues in the active site through π-stacking interactions. The cyclization is terminated either by deprotonation by an active site base (as in the case of **27**), or by nucleophilic capture of the carbocation by water.

Replicating the level of control that nature exerts over the outcome of these cascade cyclizations is still a daunting challenge in synthetic chemistry. A large part of the difficulty comes from the number of potential rearrangements that are available to carbocationic intermediates in

[31] a) Smentek, L.; Hess, B. A., Jr. *J. Am. Chem. Soc.* **2010**, *132*, 17111. b) Hess, B. A., Jr.; Smentek, L. *Org. Lett.* **2004**, *6*, 1717. c) Hess, B. A., Jr. *Org. Lett.* **2003**, *5*, 165.
[32] a) Hong, Y. J.; Tantillo, D. J. *J. Am. Chem. Soc.* **2010**, *132*, 5375. b) Lodewyk, M. W.; Gutta, P.; Tantillo, D. J. *J. Org. Chem.* **2008**, *73*, 6570.

complex carbocyclic frameworks.[32] This has led to the search for efficient, highly selective reagents that can be employed in biomimetic polyene cascade cyclizations.

A significant development in this area came with the report of Yamamoto's Lewis acid-assisted chiral Brønsted acid (LBA) systems.[33] These systems combine a Lewis acid with a chiral Brønsted acid to restrict directional access to the proton, in addition to increasing the proton's acidity. This helped overcome problems in asymmetric synthesis employing only chiral Brønsted acids, such as the conformational flexibility between the proton and its conjugate base and the small steric size of the proton, which allows a large amount of directional approaches to Brønsted basic sites and in turn reduces the reaction selectivity. LBAs were utilized in the first enantioselective biomimetic cyclization of polyprenoids (Scheme 1.9).[33a] The diastereoselectivity seen in these reactions was generally quite high (ca. 90:10 or greater) but enantioselectivities were moderate in most cases (ca. 50-80%).

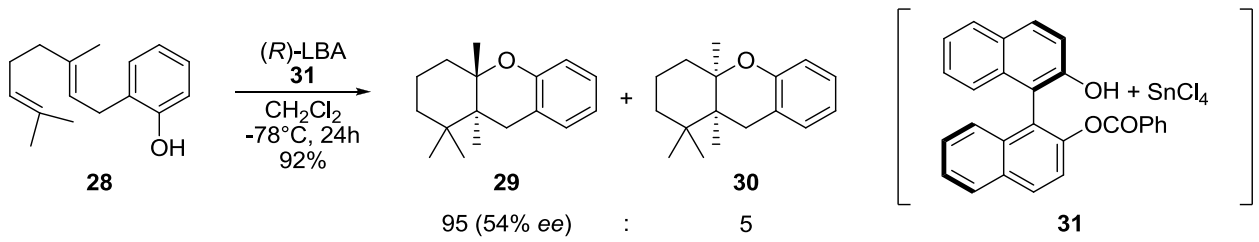

Scheme 1.9. LBA-mediated biomimetic cyclization of polyene substrates.

In a subsequent study the Yamamoto group applied LBA systems to polyene substrates with an aprotic terminating group (Scheme 1.10a).[33c] In this case it was pyrogallol derivatives that were the chiral Brønsted acids paired with $SnCl_4$. Unfortunately without a protic terminating group the selectivity of the reaction was much lower and with most of the LBA complexes employed the major product was the incomplete cyclization product, **35**. LBA **37** (Scheme 1.10b) was found to cyclize **32** in the highest enantioselectivity of the desired product (**33**), but in poor yield. Modest yields of **33** could be obtained with different LBAs, but with little or no enantioselectivity. It was also noted that

[33] a) Ishihara, K.; Nakamura, S.; Yamamoto, H. *J. Am. Chem. Soc.* **1999**, *121*, 4906. b) Ishibashi, H.; Ishihara, K.; Yamamoto, H. *Chem. Rec.* **2002**, *2*, 177. c) Kumazawa, K.; Ishihara, K.; Yamamoto, H. *Org. Lett.* **2004**, *6*, 2551.

in some cases a chlorinated compound of undetermined structure was formed in low yields (**36**). When these LBA complexes were tested with substrate **28** they gave products with similar selectivity to the BINOL-derived complexes.

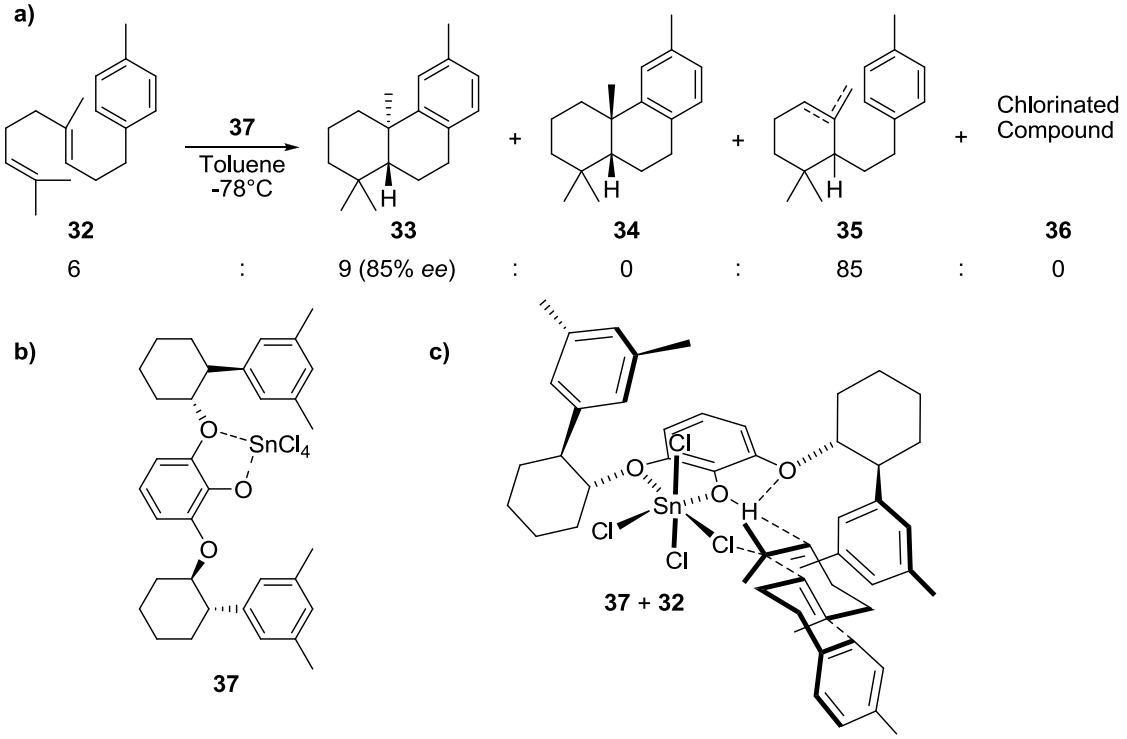

Scheme 1.10. Experimental results of cascade cyclizations with LBA 37 and rationalization for observed absolute stereochemistry.

The observed absolute stereochemistry is proposed to come from formation of LBA-ligand complexes such as that show in Scheme 1.10c. The protic O-H bond is fixed in the phenoxy plane by chelation with $SnCl_4$ and hydrogen bonding to the adjacent ethereal oxygen. Steric congestion is believed to cause the substrate (**32**) to approach the activated proton perpendicular to the phenoxy plane, with the methyl groups positioned away from the bulky carbocycles. While demonstrating the first enantioselective example of a biomimetic polyene cyclization, these systems had the disadvantage of incomplete cyclization with aprotic substrates, as well as most cases requiring a stoichiometric amount of the LBA.

Another Lewis acid system that has been employed for carbophilic activation and biomimetic cyclizations is $Hg(OTf)_2$. Originally formulated as a mercury(II) triflate-amine complex, this soft

Lewis acid was utilized for the bicyclization of a number of polyene substrates (Table 1.2).[34] The system was tolerant of oxygen- and sulfur-containing functional groups, providing the product compounds in moderate to good yields. The stable alkyl-mercury bond formed provided a handle for further synthetic elaboration, but also prevented catalytic turnover, requiring use of a stoichiometric amount of mercury, an undesirable feature for large scale preparations.

Table 1.2. Mercury(II) triflate mediated cyclization of polyenes.

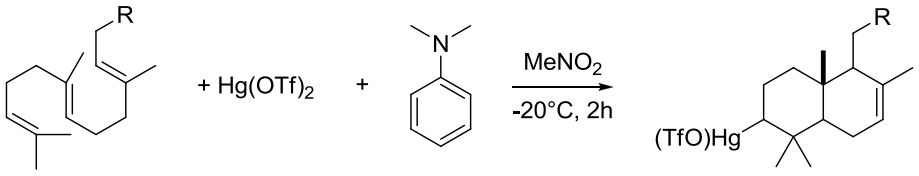

Entry	Substrate	Product (Yield %)
1	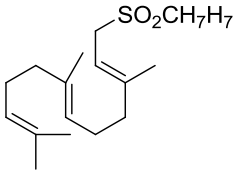	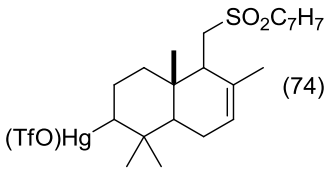 (74)
2	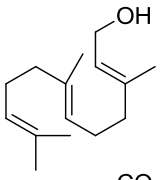	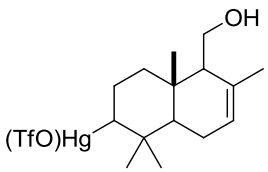 (51)
3	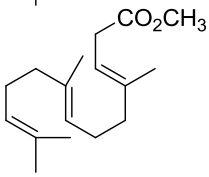	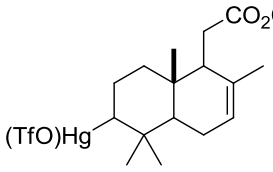 (56)

These systems could be rendered catalytic in Hg(II) by clever design of the substrate.[35] It was discovered that if an acid labile moiety is present (e.g. hydroxyl, ether) protonation of the alkylmercury intermediate (**38**) with *in situ* generated triflic acid can lead to demercuration with concomitant release of the conjugate base (e.g. water, alcohol), as shown in Scheme 1.11. Catalyst loadings could be quite low (0.5-1.0 mol%) but the reactions were limited to monocyclizations. The

[34] Nishizawa, M.; Takenaka, H.; Nishide, H.; Hayashi, Y. *Tetrahedron Lett.* **1983**, *24*, 2581.
[35] Namba, K.; Yamamoto, H.; Sasaki, I.; Mori, K.; Imagawa, H.; Nishizawa, M. *Org. Lett.* **2008**, *10*, 1767.

authors also reported no asymmetric induction when chiral auxiliaries were employed for a similar enyne cyclization.

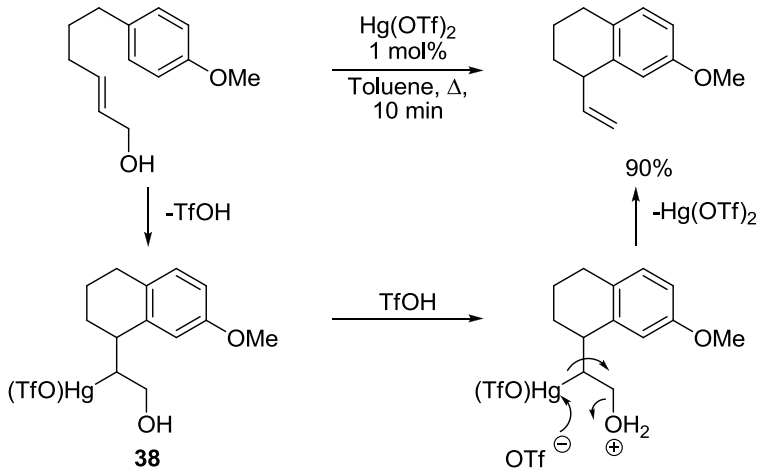

Scheme 1.11. Catalytic monocyclizations mediated by $Hg(OTf)_2$.

While it had been known since Overman's Pd-catalyzed Cope rearrangement (see Scheme 1.7) that Pd(II) could electrophilically activate carbon-carbon π-bonds it wasn't until the late 1990's and early 2000's that this idea began to be applied towards biomimetic cascade cyclizations. Building off the work of Overman,[18] as well as demonstrations of intermolecular additions to electrophilically activated olefins by Vitagliano,[36] the Gagné group reported the cyclization of polyene chains into multicyclic compounds using a Pd(II) catalyst (Scheme 1.12).[37]

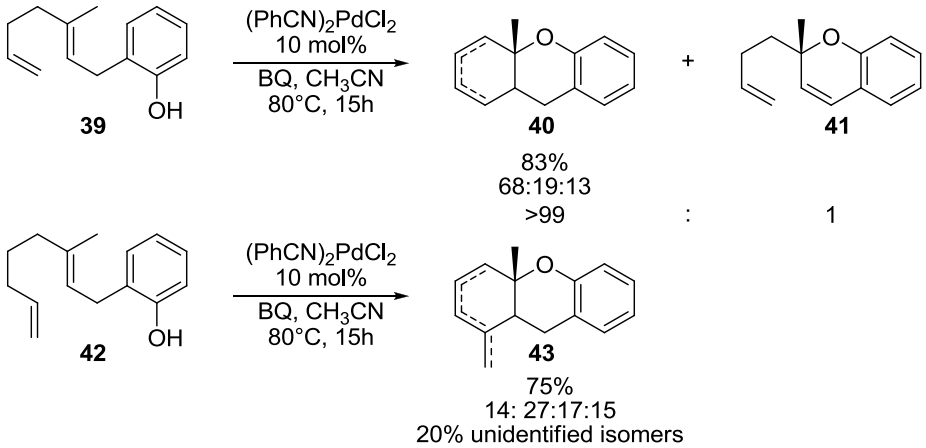

Scheme 1.12. Pd(II) catalyzed cyclizations of polyene substrates.

[36] a) Hahn, C.; Vitagliano, A.; Giordano, F.; Taube, R. *Organometallics* **1998**, *17*, 2060. b) Hahn, C.; Morvillo, P.; Vitagliano, A. *Eur. J. Inorg. Chem.* **2001**, 419.
[37] Koh, J. H.; Mascarenhas, C.; Gagné, M. R. *Tetrahedron* **2004**, 7405.

Utilizing $(PhCN)_2PdCl_2$ as the catalyst and benzoquinone (BQ) as the stoichiometric oxidant, the cyclized products could be obtained in good yield as a mixture of alkene isomers. For instance, the cyclization of 1,5-diene **39** could be performed efficiently under optimized conditions to provide the cyclized product, **40**, as a mixture of isomers with minimal formation of the undesired Wacker-type product (**41**). Under the same conditions 1,6-diene **42** formed the cyclized product, **43**, as a mixture of four alkene isomers and gave an additional 20% yield of unidentified alkene isomers. The poor product regioselectivity is attributed to the high propensity of Pd(II) to isomerize alkenes by sequential migratory-insertion/β-hydride elimination reactions.

Further exploration of these Pd(II) systems for polyene cyclizations revealed that the outcome products formed were highly dependent on the structural features of the substrate.[38] It was found that while 1,5-diene substrates were reasonably well behaved, alkenes separated by more than 2 methylene units demonstrated poor cyclization reactivity (Scheme 1.13). Reaction of 1,6-diene **44** gave a combined 22% of the desired pinacol rearrangement product (**45**) and isomerized starting material, in addition to a 45% yield of dehydration/aromatization products. Reaction of 1,8-diene **46** gave, after hydrogenation of the product alkene isomers, only 28% yield of saturated **47**. As the reaction pathways and product distributions were strongly affected by the structural features of the substrate these systems demonstrated little sensitivity to optimization attempts through changing reaction conditions.

[38] Korotchenko, V. N.; Gagné, M. R. *J. Org. Chem.* **2007**, *72*, 4877.

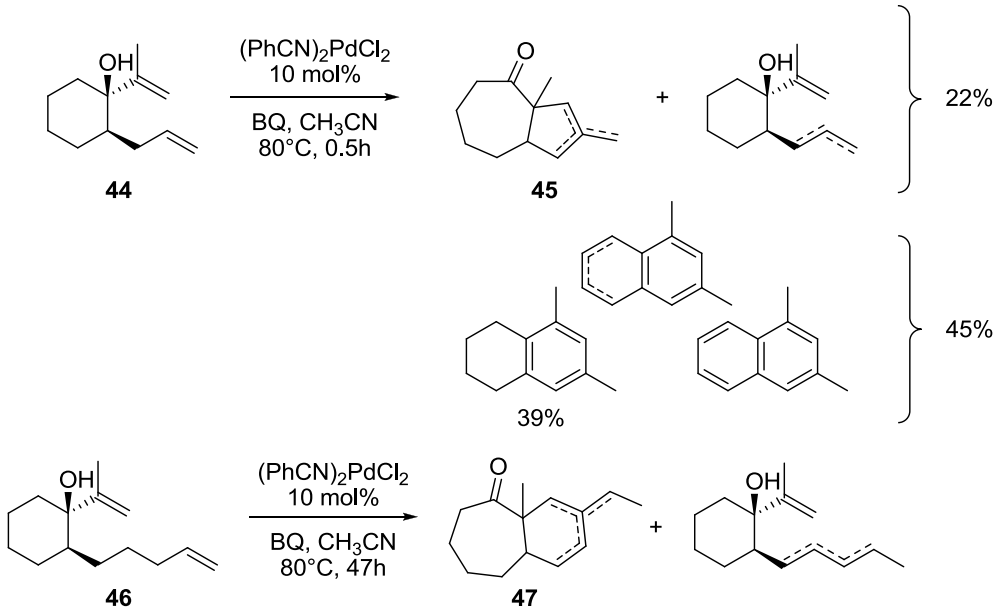

Scheme 1.13. Pd(II) catalyzed cyclization of 1,*n*-dienes.

Due to the tendency for alkene isomerization and undesirable rearrangement pathways displayed by Pd(II), this system was deemed unsuitable for biomimetic cascade cyclization reactions. Pt(II) and Au(I), however, just one row down in the periodic table, have some distinct characteristics that have allowed them to be used effectively in a number of electrophilic activation reactions, including biomimetic polyene cascades.

Electrophilic Pt(II) Systems

Pt(II) and Au(I) have many similar chemical properties that manifest in their soft Lewis acidic character. Despite this, the two transition metal elements can, and often do, display greatly differing reactivity and this has been used to develop a plethora of novel reaction systems for the electrophilic activation of alkynes, allenes, and alkenes.[2,20,39] Indeed, one of the most fundamental ways in which these elements differ is in their preferred complexation geometry. The d^8 metal Pt(II) adopts square planar geometry while the d^{10} Au(I) adopts linear complexation geometries, which has important implications on asymmetric applications as the source of chirality in Au(I) complexes is necessarily held relatively far from the reacting center (Figure 1.10).

[39] Fürstner, A. *Chem. Soc. Rev.* **2009**, *38*, 3208.

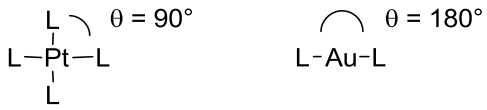

Figure 1.10. Common coordination geometries of Pt(II) and Au(I) ligand (L) complexes.

However, these two elements also share a lot of chemical properties that help to explain their reactivity profiles which differ significantly from many other transition metal elements. Perhaps the most significant elemental properties on the reactivity of these two metals are the lanthanide contraction and relativistic effects.[2,40] The lanthanide contraction is a larger than expected decrease in atomic radii for the lanthanide and post-lanthanide elements due to an increase in the number of protons in the nucleus having a disproportionate attractive effect on the 6*s* orbitals, a result of population of the weakly shielding 4*f* orbitals. The result is a contraction of the 6*s* orbitals towards the nucleus.

Relativistic effects become significant with the heavy, late transition metals where the velocity of electrons becomes significant enough to cause an increase in their mass and a further contraction of the core shell orbitals. This contraction of the atomic *s* orbitals leads to increased shielding by the core electrons and even more diffuse *d* and *f* orbitals.[40] The diffuse nature of the *d* orbitals in these elements has two important implications on reactivity. It can be interpreted as giving Au(I) and Pt(II) their soft Lewis acidic character due to a higher degree of polarizability of these orbitals, allowing better overlap with approaching nucleophiles. This, in conjunction with contraction of the atomic *s* orbitals, results in shorter bond lengths and stronger bonds. Another important implication is there is less electron-electron repulsion in the diffuse orbitals, leading to the 5*d* electrons being held especially strongly. Theoretical studies indicate the 5*d* electrons of Au are actually held more strongly than the 3*d* electrons of Cu.[41] This has an important effect on reactivity as it makes Au(I) and Pt(II) resistant to normal oxidation-reduction processes common to other

[40] Gorin, D. J.; Toste, F. D. *Nature* **2007**, *446*, 395 and references therein.
[41] Nakanishi, W.; Yamanaka, M.; Nakamura, E. *J. Am. Chem. Soc.* **2005**, *127*, 1446.

transition metals such as Pd(II). This leads to broad functional group tolerance and often air and moisture stability for isolable complexes of these metals.

As Pd(II) complexes are highly reactive toward ligand substitution, pathways such as β-hydride elimination become facile processes for catalytic turnover. Pt(II) and Au(I) complexes, however, are relatively inert towards ligand substitutions and tend to form strong M-alkyl and M-hydride bonds. This leads to less competitive alkene isomerization pathways than in analogous Pd(II) systems, but also necessitates different catalytic turnover methods than the oxidative techniques commonly employed with Pd(II)/Pd^0 systems. This makes protonolysis pathways common (especially for Au(I) systems) but also opens up opportunities for more unusual pathways, such as cyclopropanation (Scheme 1.14).[42]

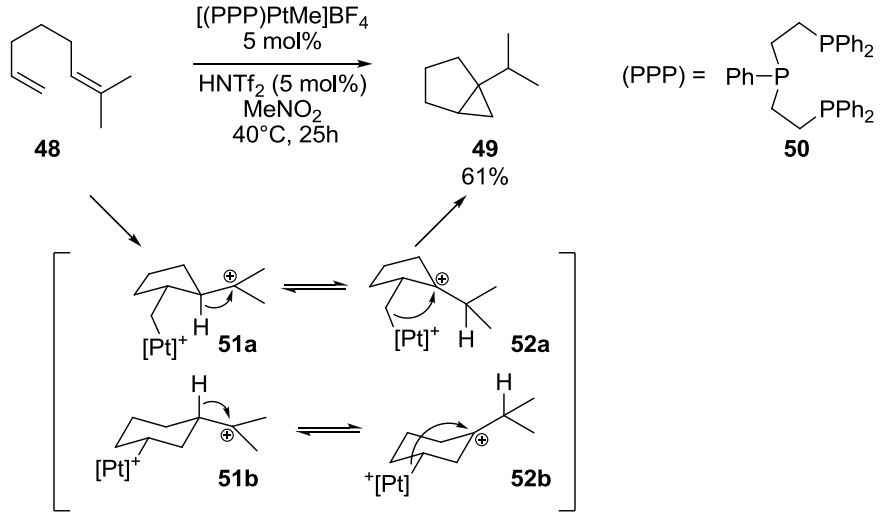

Scheme 1.14. Cyclopropanation reaction catalyzed by an *in situ* activated Pt(II) complex.

Cyclopropanation begins with *in situ* activation of [(PPP)PtMe][BF_4] (PPP = triphos, Bis(diphenylphosphinoethyl)phenylphosphine, **50**) by protonation and release of methane by $HNTf_2$. Coordination of the active Pt(II) complex to the least substituted double bond of **48** electrophilically activates the alkene, leading to cyclization by attack of the internal alkene. This reaction was found to proceed by both initial 5-*exo* and 6-*endo* cyclization modes, as demonstrated by experiments in the

[42] a) Kerber, W. D.; Gagné, M. R. *Org. Lett.* **2005**, *7*, 3379. b) Kerber, W. D.; Koh, J. H.; Gagné, M. R. *Org. Lett.* **2004**, *6*, 3013.

presence of benzyl alcohol in which carbocations **51a** and **51b** could both be trapped. In the absence of a base, a hydride shift from the initial cyclization intermediate occurs (to **52a** and **52b** for 5-*exo* and 6-*endo*, respectively), followed by elimination of the Pt-alkyl to produce **49**, the same product by either cyclization pathway. Notably, the tridentate triphos (PPP) ligand blocks an open coordination site necessary for β-hydride elimination to occur, resulting in trapping of the carbocation by cyclopropanation. The Pt-center did not proceed through a 5-coordinate Pt(IV) state to undergo β-hydride elimination due to its resistance to oxidation-reduction reactions. Use of a similar P_2P system employing a chiral, bidentate diphosphine ligand and a monophosphine ligand to block β-hydride elimination allowed these reactions to be rendered highly enantioselective.[43]

The triphos ligand was also employed in Pt(II)-mediated biomimetic polyene cyclizations. Reacting diene-phenol **39** with isolable Pt(II) catalyst $[(PPP)Pt(NCC_6F_5)][BF_4]_2$, cyclization proceeded efficiently to provide Pt-alkyl **53** (Scheme 1.15).[44] Reduction of the Pt-C bond with $NaBH_4$ provided the product, **40a**, in 90% yield and a diastereomeric ratio in excess of 99:1.

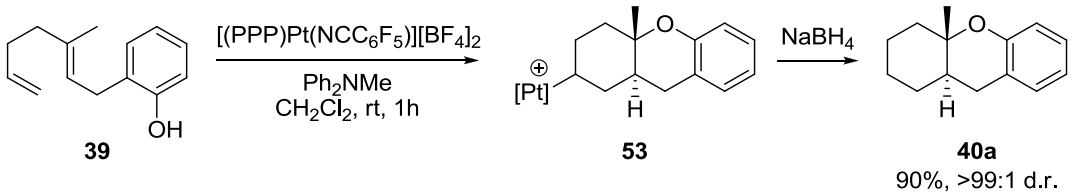

Scheme 1.15. Polyene cyclization using tridentate (PPP)Pt(II) catalysts.

The ability of the Pt(II) center to initiate the cascade cyclization was found to be sensitive to the electron donating ability of the phosphine ligands bound to the metal.[45] To explore these effects a number of triphos derivatives were synthesized (Figure 1.11). It was found that with the parent triphos ligand and an additive base all substrates investigated would cyclize until only the Pt-alkyl species was detected by ^{31}P NMR. With more strongly electron donating ligands such as EtPPPEt, it was observed that an equilibrium would be established with some of the Pt(II) species present as the

[43] Feducia, J. A.; Campbell, A. N.; Doherty, M. Q.; Gagné, M. R. *J. Am. Chem. Soc.* **2006**, *128*, 13290.
[44] Koh, J. H.; Gagné, M. R. *Angew. Chem. Int. Ed.* **2004**, *43*, 3459.
[45] Feducia, J. A.; Gagné, M. R. *J. Am. Chem. Soc.* **2008**, *130*, 592.

Pt-alkene complex. This indicates there is a threshold to how strong electron donation can be from bound ligands and still allow Pt(II) to initiate cyclization.

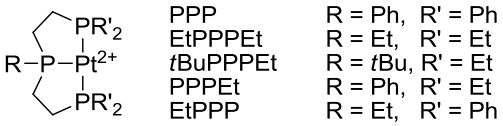

Figure 1.11. Triphos derivatives synthesized in order to explore the effect of ligand electron donating ability on Pt(II) initiated cyclizations.

In addition to 1,5-dienes, cyclization of a 1,6-diene phenol substrate, **54**, was also demonstrated and this served as the basis for a follow-up computational study into the mechanism of the reaction (Figure 1.12).[46] Two possible pathways were explored: a concerted cyclization whereby closure of the A ring occurs with trapping by the oxygen nucleophile and formation of the B ring in a single step and, alternatively, a stepwise path where a carbocation intermediate, **55**, is formed prior to oxygen addition and deprotonation to form the product (**56**).

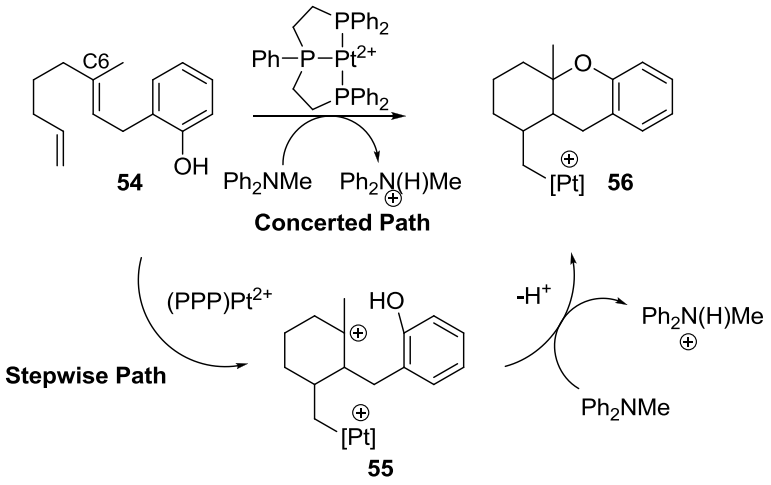

Figure 1.12. Possible mechanistic pathways of Pt(II) initiated cascade cyclization reaction.

Density functional theory (DFT) calculations at the B3LYP level of theory revealed that the concerted mechanism proceeds without formation of a distinct carbocationic intermediate and with essentially no barrier when the amine base is hydrogen bonding with the hydroxyl group. This hydrogen bonding enhances the ability of the oxygen atom to stabilize the developing positive charge on C6 through neighboring group participation. Neighboring group participation is the ability of an

[46] Nowroozi-Isfahani, T.; Musaev, D. G.; Morokuma, K.; Gagné, M. R. *Organometallics*, **2007**, *26*, 2540.

electron donating group (e.g. Lewis base, alkene, hydroxyl, etc.) to interact with and stabilize a developing positive charge, often while simultaneously advancing the reaction coordinate.[47] This stabilization lowers the enthalpic cost of the reaction by mitigating the penalty of localizing a positive charge on a single atom, but increases the entropic cost of the reaction due to the additional preorganization required to align relevant orbitals to allow neighboring group participation. In the case of **54**, hydrogen bonding, the first step of deprotonation, by the amine base allows the oxygen atom to donate electron density more strongly into the orbital developing positive charge, resulting in a near-barrierless reaction.

The activation barrier for monocyclization in the stepwise path was found to be ca. 2 kcal/mol and leads to intermediate carbocation **55**. Trapping of the carbocation by the phenol moiety with simultaneous deprotonation completes the cyclization. A transition state for this transformation could not be located, but would most likely occur without a barrier, analogous to the deprotonation/cyclization in the concerted pathway. The results of this study indicate that these Pt(II) initiated cyclizations most likely proceed through a concerted pathway, with very small reaction barriers when hydrogen bonding to a base is possible.

In recent years advances have been made in the scope and selectivity of Pt(II) mediated biomimetic polyene cyclizations. A recent study by the Gagné group explored the polycyclizations of various substrates with aprotic terminating groups.[48] Utilizing $[(PPP)Pt][BF_4]_2$, generated *in situ* by halide abstraction from $[(PPP)PtI_2][BF_4]$ using $AgBF_4$, and a piperidine resin base, a number of substrates were efficiently cyclized to the isolable Pt-alkyl product (Table 1.3). Both bi- (entries 1, 5) and tricyclizations (entries 2-4) were found to work well, with one product isomer observed in most cases. A limitation to the reaction was observed, however, with squalene analog **57** (Scheme 1.16). Cyclization of the first three rings proceeded analogously to the proposed enzymatic cyclization (see

[47] a) Eschenmoser, A.; Arigoni, D. *Helv. Chim. Acta* **2005**, *88*, 3011. b) Johnson, W. S.; Bailey, D. M.; Owyang, R.; Bell, R. A.; Jacques, B.; Crandall, J. K. *J. Am. Chem. Soc.* **1964**, *86*, 1959. c) Poulter, C. D.; King, C. R. *J. Am. Chem. Soc.* **1982**, *104*, 1422.
[48] Sokol, J. G.; Korapala, C. S.; White, P. S.; Becker, J. J.; Gagné, M. R. *Angew. Chem. Int. Ed.* **2011**, *50*, 5658.

Scheme 1.8) with formation of the 5-membered C-ring in order to generate the most stable, tertiary carbocation. At this point, however, the cyclization stalls. Instead of ring expansion to form the 6-membered C-ring and allow cyclization to continue, a Wagner-Meerwein rearrangement occurs to give the tricyclic product **58**. This indicates that without the carbocation stabilizing environment that is present in cyclase enzymes, lower energy rearrangement pathways can become active in these Pt(II) systems.

Table 1.3. (PPP)Pt^{2+} initiated polycyclization reactions.

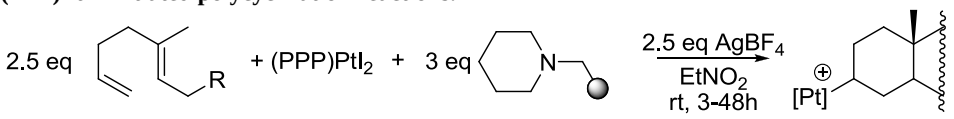

Entry	Substrate	Product	Yield
1	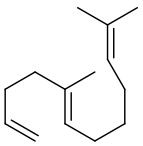	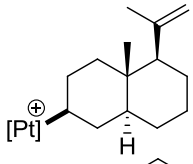	80%
2	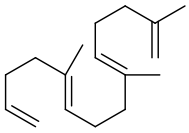	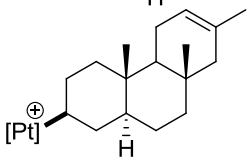	74%
3	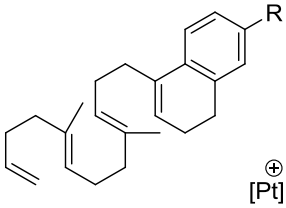	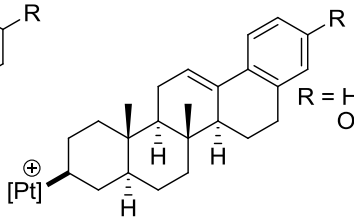	R = H 89%
4			OMe 97%
5	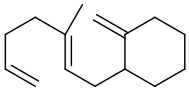	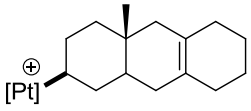	76%

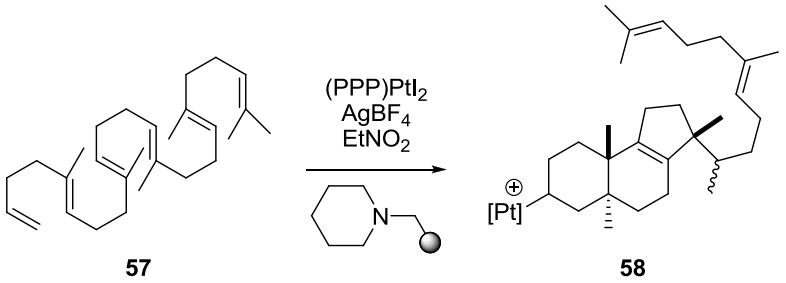

Scheme 1.16. Cyclization of a squalene analog with *in situ* generated (PPP)Pt^{2+}.

Using Pt(II) complexes with bidentate phosphorous ligands, a catalytic system was developed for cascade cyclizations.[49] Initiation of the catalytic cycle begins with coordination of the Pt(II) center to the least substituted alkene (Figure 1.13, structure **A**). Cyclization proceeds with concomitant deprotonation by Ph_2NH to produce Pt-alkyl intermediate **B**. Transfer of the proton from $Ph_2NH_2^+$ to resin-bound trityl methyl ether releases methanol and forms active hydride abstracting reagent trityl cation (Tr^+). β-hydride elimination from intermediate **B** occurs to release the product, **40b**, while producing Pt-hydride, **C**. Trityl cation then abstracts the hydride to turn over the catalytic cycle. Employment of hydride abstracting agents was found to be vital to the catalytic process as the Pt-hydride is a relatively stable oxidation-resistant species.

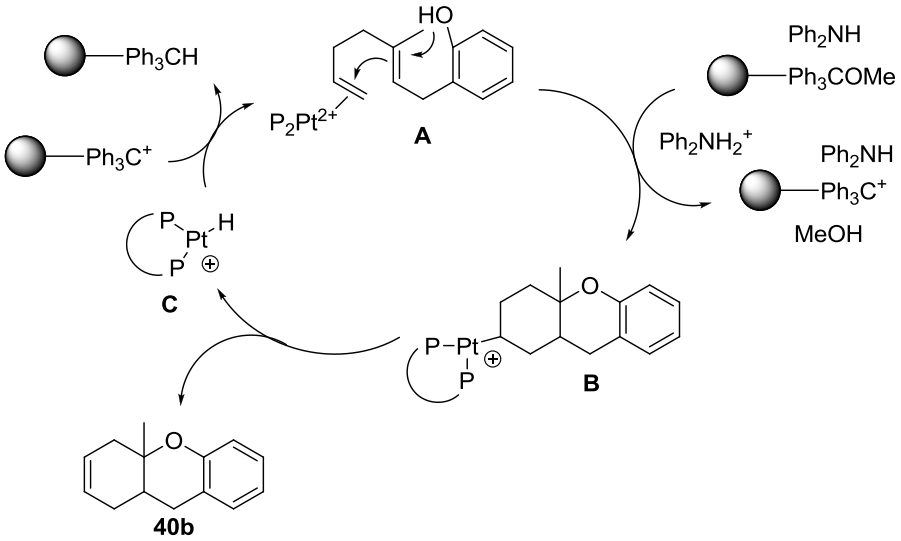

Figure 1.13. Catalytic cycle for Pt(II) initiated polyene cascade cyclizations.

[49] Mullen, C. A.; Gagné, M. R. *J. Am. Chem. Soc.* **2007**, *129*, 11880.

Using *in situ* generated $[(dppe)Pt][BF_4]_2$, (dppe = 1,2-bis(diphenylphosphino)ethane) it was found that bi- (Table 1.4, entries 1-4) and tricyclizations (entry 5) could be performed efficiently and the products obtained in good isolated yields. Both (*E*)- and (*Z*)- terminal alkenes could be cyclized with the (*Z*) substrate giving slightly higher yield (compare entries 3 and 4). A limitation was noted with a trisubstituted terminal alkene substrate, which failed to give any cyclization product (entry 6). This was attributed to the increased steric demand of the trisubstituted alkene disfavoring complexation to the Pt(II) center.

Table 1.4. Substrate scope of catalytic cyclizations with $(dppe)PtI_2$.

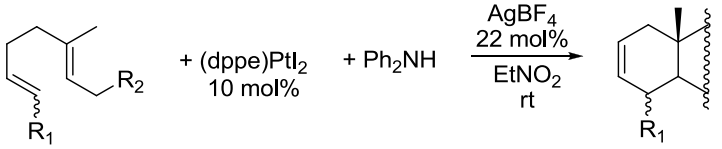

Entry	Substrate	Product	Time(h)	Yield
1	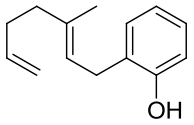	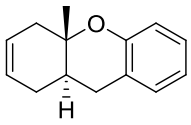	8	73%
2	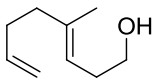	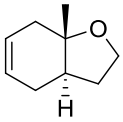	8	84%
3	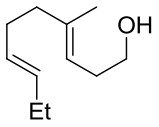	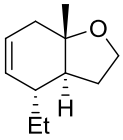	12	65%
4	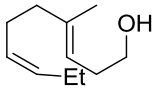	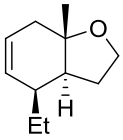	12	72%
5	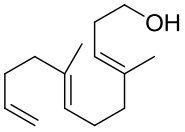	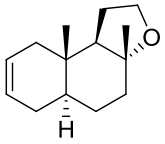	12	90%
6	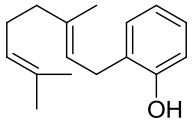			NR

Employment of the chiral (*S*)-xylyl-PHANEPHOS ligand (**59**) allowed these reactions to be performed enantioselectively.[50] In this case, however, a reactivity difference was displayed by (*E*)- and (*Z*)- alkenes (Scheme 1.17). With the chiral ligand the (*Z*)-alkene (**60a**) still cyclized, providing **61a** in 61% yield and 87% *e.e.* The (*E*)-alkene, **60b**, behaved poorly with no product being isolable and only a slight enantiomeric excess being detectable by GC. Greater quadrant differentiation by the chiral ligand most likely makes the binding environment around the Pt center more sterically demanding. As a result (*E*)-alkenes are unsuitable substrates in the chiral system.

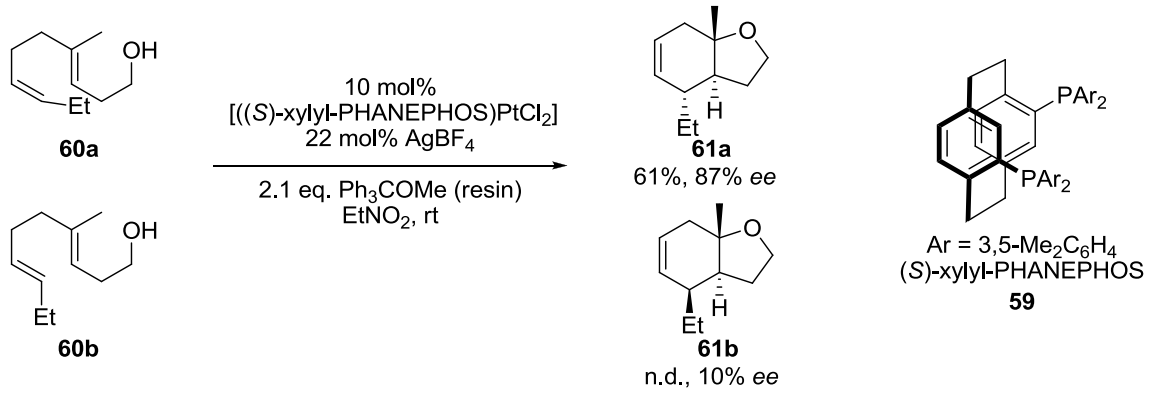

Scheme 1.17. Cyclization of (*E*)- and (*Z*)- alkenes with a chiral Pt(II) complex.

A large number of natural products have geminal disubstitution on the A-ring (e.g hopene, **27**, see Figure 1.9). Unfortunately, trisubstituted alkenes, which upon cyclization would lead directly to these types of compounds, are poor ligands for Pt(II) and will not cyclize with the current systems. It was the exploration of a potential way to circumvent this limitation that led to development of a Au(I)-catalyzed system and the investigations pertaining to it that comprise the majority of chapters 2 and 3 of this thesis.

Electrophilic Au(I) Systems

Many of the defining characteristics of the electrophilic activation chemistry of Pt(II) and Au(I) have been summarized (see Electrophilic Pt(II) Systems) but there are a few characteristics of Au(I) worth pointing out separately. One difference that is especially pertinent to catalytic chemistry

[50] Mullen, C. A.; Campbell, A. N.; Gagné, M. R. *Angew. Chem. Int. Ed.* **2008**, *47*, 6011.

is the labile nature of the Au-carbon single bond. These bonds are kinetically labile and Au-alkyl complexes tend to undergo rapid protodemetallation, even in the presence of relatively weak acids.[51] This provides a convenient turnover mechanism for catalytic cycles involving Au(I)-alkyl bonds, in many cases making the presence of additional reagents (e.g. oxidizing agents, hydride abstractors) unnecessary.

Au(I) also has a demonstrated affinity for initiating reactivity at alkynes. This "alkynophilicity," however, seems to be kinetic rather than thermodynamic in nature. Computational studies have indicated that ethylene is a slightly better ligand than acetylene for Au(I).[26] Initiation of chemistry at the alkyne moiety in enyne systems, then, seems to be due to preferential attack of the incoming nucleophile at the coordinated alkyne. Another explanation, proposed by Toste, invokes the characteristic lower HOMOs and LUMOs of alkynes compared to alkenes.[40] Due to lower energy HOMOs alkynes are less capable electron donors than alkenes, but their lower energy LUMOs make them more electrophilic as well. This is posited to translate into Au(I)-alkyne complexes having lower energy LUMOs, leading to greater electrophilic reactivity, than Au(I)-alkene complexes.

Au(I) complexes preferentially adopt linear coordination complexes. As stated earlier, this negatively impacts asymmetric applications as the source of chirality is necessarily held far from the reacting substrate. This property also makes it hard to chelate bisphosphine ligands to a single gold atom, the most commonly employed technique for realizing asymmetric transformations involving square planar Pd(II) and Pt(II) complexes. Prior to 2005 there was only one reported enantioselective Au(I)-catalyzed reaction.[52] In the years since Echavarren first reported[53] the alkoxycyclization of 1,6-enynes, there has been an influx of asymmetric Au(I) catalyzed reactions (Scheme 1.18).[54]

[51] Weber, D.; Jones, T. D.; Adduci, L. L.; Gagné, M. R. *Angew. Chem. Int. Ed.* **2012**, *51*, 2452.
[52] Ito, Y.; Sawamura, M.; Hayashi, T. *J. Am. Chem. Soc.* **1986**, *108*, 6405.
[53] Muñoz, M. P.; Adrio, J.; Carretero, J. C.; Echavarren, A. M. *Organometallics* **2005**, *24*, 1293.
[54] a) Widenhoefer, R. A. *Chem. Eur. J.* **2008**, *14*, 5382. b) Sengupta, S.; Shi, X. *ChemCatChem* **2010**, *2*, 609. c) Lee, A.-L. *Annu. Rep. Prog. Chem., Sect. B* **2011**, *107*, 369-389.

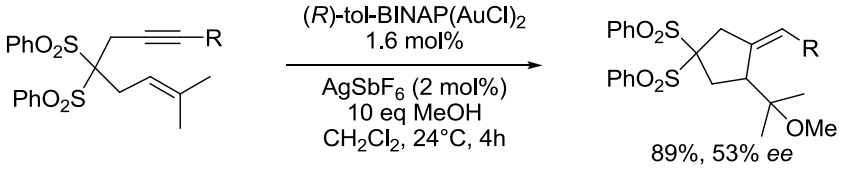

Scheme 1.18. Enantioselective alkoxycyclization catalyzed by a chiral Au(I) complex.

The most effective and widely employed systems have been bis-gold phosphine complexes of type **62** (Figure 1.14). The discovery of these dinuclear species for enantioselective Au(I) catalysis opened up the field to the use of the large library of chiral phosphorus ligands common in Pd(II) and Pt(II) chemistry. Also proven to be effective have been chiral phosphoramidite complexes (**63**) and the use of chiral counterions for activation of the catalyst precursor (**64**). These chiral counterions have seen use with both chiral and achiral ligands coordinated to the Au(I) center. Together these systems comprise the majority of the reported examples of asymmetric Au(I) catalysis. It should also be noted that the counterion (chiral or achiral) can have a large effect on selectivity, leaving open more opportunities for the fine-tuning of reaction systems than is observed in many other transition metal systems.

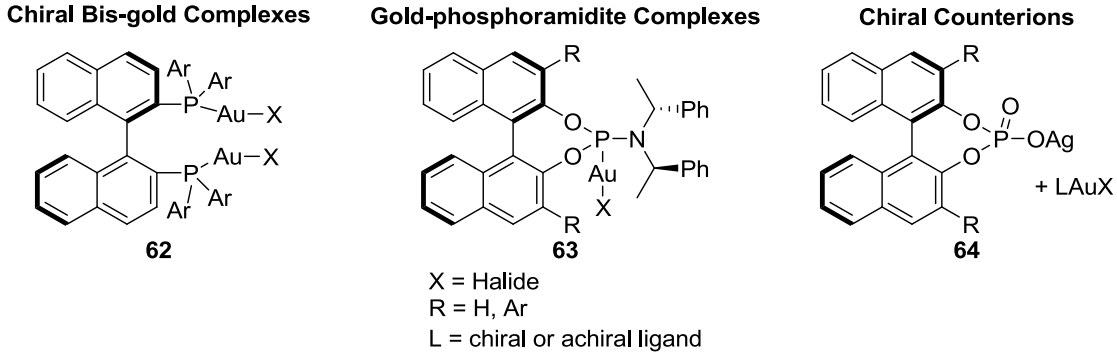

Figure 1.14. Examples of Au(I) complexes commonly utilized in asymmetric transformations.

A number of carbophilic activation reactions have been successfully rendered enantioselective by Au(I) catalysts including cyclizations,[55] hydroaminations,[56] and cycloadditions.[57]

[55] a) Sethofer, S. G.; Mayer, T.; Toste, F. D. *J. Am. Chem. Soc.* **2010**, *132*, 8276. b) Tarselli, M. A.; Chianese, A. R.; Lee, S. J.; Gagné, M. R. *Angew. Chem. Int. Ed.* **2007**, *46*, 6670.
[56] a) LaLonde, R. L.; Sherry, B. D.; Kang, E. J.; Toste, F. D. *J. Am. Chem. Soc.* **2007**, *129*, 2452. b) Zhang, Z.; Bender, C. F.; Widenhoefer, R. A. *J. Am. Chem. Soc.* **2007**, *129*, 14148.
[57] a) Alonso, I.; Trillo, B.; López, F.; Montserrat, G.; Ujaque, L.; Castedo, A.; Lledós, J. L.; Mascarenhas, C. *J. Am. Chem. Soc.* **2009**, *131*, 13020. b) Liu, F.; Yu, Y.; Zhang, J. *Angew. Chem. Int. Ed.* **2009**, *48*, 5505.

For example, activating the chiral phosphoramidite Au(I)-chloride complex with $AgSbF_6$ allowed the [4+2] cycloaddition of allenediene **65** to proceed at low temperature to provide the product (**66**) in high yield and excellent enantioselectivity (Scheme 1.19).[57a]

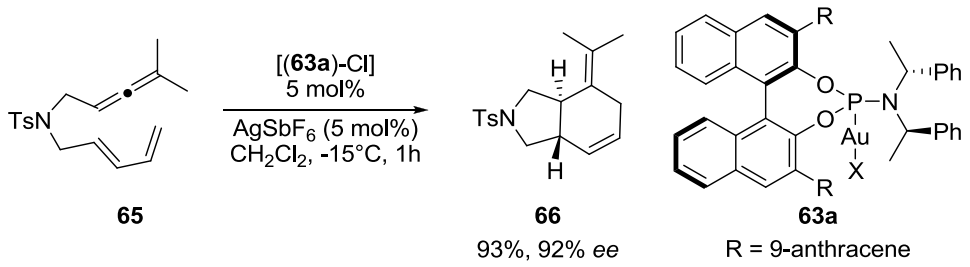

Scheme 1.19. Enantioselective [4+2] cycloaddition reaction catalyzed by a chiral Au(I)-phosphoramidite complex.

Research Objectives

The complex carbocyclic structures of natural products derived from terpenes, such as cholesterol and progesterone, still present daunting and inspiring challenges to synthetic chemists. No methodology currently developed is capable of approaching the level of control and selectivity demonstrated by enzymes in polyene cascade cyclizations. Biomimetic cyclizations by carbophilic transition metal Lewis acids offers a promising path towards this type of selectivity, however, through the creation of multiple rings in a single step with the potential for enantio-control provided by chiral ligands. The purpose of the research reported herein was to *develop new methodology for the electrophilic activation of alkenes*, as well as to *explore factors affecting the initial steps of polyene cascade cyclizations*. The work was initiated as an extension of cascade cyclizations previously reported by the Gagné group and aimed at utilizing ring strain present in cyclopropylidenes to provide a solution to the limitation that alkene trisubstitution imposes on Pt(II) initiated reactions. Substrates from this work were reacted with a Au(I) compound and led to the discovery and development of an enantioselective Au(I)-catalyzed Cope rearrangement (**Chapter 2**). In attempting to utilize this methodology to access medium-sized rings a unique rearrangement was discovered that leads to the creation of tricyclic compounds with a bicyclo[4.2.0]oct-1-ene core (**Chapter 3**). Simultaneously with this undertaking a theoretical investigation into the factors affecting the regioselectivity of Pt(II)

cyclization was begun in collaboration with the Tantillo group at the University of California-Davis (**Chapter 4**).

Chapter 2 - Au(I)-Catalyzed Cope Rearrangement

Hypothesis – Overcoming Trisubstitution Limitation of Pt(II)-Mediated Cyclizations

Parts of this chapter have been reported in a paper published in *Nature Chemistry* in 2012.[58]

As was previously stated, limitations were observed for Pt(II)-mediated cascade cyclizations; reaction efficiency decreased with increasing substitution on the terminal olefin (see Electrophilic Pt(II) Systems).[49,50] The nature of these limitations are believed to be steric, resulting from unfavorable clashes between the polyene substrate and the bi- or tridentate phosphine ligands bound to the Pt(II) center. This makes coordination of the alkene energetically unfavorable, preventing the electrophilic activation and subsequent cyclization of the substrate.

A proposed way of circumventing this limitation was to utilize the ring strain inherent in methylenecyclopropanes (MCP, cyclopropylidenes) to assist coordination of the substrate to the metal complex. The strain of the exocyclic double bond in the MCP moiety is ca. 12 kcal/mol (Scheme 2.1).[59] It has been successfully demonstrated that utilizing the strain energy of small ring systems can drive a large number of chemical transformations.[60]

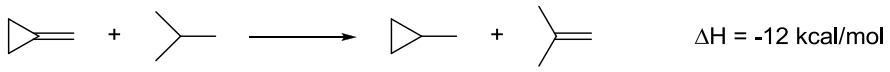

Scheme 2.1. Isodesmic reaction of methylenecyclopropane with isopropane.

The hypothesis was that coordination of the cyclopropylidene by Pt(II) would relieve some of the ring strain present in this moiety, making coordination energetically favorable despite the steric

---

[58] Felix, R. J.; Weber, D.; Gutierrez, O.; Tantillo, D. J.; Gagné, M. R. *Nature Chem.* **2012**, *4*, 405.
[59] a) Johnson, W. T. G.; Borden, W. T. *J. Am. Chem. Soc.* **1997**, *119*, 5930. b) Bach, R. D.; Dmitrenko, O. *J. Am. Chem. Soc.* **2004**, *126*, 4444.
[60] a) Lu, B.-L.; Dai, L.; Shi, M. *Chem. Soc. Rev.* **2012**, *41*, 3318. b) Seiser, T.; Cramer, N. *Org. Biomol. Chem.* **2009**, *7*, 2835. c) Leemans, E.; D'hooghe, M.; De Kimpe, N. *Chem. Rev.* **2011**, *111*, 3268. d) Seiser, T.; Saget, T.; Tran, D. N.; Cramer, N. *Angew. Chem. Int. Ed.* **2011**, *50*, 7740. e) Mauleón, P.; Krinsky, J. L.; Toste, F. D. *J. Am. Chem. Soc.* **2009**, *131*, 4513.

interactions of the trisubstituted olefin (Figure 2.1). In the case of substrate **67,** coordination would lead to structure **68** and the equivalent "slipped" structures **68a** and **68b** (see also Figure 1.4). It was envisioned that electron donation from the π-bond of the methylenecyclopropane to the Pt(II) center would weaken the double bond, releasing some of the ring strain and making the coordination more energetically favorable. From structure **68,** cyclization could occur to give Pt-alkyl **69**. Compound **69** could potentially be isolable if a tridentate phosphine ligand such as (PPP) were employed; if a bidentate ligand were complexed with the Pt(II) center two elimination mechanisms could be envisioned. One is β-alkyl elimination to give primary Pt-alkyl **70**, which would provide different product regioisomers than have previously been observed in the Gagné systems. More interesting to the proposed goal, however, was β-hydride elimination to provide the alkene **71**, which could theoretically undergo reductive opening of the cyclopropane to the geminal disubstituted compound **72**.

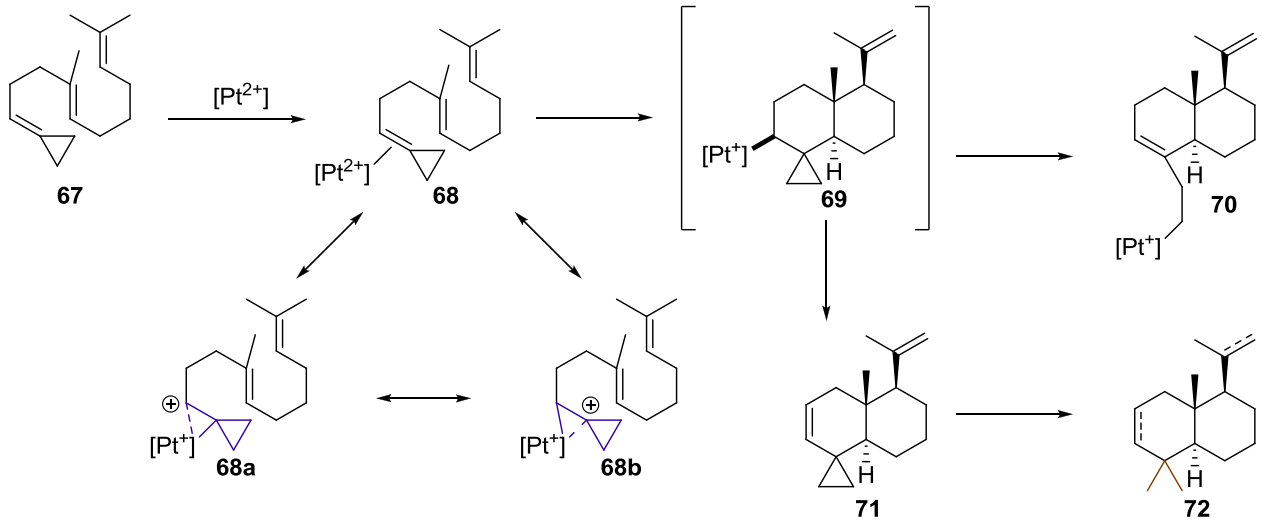

Figure 2.1. Proposed coordination and cyclization modes of methylenecyclopropanes with Pt(II).

Attempted Biomimetic Synthesis with Pt(II)

Research was then initiated to synthesize polyene substrates with terminal cyclopropylidene moieties. Starting from δ-valerolactone (**73**) substrate **67** could be synthesized in 7 steps (Scheme 2.2).[48] The synthesis begins with reduction of **73** using DIBAL-H to provide compound **74** in good

yield. A Wittig reaction using isopropyltriphenylphosphonium iodide provides compound **75** which can then be transformed to aldehyde **76** via the Swern oxidation in excellent yield. Grignard addition to **76** provides allylic alcohol **77** in moderate yield, which can then be converted into **78** via a Hg(II)-catalyzed vinyl ether synthesis and a subsequent Claisen rearrangement. Finally, a Wittig reaction employing cyclopropyltriphenylphosphonium bromide and TDA-1 as a phase transfer catalyst provides the methylenecyclopropane substrate (**67**) in moderate yield.[61]

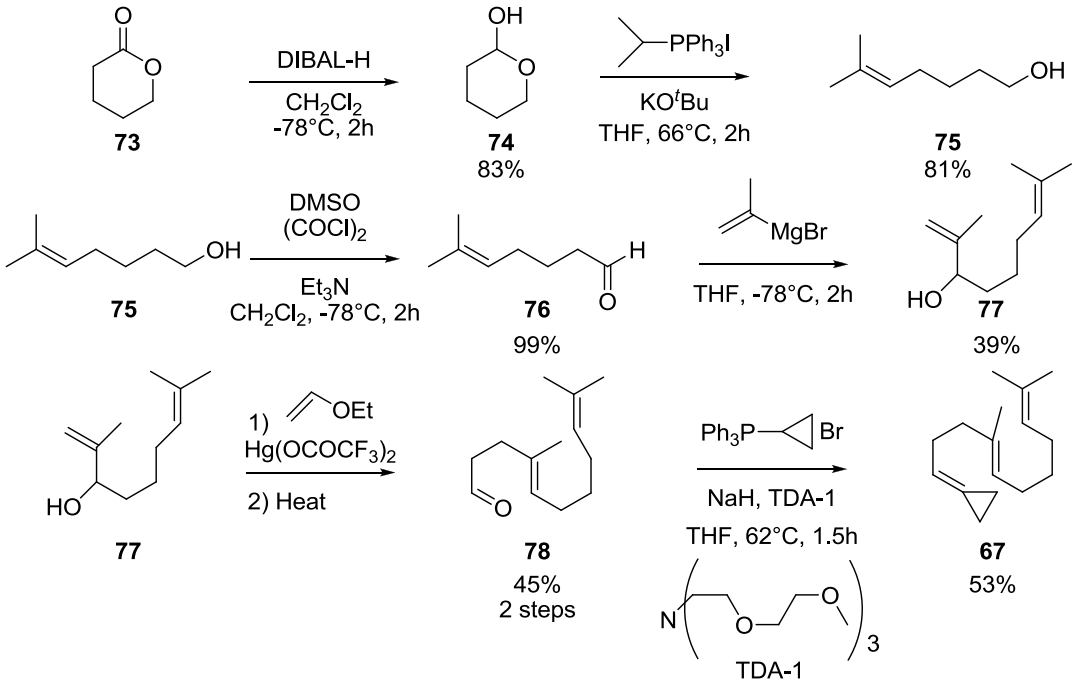

Scheme 2.2. Synthesis of substrate 67.

With MCP substrate **67** in hand, various reaction conditions were explored in an attempt to cyclize the polyene (Table 2.1). Activation of (PPP)PtI_2 using $AgBF_4$ in nitromethane in the presence of NCC_6F_5 provides a stable Pt(II) species, $[(PPP)Pt(NCC_6F_5)][BF_4]_2$. After the *in situ* activation the substrate was added, along with a base. Using a slight excess of the nitrile, a four-fold excess of **67,** and a piperidinomethyl resin base, no cyclization was detected (Table 2.1, entry 1); in monitoring the reaction by ^{31}P NMR spectroscopy only the complex $[(PPP)Pt\text{-}NCC_6F_5][BF_4]_2$ was observed. The absence of Pt-alkene complexes indicated coordination of the polyene was still energetically

[61] Stafford, J. A.; McMurry, J. E. *Tetrahedron Lett.* **1988**, *29*, 2531.

unfavorable. Over time or upon heating the reaction to 40˚C, formation of $[(PPP)Pt\text{-}CD_2NO_2][BF_4]_2$ was observed, resulting from deprotonation of the solvent (entry 2). A weaker base, Ph_2NH, was employed to avoid formation of the Pt(II)-enolate, but there was still no coordination or cyclization of the substrate observed (entry 3). Reasoning that the nitrile ligand was preventing coordination, a reaction was performed utilizing no added NCC_6F_5 and no base, in an attempt to observe formation of the Pt-alkene (entry 4). Unfortunately, while a number of unknown Pt(II) species were formed, none had the characteristic shift in the ^{31}P NMR spectrum for a coordinated alkene (e.g. $[(PPP)Pt(1\text{-hexene})][BF_4]_2$ shows a signal for the phosphorus *trans* to the alkene at 106-108 ppm and has a coupling constant, $J_{Pt\text{-}P}$, of ca. 2900 Hz, slightly dependent upon solvent). Analysis of the reaction mixture by gas chromatography-mass spectroscopy (GC-MS) showed a number of starting material isomers, presumably formed by interaction of a Pt(II) species with the cyclopropylidene moiety leading to unproductive alkene isomerization. To probe whether the silver salt was having an adverse effect on coordination of the olefin to the Pt(II) species the pre-activated, isolated complex $[(PPP)Pt\text{-}NCC_6F_5][BF_4]_2$ was reacted with **67** in nitromethane. Only the Pt(II)-nitrile complex was observed under these conditions.

Table 2.1. Attempted cyclization of substrate 67 with (PPP)PtI_2.

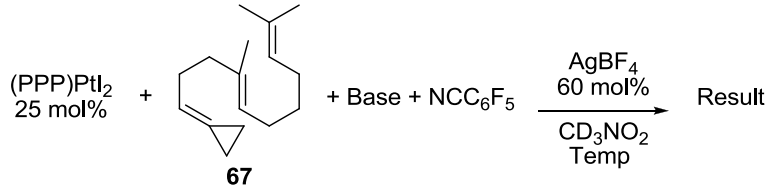

Entry	NCC_6F_5 (eq)	Base (eq)	Temp	Result
1	1.1	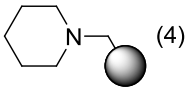 (4)	rt	Pt-NCC_6F_5
2	1.1	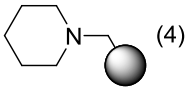 (4)	40°C	Pt-CD_2NO_2
3	1.1	Ph_2NH	rt	Pt-NCC_6F_5
4	-	-	rt	Starting Material Isomerization

As no coordination or cyclization of **67** could be detected with the tridentate (PPP) ligand bound to the Pt(II) center, it was hypothesized that perhaps a bidentate phosphine ligand, filling only two of the four coordination sites available to d^8 Pt(II) species, would result in less unfavorable steric interactions, allowing coordination and cyclization of the substrate. Proper choice of the bidentate ligand could also increase the electrophilicity of the Pt(II) center due to there being a smaller number of electron donating groups bound to the metal. Synthesis of bi- and tridentate phosphine Pt(II) complexes start with transformation of potassium tetrachloroplatinate(II) (K_2PtCl_4, **79**). Heating **79** with an excess of 1,5-cyclooctadiene in a solution of 2:3 H_2O:HOAc gives 1,5-cyclooctadiene platinum(II) chloride ((COD)$PtCl_2$, **80**, see Scheme 2.3). This complex is then converted to the Pt(II)-iodide by reaction at room temperature with NaI to give **81**. At this point addition of the desired phosphine ligand in DCM results in displacement of the COD ligand to give the phosphine bound Pt(II) halide.

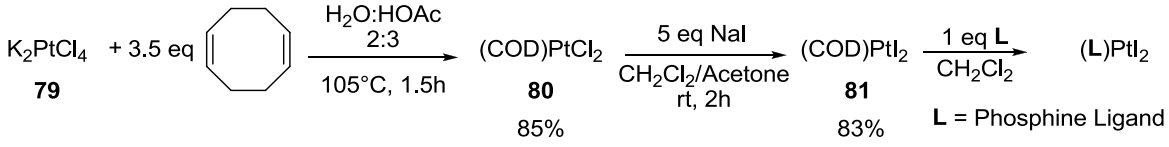

Scheme 2.3. Synthesis of Pt(II) complexes for use in polyene cascade cyclizations.

In hopes of cyclizing compound **67**, another series of experiments were attempted using 2,2′-Bis(diphenylphosphino)-1,1′-binaphthalene (BINAP) as the bidentate phosphine ligand (Table 2.2). Employing a racemic mixture of the (*S*)- and (*R*)-(BINAP)PtI_2 complexes in 20 mol% with NCC_6F_5 present at either room temperature or 40˚C led only to observation of the Pt-nitrile complex, [(*rac*)-(BINAP)$Pt(NCC_6F_5)_2][BF_4]_2$ (entries 1 and 2). When the nitrile was excluded unknown Pt(II) species were detected by ^{31}P NMR and no cyclization products were found by GC-MS. Both the resin base and diphenylamine gave similar mixtures of starting material isomerization (entries 3 and 4).

Table 2.2. Attempted cyclization of substrate 67 with (*rac*)-(BINAP)PtI_2.

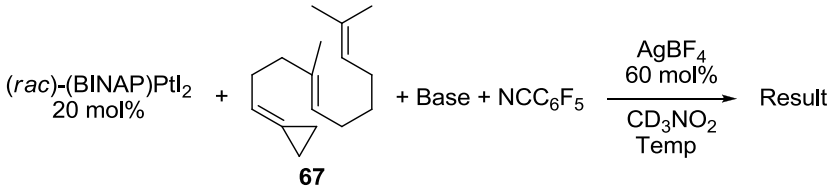

Entry	NCC_6F_5 (eq)	Base (eq)	Temp	Result
1	2.2	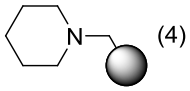 (4)	rt	Pt-NCC_6F_5
2	2.2	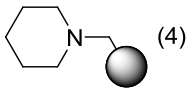 (4)	40°C	Pt-NCC_6F_5
3	-	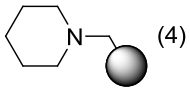 (4)	rt	Starting Material Isomerization
4	-	Ph_2NH	rt	Starting Material Isomerization

At the same time these experiments were being conducted Dieter Weber suggested that substrate **67** be reacted with a Au(I) catalyst as the linear coordination is less sensitive to steric clashes than Pt(II) complexes. In light of the promising results of an initial experiment utilizing Au(I), and the lack of positive results with Pt(II) mediated reactivity, the focus of the project was shifted to identifying the product of the reaction and further developing this new Au(I)-catalyzed system.

Au(I)-Catalyzed Cope Rearrangement

D. Weber conducted the initial reaction of compound **67** with a Au(I) catalyst. For this reaction the Gagosz catalyst,[62] $Ph_3PAuNTf_2$ (Tf = trifluoromethanesulfonyl), was employed in 10 mol% (Scheme 2.4). The starting material converted cleanly over 2 hours into a single product at room temperature in DCM. The species formed was eventually identified as the product of a Cope rearrangement (**82**).

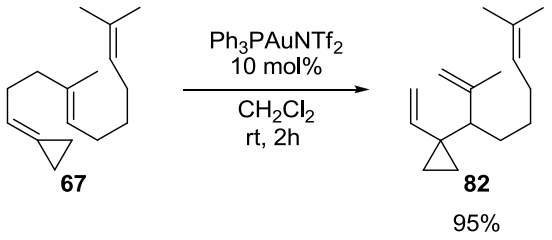

Scheme 2.4. Initial reaction of a methylenecyclopropane substrate with a Au(I) catalyst.

With the discovery of a Au(I)-catalyzed Cope rearrangement a number of transition metals known to catalyze Cope rearrangements were tested (see Scheme 2.5).[63] In no other case was a Cope rearrangement observed. For example no reaction was seen when using $PdCl_2(CH_3CN)_2$ in MeCN or $PdCl_2(PhCN)_2$ in MeCN or THF. $PtCl_2$ was unreactive at room temperature, and heating in toluene led to a large number of unidentified products. These reactions demonstrate the unique ability of Au(I) to catalyze this Cope rearrangement.

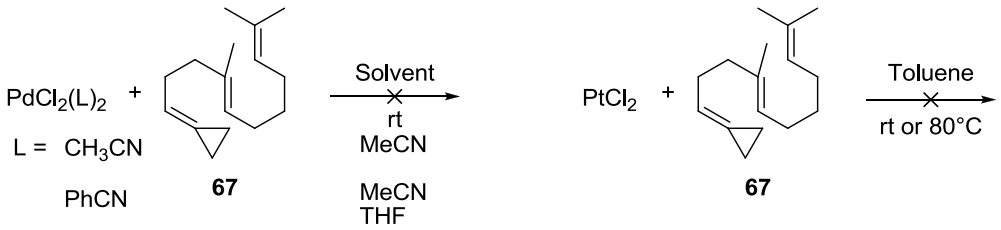

Scheme 2.5. Reaction of substrate 67 with other transition metals known to catalyze the Cope rearrangement.

[62] Mézailles, N.; Ricard, L.; Gagosz, F. *Org. Lett.* **2005**, *7*, 4133.
[63] a) Overman, L. E.; Renaldo, A. F. *J. Am. Chem. Soc.* **1990**, *112*, 3945. b) Nakamura, H.; Iwama, H.; Ito, M.; Yamamoto, Y. *J. Am. Chem. Soc.* **1999**, *121*, 10850. c) Fanning, K. N.; Jamieson, A. G.; Sutherland, A. *Curr. Org. Chem.* **2006**, *10*, 1007. d) Fürstner, A.; Aissa, C. *J. Am. Chem. Soc.* **2006**, *128*, 6306.

The Cope rearrangement is a [3,3]-sigmatropic rearrangement of 1,5-dienes, originally reported by Cope and Hardy over 70 years ago (see Scheme 1.7, Figure 2.2).[64] In this rearrangement an equilibrium is established between two 1,5-dienes (Figure 2.2a). For unsubstituted alkenes reaction barriers are high, requiring elevated temperatures for equilibrium to be reached. Under these conditions the more thermodynamically stable product is the major species, and this principle can be used to drive Cope rearrangements in a single direction (i.e. to more substituted dienes, see Figure 2.2b). Substituents at C2, C3, C4, and C5 can lower the reaction barrier significantly through stabilization of the transition state (usually chair-like), but the major product of the reaction is still the thermodynamically favored one (Figure 2.2c) and elevated temperatures are usually still required. Nevertheless the Cope rearrangement has found applications in complex synthetic settings.[65] However, as these reactions typically convert less-substituted alkenes into more-substituted alkenes large classes (directions) of the Cope rearrangement are not feasible.[66]

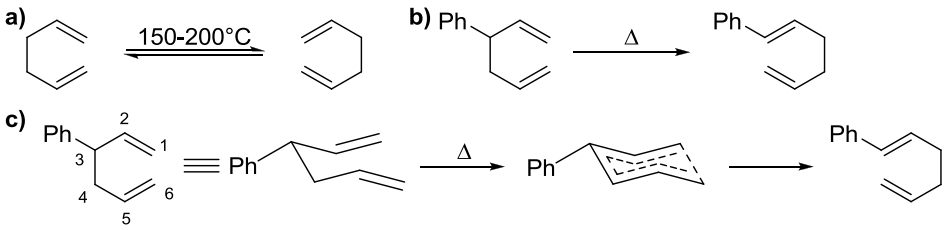

Figure 2.2. Classical Cope rearrangement conditions and representation of the typically chair-like transition state of Cope rearrangements.

The Cope rearrangement shown in Scheme 2.4 is therefore notable for a number of reasons. One is that the reaction takes place efficiently at room temperature, well below the temperatures required under thermal conditions for similar, unsubstituted 1,5-dienes. A second feature is that the π-bonds in the product (**82**) are less substituted than those in the starting diene. While this at first seems counter-intuitive, it is the relief of the ring strain present in the cyclopropylidene moiety that serves as the thermodynamic driving force for this rearrangement.[59] These aspects were explored both experimentally and computationally and will be discussed in more detail below (see

[64] Cope, A. C.; Hardy, E. M. *J. Am. Chem. Soc.* **1940**, *62*, 441.
[65] Nowicki, J. *Molecules* **2000**, *5*, 1033.
[66] Hoffman, R.; Stohrer, W.-D. *J. Am. Chem. Soc.* **1971**, *93*, 6941.

Thermodynamic and Mechanistic Considerations). Collaboration with the Tantillo group from the University of California at Davis provided supporting computational data and insight into the mechanistic pathways of the reaction. A last significant characteristic of this reaction is that a chiral compound is created from an achiral starting material. The presence of a chiral center in the product resulted in the exploration of whether this system could be made enantioselective, leading to the first report of an enantioselective Cope rearrangement from achiral starting materials.

Enantioselective Au(I)-Catalyzed Cope

While exploring the initial reaction conditions a second methylenecyclopropane substrate was synthesized (**83**). Due to the significantly shorter synthesis (see Scheme 2.6)[67] and the larger scale on which this substrate could be prepared, **83** was used as the substrate for the optimization of reaction parameters in pursuit of an enantioselective Cope rearrangement. Starting with geranyl acetate (**84**) reaction with the electrophilic epoxidizing agent *meta*-chloroperoxybenzoic acid (mCPBA) provided compound **85** in good yield. A lithium cuprate catalyzed coupling reaction with phenylmagnesium bromide then provided phenyl substituted **86** in moderate yield. Sodium periodate oxidation of **86** provided aldehyde **87**, which upon Wittig reaction provided substrate **83** in 34% yield.

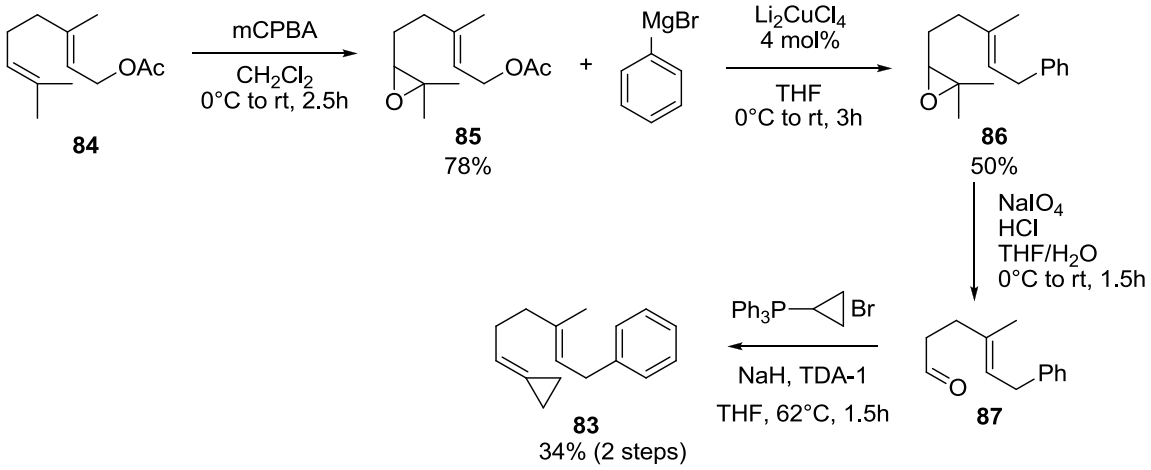

Scheme 2.6. Synthesis of substrate 83.

[67] Zhao, J.-F.; Loh, T.-P. *Angew. Chem. Int. Ed.* **2009**, *48*, 7232.

The first Au(I) catalysts investigated were bis-gold complexes bound by chiral phosphines (see structure **62**, Figure 1.14). Phosphine (bisphosphine and phosphoramidite, see structure **63**) ligands can be added to Au(I) by reacting the ligand with a stoichiometric (to P) amount of Me_2S-AuCl in DCM (see Figure 2.3). After removal of the solvent, drying the complex *in vacuo* provides the Au(I) catalyst precursor in high yield.

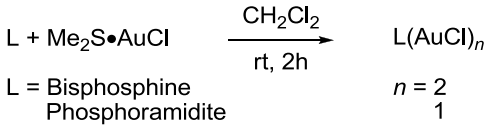

Figure 2.3. Synthesis of phosphine coordinated Au(I) complexes.

Using substrate **83** solvent effects were explored first, utilizing (*R*)-BINAP$(AuCl)_2$ and (*R*)-xyl-BINAP$(AuCl)_2$ (see Table 2.3). Activating the Au(I) chloride with a slight excess of $AgBF_4$ allowed clean rearrangement of **83** to **88** at room temperature over 3h. (*R*)-xyl-BINAP$(AuCl)_2$ was found to give slightly higher enantioselectivity (compare entries 2 and 3), but only slight improvements to the *e.e.* could be gained with different solvent systems (entries 3-6). As 1,2-dichloroethane (1,2-DCE) was found to be slightly more effective than the other solvents investigated it was employed as the solvent to explore most other reaction parameters.

Table 2.3. Solvent effects on the Au(I) catalyzed Cope rearrangement.

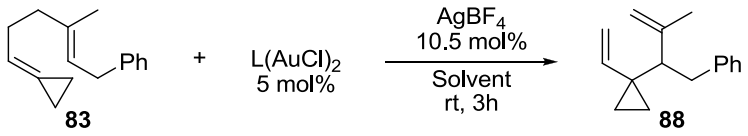

Entry	Ligand	Solvent	*e.e.* (%)
1	(R)-BINAP	DCM	15
2	(R)-BINAP	$MeNO_2$	19
3	(R)-xylyl-BINAP	$MeNO_2$	20
4	(R)-xylyl-BINAP	1,2-DCE	24
5	(R)-xylyl-BINAP	Toluene	15
6	(R)-xylyl-BINAP	Et_2O	0

The effect of temperature was explored using (*R*)-xyl-BINAP(AuCl)$_2$ in nitromethane (Table 2.4). Similar to changing the solvent, temperature had only a minor effect on the enantioselectivity of the reaction, with up 25% *e.e.* obtained at -20˚C. At the lower temperatures employed the reaction time was elongated, requiring 18h for complete conversion of the starting material.

Table 2.4. Temperature effects on the Au(I) catalyzed Cope rearrangement.

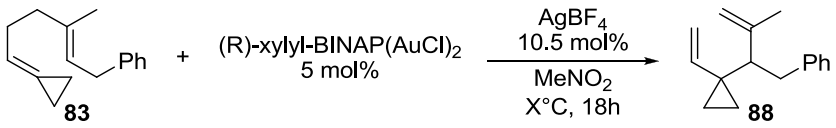

83 **88**

Temperature (°C)	*e.e.* (%)
R.T.	20
0	22
-5	24
-20	25

The next parameter explored was the effect of the counter-ion on the enantioselectivity (Table 2.5). A mild improvement was observed in changing the silver salt from $AgBF_4$ to AgOTf, however the reaction only proceeded to 50% conversion, as seen by GC-MS (compare entries 1 & 2). A more modest improvement was seen using $AgPF_6$, but in this case the reaction gave full conversion (entry 3). The two silver salts, $AgSbF_6$ and $AgNTF_2$, gave slightly lower enantioselectivities than $AgPF_6$, resulting in $AgPF_6$ being employed as the silver activating agent to explore the effects of chiral ligands on the reaction enantioselectivity.

Table 2.5. Counter-ion effects on the Au(I) catalyzed Cope rearrangement.

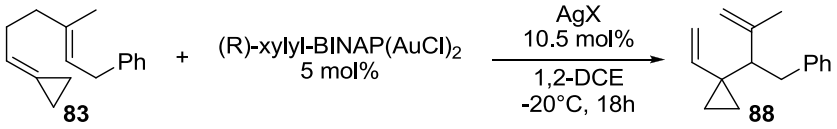

Entry	X^-	*e.e.* (%)
1	BF_4	25
2	OTf	37[a]
3	PF_6	34
4	SbF_6	32
5	NTf_2	32

[a] Reaction only proceeded to 50% conversion (GC-MS).

A number of bis-gold catalysts were explored at either 0˚C or -20˚C (Table 2.6). With (*R*)-xylyl-BINAP$(AuCl)_2$ providing the product in 34% *e.e.* as a starting point (entry 2), various other chiral aromatic bisphosphine ligands were investigated. Unfortunately, most of these catalysts performed poorly, giving lower enantioselectivity than (*R*)-xylyl-BINAP (entries 3, 4, 5. 7, 9). The more bulky (*R*)-DTBM-SEGPHOS gave higher enantioselectivity than (*R*)-SEGPHOS, but still lower than the xylyl-BINAP complex (compare entries 2, 4, and 7). Chiral alkyl backbone moieties in the ligands proved less effective than the aromatic ligands (entries 6, 8). However, upon utilization of (*S*)-3,5,-xylyl-PHANEPHOS (**59**) as the chiral ligand, a significant increase in the enantioselectivity of the reaction was observed, providing compound **88** in 79% *e.e*. A chiral phosphoramidite ligand was also tested but proved to be ineffective for this system (entry 11). A chiral counterion (**64**, R = H) Au-PPh_3 complex, synthesized by D. Weber, was also screened, but notably this system did not demonstrate any aptitude for the Cope rearrangement, with starting material being observed after 24h at room temperature (entry 12).

Table 2.6. Ligand effects on the Au(I) catalyzed Cope rearrangement.

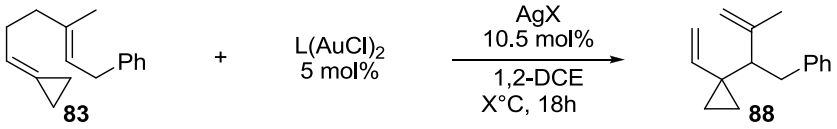

Entry	Ligand	T (°C)	*e.e.* (%)
1	(*R*)-xylyl-BINAP	0	28
2	(*R*)-xylyl-BINAP	-20	34
3	(*R*)-xylyl-MeO-BIPHEP	-20	19
4	(*R*)-SEGPHOS	-20	16
5	(*R*)-DIFLUORPHOS	-20	9
6	(*R*)-xyl-SDP	-20	5
7	(*R*)-DTBM-SEGPHOS	-20	25
8	(*R*,*R*)-Me-DuPHOS	0	2
9	(*R*)-SYNPHOS	0	15
10	(*S*)-3,5-xylyl-PHANEPHOS (**59**)	-20	79
11	(*S*)-SIPHOS-PE	0	7
12	(*R*)-(**64**)-Au(PPh_3)	rt	-

With a competent catalyst (**59**-$(AuCl)_2$) for the asymmetric Cope rearrangement of **83**, a second round of catalyst optimization was undertaken (Table 2.7). The first parameter explored was the equivalents of the silver salt necessary to provide the product in high enantioselectivity. With less than two equivalents of $AgPF_6$ the reaction did not give complete conversion of starting material and provided significantly lower enantioselectivity (compare entries 1 and 2). Employing four equivalents of the Ag(I) salt, however, slightly improved the enantiomeric excess to 82% (compare entries 2 and 3). Next, the solvent was investigated (entries 3-5). The solvents 1,2-DCE and nitromethane ($MeNO_2$) were found to give similar enantioselectivities, with both solvents being modestly more effective than DCM. Further reducing the temperature of the reaction in DCM did not improve the enantioselectivity and also prevented the reaction from proceeding to completion (entry 6). Different Ag(I) salts were then screened and $AgSbF_6$ was found to provide **88** in the highest enantioselectivity (compare entries 3, 7-10). The optimized conditions were found to consist of a 1:9 solution of DCM and 1,2-DCE (by volume), which allowed the temperature to be lowered to -35˚C,

and four equivalents of $AgSbF_6$, providing the product compound in 87% *e.e.* (entry 11). This marks the first reported example of an asymmetric Cope rearrangement of achiral 1,5-dienes.

Table 2.7. Optimization of Au(I) catalyzed Cope rearrangement with (*S*)-xylyl-PHANEPHOS(AuCl)$_2$.

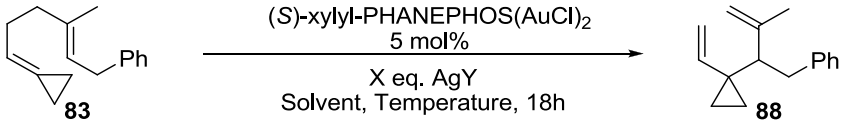

Entry	X	Y^-	T (°C)	Solvent	*e.e.* (%)
1[a]	1	PF_6	-20	1,2-DCE	58
2	2.1	PF_6	-20	1,2-DCE	79
3	4	PF_6	-20	1,2-DCE	82
4	4	PF_6	-20	DCM	77
5	4	PF_6	-20	$MeNO_2$	81
6[a]	4	PF_6	-50	DCM	66
7	4	BF_4	-20	1,2-DCE	81
8	4	OTf	-20	1,2-DCE	74
9	4	SbF_6	-20	1,2-DCE	83
10	4	NTf_2	-20	1.2-DCE	82
11	4	SbF_6	-35	DCM:1,2-DCE (1:9)	87

[a] Reaction did not go to completion.

Asymmetric Cope Rearrangement

Numerous variants of the Cope rearrangement have yielded to asymmetric methodology (e.g. the aza-Cope, Claisen) but in the over 70 years the Cope reaction has been known no asymmetric Cope rearrangement, starting from achiral 1,5-dienes, had been developed.[68] A notable Cope variant is the enantioselective hetero-Cope rearrangement of allylic trichloroacetimidiates reported by Overman (Figure 2.4).[69] In this system achiral compounds (**89**) can be transformed by chiral Pd(II) catalysts into chiral enones (**90**) with high enantioselectivities.

[68] a) Nubbemeyer, U. *Synthesis* **2003**, 961. b) Allin, S. M.; Baird, R. D. *Curr. Org. Chem.* **2001**, *5*, 395.
[69] a) Anderson, C. E.; Overman, L. E. *J. Am. Chem. Soc.* **2003**, *125*, 12412. b) Watson, M. P.; Overman, L. E.; Bergman, R. G. *J. Am. Chem. Soc.* **2007**, *129*, 5031.

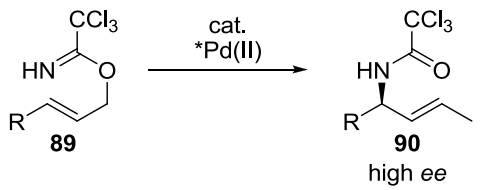

Figure 2.4. Pd(II) catalyzed hetero-Cope rearrangement of allylic trichloroacetimidiates.

It was known that chirality transfer was possible from a chiral starting material due to the chair-like transition state of the Cope rearrangement (see Figure 2.2c). The system most resembling an enantioselective Cope rearrangement that had been reported prior to this Au(I)-catalyzed reaction was the combined C-H functionalization/Cope rearrangement reported by Davies (Figure 2.5).[70] In this reaction a Rh(II) catalyst initiates a domino reaction in which an allylic C-H insertion is diverted mid-insertion by a competing Cope rearrangement. During this intermolecular reaction a transiently formed chiral intermediate leads to arrangement of the reactants to minimize steric repulsions in the chair-like transition state, yielding the product compounds in high diastereo- and enantioselectivities.

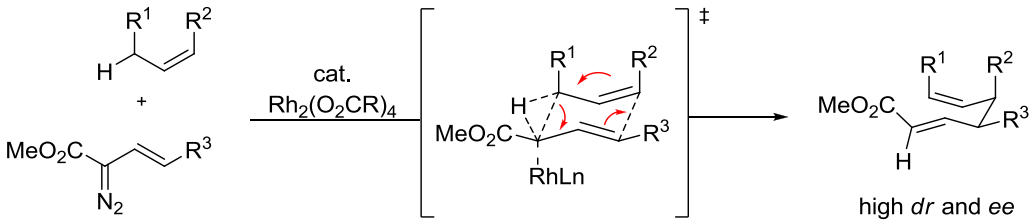

Figure 2.5. Rh(II) catalyzed intermolecular process resembling the Cope rearrangement.

However, unlike these noteworthy systems, this Au(I)-catalyzed system is the first example of a Cope rearrangement in which the enantioselectivity is not provided by either a pre-existing stereocenter or through a multistep sequence. This reaction also demonstrated a wide range of functional group tolerance and provided most product compounds in high yields and enantioselectivities.

[70] a) Hansen, J. H.; Gregg, T. M.; Ovalles, S. R.; Lian, Y.; Autschbach, J.; Davies, H. M. L. *J. Am. Chem. Soc.* **2011**, *133*, 5076. b) Lian, Y.; Davies, H. M. L. *J. Am. Chem. Soc.* **2011**, *133*, 11940.

Substrate Scope and Limitations

A variety of substrates could be obtained from aldehydes, whose preparations had previously been reported in the literature,[44,71] by Wittig reaction using cyclopropyltriphenylphosphonium bromide, NaH, and TDA-1 (see Scheme 2.6). These Wittig reactions gave low to moderate yields of the desired compounds in all cases except for dienylphenol substrate **91**. In this case the starting material aldehyde would decompose under the reaction conditions and alternative conditions[72] had to be employed for synthesis of the cyclopropylidene (Scheme 2.7). Utilizing an excess of KO^{t}Bu to both activate the Wittig salt and deprotonate the phenol moiety, **91** could be obtained in 17% yield after 60h at 45˚C.

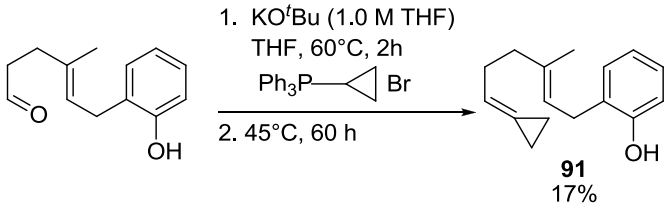

Scheme 2.7. Synthesis of dienylphenol substrate 91.

Substrates with a range of alkyl, aromatic, oxygen, and nitrogen functionality were synthesized and rearranged using **59**-$(AuCl)_2$ (Table 2.8). It should be noted that in all cases complete conversion to a single product was observed by GC-MS except for substrates **103** and **105**. Alkyl, aromatic, and ether functionalized compounds were found to be good reactants and gave high product yields and excellent enantioselectivities (entries 1, 2, 4, 5, 6). The highest enantioselectivity came from rearrangement of triene **67**, which provided **82** in 93% *ee* (entry 1). The efficiency of the reaction was unimpeded by increasing the steric bulk on the internal double bond (entries 4 and 6). Ether **95** gave the highest yielding reaction with an isolated 98% yield of **96**, albeit without a chiral center in this molecule (entry 5). Dienylphenol substrate **91** demonstrated slightly lower efficiency, with the product being isolated in only 71% yield and 70% *e.e.* (entry 3)

[71] a) Surendra, K.; Qiu, W.; Corey, E. J. *J. Am. Chem. Soc.* **2011**, *133*, 9724. b) Dérien, S.; Jan, D.; Dixneuf, P. H. *Tetrahedron* **1996**, *52*, 5511.
[72] Maercker, A.; Daub, V. E. E. *Tetrahedron* **1994**, *50*, 2439.

Table 2.8. Substrate scope of Au(I) catalyzed Cope rearrangement.

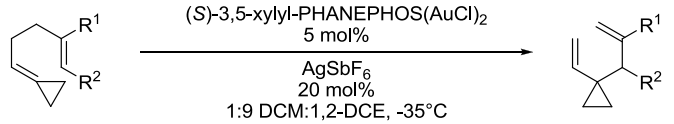

Entry	Substrate	Product	Yield (%)[b]	ee (%)[c]	Entry	Substrate	Product	Yield (%)[b]	ee (%)[c]
1	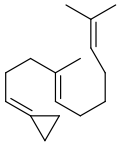 **67**	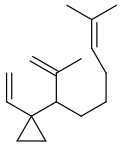 **82**	94	93	*7*	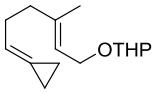 **99**	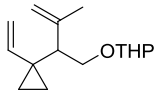 **100**	60	73[d]
2	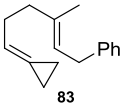 **83**	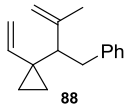 **88**	89	87	*8*	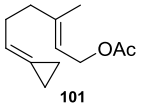 **101**	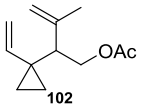 **102**	70	82[e]
3	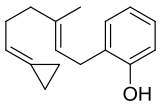 **91**	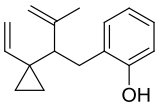 **92**	71	70	*9*	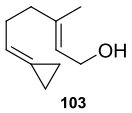 **103**	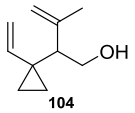 **104**	35	76[f]
4	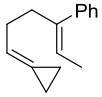 **93**	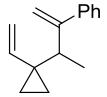 **94**	90	82	*10*	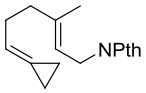 **105**	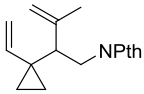 **106a**	45	58[g]
5	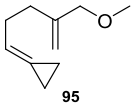 **95**	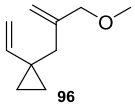 **96**	98	-			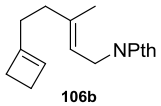 **106b**	23	-
6	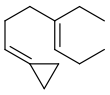 **97**	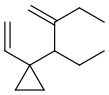 **98**	87	84	*11*	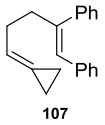 **107**	-	-	-

[a]Reaction conditions: **59**-$(AuCl)_2$ (5 mol%), AgSbF6 (20 mol%), 1:9 DCM:1,2-DCE, -35˚C, 18h. [b]Isolated yield. [c]*e.e.* determined by chiral GC. [d]72 hours at -35˚C, 1:1 diastereomeric ratio. [e]72 hours at -35˚C. [f]*e.e.* determined by conversion to the acetate **102**. [g]*e.e.* determined by chiral supercritical fluid chromatography.

THP- (**99**) and acetyl-protected (**101**) alcohols were also found to rearrange in good yields and enantioselectivities (entries 7 and 8). For these substrates reaction times had to be extended to 72 hours at -35˚C to give complete conversion of the starting material. Unprotected alcohol **103** gave a diminished yield due to deleterious, unidentified side reactions (entry 9). While there were a number of side products observed by GC-MS in the reaction of **103**, only the Cope rearrangement products (**100**, **102**) were observed using the protected alcohols (**99**, **101**, respectively). The naphthalimide protected amine substrate **105** afforded the Cope rearranged product **106a** in only 45% yield and 58%

e.e., but also gave a 23% yield of cyclobutene product **106b** (entry 10). Interestingly, this was the only substrate in which ring expansion to a cyclobutene ring structure was observed. Ring expansion of methylenecyclopropanes to cyclobutenes has previously been documented utilizing $PtCl_2$/CO conditions.[63d] The proposed mechanisms of both the Cope rearrangement and the cyclopropylidene to cyclobutene ring expansion will be discussed in detail in the next section.

A limitation of the system was discovered when attempting to rearrange substrate **107**, a unique substrate in that it bears two aromatic rings brought into conjugation by the C5-C6 π-bond. No reactivity was observed and starting material could be isolated cleanly from the reaction mixture. The driving force for the Au(I) catalyzed Cope rearrangement is the relief of the ring strain present in the cyclopropylidene moiety. It seems that breaking the extended conjugated system formed by the two aromatic rings in compound **107** is too energetically unfavorable for the Cope rearrangement product to persist.

Thermodynamic and Mechanistic Considerations

To explore the energetics of this system, calculations were performed using Mac Spartan '10.[73] Calculations were carried out by first building the molecule using the program's molecular modeling interface, then performing an energy minimization routine to roughly estimate the lowest energy bond angles in the molecule. A semi-empirical conformer distribution calculation would then be performed using the AM1 basis set. The results of this calculation would be examined and conformers greater than ca. 2 kcal/mol higher in energy than the lowest energy conformer would be discarded to improve computational times for subsequent calculations. With the remaining conformers another conformer distribution calculated would be executed, this time at the Hartree-Fock level of theory with the 3-21G basis set. Again the conformers would be examined and those greater than ca. 2 kcal/mol higher in energy than the lowest energy conformer would be discarded. Finally a calculation would be performed using density functional theory and the B3LYP/6-31G(d)

[73] *Mac Spartan '10*, Wavefunction, Inc.: Irvine, CA, 2011.

basis set. These calculations were used to find the ground state energies of a number of compounds and predict whether the Cope rearrangement would be energetically favorable (Scheme 2.8).

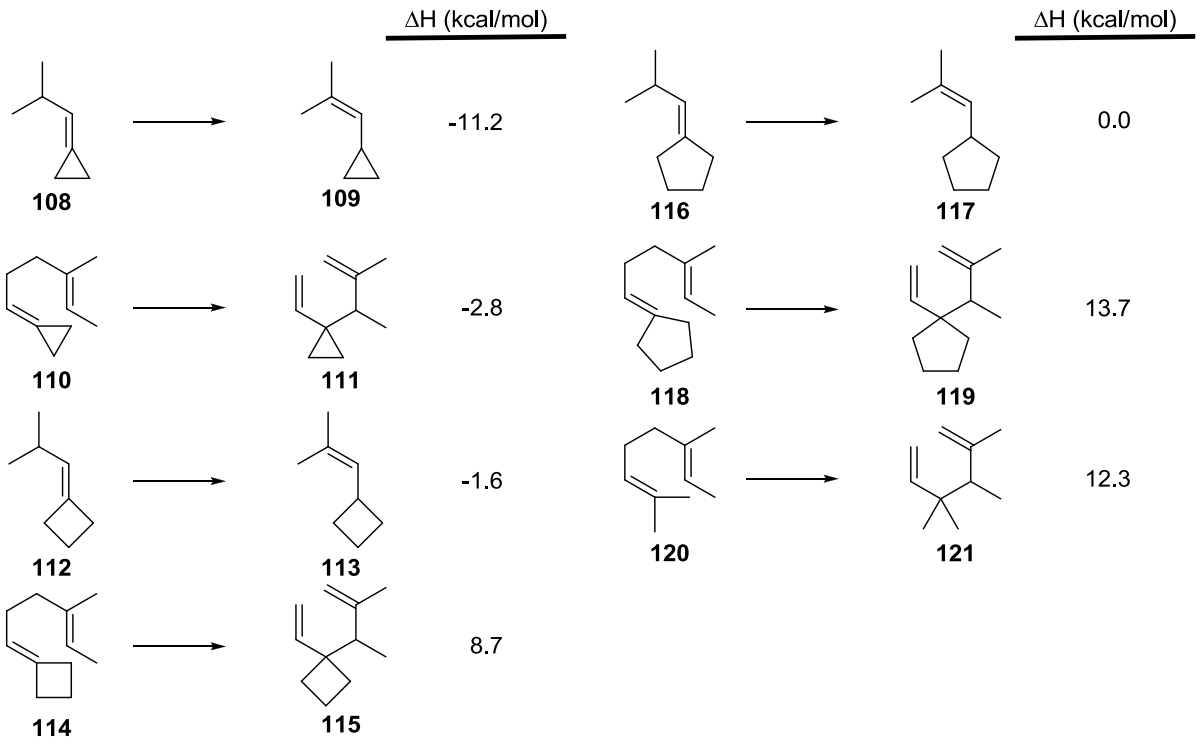

Scheme 2.8. Calculated energy differences between cycloalkylidenes and their expected Cope rearrangement products (using the DFT B3LYP/6-31G(d) method).

The first calculation was performed to find the energy difference between compounds **108** and **109**, which could serve as both an estimate for the ring strain in the cyclopropylidene moiety and as a reference point for other calculations reported in the literature (see Scheme 2.1).[59] The calculated energy difference was ca. -11.2 kcal/mol, close to, but slightly lower than, the ca. -12 kcal/mol which had been previously reported. Next the energy difference was calculated for **110** and **111**, a model system for the rearrangement of substrate **67** to **82** (see Scheme 2.4). The rearrangement for this model system was found to be exergonic by -2.8 kcal/mol, reflecting the relief of ring strain in the product overcoming the thermodynamic penalty of forming less substituted double bonds.

Calculations were then performed on cyclobutylidene (**112**-**115**) and cyclopentylidene (**116**-**119**) analogs. These investigations revealed that the ring strain caused by the exocyclic double bond in the cyclobutylidene moiety is ca. 1.6 kcal/mol (**112** to **113**), which is not enough energy to

overcome the conversion of more substituted double bonds to less substituted olefins (**114** to **115**). Going from a 4-membered to a 5-memebered ring essentially removed ring strain caused by the exocyclic double bond (**116** to **117**). Consequently, the Cope rearrangement of compound **118** to compound **119** was predicted to be endergonic by ca. 14 kcal/mol. Finally the rearrangement of a trisubstituted, acyclic analog was calculated and found to be endergonic by ca. 12 kcal/mol (**120** to **121**).

These predictions were confirmed experimentally by synthesis of the substrates shown in Figure 2.6. These substrates could be prepared in moderate yields by Wittig reaction of aldehyde **87** with isopropyl (**122**), cyclobutyl (**123**), or cyclopentyltriphenylphosphonium (**124**) halide. No reactivity was seen for compounds **122** or **124** at -35˚C or at room temperature. Cyclobutylidene **123** was reactive towards gold catalysis but gave several products. No indication of the Cope rearranged product was observed by ^{1}H NMR. These outcomes are consistent with the notion that it is the ring strain present in the methylenecyclopropane that drives the reaction.

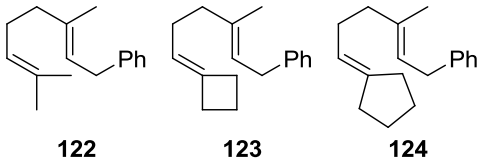

Figure 2.6. Control substrates tested under Au(I)-catalyzed Cope rearrangement conditions.

The following computational work was performed by Osvaldo Gutierrez and Dean Tantillo (UC-Davis) in a collaborative effort aimed at gaining a deeper insight into the mechanism and thermodynamics of this reaction. Calculations were performed using DFT (M06-2X/6-31G(d) in the gas phase for uncatalyzed systems and in 1,2-DCE (CPCM[74] model) using M06/6-31G(d)-(LANL2DZ for Au) for organometallic systems) as implemented in Gaussian09.[75] While the Tantillo

[74] Barone, V.; Cossi, M. *J. Phys. Chem. A* **1998**, *102*, 1995.
[75] Gaussian 09, Revision B.01, M. J. Frisch, G. W. Trucks, H. B. Schlegel, G. E. Scuseria, M. A. Robb, J. R. Cheeseman, G. Scalmani, V. Barone, B. Mennucci, G. A. Petersson, H. Nakatsuji, M. Caricato, X. Li, H. P. Hratchian, A. F. Izmaylov, J. Bloino, G. Zheng, J. L. Sonnenberg, M. Hada, M. Ehara, K. Toyota, R. Fukuda, J. Hasegawa, M. Ishida, T. Nakajima, Y. Honda, O. Kitao, H. Nakai, T. Vreven, J. A. Montgomery, Jr., J. E. Peralta, F. Ogliaro, M. Bearpark, J. J. Heyd, E. Brothers, K. N. Kudin, V. N. Staroverov, T. Keith, R. Kobayashi, J. Normand, K. Raghavachari, A. Rendell, J. C. Burant, S. S. Iyengar, J. Tomasi, M. Cossi, N. Rega,

group performed these calculations it is important to report the findings here for a thorough discussion of the energetics of this system.

Rearrangement barriers in the absence of catalyst were examined (Table 2.9). The predicted barriers for this rearrangement were high, greater than 30 kcal/mol in all cases, but the rearrangements were significantly exothermic, reflecting release of the ring strain from the methylenecyclopropane. The general trend seen was increasing exothermicity of the reaction with decreasing substitution on the acyclic alkene (compare entries 2, 3, 4). Methyl substitution at both R_1 and R_2 was found to be slightly less exothermic than when R_1 was H and R_2 was methyl, possibly due to $A^{1,2}$ strain present in the former case (compare entries 1 and 2). It is noteworthy that the B3LYP calculations performed on Spartan underestimate the exothermicity of these reactions, an aspect the Tantillo group also noted while investigating different basis sets to find the most suitable for the kinetic and thermodynamic parameters of these systems.

Table 2.9. Gas-phase free energies for uncatalyzed Cope rearrangement of substituted methylenecyclopropanes.

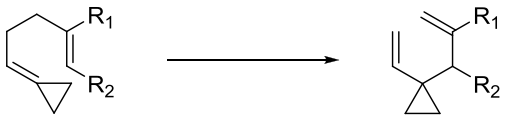

Entry		$\Delta G^{\ddagger}$ ($\Delta H^{\ddagger}$)	ΔG (ΔH)
1	$R_1 = R_2 =$ Me	35.1 (30.1)	-3.6 (-6.2)
2	$R_1 =$ H, $R_2 =$ Me	36.1 (32.4)	-4.4 (-6.0)
3	$R_1 =$ Me, $R_2 =$ H	32.0 (29.5)	-7.0 (-7.5)
4	$R_1, R_2 =$ H	33.4 (30.1)	-7.3 (-8.4)

Two possible mechanistic pathways for the rearrangement were explored computationally using PMe_3 as a model ligand for Au(I) (Figure 2.7). These pathways differ based on which double bond the Au(I) catalyst initiates the rearrangement at, either the dimethyl substituted alkene (pathway a) or the cyclopropylidene (pathway b).

J. M. Millam, M. Klene, J. E. Knox, J. B. Cross, V. Bakken, C. Adamo, J. Jaramillo, R. Gomperts, R. E. Stratmann, O. Yazyev, A. J. Austin, R. Cammi, C. Pomelli, J. W. Ochterski, R. L. Martin, K. Morokuma, V. G. Zakrzewski, G. A. Voth, P. Salvador, J. J. Dannenberg, S. Dapprich, A. D. Daniels, O. Farkas, J. B. Foresman, J. V. Ortiz, J. Cioslowski, and D. J. Fox, Gaussian, Inc., Wallingford CT, 2010.

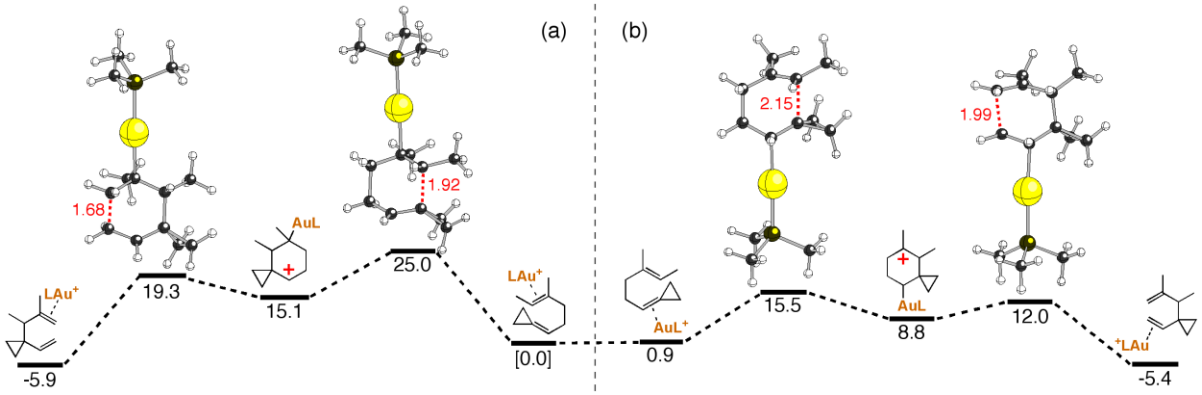

Figure 2.7. Potential mechanistic pathways for the Au(I)-catalyzed Cope rearrangement.

Initiation of the rearrangement at the dimethyl substituted alkene leads to formation of a secondary carbocation intermediate, which then continues the Cope rearrangement to provide the Au(I)-alkene complex. When the rearrangement is initiated by coordination of the cyclopropylidene moiety a more stable tertiary carbocation is formed, via a lower energy transition state. The difference in transition state energies between the pathways reflects the developing carbocationic character of the initially formed intermediate. In pathway (a) secondary carbocation character is developing, whereas in pathway (b) it is tertiary carbocation character that is developing. This leads to pathway (b) having a lower reaction barrier and being the kinetically preferred pathway. The overall predicted reaction barrier was found to be ca. 15 kcal/mol. This is approximately 20 kcal/mol lower than for the uncatalyzed reaction, explaining the efficiency of this reaction at low temperatures.

The failure of substrate **67** to undergo cyclization was also investigated computationally (Figure 2.8). The calculations revealed that from common intermediate **125** pathways were energetically accessible which would lead to either the Au(I) coordinated product ([Au]-**82**) or a bicyclic carbocationic intermediate (**126**). Surprisingly, the predicted barrier for cyclization (TS-3) was ca. 3 kcal/mol lower than the predicted barrier for the Cope pathway (TS-2). However, formation of **126** is less exergonic than formation of the Cope product and reversible, allowing the thermodynamically favored [Au]-**82** to form preferentially.

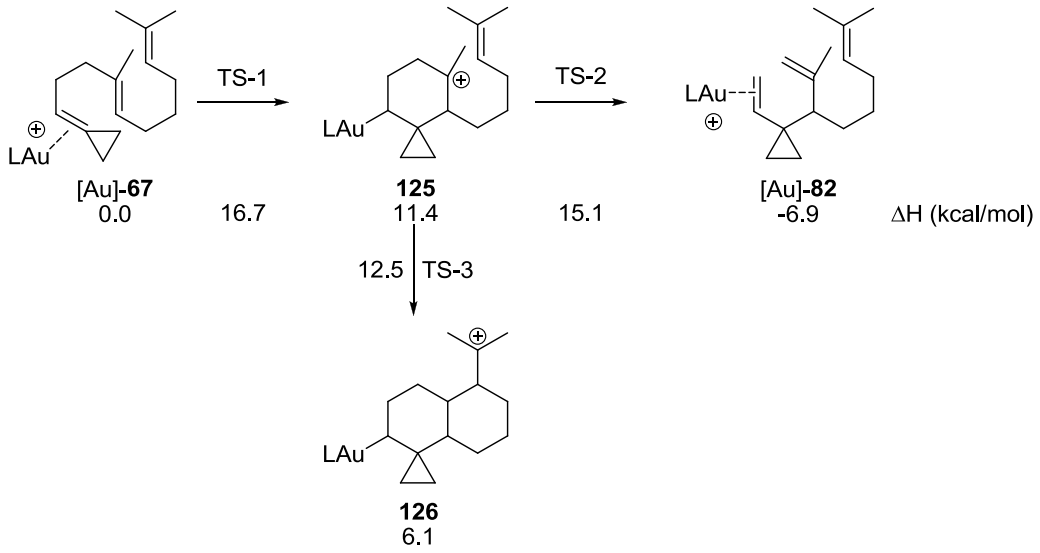

Figure 2.8. Investigation of Cope rearrangement versus cyclization for substrate 67.

A mechanistic pathway for the ring expansion of the cyclopropylidene to a cyclobutene was also investigated (Figure 2.9). Ring expansion would begin with slippage of the η^2 coordinated Au(I) –alkene to a state more resembling structure **B**. Transition states for the first two steps of the ring expansion (**B-TS1**, **B-TS2**) could not be located but it is worth noting that the intermediates are much higher in energy than any species observed on the Cope rearrangement pathway (**A** through **A2**). The one transition state structure that could be located, **B-TS3**, which corresponds to a proton shift, was significantly higher in energy than the barriers in the Cope pathway (ca. 28 kcal/mol). These calculations indicate that the ring expansion pathway is not kinetically feasible. The observation of some ring expanded product for substrate **105** (compound **106b**, see Table 2.8) is intriguing. It is unknown why this substrate is able to undergo ring expansion but investigation into this side reactivity could serve as a focus for future research.

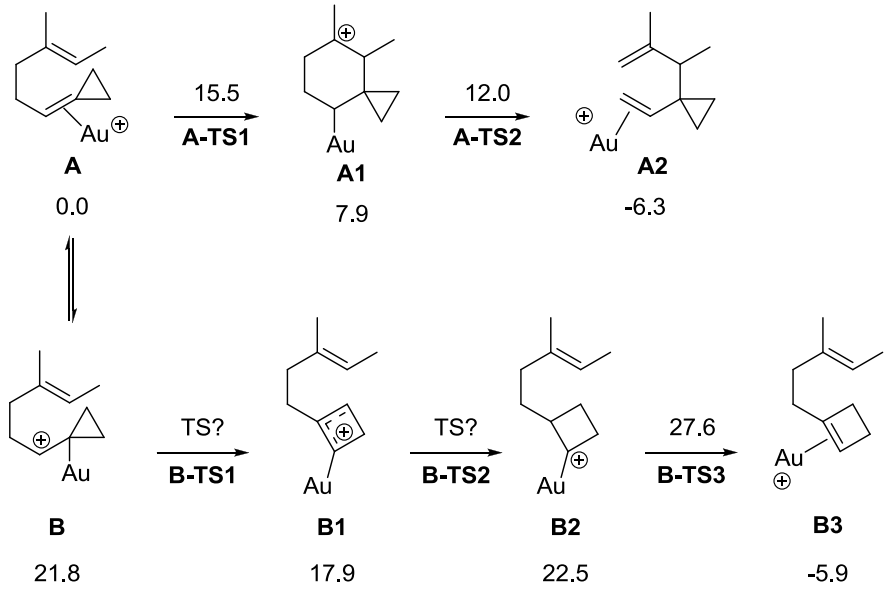

Figure 2.9. Relative free energies (kcal/mol) of cyclopropylidene to cyclobutene ring expansion.

Conclusions

This research was the first report of an enantioselective Cope rearrangement of achiral 1,5-dienes. Utilizing chiral bis-gold catalysts to significantly lower the reaction barrier, this reaction was successfully applied to alkyl, aromatic and oxygen- and nitrogen-containing substrates with high yields and good-to-excellent enantioselectivities. Quantum chemical calculations revealed that the release of ring strain from the cyclopropylidene moiety was the thermodynamic driving force for the reaction and that the predicted mechanism proceeds through a tertiary carbocation intermediate. Attempts to expand the utility of this novel Au(I)-catalyzed system to the synthesis of medium sized rings are the focus of the following chapter.

Experimental Section

General Information

All chemicals were reagent grade quality and used as received from Aldrich unless otherwise noted. Anhydrous THF (Stabilized, 99.9%, Acros Organics) and 1,2-Dichloroethane (99.8+%, extra pure) were purchased from Fisher Scientific and used as received. Phosphorous ligands were purchased from Strem Chemicals, Inc. and used without further purification. All glassware was flame dried

under vacuum unless otherwise indicated. Anhydrous CH_2Cl_2, diethyl ether, and pentanes were passed through a column of alumina.[76] Column chromatography was performed using SilaFlash P60 40-63 μm (230-400 mesh). All NMR spectra were recorded on either a Bruker Avance 600 MHz or 400 MHz spectrometer at STP. All deuterated solvents were used as received from Cambridge Isotope Laboratories, Inc. ^{1}H, ^{13}C, and ^{31}P NMR chemical shifts are reported in parts per million (ppm) relative to residual solvent resonances ($CDCl_3$ or CD_2Cl_2) or an external standard (H_3PO_4, 85%, 0 ppm). GC-MS data was obtained using an Agilent G2570A GC/MSD system containing a 6850 GC equipped with an HP-5MS column (length 30 m,; I.D. 0.250 mm) connected to an Agilent 5983N MSD. Enantiomeric excess (*e.e.*'s) were determined on a HP-6890 GC using an Agilent β-Cyclosil column (length 30 m, I.D. 0.250 mm) or using a Berger Instruments SFC equipped with a Chiralpak AD-H column (length 250 mm, I.D. 4.6 mm). High resolution mass spectra (HRMS) were obtained from the University of Illinois Mass Spectrometry lab (Dr. Furong Sun).

General Procedure for Synthesis of Au(I) Catalysts

Bis(phosphine) gold(I) catalysts were prepared by a modification to a procedure previously reported.[77] Spectroscopic data for the Au(I) complexes used in the optimization study have been reported previously.[78] To a solution of (S)-3,5-xylyl-PHANEPHOS (0.094 g, 0.136 mmol, 1.00 eq.) in CH_2Cl_2 (4 mL) at rt under air was added $Me_2S{\cdot}AuCl$ (0.080 g, 0.272 mmol, 2.00 eq.). The reaction was stirred for 2 h at rt, then concentrated and dried under vacuum overnight to provide the product compound as a white solid (0.128 g, 82% yield).

[76] Pangborn, A. B.; Giardello, M. A.; Grubbs, R. H.; Rosen, R. K.; Timmers, F. J. *Organometallics* **1996**, *15*, 1518.
[77] Kleinbeck, F.; Toste, F. D. *J. Am. Chem. Soc.* **2009**, *131*, 9178.
[78] a) Johansson, M. J.; Gorin, D. J.; Stabe, S. T.; Toste, F. D. *J. Am. Chem. Soc.* **2005**, *127*, 18002. b) Melhado, A. D.; Luparia, M.; Toste, F. D. *J. Am. Chem. Soc.* **2007**, *129*, 12638. c) Pradal, A.; Chao, M-C.; Vitale, M. R.; Toullec, P. Y.; Michelet, V. *Tetrahedron*, **2011**, *67*, 4371. d) Hamilton, G. L.; Kang, E. J.; Mba, M.; Toste, F. D. *Science*, **2007**, *317*, 496.

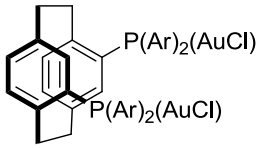

Ar = 3,5-xylyl

59-(AuCl)$_2$

(S)-3,5-xylyl-PHANEPHOS(AuCl)$_2$ (59-(AuCl)$_2$): **^{1}H-NMR** (600 MHz, CD_2Cl_2) δ 7.28-7.19 (m, 8H), 7.10-7.05 (m, 6H), 6.82-6.80 (m, 2H), 6.74-6.72 (m, 2H), 3.76-3.69 (m, 2H), 3.30 (t, *J* = 12 Hz, 2H), 3.07 (t, *J* = 12 Hz, 2H), 2.80-2.78 (m, 2H), 2.43 (s, 12H), 2.21 (s, 12H); **^{13}C-NMR** (150 MHz, CD_2Cl_2) δ 145.0, 144.9, 140.7, 140.6, 139.9, 139.8, 139.2, 139.1, 137.5, 135.9, 135.8, 135.0, 134.9, 133.8, 133.7, 133.6, 133.5, 132.8, 132.4, 131.7, 131.6, 128.2, 127.8, 127.4, 34.9, 34.8, 34.4, 22.0, 21.5; **^{31}P-NMR** (162 MHz, CD_2Cl_2) δ 31.5.

Synthesis of 1,5-Dienes

General Procedure for Wittig cyclopropylidination.[61]

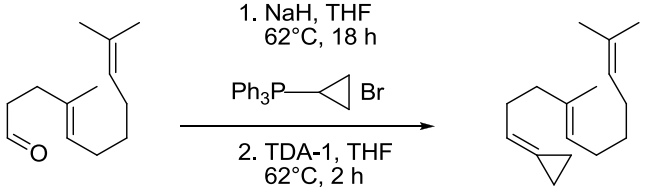

78 53% **67**

To a Schlenk flask loaded with a suspension of dry NaH (0.075 g, 3.15 mmol, 1.30 eq.) in THF (13 mL) under N_2 atmosphere was added cyclopropyltriphenylphosphonium bromide (1.21 g, 3.15 mmol, 1.30 eq.) at rt. The reaction flask was then equipped with a condenser and heated to 62°C for 18 h. To the resulting orange suspension was then added (E)-4,10-dimethylundeca-4,9-dienal[48] (0.469 g, 2.42 mmol, 1.00 eq.) and tris[2-(2-methoxyethoxy)ethyl]amine (TDA-1) (0.077 mL, 0.242 mmol, 0.10 eq.) in THF (4 mL). The reaction was stirred for 2 h at 62°C before cooling to rt and quenching with saturated aqueous $NaHCO_3$. The reaction was diluted with deionized H_2O and Et_2O before separating the layers. The aqueous layer was extracted with Et_2O (2x) and the combined organic layers were then washed with brine (2x). The organic layer was then dried over $MgSO_4$, filtered, and concentrated *in vacuo*. Purification by silica gel chromatography (Hexanes) provided the product

compound as a colorless oil (0.283 g, 53% yield). A small amount of CH_2Cl_2 was used to load the material onto the column.

(E)-(4,10-dimethylundeca-4,9-dienylidene)cyclopropane (67): **^{1}H-NMR** (600 MHz, CD_2Cl_2) δ 5.75-5.72 (m, 1H), 5.16-5.10 (m, 2H), 2.29-2.25 (m, 2H), 2.12-2.09 (m, 2H), 1.99-1.94 (m, 4H), 1.68 (s, 3H), 1.60 (s, 3H), 1.59 (s, 3H), 1.37-1.32 (m, 2H), 1.02-1.00 (m, 4H); **^{13}C-NMR** (150 MHz, CD_2Cl_2) δ 135.4, 131.8, 125.2, 125.2, 121.5, 118.5, 39.9, 31.0, 30.6, 28.1, 28.0, 26.0, 17.9, 16.2, 2.5, 2.1. HRMS (EI+) calculated for $C_{16}H_{26}$ 218.20345, found 218.20366.

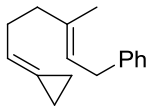

83

(E)-(6-cyclopropylidene-3-methylhex-2-enyl)benzene (83): Prepared using the same general procedure as for (**67**) from (E)-4-methyl-6-phenylhex-4-enal.[67] Purified by silica gel chromatography (Hexanes). Colorless oil, 34% yield. **^{1}H-NMR** (600 MHz, CD_2Cl_2) δ 7.27-7.24 (m, 2H), 7.17-7.14 (m, 3H), 5.75-5.73 (m, 1H), 5.36-5.32 (m, 1H), 3.35 (d, *J* = 7.8 Hz, 1H), 2.34-2.30 (m, 2H), 2.19-2.17 (m, 2H), 1.73 (s, 3H), 1.00 (s, 4H); **^{13}C-NMR** (150 MHz, CD_2Cl_2) δ 142.5, 136.6, 128.8, 126.1, 123.7, 121.7, 118.4, 39.9, 34.7, 30.9, 16.4, 2.5, 2.2. HRMS (EI+) calculated for $C_{16}H_{20}$ 212.15650, found 212.15613.

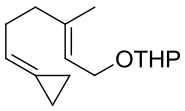

99

(E)-2-(6-cyclopropylidene-3-methylhex-2-enyloxy)tetrahydro-2H-pyran (99): Prepared using the same general procedure as for (**67**) from (E)-4-methyl-6-(tetrahydro-2H-pyran-2-yloxy)hex-4-enal.[44] Purified by silica gel chromatography (10:1 Hexanes:Et_2O). Colorless oil, 45% yield. **^{1}H-NMR** (600 MHz, $CDCl_3$) δ 5.75-5.72 (m, 1H), 5.39-5.36 (m 1H), 4.62-4.61 (m, 1H), 4.23 (dd, *J* = 11.9 Hz, 6.4 Hz, 1H), 4.02 (dd, *J* = 11.9 Hz, 7.4 Hz, 1H), 3.91-3.87 (m, 1H), 3.52-3.49 (m, 1H), 2.33-2.29 (m, 2H), 2.18-2.16 (m, 3H), 1.86-1.81 (m, 1H), 1.74-1.69 (m, 1H), 1.69 (s, 3H), 1.60-1.56 (m, 3H), 1.55-

1.51 (m, 2H), 1.01 (bs, 4H); **^{13}C-NMR** (150 MHz, $CDCl_3$) δ 140.1, 121.3, 120.6, 117.6, 97.8, 63.6, 62.3, 39.2, 30.7, 30.1, 25.5, 19.6, 16.4, 2.2, 1.8.

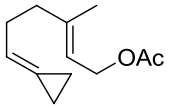

101

(E)-6-cyclopropylidene-3-methylhex-2-enyl acetate (101): Prepared using the same general procedure as for (**67**) from (E)-3-methyl-6-oxohex-2-enyl acetate.[71a] Purified by an silica gel chromatography using 9:1 Hexanes:EtOAc in an initial column, followed by a second silica gel column utilizing 15:1 Hexanes:EtOAc as the eluant. Colorless oil, 22% yield. **^{1}H-NMR** (600 MHz, $CDCl_3$) δ 5.74-5.72 (m, 1H), 5.37-5.34 (m, 1H), 4.58 (d, *J* = 7.1 Hz, 2H), 2.33-2.29 (m, 2H), 2.19-2.16 (m, 2H), 2.05 (s, 3H), 1.71 (s, 3H), 1.01 (bs, 4H); **^{13}C-NMR** (150 MHz, $CDCl_3$) δ 171.2, 142.2, 121.6, 118.3, 117.4, 61.4, 39.1, 30.0, 21.1, 16.5, 2.2, 1.8.

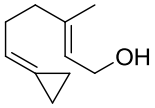

103

(E)-6-cyclopropylidene-3-methylhex-2-en-1-ol (103): Prepared by removal of the tetrahydropyran protecting group from **101**. To a small vial loaded with **1g** (0.250 g, 1.06 mmol, 1 eq.) was added MeOH (2.5 mL). *p*-Toluenesulfonic acid monohydrate was then added (0.010 g, 0.053 mmol, 5 mol%) and the reaction was stirred for 30 minutes at room temperature. The reaction mixture was then concentrated *in vacuo* and purified by silica gel chromatography (5:1 Hexanes:EtOAc) to give 0.1136 of the product compound as a colorless oil. 71% yield. **^{1}H-NMR** (600 MHz, $CDCl_3$) δ 5.75-5.72 (m, 1H), 5.44-5.41 (m, 1H), 4.15 (d, *J* = 6.9 Hz, 2H), 2.32-2.29 (m, 2H), 2.17-2.15 (m, 2H), 1.69 (s, 3H), 1.21 (bs, 1H), 1.01 (bs, 4H); **^{13}C-NMR** (150 MHz, $CDCl_3$) δ 139.7, 123.4, 121.5, 117.5, 59.4, 39.1, 30.1, 16.2, 2.2, 1.81.

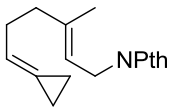

105

(E)-2-(6-cyclopropylidene-3-methylhex-2-enyl)isoindoline-1,3-dione (105): Prepared by a Mitsunobu reaction of compound **103**. To a small flask was added THF (4 mL), **103** (0.050 g, 0.328 mmol, 1eq.), phthalimide (0.063 g, 0.426 mmol, 1.3 eq.), then triphenylphosphine (0.112 g, 0.426 mmol, 1.3 eq.). The reaction flask was then wrapped in aluminum foil and diisopropyl azodicarboxylate (0.084 mL, 0.426 mmol, 1.3 eq.) was then added dropwise. The reaction was stirred for 4.5 h at room temperature before being poured into 16 mL H_2O. The layers were separated and the aqueous layer was extracted twice each with Et_2O and Hexanes. The combined organics were washed with two times with brine, dried over $MgSO_4$, filtered and concentrated *in vacuo*. The product compound was purified by silica gel chromatography (10:1 Hexanes:Et_2O) to give 0.0597 of product as a colorless oil which solidified upon placing in the freezer. 65% yield. **^{1}H-NMR** (600 MHz, $CDCl_3$) δ 7.84-7.82 (m, 2H), 7.71-7.69 (m, 2H), 5.69-5.67 (m, 1H), 5.29-5.26 (m, 1H), 4.27 (d, *J* = 7.1 Hz, 2H), 2.29-2.25 (m, 2H), 2.13-2.11 (m, 2H), 1.83 (s, 3H), 0.97 (bs, 4H); **^{13}C-NMR** (150 MHz, $CDCl_3$) δ 168.1, 140.4, 133.8, 132.3, 123.1, 121.5, 118.0, 117.4, 39.0, 35.8, 30.0, 16.4, 2.2, 1.8.

Alkylidenecyclopropanes **93**, **95**, **97**, and **107** were prepared from aldehydes synthesized using a published ruthenium-catalyzed coupling procedure.[71b]

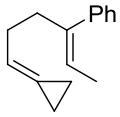

93

(Z)-(6-cyclopropylidenehex-2-en-3-yl)benzene (93): Prepared using the same general procedure as for (**67**). Purified by silica gel chromatography (Hexanes). Colorless oil, 25% yield. **^{1}H-NMR** (600 MHz, CD_2Cl_2) δ 7.35-7.33 (m, 2H), 7.25-7.23 (m, 1H), 7.17-7.15 (m, 1H), 5.74-5.71 (m, 1H), 5.60-5.56 (m, 1H), 2.49 (t, *J* = 7.8 Hz, 2H), 2.22 (q, *J* = 7.8 Hz, 2H), 1.60 (d, *J* = 7.2 Hz, 3H), 1.01-0.95 (m, 4H); **^{13}C-NMR** (150 MHz, CD_2Cl_2) δ 142.0, 141.6, 129.1, 128.5, 126.9, 121.8, 121.7, 118.2, 39.4, 31.2, 15.0, 2.5, 2.2. HRMS (EI+) calculated for $C_{15}H_{18}$ 198.14085, found 198.13973.

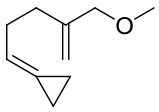

95

(4-(methoxymethyl)pent-4-enylidene)cyclopropane (95): Prepared using the same general procedure as for (**67**). Purified by silica gel chromatography (5:1 Pentanes:Et_2O). Colorless oil, 31% yield. **^{1}H-NMR** (600 MHz, CD_2Cl_2) δ 5.76-5.74 (m, 1H), 4.97 (s, 1H), 4.89 (s, 1H), 3.83 (s, 2H), 3.27 (s, 3H), 2.35-2.31 (m, 2H), 2.17 (t, *J* = 7.8 Hz, 2H), 1.01 (bs, 4H); **^{13}C-NMR** (150 MHz, CD_2Cl_2) δ 146.7, 121.9, 118.1, 111.4, 75.9, 58.2, 33.2, 30.5, 2.5, 2.2. HRMS (EI+) calculated for $C_{10}H_{15}O$ ([M^+ - H^+]) 151.11230, found 151.11278.

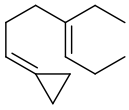

97

(E)-(4-ethylhept-4-enylidene)cyclopropane (97): Prepared using the same general procedure as for (**67**). Purified by silica gel chromatography (Hexanes). Colorless oil, 56% yield. **^{1}H-NMR** (600 MHz, CD_2Cl_2) δ 5.76-5.73 (m, 1H), 5.10 (t, *J* = 7.2 Hz, 1H), 2.26 (q, *J* = 7.7 Hz, 2H), 2.11 (t, *J* = 7.2 Hz, 2H), 2.04 (q, *J* = 7.6 Hz, 2H), 2.00 (m, 2H), 1.01 (bs, 4H), 0.96 (t, *J* = 7.6 Hz, 3H), 0.93 (t, *J* = 7.7 Hz, 3H); **^{13}C-NMR** (150 MHz, CD_2Cl_2) δ 140.7, 126.6, 121.4, 118.6, 36.7, 31.2, 23.5, 21.3, 15.1, 13.7, 2.5, 2.2. HRMS (EI+) calculated for $C_{12}H_{20}$ 164.15650, found 164.15546.

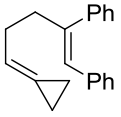

107

(Z)-(5-cyclopropylidenepent-1-ene-1,2-diyl)dibenzene (107): Prepared using the same general procedure as for (**67**). Purified by silica gel chromatography (Hexanes). Colorless oil, 39% yield. **^{1}H-NMR** (600 MHz, CD_2Cl_2) δ 7.31-7.28 (m, 2H), 7.27-7.24 (m, 1H), 7.16-7.14 (m, 2H), 7.08-7.02 (m, 3H), 6.92-6.90 (m, 2H), 6.47 (s, 1H), 5.79 (tt, *J* = 6.6 Hz, 2.4 Hz, 1H), 2.64 (ddd, *J* = 9.0 Hz, 6.6 Hz, 1.2 Hz, 2H), 2.31-2.27 (m, 2H), 1.03-0.98 (m, 4H); **^{13}C-NMR** (150 MHz, CD_2Cl_2) δ 143.7, 141.9, 138.2, 129.5, 129.2, 129.0, 128.3, 127.4, 126.9, 126.6, 122.1, 117.9, 40.8, 30.8, 2.5, 2.3. HRMS (EI+) calculated for $C_{20}H_{20}$ 260.15650, found 260.15682.

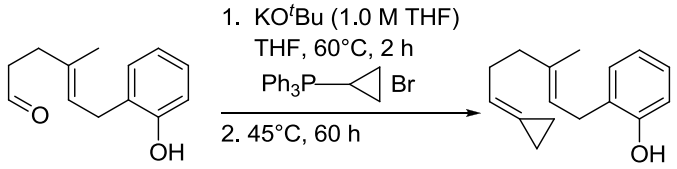

91

(**E)-2-(6-cyclopropylidene-3-methylhex-2-enyl)phenol (91)**: The general procedure for the Wittig reaction did not work to synthesize **91** as decomposition of the aldehyde was observed. Instead a procedure employing KO^{t}Bu to activate the phosphonium salt was utilized.[72] To a Schlenk flask loaded with cyclopropyltriphenylphosphonium bromide (1.00 g, 2.61 mmol, 1.33 eq.) and THF (20 mL) under N_2 atmosphere was slowly added KO^{t}Bu (1.0 M in THF, 5.22 mL, 5.22 mmol, 2.66 eq.) at rt. The reaction changed from yellow upon initial addition of the KO^{t}Bu and was orange by the end of the addition. The reaction was then heated to 60°C for 2 h. The aldehyde, (E)-6-(2-hydroxyphenyl)-4-methylhex-4-enal,[37] dissolved in THF (2.5 mL), was then added and the reaction was heated at 45°C for 60 h. After allowing the reaction to cool to rt, H_2O was added then saturated aqueous NH_4Cl. The layers were separated and the aqueous layer extracted with Et_2O (2x). The combined organic layers were washed with brine (1x), dried over $MgSO_4$, filtered, and concentrated *in vacuo*. The product compound was then purified by silica gel chromatography using 5:1 Pentanes:Et_2O. Compound **1f** was obtained as a colorless oil (0.075g, 17% yield). **^{1}H-NMR** (600 MHz, CD_2Cl_2) δ 7.09-7.07 (m, 2H), 6.89 (dt, *J* = 7.8 Hz, 1.2 Hz, 1H), 6.78-6.76 (m, 1H), 5.73-5.70 (m, 1H), 5.33-5.31 (m, 1H), 5.11-5.09 (m, 1H), 3.35 (d, *J* = 7.2 Hz, 2H), 2.35-2.31 (m, 2H), 2.21-2.19 (m, 2H), 1.76 (s, 3H), 1.02-0.99 (m, 4H); **^{13}C-NMR** (150 MHz, CD_2Cl_2) δ 154.9, 138.6, 130.4, 127.9, 127.6, 122.3, 122.1, 121.1, 118.1, 116.0, 39.8, 30.7, 30.0, 16.4, 2.6, 2.2. HRMS (EI+) calculated for $C_{16}H_{20}O$ 228.15142, found 228.15209.

General Procedure for Au(I)-Catalyzed Cope Rearrangement

To a vial loaded with silver hexafluoroantimonate (3.2 mg, 0.0092 mmol, 0.2 eq.) was added a 1:9 CH_2Cl_2:1,2-DCE solution (1 mL). Au(I) catalyst precursor **59-$(AuCl)_2$** (2.6 mg, 0.0023 mmol, 0.05 eq.) was then added and the reaction stirred at rt for 15 min. The reaction was then placed into a

NesLab Cryobath CB-80 maintained at -35°C and stirred for 10 min before addition of **67** (10 mg, 0.046 mmol, 1 eq.). The reaction was then stirred for 18 h at -35°C before concentrating the reaction *in vacuo*. The product was then isolated by a pipette column.

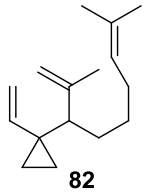

82

1-(2,8-dimethylnona-1,7-dien-3-yl)-1-vinylcyclopropane (82): Silica gel column (Hexanes). Product isolated as a colorless oil (9.4 mg, 94% yield). **^{1}H-NMR** (600 MHz, $CDCl_3$) δ 6.09 (dd, *J* = 15.6 Hz, 10.5 Hz, 1H), 5.12-5.09 (m, 1H), 4.85-4.80 (m, 2H), 4.80 (bs, 1H), 4.66 (bs, 1H), 1.97-1.92 (m, 2H), 1.71 (s, 3H), 1.68 (s, 3H), 1.52-1.47 (m, 2H), 1.33-1.28 (m, 2H), 0.64-0.58 (m, 3H), 0.54-0.51 (m, 1H); **^{13}C-NMR** (150 MHz, $CDCl_3$) δ 147.1, 141.5, 131.5, 124.9, 111.3, 111.1, 52.7, 30.3, 28.4, 28.3, 25.9, 25.6, 22.2, 17.9, 14.6, 12.9. HRMS (EI+) calculated for $C_{16}H_{26}$ 218.20345, found 218.20224.

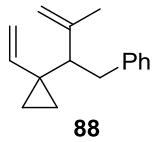

88

(3-methyl-2-(1-vinylcyclopropyl)but-3-enyl)benzene (88): Silica gel column (Hexanes). Product isolated as a colorless oil (89% yield). **^{1}H-NMR** (600 MHz, $CDCl_3$) δ 7.25-7.23 (m, 2H), 7.17-7.14 (m, 3H), 6.13 (dd, *J* = 17.1 Hz, 10.5 Hz, 1H), 4.94-4.88 (m, 2H), 4.82 (bs, 1H), 4.70 (bs, 1H), 2.90 (dd, *J* = 13.8 Hz, 6.0 Hz, 1H), 2.85 (dd, *J* = 13.8 Hz, 8.7 Hz, 1H) 1.92 (dd, *J* = 8.7 Hz, 6.0 Hz, 1H), 1.76 (s, 3H), 0.66-0.64 (m, 2H), 0.60-0.58 (m, 1H), 0.33-0.30 (m, 1H); **^{13}C-NMR** (150 MHz, $CDCl_3$) δ 146.3, 141.6, 140.9, 129.1, 128.1, 125.7, 112.0, 111.8, 54.2, 37.3, 25.3, 23.3, 14.1, 13.9. HRMS (EI+) calculated for $C_{16}H_{20}$ 212.15650, found 212.15739.

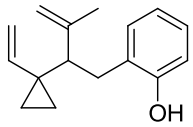

92

2-(3-methyl-2-(1-vinylcyclopropyl)but-3-enyl)phenol (92): Silica gel column (10:1 Pentanes:Et_2O). Product isolated as a colorless oil (71% yield). **^{1}H-NMR** (600 MHz, $CDCl_3$) δ 7.08-7.05 (m, 2H), 6.83 (td, *J* = 7.2 Hz, 1.2 Hz, 1H), 6.75-6.74 (m, 1H), 6.16 (dd, *J* = 17.1 Hz, 10.8 Hz, 1H), 4.96 (dd, *J* = 10.8 Hz, 1.8 Hz, 1H), 4.94 (dd, *J* = 17.1 Hz, 1.8 Hz, 1H), 2.88 (dd *J* = 14.4 Hz, 7.8 Hz, 1H), 2.85 (dd, *J* = 14.4 Hz, 7.2 Hz, 1H), 1.95 (pt, *J* = 7.8 Hz, 7.2 Hz, 1H), 1.80 (s, 3H), 0.67-0.59 (m, 3H), 0.33-0.30 (m, 1H); **^{13}C-NMR** (150 MHz, $CDCl_3$) δ 153.8, 147.2, 140.9, 131.0, 127.5, 127.3, 120.7, 115.5, 112.1, 111.7, 52.4, 31.8, 24.9, 23.6, 14.5, 13.5. HRMS (EI+) calculated for $C_{16}H_{20}O$ 228.15142, found 228.15274.

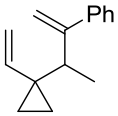

94

(3-(1-vinylcyclopropyl)but-1-en-2-yl)benzene (94): Silica gel column (Hexanes). Product isolated as a colorless oil (90% yield). **^{1}H-NMR** (600 MHz, $CDCl_3$) δ 7.31-7.29 (m, 4H), 7.27-7.25 (m, 1H), 6.00 (dd, *J* = 17.1 Hz, 10.8 Hz), 5.21 (bs, 1H), 5.11 (bs, 1H), 4.90 (d, *J* = 10.8 Hz, 1H), 4.84 (d, *J* = 17.1 Hz, 1H), 2.45 (q, *J* = 7.2 Hz, 1 H), 1.19 (d, *J* = 7.2 Hz, 3H), 0.61-0.58 (m, 1H), 0.48-0.38 (m, 3H); **^{13}C-NMR** (150 MHz, $CDCl_3$) δ 152.1, 144.0, 141.1, 128.1, 127.1, 127.0, 113.0, 111.5, 43.4, 25.7, 17.3, 14.2, 13.5. HRMS (EI+) calculated for $C_{15}H_{18}$ 198.14085, found 198.14154.

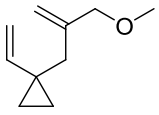

96

1-(2-(methoxymethyl)allyl)-1-vinylcyclopropane (96): Silica gel column (10:1 Pentanes:Et_2O). Product isolated as a colorless oil (98% yield). **^{1}H-NMR** (600 MHz, $CDCl_3$) δ 5.62 (dd, *J* = 17.4 Hz, 10.8 Hz, 1H), 5.07 (bs, 1H), 5.03 (bs, 1H), 4.89 (d, *J* = 17.4 Hz, 1H), 4.86 (d, *J* = 10.8 Hz, 1H), 3.86 (s, 2H), 3.30 (s, 3H), 2.20 (s, 2H), 0.68-0.63 (m, 4H); **^{13}C-NMR** (150 MHz, $CDCl_3$) δ 143.9, 143.6,

113.6, 110.8, 75.9, 57.9, 39.6, 20.3, 14.7. HRMS (EI+) calculated for $C_{10}H_{15}O$ ([M^+ - H^+]) 151.11230, found 151.11209.

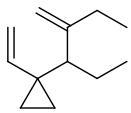

98

1-(4-methylenehexan-3-yl)-1-vinylcyclopropane (98): Silica gel column (Hexanes). Product isolated as a colorless oil (87% yield). **^{1}H-NMR** (600 MHz, $CDCl_3$) δ 6.02 (dd, *J* = 16.8 Hz, 10.8 Hz, 1H), 4.85-4.80 (m, 2H), 4.83 (bs, 1H), 4.70 (bs, 1H), 2.10-2.03 (m, 1H), 2.02-1.95 (m, 1H), 1.59-1.50 (m, 3H), 1.01 (t, *J* = 7.8 Hz, 3H), 0.86 (t, *J* = 7.2 Hz, 3H), 0.61-0.57 (m, 3H), 0.51-0.48 (m, 1H); **^{13}C-NMR** (150 MHz, $CDCl_3$) δ 151.9, 141.9, 110.0, 108.3, 53.0, 28.7, 25.4, 24.1, 14.4, 12.8, 12.6, 12.3.

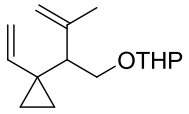

100

2-(3-methyl-2-(1-vinylcyclopropyl)but-3-enyloxy)tetrahydro-2H-pyran (100): Silica gel column (10:1 Hexanes:Et_2O). Product isolated as a colorless oil, in a 1:1 mixture of diasteromers (60% yield). **^{1}H-NMR** (600 MHz, $CDCl_3$) δ 6.01 (dd, *J* = 7.2 Hz, 6.5 Hz, 1H), 4.87-4.73 (m, 4H), 4.56 (bs, 1H), 3.95-3.91 (m, 1H), 3.85-3.83 (m, 1H), 3.54-3.47 (m, 2H), 1.86 (bs, 1H), 1.78 (bs, 4H), 1.55 (bs, 1H), 1.53-1.47 (m, 4H), 0.67-0.64 (m, 4H); **^{13}C-NMR** (150 MHz, $CDCl_3$) δ 145.0, 140.8, 111.7, 111.5, 99.3, 68.6, 62.2, 51.9, 30.9, 25.5, 23.4, 23.1, 19.5, 13.9, 13.4.

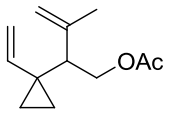

102

3-methyl-2-(1-vinylcyclopropyl)but-3-enyl acetate (102): Silica gel column (10:1 Hexanes:Et_2O). Product isolated as a colorless oil (70% yield). **^{1}H-NMR** (600 MHz, $CDCl_3$) δ 5.94 (dd *J* = 16.9 Hz, 10.8 Hz, 1H), 4.90 (m, 2H), 4.87 (dd, *J* = 8.4 Hz, 1.4 Hz, 1H), 4.73 (bs, 1H), 4.26 (d, *J* = 7.2 Hz, 2H), 2.03 (s, 3H), 1.94 (t, *J* = 7.2 Hz, 1H), 1.79 (s, 3H), 0.72-0.65 (m, 3H), 0.63-0.60 (m, 1H); **^{13}C-NMR** (150 MHz, $CDCl_3$) δ 171.1, 143.7, 139.8, 112.3, 112.0, 64.8, 50.6, 23.0, 21.0, 13.6, 13.1.

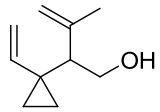

104

3-methyl-2-(1-vinylcyclopropyl)but-3-en-1-ol (104): Silica gel column (10:1 Hexanes:EtOAc). Product isolated as a colorless oil (35% yield). **^{1}H-NMR** (600 MHz, $CDCl_3$) δ 5.97 (dd, *J* = 17.4 Hz, 10.3 Hz, 1H), 4.98 (bs, 1H), 4.90 (pd, *J* = 1.8 Hz, 1H), 4.87 (pd, *J* = 2.9 Hz, 1H), 4.80 (bs, 1H), 3.77-3.75 (m, 2H), 1.90 (t, *J* = 7.2 Hz, 1H), 1.81 (s, 3H), 1.54 (bs, 1H), 0.73-0.70 (m, 1H), 0.67-0.62 (m, 2H), 0.61-0.58 (m, 1H); **^{13}C-NMR** (150 MHz, $CDCl_3$) δ 144.4, 140.4, 112.0, 112.0, 62.9, 54.1, 31.6, 23.1, 13.0, 12.9

Conversion of 104 to 102: Dissolved alcohol **104** (13 mg, 0.085 mmol, 1 eq.) in pyridine (0.12 mL) and cooled to 0°C. Added a single small crystal of 4-(dimethylamino)pyridine (DMAP) then acetic anhydride (0.0126 mL, 0.133 mmol, 1.5 eq.). The reaction was stirred briefly at 0° then allowed to warm to room temperature and stirred for 2 h. The reaction was then diluted with hexanes and quenched with ice/H_2O. The layers were separated and the aqueous layer was washed with hexanes (2x). The combined organic layers were then washed with 10% HCl (2x) and saturated $NaHCO_3$ (2x) before drying over $MgSO_4$. The product was then concentrated *in vacuo* to give the product as a colorless oil (7.6 mg, 46% yield). ^{1}H and ^{13}C NMR spectra matched that of compound **102**.

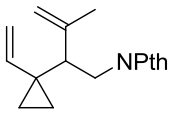

106a

2-(3-methyl-2-(1-vinylcyclopropyl)but-3-enyl)isoindoline-1,3-dione (106a): Silica gel column (10:1 Hexanes:Et2O). Product isolated as a pale green oil, as an intractable mixture with **106b** (45% yield). **^{1}H-NMR** (600 MHz, $CDCl_3$) δ 7.84-7.81 (m, 2H), 7.71-7.69 (m, 2H), 6.08 (dd, *J* = 17.1 Hz, 10.5 Hz, 1H), 4.96 (dd, *J* = 17.1 Hz, 1.3 Hz, 1H), 4.93 (dd, *J* = 17.1 Hz, 1.3 Hz, 1H), 3.97 (dd, *J* = 13.8 Hz, 9.5 Hz, 1H), 3.79 (dd *J* = 13.8 Hz, 6.1 Hz, 1H), 2.39 (dd, *J* = 9.5 Hz, 6.1 Hz, 1H), 1.78 (s, 3H), 0.71-0.68 (m, 1H), 0.67-0.62 (m, 3H); **^{13}C-NMR** (150 MHz, $CDCl_3$) δ 168.4. 144.0, 140.0, 133.8, 132.0, 123.1, 112.8, 112.3, 49.5, 39.3, 23.4, 22.5, 13.8, 12.3.

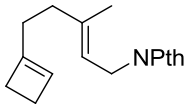

106b

(E)-2-(5-cyclobutenyl-3-methylpent-2-enyl)isoindoline-1,3-dione (106b): Silica gel column (10:1 Hexanes:Et2O). Product isolated as a pale green oil, as an intractable mixture with **106a** (23% yield). **^{1}H-NMR** (600 MHz, $CDCl_3$) δ 7.84-7.81 (m, 2H), 7.71-7.69 (m, 2H), 5.62 (bs, 1H), 5.28 (t, *J* = 7.1 Hz, 1H), 4.27 (d, *J* = 7.1 Hz, 2H), 2.36 (bs, 2H), 2.26 (bs, 2H), 2.12-2.07 (m, 4H), 1.82 (s, 3H); **^{13}C-NMR** (150 MHz, $CDCl_3$) δ 168.1, 149.8, 140.4, 133.8, 132.3, 127.0, 123.1, 118.0, 36.6, 35.8, 31.1, 29.3, 26.5, 16.2.

Synthesis of Alkylidene Substrates

Substrates prepared by Wittig reaction of phosphonium halide salt with (E)-4-methyl-6-phenylhex-4-enal.

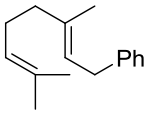

122

(E)-(3,7-dimethylocta-2,6-dienyl)benzene (122): Isopropyltriphenyphosphonium iodide (0.717 g, 1.66 mmol, 1.2 eq.) was suspended in dry THF (12 mL) and cooled to 0°C. *n*-BuLi (1.6 M, 1.04 mL, 1.66 mmol, 1.2 eq.) was added dropwise and the reaction was then stirred for 10 minutes at 0°C before adding the aldehyde (0.260 g, 1.38 mmol, 1 eq.) dissolved in THF (1 mL). The reaction was stirred 2h at 0°C before quenching at that temperature with saturated aqueous NH_4Cl. Added H_2O and Et_2O and separated the layers. The aqueous layer was extracted 2 times with Et_2O and the combined organics were then washed 2 times with brine before drying over $MgSO_4$, filtering, and concentrating *in vacuo*. The product was then purified by silica gel chromatography (Hexanes) to give 0.130 g of the product as a colorless oil. 44% yield. **^{1}H-NMR** (600 MHz, CD_2Cl_2) δ 7.27-7.25 (m, 2H), 7.18-7.14 (m, 3H), 5.34 (t, *J* = 7.0 Hz, 1H), 5.13-5.10 (m, 1H), 3.35 (d, *J* = 7.4 Hz, 2H), 2.14-2.10 (m, 2H), 2.07-2.04 (m, 2H), 1.72 (s, 3H), 1.68 (s, 3H), 1.60 (s, 3H); **^{13}C-NMR** (150 MHz, CD_2Cl_2) δ 142.3, 136.5, 131.7, 128.6, 128.6, 125.9, 124.6, 123.4, 40.0, 34.4, 26.9, 25.8, 17.7, 16.1.

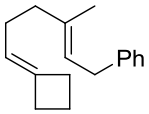

123

(E)-(6-cyclobutylidene-3-methylhex-2-enyl)benzene (123): Added cyclobutyltriphenylphosphonium bromide (0.505 g, 1.27 mmol, 1.2 eq.) to a small flask and suspended in THF (25 mL). Added PhLi (2.0M, 0.70 mL, 1.40 mmol, 1.3 eq.) slowly at room temperature. Stirred 2h at room temperature then added aldehyde (0.200 g, 1.06 mmol, 1 eq.) in THF (1 mL) to the dark red solution. The reaction turned green with the formation of a precipitate and stirred for 3h. The reaction was then quenched with H_2O and saturated aqueuous NH_4Cl. Et_2O was added and the layers were separated before extracting the aqueous layer 2 times with Et_2O. The combined organic layers were washed 2 times with brine before drying over $MgSO_4$, filtering, and concentrating *in vacuo*. The product was then purified via silica gel chromatography (Hexanes) to give 0.154 g of the product as an intractable mixture with biphenyl. **^{1}H-NMR** (600 MHz, CD_2Cl_2) δ 7.28-7.25 (m, 2H), 7.19-7.15 (m, 3H), 5.34-5.31 (m, 1H), 5.04-5.01 (m, 1H), 3.35 (d, *J* = 7.3 Hz, 2H), 2.64-2.60 (m, 4H), 2.07-2.04 (m, 2H), 2.02-1.99 (m, 2H), 1.91 (p, *J* = 7.9 Hz, 2H), 1.71 (s, 3H); **^{13}C-NMR** (150 MHz, CD_2Cl_2) δ 142.3, 140.3, 136.5, 128.6, 128.6, 125.9, 123.4, 120.3, 40.0, 34.5, 31.2, 29.5, 26.8, 17.4, 16.1.

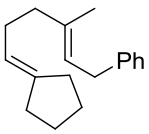

124

(E)-(6-cyclopentylidene-3-methylhex-2-enyl)benzene (124): Cyclopentyltriphenylphosphonium bromide (0.522 g, 1.27 mmol, 1.2 eq.) was suspended in dry THF (12 mL) and cooled to 0°C. *n*-BuLi (1.6 M, 0.793 mL, 1.27 mmol, 1.2 eq.) was added dropwise and the reaction was then stirred for 30 minutes at 0°C before adding the aldehyde (0.200 g, 1.06 mmol, 1 eq.) dissolved in THF (1 mL). The reaction was stirred 1.5h at 0°C before quenching at that temperature with saturated aqueous NH_4Cl. Added H_2O and Et_2O and separated the layers. The aqueous layer was extracted 2 times with Et_2O and the combined organics were then washed 2 times with brine before drying over $MgSO_4$, filtering,

and concentrating *in vacuo*. The product was then purified by silica gel chromatography (Hexanes) to give 0.130 g of the product as a colorless oil. 51% yield. **^{1}H-NMR** (600 MHz, CD_2Cl_2) δ 7.27-7.25 (m, 2H), 7.19-7.14 (m, 3H), 5.33 (t, *J* = 7.3 Hz, 1H), 5.23 (bs, 1H), 3.35 (d, *J* = 7.4, 2H), 2.19 (dt, *J* = 19.7 Hz, 7.2 Hz, 4H), 2.12-2.06 (m, 4H), 1.72 (s, 3H), 1.65 (p, *J* = 7.0 Hz, 2H), 1.58 (p, *J* = 6.8 Hz, 2H); **^{13}C-NMR** (150 MHz, CD_2Cl_2) δ 143.5, 142.3, 136.6, 128.6, 128.6, 125.9, 123.3, 120.0, 39.9, 34.5, 33.9, 28.8, 28.5, 26.8 26.7, 16.2.

Gas Chromatography Results

Enantiomeric excess (ee's) were determined on a HP-6890 GC using an Agilent β-Cyclosil column. Inlet temperature was maintained at 250°C, 19.99 psi H_2.

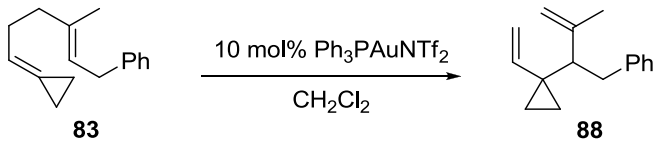

83 **88**

Initial: 80°C (5 min) *Ramp 1*: 2.0°C/min to 170°C (30 min)

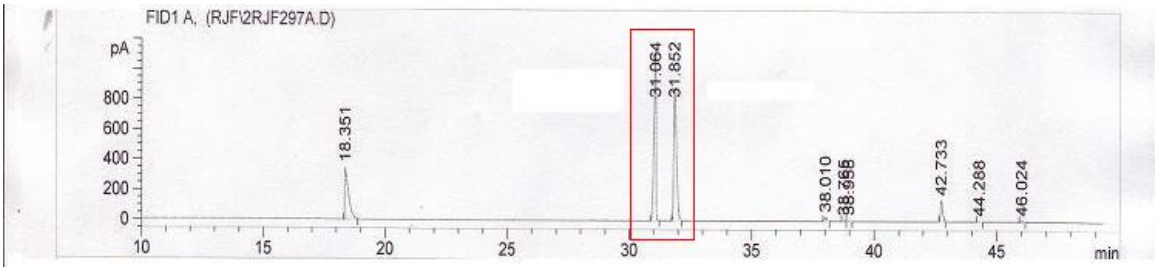

Signal 1: FID1 A,

Peak #	RetTime [min]	Type	Width [min]	Area [pA*s]	Height [pA]	Area %
1	18.351	BB	0.1283	3587.17651	343.44250	19.33022
2	31.064	BB	0.0818	6880.26758	1137.30103	37.07570
3	31.852	BB	0.0961	6878.80225	886.57819	37.06780
4	38.010	PB	0.0777	151.59846	25.96917	0.81692
5	38.765	BV	0.0722	34.87588	6.17979	0.18794
6	38.958	VB	0.0740	36.81094	6.43266	0.19836
7	42.733	BB	0.0791	874.75201	138.75943	4.71378
8	44.288	BP	0.0731	28.37593	4.90221	0.15291
9	46.024	BP	0.0664	47.55323	8.67448	0.25625
10	53.411	BB	0.0841	37.13955	5.35386	0.20013
Totals :				1.85574e4	2563.59331	

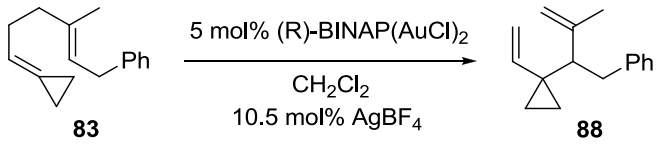

83 **88**

Initial: 80°C (5 min) *Ramp 1*: 2.0°C/min to 170°C (30 min)

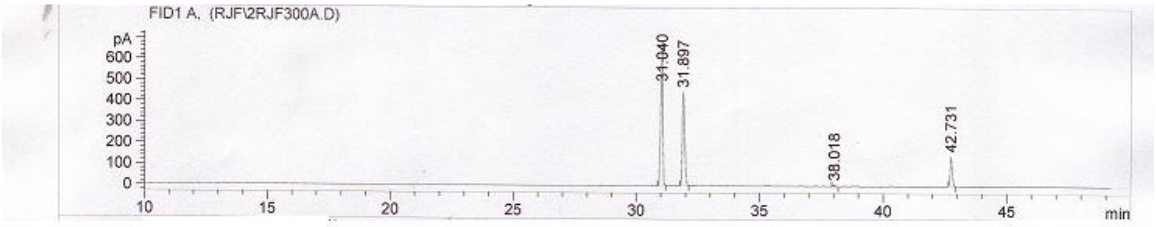

Signal 1: FID1 A,

Peak #	RetTime [min]	Type	Width [min]	Area [pA*s]	Height [pA]	Area %
1	31.040	BB	0.0760	4052.35669	687.12292	50.85804
2	31.897	BB	0.0864	2997.06396	446.25327	37.61387
3	38.018	BB	0.0715	37.64063	6.66853	0.47240
4	42.731	BB	0.0801	880.91492	142.46346	11.05569
Totals :				7967.97620	1282.50818	

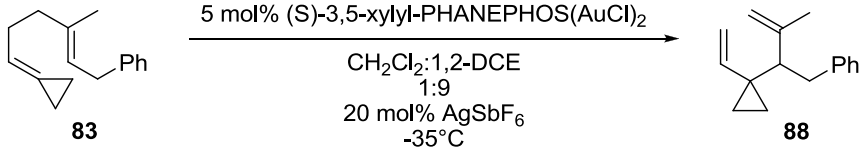

83 **88**

Initial: 80°C (14 min) *Ramp 1*: 2.0°C/min to 130°C (0 min) *Ramp 2*: 20°C/min to 170°C (7 min)

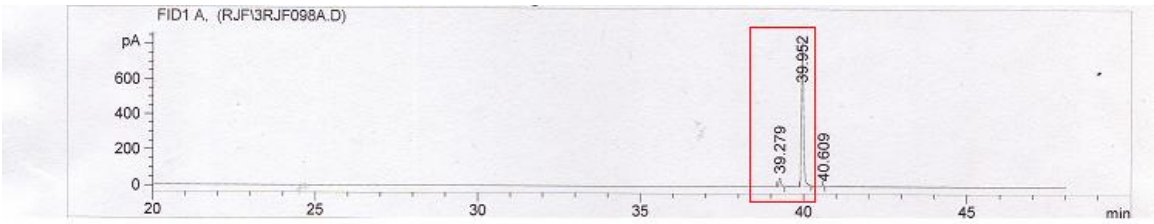

Signal 1: FID1 A,

Peak #	RetTime [min]	Type	Width [min]	Area [pA*s]	Height [pA]	Area %
1	39.279	BB	0.0643	239.81931	47.64743	6.49692
2	39.952	PB	0.0583	3447.78027	812.22766	93.40341
3	40.609	BB	0.0293	3.67938	1.75539	0.09968
Totals :				3691.27896	861.63048	

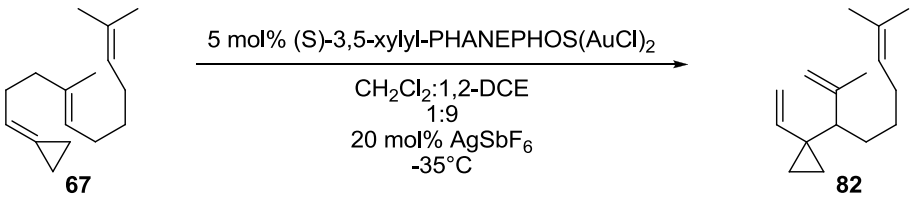

67 **82**

Initial: 60°C (14 min) *Ramp 1*: 5.0°C/min to 100°C (10 min) *Ramp 2*: 10°C/min to 130°C (10 min)

Ramp 3: 10°C/min to 170°C (0 min)

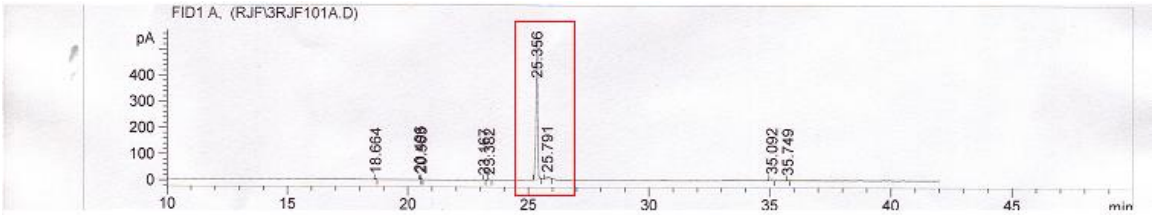

Signal 1: FID1 A,

Peak #	RetTime [min]	Type	Width [min]	Area [pA*s]	Height [pA]	Area %
1	3.689	BB	0.0413	20.53978	7.75835	0.74254
2	18.664	BB	0.0371	9.26258	3.81891	0.33485
3	20.496	BV	0.0330	19.74739	9.52839	0.71389
4	20.563	VB	0.0310	10.96064	5.55833	0.39624
5	23.167	BB	0.0411	4.65947	1.72743	0.16845
6	23.382	PB	0.0474	9.05670	3.12747	0.32741
7	25.356	PB	0.0696	2555.77490	539.78345	92.39462
8	25.791	PB	0.1222	97.33476	9.48041	3.51878
9	35.092	BB	0.0582	26.40583	6.44400	0.95461
10	35.749	PB	0.0525	12.40914	3.37542	0.44861
Totals :				2766.15120	590.60217	

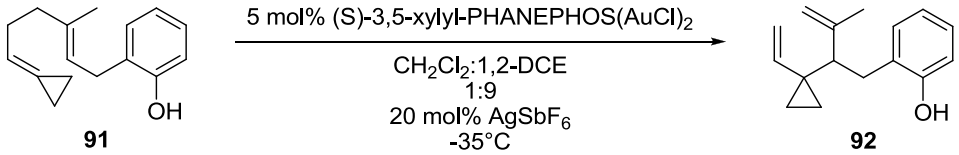

91 **92**

Initial: 100°C (10 min) *Ramp 1*: 2.0°C/min to 130°C (5 min) *Ramp 2*: 5.0°C/min to 170°C (20 min)

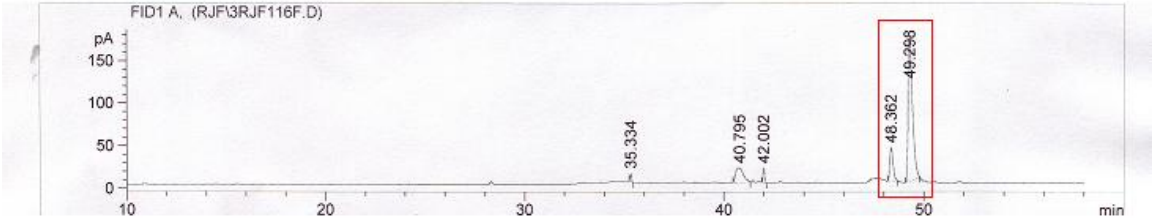

Signal 1: FID1 A,

Peak #	RetTime [min]	Type	Width [min]	Area [pA*s]	Height [pA]	Area %
1	2.091	BB	0.0239	4.95926	3.03597	0.13714
2	35.334	BP	0.0631	48.37317	10.23862	1.33770
3	40.795	BB	0.3064	449.57294	17.25171	12.43242
4	42.002	PB	0.0805	96.58465	17.47247	2.67094
5	48.362	PB	0.1344	446.71997	39.49307	12.35352
6	49.298	PB	0.1806	2569.92480	169.01466	71.06828
Totals :				3616.13479	256.50651	

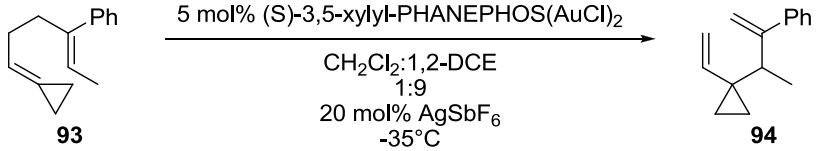

93 **94**

Initial: 80°C (14 min) *Ramp 1*: 2.0°C/min to 130°C (0 min) *Ramp 2*: 20°C/min to 170°C (7 min)

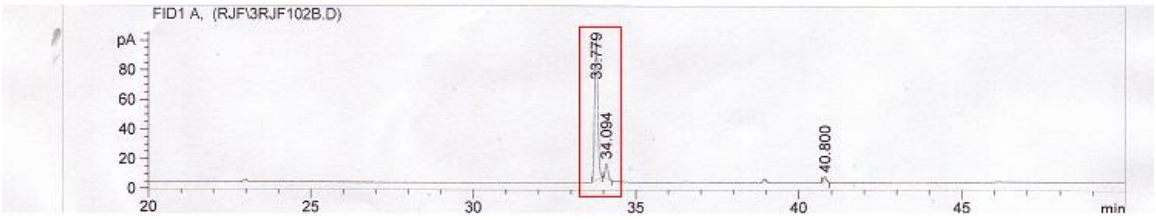

Signal 1: FID1 A,

Peak #	RetTime [min]	Type	Width [min]	Area [pA*s]	Height [pA]	Area %
1	33.779	PB	0.0833	638.82385	94.93727	87.86691
2	34.094	PP	0.0782	61.79708	10.03902	8.49987
3	40.800	BB	0.0850	26.41479	3.95970	3.63322
Totals :				727.03573	108.93599	

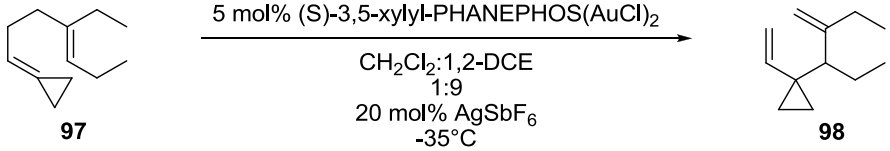

97 **98**

Initial: 60°C (14 min) *Ramp 1*: 10°C/min to 170°C (10 min)

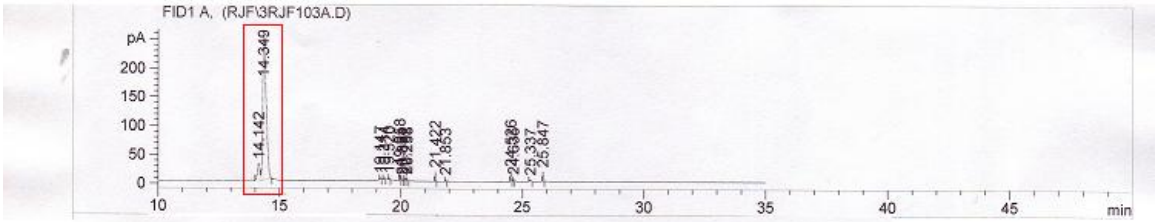

Signal 1: FID1 A,

Peak #	RetTime [min]	Type	Width [min]	Area [pA*s]	Height [pA]	Area %
1	3.693	BB	0.0387	9.44923	3.79004	0.32730
2	14.142	BV	0.1130	218.44730	28.90483	7.56651
3	14.349	VB	0.1450	2463.99634	247.37848	85.34711
4	19.147	BB	0.0370	8.85403	3.65790	0.30668
5	19.314	PB	0.0359	7.43450	3.20224	0.25751
6	19.520	BP	0.0356	7.12740	3.19425	0.24688
7	19.958	BB	0.0313	34.99399	17.49883	1.21211
8	20.054	BB	0.0328	3.94372	1.85828	0.13660
9	20.162	BB	0.0309	7.57995	3.85682	0.26255
10	20.258	BP	0.0310	7.78298	3.94491	0.26958
11	21.422	BB	0.0267	27.71542	16.59258	0.96000
12	21.853	PP	0.0261	5.39276	3.32735	0.18679
13	24.526	BP	0.0320	35.67371	17.95411	1.23565
14	24.635	PB	0.0268	7.60393	4.34342	0.26338
15	25.337	PB	0.0383	8.25134	3.01471	0.28581
16	25.847	BP	0.0322	32.78294	16.36681	1.13553
Totals :				2887.02954	378.88555	

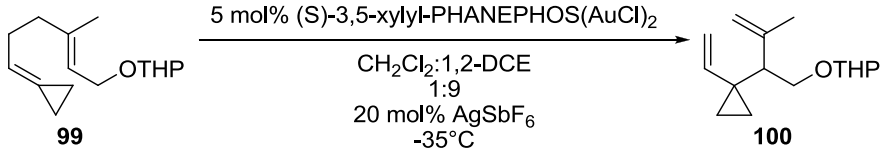

99 **100**

Initial: 80°C (10 min) *Ramp 1*: 1.0°C/min to 100°C (10 min) *Ramp 2*: 1.0°C/min to 110 (15 min) *Ramp 3*: 1.0°C/min to 115°C (12 min) *Ramp 4*: 1°C/min 120 (10 min) *Ramp 5*: 20°C/min to 170°C (7 min)

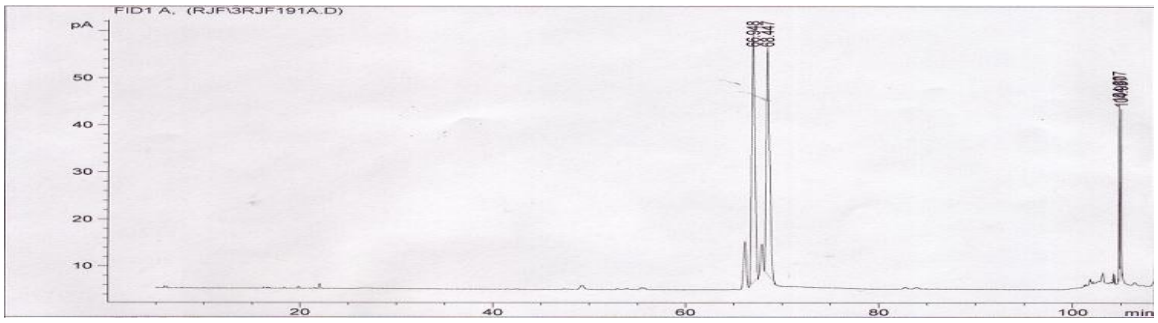

Signal 1: FID1 A,

Peak #	RetTime [min]	Type	Width [min]	Area [pA*s]	Height [pA]	Area %
1	66.147	PV	0.3196	203.32793	10.03438	6.26077
2	66.946	VV	0.3472	1302.15051	53.64042	40.09513
3	67.901	VV	0.3445	204.95366	9.04174	6.31082
4	68.443	VB	0.3930	1312.88062	50.48575	40.42552
5	105.002	VB	0.0959	224.33992	35.60491	6.90776
Totals :				3247.65263	158.80720	

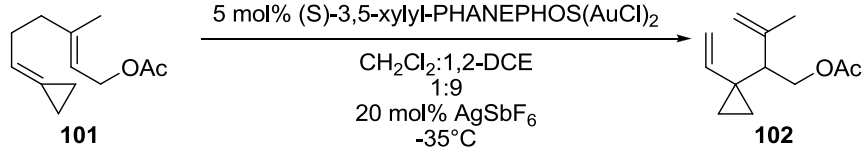

101 **102**

Initial: 100°C (10 min) *Ramp 1*: 2°C/min to 130°C (5 min) *Ramp 2*: 5°C/min to 170°C (20 min)

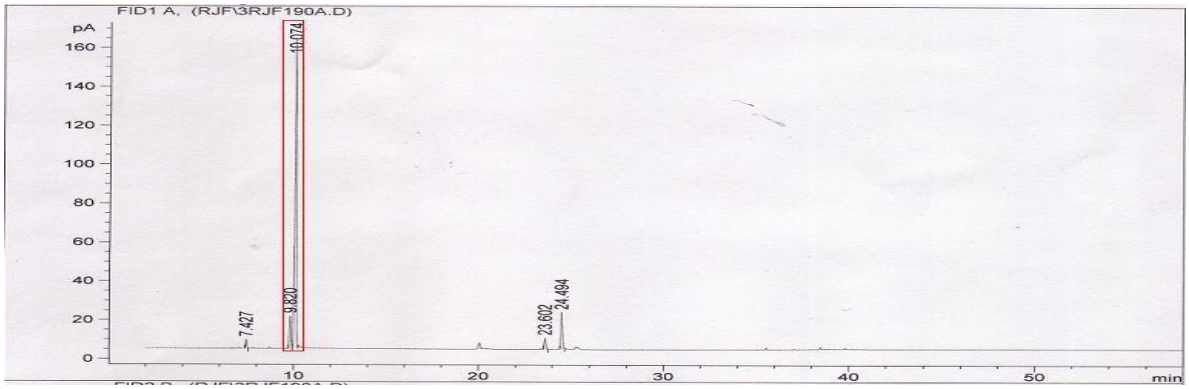

Signal 1: FID1 A,

Peak #	RetTime [min]	Type	Width [min]	Area [pA*s]	Height [pA]	Area %
1	7.427	PB	0.0673	19.44063	4.56688	1.63949
2	9.820	BV	0.0882	93.14408	16.30516	7.85512
3	10.074	VB	0.0909	929.99030	158.30988	78.42885
4	23.602	BB	0.0912	32.36367	5.68944	2.72932
5	24.494	BB	0.0937	110.83716	18.77416	9.34723
Totals :				1185.77584	203.64552	

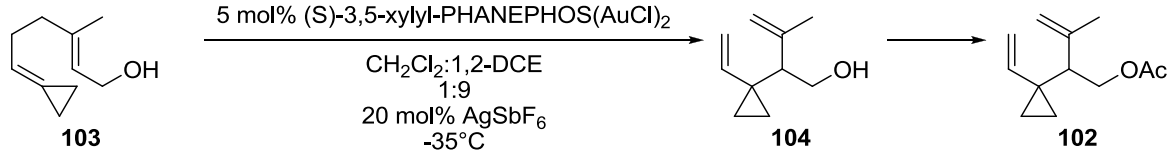

103 **104** **102**

Initial: 100°C (10 min) *Ramp 1*: 2°C/min to 130°C (5 min) *Ramp 2*: 5°C/min to 170°C (20 min)

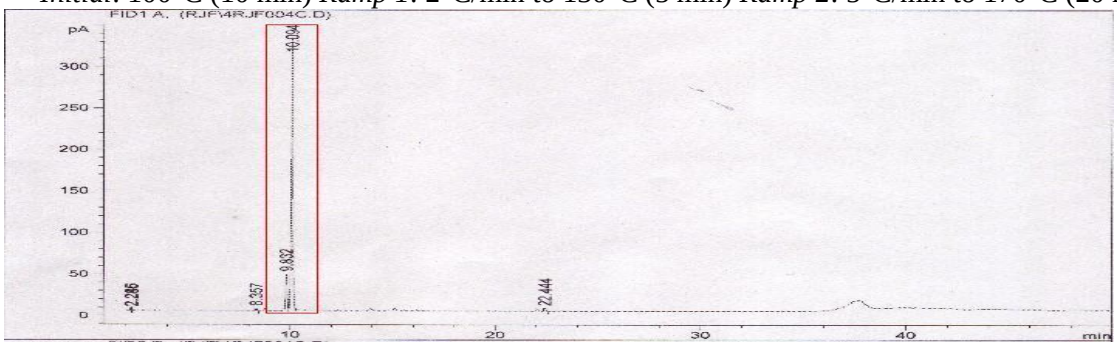

Signal 1: FID1 A,

Peak #	RetTime [min]	Type	Width [min]	Area [pA*s]	Height [pA]	Area %
1	2.246	PV	0.0280	3.91561	2.11341	0.17742
2	2.285	VB	0.0213	2.41829	1.70988	0.10957
3	8.357	BB	0.0712	13.81585	2.91884	0.62600
4	9.832	BV	0.0930	261.71375	43.74424	11.85830
5	10.094	VB	0.0872	1906.02380	327.19940	86.36231
6	22.444	BB	0.0893	19.12160	3.37252	0.86640
Totals :				2207.00889	381.05829	

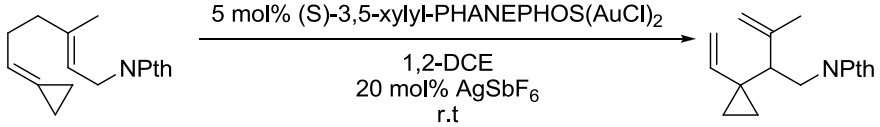

105 **106a**

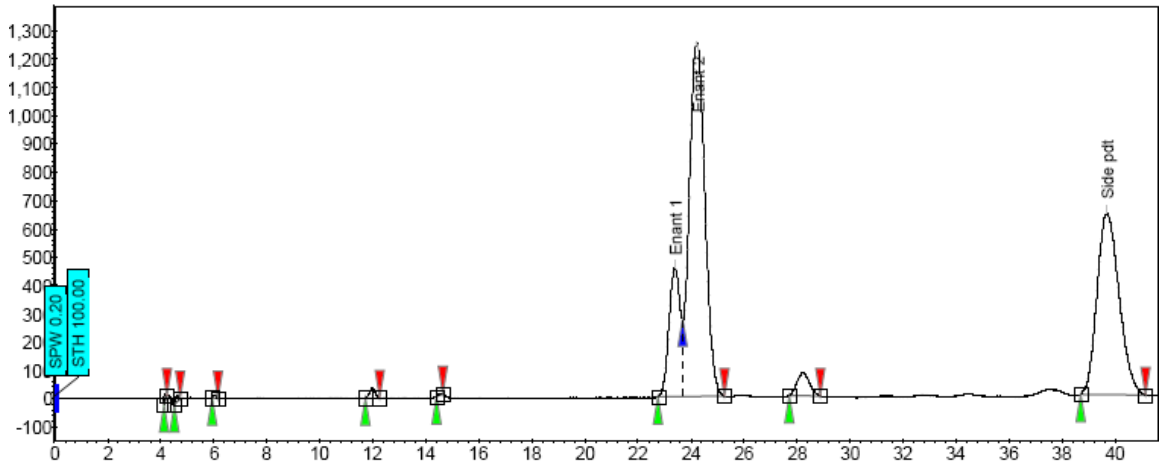

Index	Name	Start	Time	End	RT Offset	Quantity	Height	Area	Area
		[Min]	[Min]	[Min]	[Min]	[% Area]	[µV]	[µV.Min]	[%]
1	UNKNOWN	4.13	4.15	4.24	0.00	0.10	30.0	1.7	0.098
2	UNKNOWN	4.52	4.59	4.73	0.00	0.17	22.3	2.9	0.165
3	UNKNOWN	5.95	6.04	6.16	0.00	0.05	8.0	0.9	0.050
4	UNKNOWN	11.72	11.96	12.25	0.00	0.46	34.2	8.0	0.458
5	UNKNOWN	14.39	14.53	14.63	0.00	0.04	5.4	0.8	0.044
6	Enant 1	22.76	23.39	23.69	0.00	12.77	457.0	224.0	12.774
7	Enant 2	23.69	24.22	25.25	0.00	48.72	1253.8	854.1	48.716
8	UNKNOWN	27.71	28.22	28.87	0.00	2.49	80.4	43.7	2.492
9	Side pdt	38.68	39.68	41.13	0.00	35.20	644.0	617.2	35.203
Total						100.00	2535.0	1753.2	100.000

Chapter 3 - Au(I)-Catalyzed Ring Expansions

Hypothesis – Ring Expansion to Medium-Sized Rings

With the discovery and development of a Au(I)-catalyzed Cope rearrangement, driven by the release of ring strain in the methylenecyclopropane functional group, the next step was exploring what other reactions and rearrangements could be rendered energetically favorable by harnessing this ring strain. One rearrangement envisioned was the ring expansion of cyclic substrates to provide medium sized rings (Figure 3.1). For instance, if a Cope rearrangement is initiated at the cyclopropylidene moiety, cyclohexyl substrate **127a** could be predicted to proceed through the tricyclic intermediate **128**, before completing the rearrangement to cyclooctene **129.** Likewise, cyclopentyl (**130a**) and cycloheptyl (**132**) substrates could theoretically produce cycloheptene and cyclononene (**131** and **133**, respectively) products.

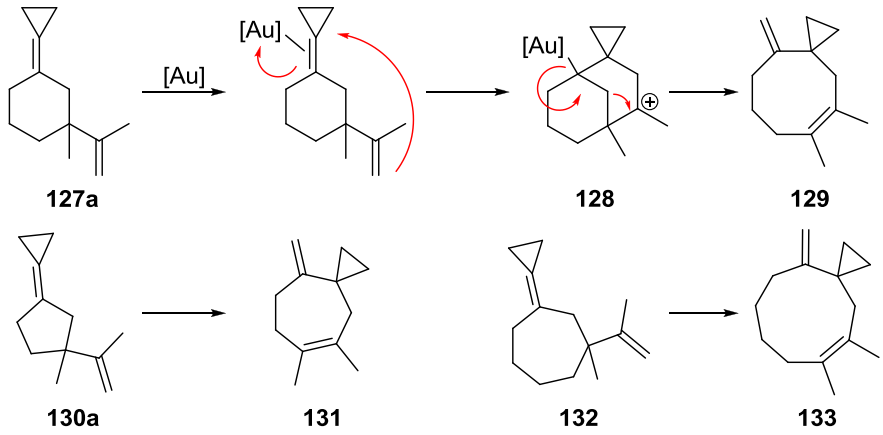

Figure 3.1. Proposed synthesis of medium sized rings.

Density functional calculations were carried out using Mac Spartan (B3LYP/6-31G(d))

to predict whether this rearrangement would be thermodynamically favorable. The rearrangement of **127** to **129** was calculated to be exothermic by ca. 9 kcal/mol, indicating that relief of ring strain from the methylenecyclopropane could serve as the driving force for the creation of medium-sized rings, which have their own inherent ring and steric strain.

Medium-Sized Rings

While not as abundant in natural products as 5- and 6-membered rings, medium-sized rings (7-12 membered rings) are still present in a variety of compounds with biological relevance (Figure 3.2).[79] The construction of medium-sized carbocycles is relatively challenging, although cycloaddition and metathesis reactions have been demonstrated to be effective in a number of synthetic settings.[79c-d,80] Even with a recent increase in research focusing on accessing these structures, there is still a relatively limited number of effective approaches. It was in hopes of expanding the methodology for construction of medium-sized rings that the work reported in this chapter was undertaken.

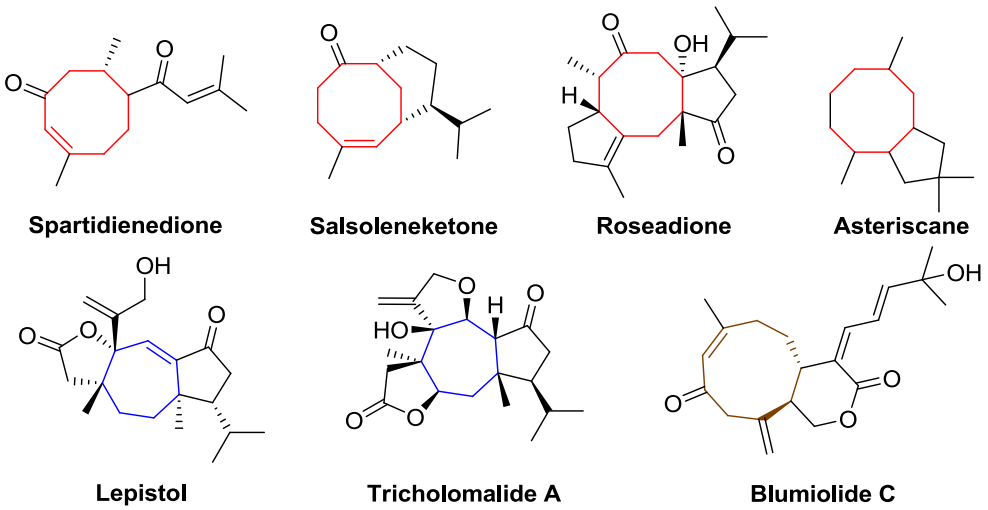

Figure 3.2. Natural products containing medium-sized rings.

[79] a) Hamel, C.; Prusov, E. V.; Gertsch, J.; Schweizer, B.; Altmann, K.-H. *Angew. Chem. Int. Ed.* **2008**, *47*, 10081. b) Williams, D. R.; Pinchman, J. R. *Can. J. Chem.* **2013**, *91*, 21. c) Mehta, G.; Singh, V. *Chem. Rev.* **1999**, *99*, 881. d) Petasis, N. A.; Patane, M. A. *Tetrahedron* **1992**, *48*, 5757.
[80] Prunet, J. *Eur. J. Org. Chem.* **2011**, 3634.

There exist both enthalpic and entropic factors that make accessing medium-sized rings more difficult than accessing smaller (5-6 membered) and larger ring structures. Ring strain arises in intermediate-sized rings primarily from two sources. The first is due to imperfect staggering of the carbon-carbon and carbon-hydrogen bonds, which results in unfavorable steric interactions. Whereas in the lowest energy conformation of cyclohexane the bonds are staggered to minimize torsional strain, in medium sized rings the geometry enforces conformations in which perfect staggering (60˚ bond angles) is not possible. This raises the energy of the ring structure. The second source of ring strain originates in the interaction of atoms across the ring coming into close proximity with one another (transannular strain). With the ring assuming a conformation to minimize torsional strain, atoms across the ring from one another can be forced close enough to experience steric repulsion.

The interplay of these two factors results in the large amounts of ring strain present in medium-sized rings.[81] For instance, the strain energy in cycloheptane has been estimated to be ca. 6-8 kcal/mol. This strain energy increases to a maximum at cyclodecane (estimated to be up to ca. 16 kcal/mol), [81a] then decreases as ring size increases further. With large rings (13-membered and up) the geometry of the ring allows for conformations that reduce both torsional and transannular strains.

In addition to the formation of medium sized rings being enthalpically less favorable than formation of smaller and larger rings, there is also an entropic barrier that must be overcome. In the formation of ring structures, of all sizes, from acyclic compounds, there is an unfavorable decrease in entropy due to a constriction of the degrees of freedom of bond rotations and molecular movement. In large rings this entropic penalty decreases as the ring becomes large enough to allow twisting and greater partial rotations in the carbon backbone.

It was postulated that harnessing the ring strain of the cyclopropylidene would provide the thermodynamic driving force necessary to overcome these barriers; this was supported by DFT

[81] a) Allinger, N. L.; Tribble, M. T.; Miller, M. A.; Wertz, D. H. *J. Am. Chem. Soc.* **1971**, *93*, 1637. b) Illuminati, G.; Mandolini, L. *Acc. Chem. Res.* **1981**, *14*, 95. c) Khoury, P. R.; Goddard, J. D.; Tam, W. *Tetrahedron* **2004**, *60*, 8103.

calculations. With the kinetic accessibility provided by Au(I) catalysts for the Cope rearrangement, the investigation was begun to develop a new method for accessing medium-sized rings.

Initial Explorations

The research began with exploration of substrate **127a**. The cyclic substrates employed in this investigation could be synthesized in two steps, as shown in Scheme 3.1. The synthesis began with a copper(I) mediated Michael addition to a cyclic enone (n = 1-3) to provide the product in a large range of yields. These reactions generally provided high yields (68-94%) when a commercially available Grignard reagent was employed, but reactions were less efficient when the Grignard reagent prepared from α-bromostyrene was utilized (18-58%). From the conjugate addition product, substrate could be prepared in low yield via Wittig reaction using the previously established conditions.[61]

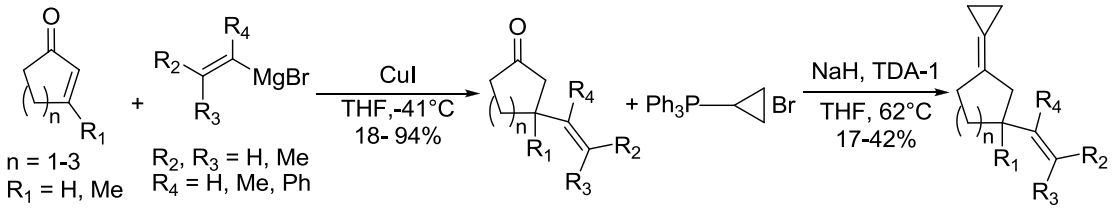

Scheme 3.1. Synthesis of cyclic substrates for creation of medium-sized rings.

This allowed the synthesis of a number of substrates with different ring sizes and pendant alkene substitution patterns (Figure 3.3).

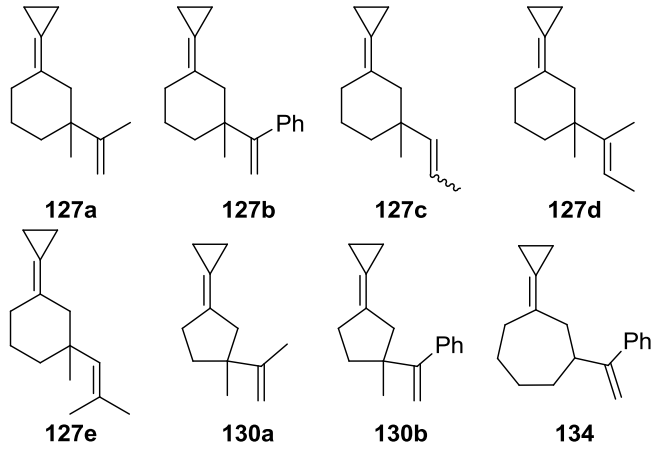

Figure 3.3. Substrates employed in attempted synthesis of medium-sized rings.

Initial reaction of substrate **127a** with the Gagosz catalyst, $Ph_3PAuNTf_2$, in DCM gave clean conversion over 12 hours at room temperature to provide a single product in 76% isolated yield (Scheme 3.2). Upon inspection of the ^1H NMR spectrum of the product of this reaction, it became immediately apparent that the compound could not be the expected cyclooctene product (**129**). Only a single vinyl proton signal (integration - 1 hydrogen) was observed. The shift of this proton was also downfield (ca. 5.2 ppm) of typical geminal vinyl protons on a disubstituted alkene (ca. 5.0-4.6 ppm). Another interesting piece of the puzzle was the observation of only two vinyl signals in the ^{13}C NMR spectrum for this compound, indicating clearly that the single product formed could not be **129**, which would have four vinyl signals. Unfortunately, overlapping signals in in the ^1H NMR spectrum made definitive compound identification problematic. To overcome this problem substrate **127b** was synthesized. It was postulated that the presence of the phenyl ring could potentially induce shift differences in both proton and carbon signals great enough to allow the structure of the product to be deduced.

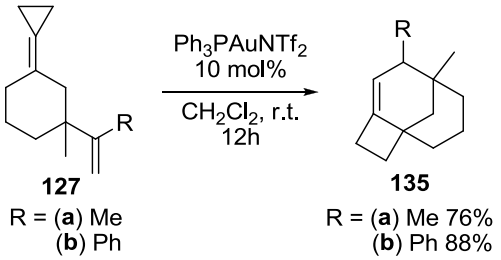

Scheme 3.2. Reaction of substrates 127a/b with Gagosz catalyst.

Reacting **127b** under identical conditions to **127a** again led to complete conversion to a single product over 12h (Scheme 3.2). This product could be isolated in slightly higher yield (88%) than the methyl analog. Fortunately, the aromatic ring did induce large enough shift differences to allow the structure of the product compound to be assigned as **135b**. The assignment of **135a** was made based on similarities in the ^1H and ^{13}C NMR spectra.

Assignment of the ring structure was made possible by an in-depth analysis of the 1D and 2D NMR spectra acquired for **135b**, which will be discussed in more detail in the next section (see Product Identification). Correlations from the NOESY spectrum that were vital to assigning the

structure are shown in Figure 3.4. The phenyl ring was assigned to the concave face of the molecule through a correlation between H_A (7.35 ppm) and H_B (1.85 ppm), but not between H_A and H_C (1.50 ppm) (Figure 3.4a), as well as the signal between H_D (3.40 ppm) and H_E (1.75 ppm) (Figure 3.4b). The *cis*-ring configuration was assigned by the key interactions between the diaxially oriented H_E (1.75 ppm) and H_F (1.85 ppm), H_G (1.90 ppm) with H_I (2.90 ppm) (Figure 3.4c), and the supporting resonance between H_A and H_B.

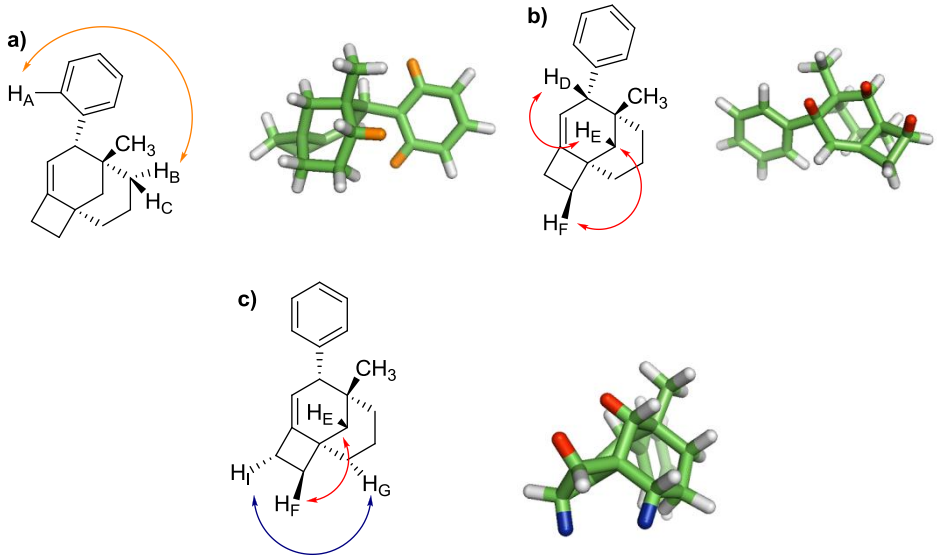

Figure 3.4. Selected NOESY correlations in NMR spectrum of 135b.

The 3D models in Figure 3.4 were made in PyMOL from the lowest energy conformer found in conformer distribution calculations performed using Mac Spartan '10 at the B3LYP 6-31G(d) level of theory.[73] These calculations were performed to determine whether the formation of compound **135b** from **127b** was thermodynamically favorable. If the calculations predicted **135b** to be energetically uphill this would indicate the assignment of the structure was most likely incorrect. Surprisingly, **135b** is predicted to be ca. 25.7 kcal/mol lower energy than **127b**. This large decrease in energy is attributed primarily to two energetically favorable processes: release of ring strain from the cyclopropylidene moiety and the conversion of a π-bond to a σ-bond. This highly exothermic

process produces a unique bicyclo[4.2.0]oct-1ene core, a skeletal feature of a number of natural products such as welwitindolinone A, and the protoilludane class of sesquiterpenes (Figure 3.5).[82]

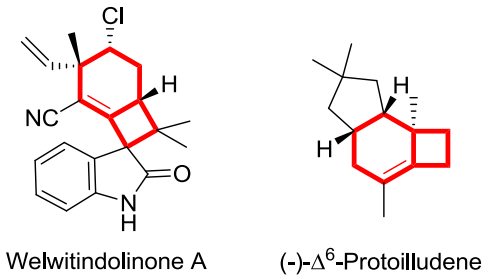

Figure 3.5. Natural products with a bicyclo[4.2.0]oct-1-ene core.

Two potential mechanistic pathways for this rearrangement are shown in Figure 3.6. The first pathway begins with coordination of the Au(I) complex to the cyclopropylidene. This initiates a Cope rearrangement that produces cyclooctene **129** (exothermic by ca. 9 kcal/mol relative to uncomplexed **127a**). At this point coordination of the Au(I) complex to the endocyclic olefin in **129** can initiate another Cope rearrangement, leading to carbocation **136**. Ring expansion from **136** would lead to tricyclic intermediate **137**, which upon deprotonation and protodemetallation would provide the product compound **135a**. The second pathway begins with coordination of Au(I) to the pendant alkene. Initiation of a Cope rearrangement at this π-bond can provide access to intermediate **136** directly, giving the final product (**135a**) via a single Cope rearrangement. The energetics of these two potential pathways will be discussed in greater detail below (see Thermodynamic and Kinetic Considerations).

[82] a) Siengalewicz, P.; Mulzer, J.; Rinner, U. *Eur. J. Org. Chem.* **2011**, *35*, 7041. b) El-Hachach, N.; Gerke, R.; Noltemeyer, M.; Fitjer, L. *Tetrahedron* **2009**, *65*, 1040. c) Zu, L.; Xu, M.; Lodewyk, M. W.; Cane, D. E.; Peters, R. J.; Tantillo, D. J. *J. Am. Chem. Soc.* **2012**, *134*, 11369. d) Abraham, W.-R. *Curr. Med. Chem* **2001**, *8*, 583.

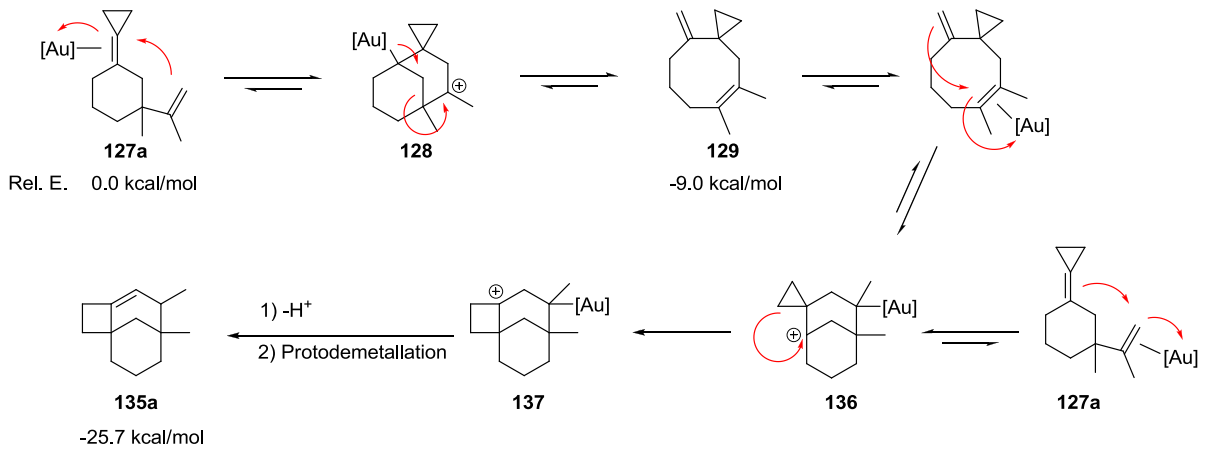

Figure 3.6. Potential mechanistic pathways for rearrangement of compound 127.

Product Identification

For the analysis of the NMR spectra of compound **135b**, the labeling scheme shown in Figure 3.7 will be used. Carbon atoms are numbered 1-16, starting with the phenyl-substituted allylic carbon and proceeding in a counter-clockwise fashion. For the protons, the labeling system is adapted from the one used above, with protons being assigned as $H_{A\text{-}N}$.

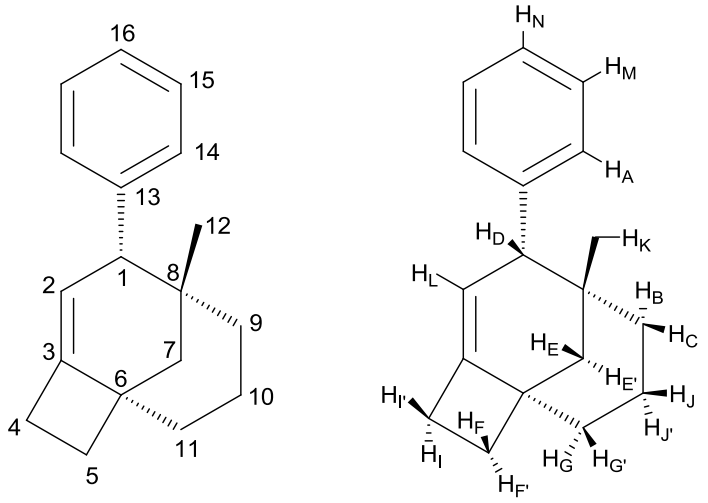

Figure 3.7. Labeling scheme employed for discussion of NMR spectra of compound 135b.

Table 3.1 gives the shifts (referenced to residual solvent in $CDCl_3$) for the carbon atoms and their associated protons. Analysis of the NMR spectra of **135b** is complicated by overlap of proton resonances both downfield in the aromatic region and upfield of 2 ppm. The aromatic region is composed of 2 multiplets. One, at 7.31-7.26 ppm, integrates to 4 protons - H_A and H_M corresponding

to C14 and C15 (130.0/127.8 ppm), respectively. The second multiplet appears at 7.22-7.20 ppm and represents a single proton H_N/C16 (126.2 ppm). Assignment of the overlapping, upfield resonances is more complicated, but possible by careful examination of the HSQC spectra, shown in Figure 3.8-3.9.

Table 3.1. Carbon and hydrogen atom shifts of compound 135b.

Carbon Atom	Carbon δ (ppm)	Hydrogen Atom	Hydrogen δ (ppm)
1	55.4	H_D	3.35
2	119.4	H_L	5.37
3	145.2	-	-
4	29.3	H_I	2.95-2.88
		$H_{I'}$	2.59
5	32.6	H_F	1.84-1.76
		$H_{F'}$	1.84-1.76
6	46.4	-	-
7	49.7	H_E	1.70
		$H_{E'}$	1.45-1.41
8	36.3	-	-
9	22.5	H_B	1.84-1.76
		H_C	1.45-1.41
10	35.4	H_J	0.79
		$H_{J'}$	1.07-1.04
11	33.7	H_G	1.91-1.88
		$H_{G'}$	1.45-1.41
12	31.4	H_K	0.97
13	142.7	-	-
14	130.0[a]	H_A	7.31-7.26
15	127.8[a]	H_M	7.31-7.26
16	126.2	H_N	7.22-7.20

[a] 2 pairs of equivalent aromatic carbons could not be assigned specifically as C14 or C15 due to overlap of aromatic proton shifts in the ^{1}H NMR spectrum, as a result the shifts assigned in the table are not to be considered definitive.

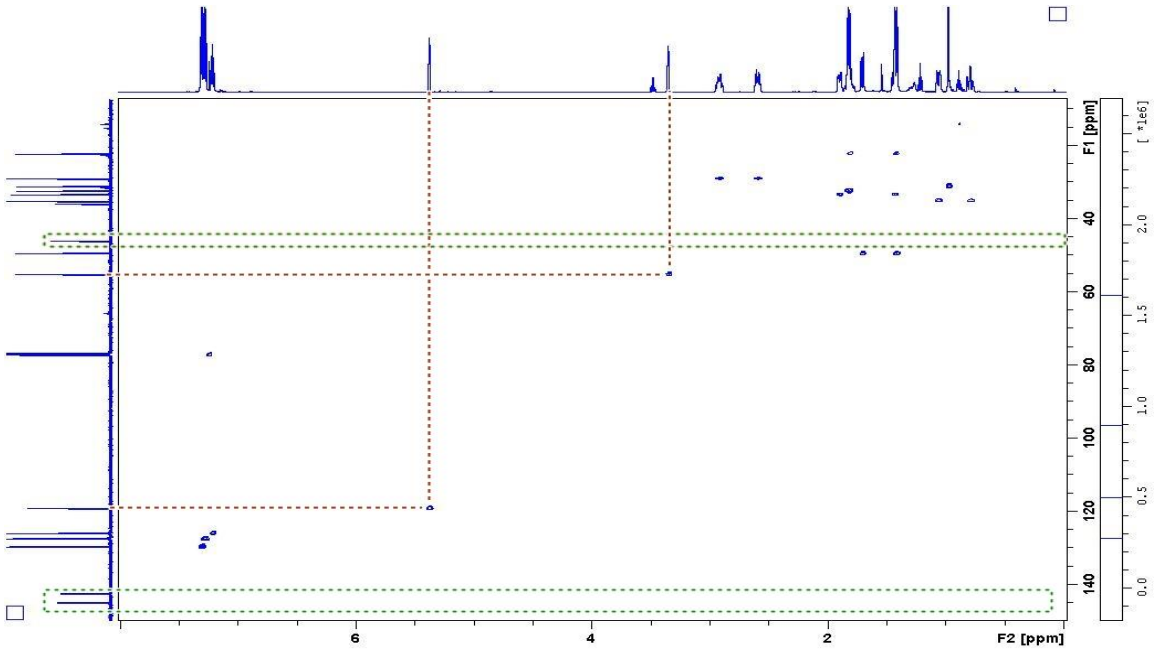

Figure 3.8. Full spectrum of HSQC of compound 135b (F2: 8.0-0.0 ppm).

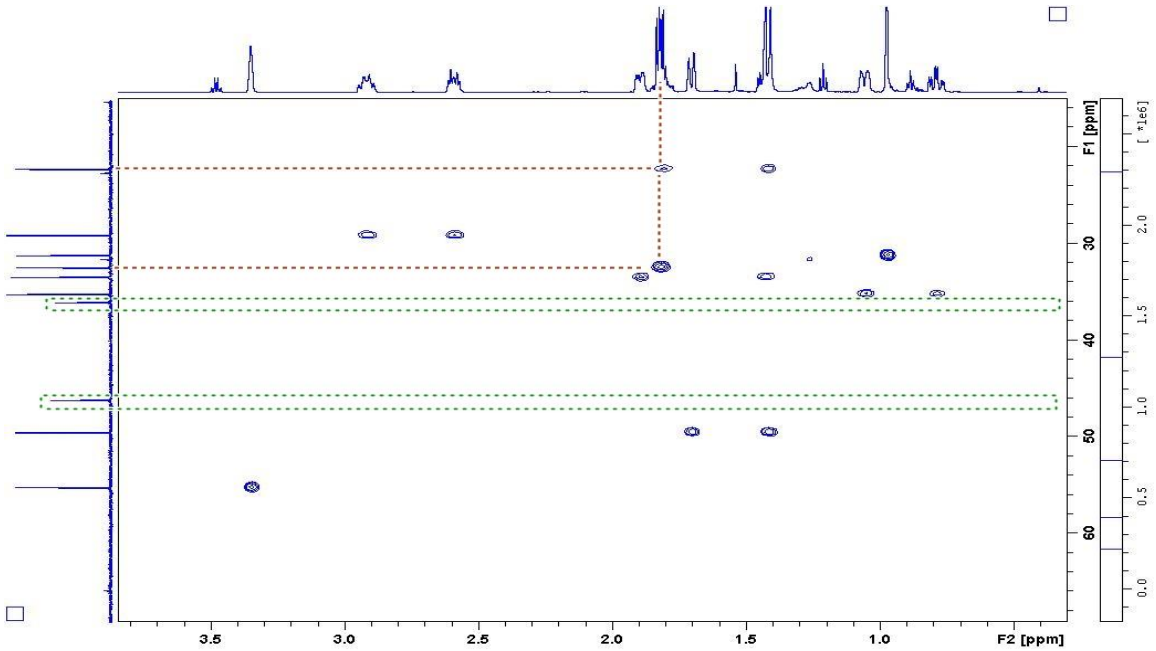

Figure 3.9. Expanded view of HSQC of 135b (F2: 3.8-0.0 ppm).

Figure 3.8 clearly shows that the one vinyl proton, H_L (5.37 ppm) is on the carbon whose resonance appears at 119.4 (C2). It can also been seen from Figure 3.8 and Figure 3.9 that the carbons at 145.7 ppm (C3), 142.7 ppm (C13), 46.4 ppm (C6) and 36.3 ppm (C8) are quaternary

carbons. The benzylic proton, H_D, has a characteristic shift of 3.35 ppm and is attached to C1 (55.4 ppm), as show in Figure 3.9.

Figure 3.9 allows the assignment of the rest of the protons to their corresponding carbon atoms. It is revealed that the resonances at 2.90 ppm and 2.59 ppm are diastereotopic protons (H_I/$H_{I'}$, respectively) on the carbon at 29.3 ppm (cyclobutane carbon C4). Two diastereotopic protons, one at 1.90 ppm (H_G) and one of the three resonances at 1.45-1.41 ppm ($H_{G'}$) are attached to C11 (33.7 ppm). The multiplet at 1.84-1.76 ppm is composed of three protons, two protons (H_F/$H_{F'}$) are attached to C5 whose resonance appears at 32.6 ppm. The third proton at 1.84-1.76 is H_B, one of the protons attached to C9 (22.5 ppm). The second proton attached to C9, H_C, is one of the three protons composing the multiplet at 1.45-1.41 ppm. The proton resonance at 1.70 ppm, H_E, is one of the two diastereotopic protons attached to C7 (49.7 ppm) with the second proton resonance in the multiplet at 1.45-1.41 ($H_{E'}$). Proton resonances at 1.07-1.04 ppm ($H_{J'}$) and 0.79 ppm (H_J) correspond to C10 (35.4 ppm). Lastly, the singlet at 0.97 ppm corresponds to the methyl H_K protons attached to C12 at 31.4 ppm.

The COSY spectrum of **135** is shown in Figure 3.10; expanded segments are shown in Figure 3.11- 3.12. It can be seen in Figure 3.10 that the vinyl proton H_L (5.37 ppm) has a correlation with the benzylic proton H_D (3.35 ppm); these two protons have no other correlations. Proton H_I (2.95-2.88 pm) has a correlation with the diastereotopic proton $H_{I'}$ (2.59 ppm) and both of these protons have correlations with the multiplet at 1.84-1.76 (H_F/$H_{F'}$). Proton H_G (1.91-1.88 ppm) has only a single correlation ($H_{G'}$, 1.45-1.41 ppm) in the COSY spectrum.

The multiplet at 1.84-1.76 is composed of 3 hydrogen atoms - cyclobutane protons H_F/$H_{F'}$ and proton H_B. Correlations from this multiplet can be seen in Figure 3.11 and Figure 3.12. As stated above, correlations to resonances at 2.95-2.88 ppm (H_I) and 2.59 ppm ($H_{I'}$) are from protons H_F/$H_{F'}$. Correlations from proton H_B can be seen to protons at 1.45-1.41 ppm (HC), 1.07-1.04 ppm ($H_{J'}$), and 0.79 ppm (H_J) (Figure 3.12).

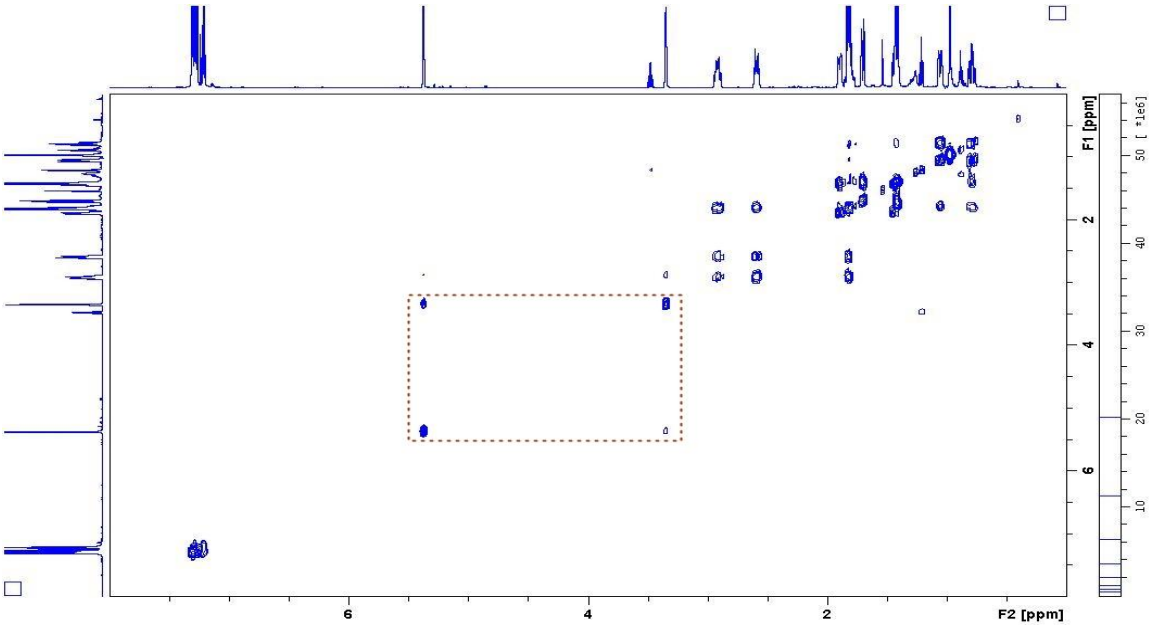

Figure 3.10. COSY spectrum of compound 135b.

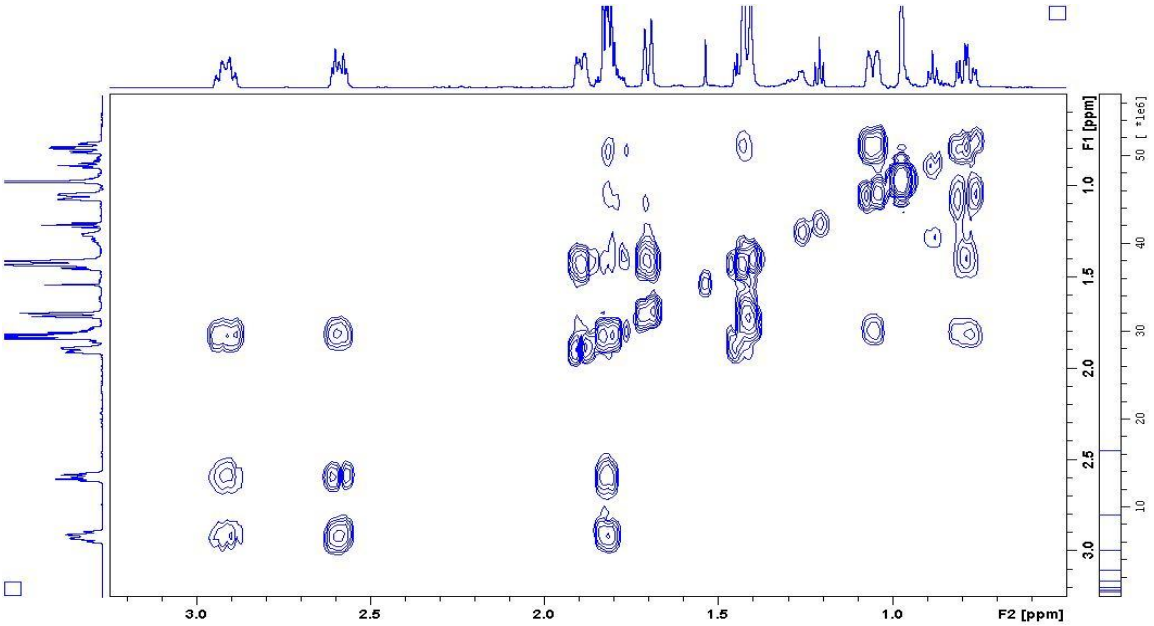

Figure 3.11. Expanded view of COSY of 135b (4.0-0.5 ppm).

Proton H_E (1.70 ppm) has only one correlation, that being with $H_{E'}$ (1.45-1.41 ppm). The multiplet at 1.45-1.41 is composed of three different hydrogens ($H_{G'}$, $H_{E'}$, H_C) and the correlations observed in the COSY can be identified as $H_{G'}$ with H_G (1.91-1.88 ppm), $H_{E'}$ with H_E (1.70 ppm), H_C

with H_B (1.84-1.76), and H_C with H_J (0.79 ppm). Proton $H_{J'}$ (1.07-1.04 ppm) has correlations with H_B (1.45-1.41 ppm) and H_J (0.79 ppm).

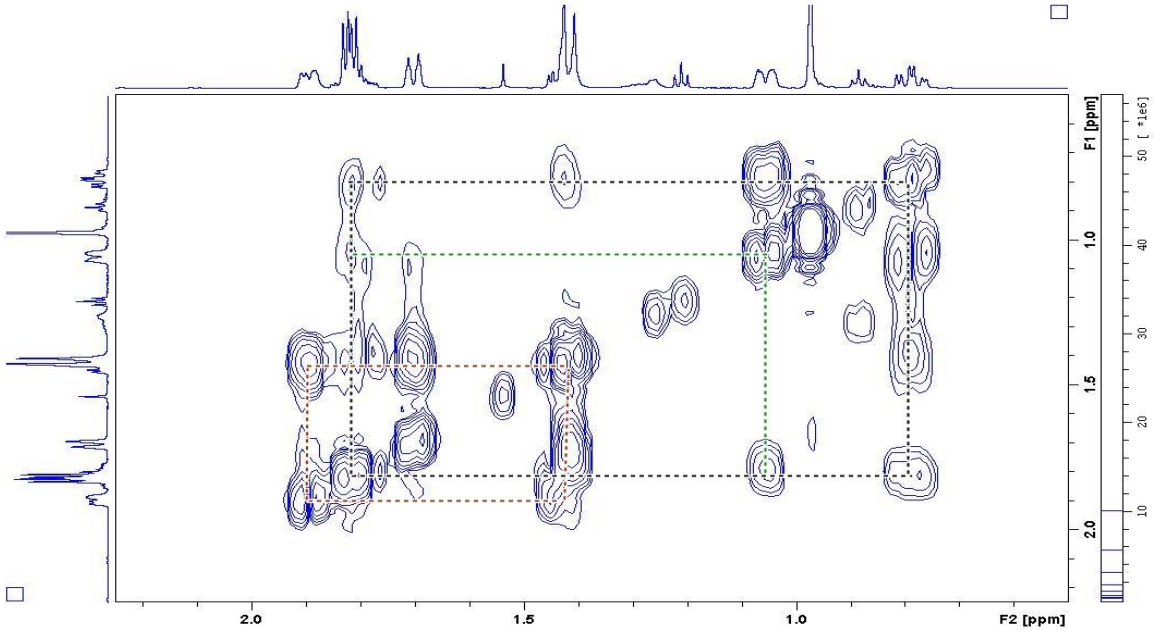

Figure 3.12. Expanded view of COSY of 135b (2.3-0.5 ppm).

The HMBC spectrum of compound **135b** also provides useful information in the deciphering of the compound structure (Figure 3.13- 3.16). Clearly visible is the correlation of C1 (55.4 ppm) to the aromatic multiplet at 7.31-7.26 (H_A). This carbon also has correlations with protons at 1.70 ppm (H_E), 1.45-1.41 ppm ($H_{E'}/H_C$), a long range coupling with the proton at 0.79 ppm (H_J) and a strong correlation with H_K (0.97 ppm). C2 (119.4 ppm) shows a weak correlation with H_D (3.35 ppm). C3 (145.2 ppm) shows correlations with H_D (3.35 ppm) H_I (2.95-2.88 ppm) and $H_{I'}$ (2.59 ppm), H_F and/or $H_{F'}$ (1.84-1.76 ppm), and $H_{E'}$ and/or $H_{G'}$ (1.45-1.41 ppm). C4 (29.3 ppm) only shows correlations with $H_F/H_{F'}$ (1.84-1.76 ppm). C5 (32.6 ppm) shows correlations with $H_I/H_{I'}$ on C4 (2.95-2.88, 2.59 ppm) and a correlation to the multiplet at 1.45-1.41 ppm ($H_{G'}$). Quaternary carbon C6 (46.4 ppm) shows correlations with H_L (5.37 ppm), $H_{I'}$ (2.59 ppm), H_G (1.91-1.88 ppm), $H_F/H_{F'}$ (1.84-1.76 ppm), H_E (1.70 ppm), and $H_{E'}$ and/or $H_{G'}$ (1.45-1.41).

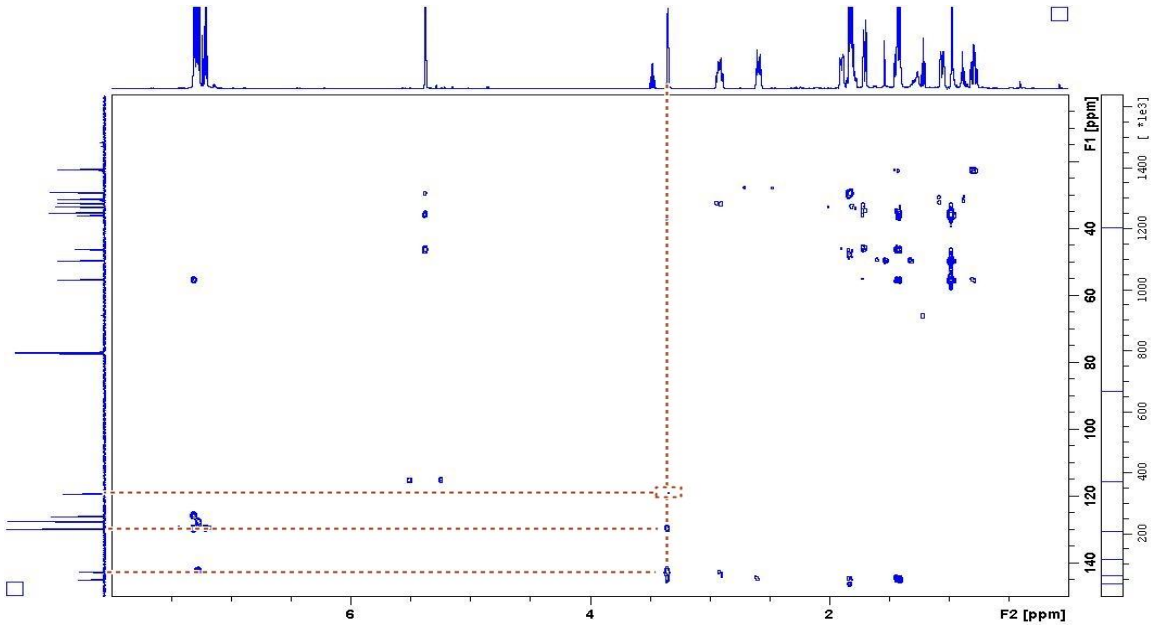

Figure 3.13. HMBC spectrum of 135b.

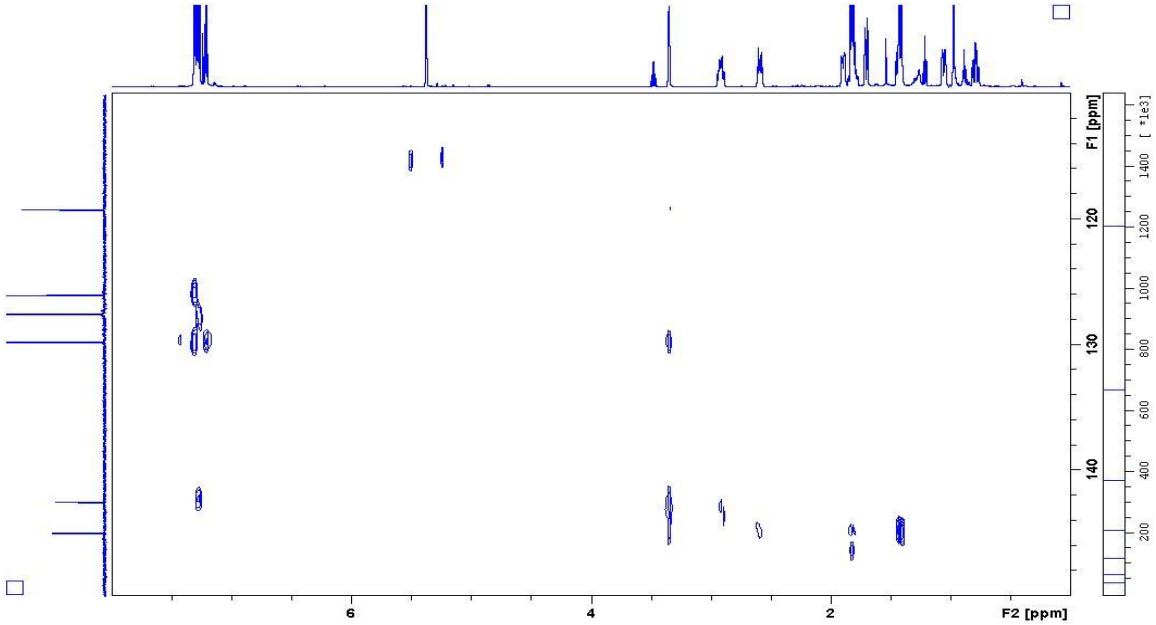

Figure 3.14. Expanded view of HMBC of 135b. F1: 150-110 ppm F2: 8.0-0.0 ppm

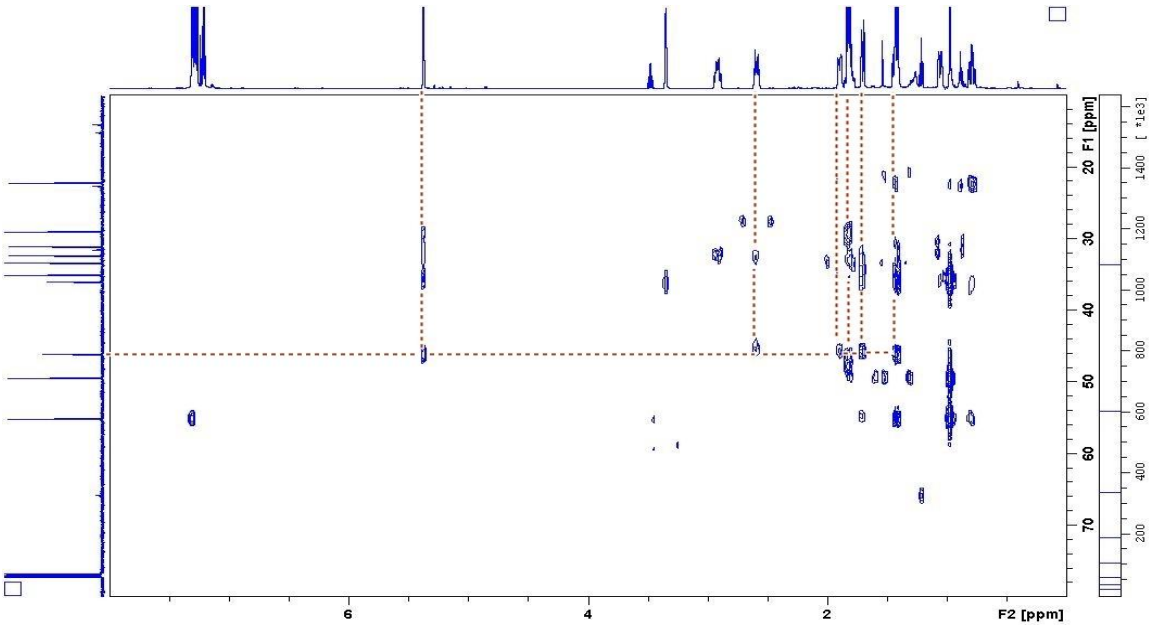

Figure 3.15. Expanded view of HMBC of 135b. F1: 80-0 ppm F2: 8.0-0.0 ppm.

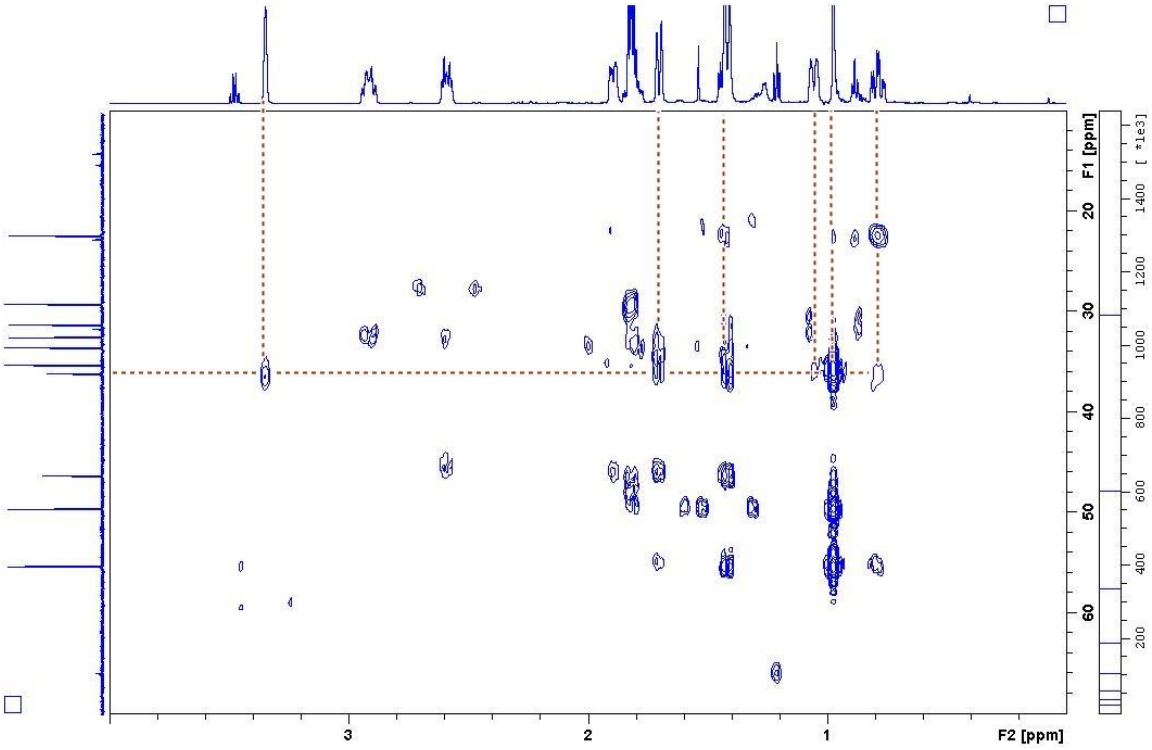

Figure 3.16. Exanded view of HMBC of 135b. F1: 70-0 ppm F2: 4.0-0.0 ppm.

C7 (49.7 ppm) demonstrates a correlation with the methyl protons H_K (0.97 ppm). Quaternary carbon C8 (36.3 ppm) has correlations with H_L (5.37 ppm), H_D (3.35 ppm), H_E (1.70 ppm), $H_{E'}$ and/or H_C (1.45-1.41 ppm), H_K (0.97 ppm) and weak correlations with $H_{J'}$ (1.07-1.04 ppm)

and H_J (0.79 ppm). C9 (22.5 ppm) shows a weak correlation with H_G (1.91-1.88 ppm), as well as correlations with $H_{G'}$ (1.45-1.41 ppm), H_K (0.97 ppm) and H_J (0.79 ppm). C10 (35.4 ppm) shows correlations with H_E (1.70 ppm), H_C and/or $H_{G'}$(1.45-1.41 ppm), and H_K (0.97 ppm). C11 shows correlations with protons H_F/$H_{F'}$ and/or H_B (1.84-1.76 ppm), H_E (1.70 ppm), and $H_{E'}$ and/or H_C (1.45-1.41 ppm).

The NOESY spectrum of compound **135b** is shown in Figure 3.17. Figure 3.18-3.21 show expanded segments of the spectrum. Resonance correlations to the aromatic multiplet at 7.31-7.26 ppm correspond to the interaction of proton H_A with protons H_D (3.35 ppm, C1), H_B (1.84-1.76 ppm, C9), and H_K (0.97 ppm, C12). Notably, H_A does not demonstrate a correlation with H_C (1.45-1.41 ppm, C9) on the convex face of the ring. The vinyl proton, H_L, shows only a single correlation and this interaction is with H_D (3.35 ppm). Benzylic proton H_D has the two correlations already described, as well as correlations with H_E (1.70 ppm, C7) and H_K (0.97 ppm) (Figure 3.19). The diastereotopic carbons on C4, H_I (2.95-2.88 ppm) and $H_{I'}$ (2.59 ppm) both show correlations with H_F/$H_{F'}$ (1.84-1.76 ppm) on C5, but only H_I shows a correlation with H_G (1.91-1.88 ppm, C11), supporting the assignment of these two protons to the concave face of the molecule (Figure 3.21). Proton H_G also shows correlations with the multiplet at 1.84-1.76 ppm ($H_{F'}$) and the multiplet at 1.45-1.41 ppm ($H_{G'}$).

Proton H_E (1.70 ppm), on carbon C7, shows through-space interactions with H_F (1.84-1.86 ppm C5), H_K (0.94 ppm C12) and the multiplet at 1.45-1.41 ppm ($H_{E'}$).

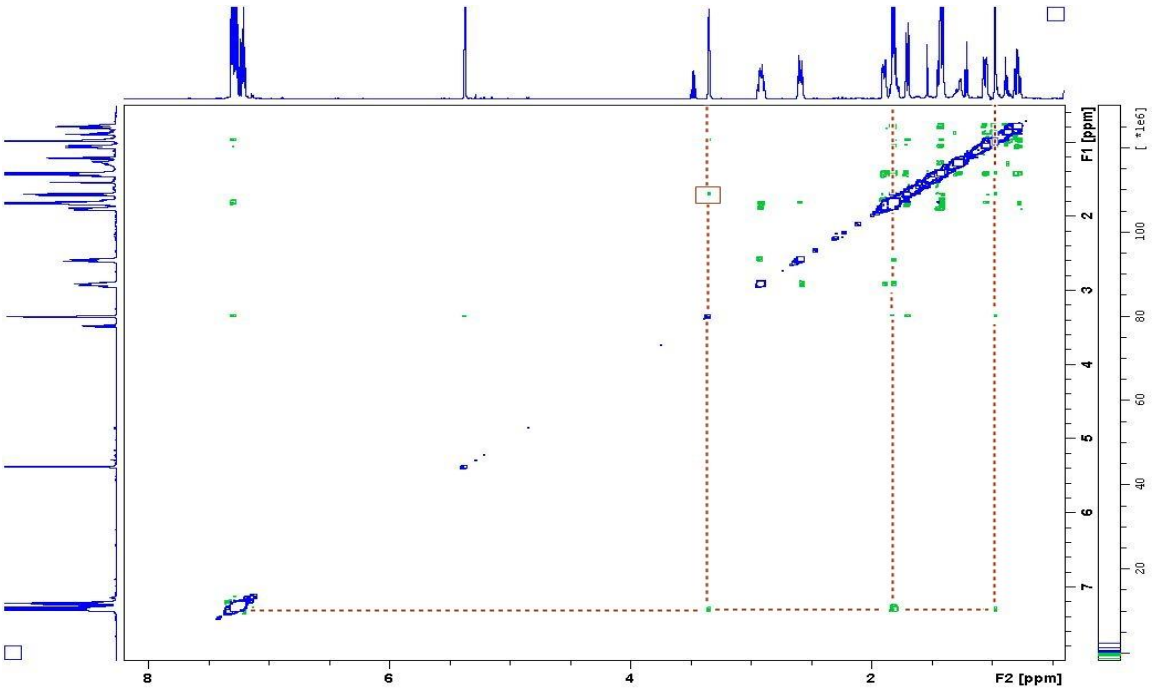

Figure 3.17. NOESY spectrum of compound 135b.

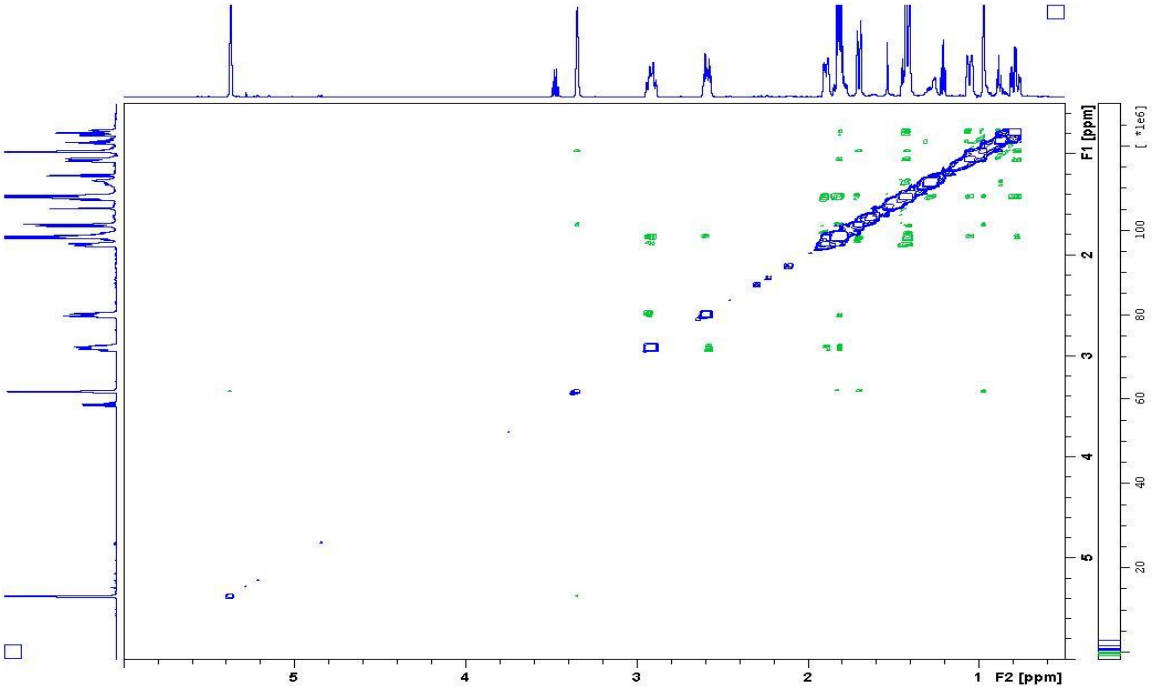

Figure 3.18. Expanded view of NOESY spectrum of 135b. (6.0-0.0 ppm).

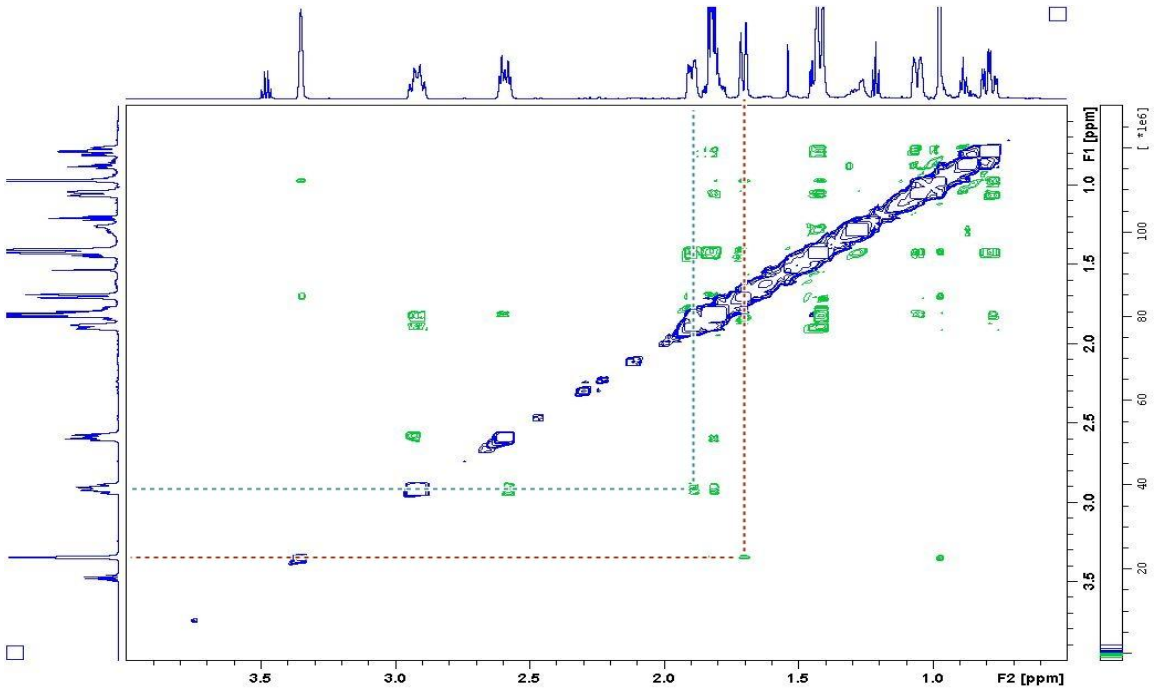

Figure 3.19. Expanded view of NOESY spectrum of 135b. (4.0-0.0 ppm).

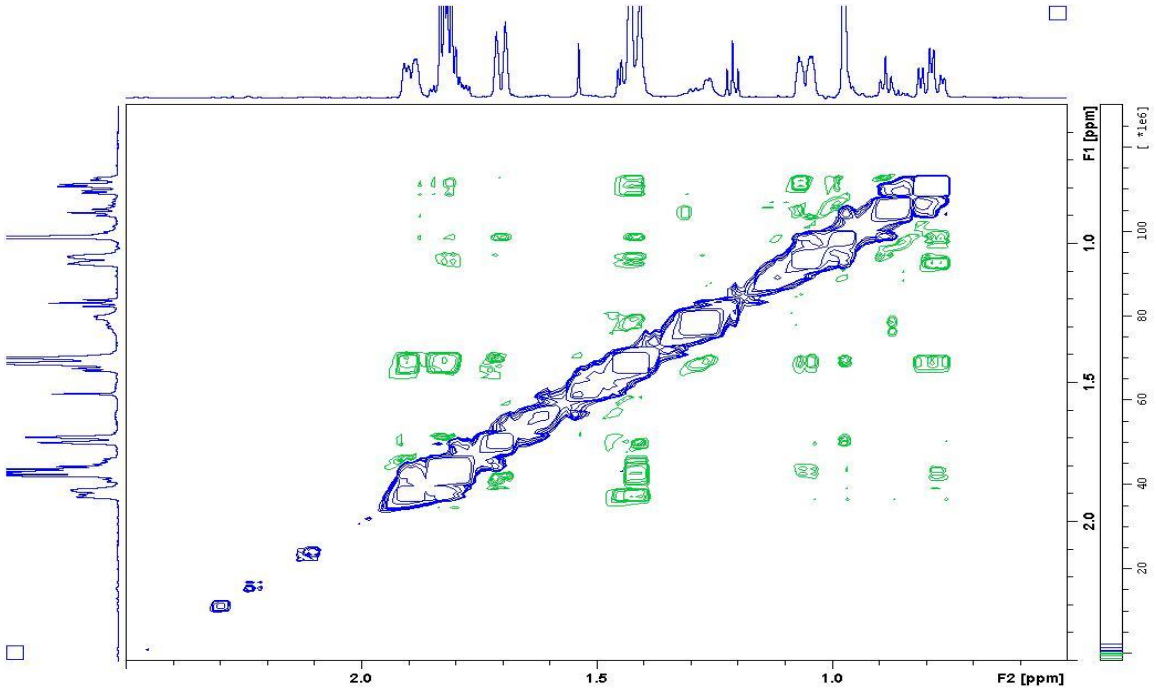

Figure 3.20. Expanded view of NOESY spectrum of 135b. (2.25-0.5 ppm).

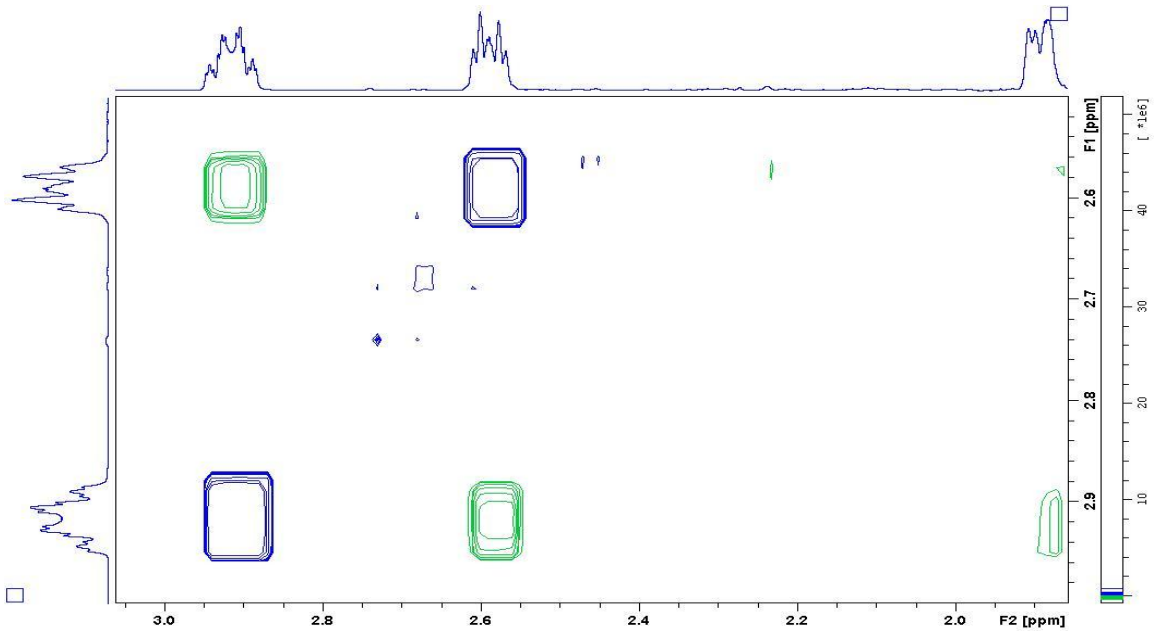

Figure 3.21. Expanded view of NOESY spectrum of 135b. (F1: 3.0-2.5 ppm F2: 3.0-1.85 ppm).

Taken together these spectra led to the determination of compound **135b** as a tricyclic species with a bicyclo[4.2.0]oct-1-ene. Overlap of signals in the ^{1}H spectrum complicated the analysis, but NOESY correlations were revealing. With the benzylic hydrogen H_D (3.35 ppm) as a starting point, the HSQC, HMBC, and NOESY spectra allowed the rest of molecule to be pieced together by the correlations listed above. HMBC was especially important in establishing the connectivity and positions of the quaternary carbons in the molecule.

Limitations on Substrate Scope

With the product identified, additional substrates were investigated (see Figure 3.3) to see if they would undergo the same rearrangement or, in the case of the cyclopentyl (**130**) and cycloheptyl (**134**) substrates, provide analogous tricyclic compounds with different ring sizes (Figure 3.22).

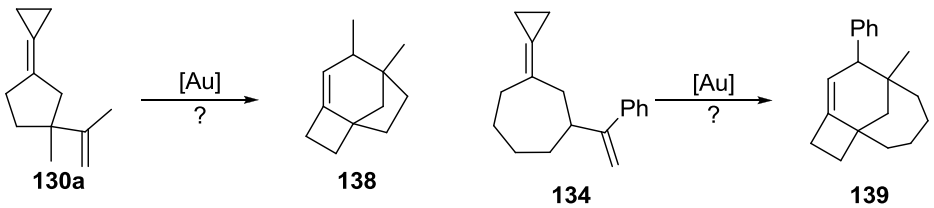

Figure 3.22. Proposed rearrangement of 5- and 7-membered ring substrates.

Unfortunately, the additional substrates gave neither the tricyclic products nor the analogous originally hypothesized medium ring products. Despite considerable experimentation compounds **127c**-**127e,** and **134** gave complex, intractable mixtures of compounds upon reaction with the Gagosz catalyst in DCM. Attempts to optimize via choice of solvent (nitromethane, 1,2-dichloroethane) and catalyst (e.g. (*R*)-BINAP($AuCl)_2$, (*S*)-xylyl-PHANEPHOS($AuCl)_2$), or activating agent ($AgBF_4$, $AgSbF_6$, $AgPF_6$), failed to simplify the reaction mixtures. Conducting the reaction at 0˚C resulted in no reactivity (GC-MS). It was observed that in the case of **134a** the identity of the counter-ion affected the ratio of products observed in the GC-MS but not the number of species formed.

For compounds **130a** and **130b** two major products were formed along with a number of minor products. Control reactions with $HCl{\cdot}Et_2O$ gave the same products in the same ratios, as did a separate control reaction between **130a** and $AgPF_6$ in DCM, suggesting unproductive, Brønsted Acid catalyzed alkene isomerization pathways. Identical control reactions with the 6- and 7- membered ring substrate analogs were sluggish and did not produce the same reaction mixtures observed as when Au(I) complexes were reacted. No tricyclic product was formed when the control reactions were run with **127a** and **127b**, supporting a gold catalyzed transformation for the production of **135a/b**. Unfortunately, despite the clean conversion of the first two substrates tested, this system was found to have limited substrate scope. The mechanistic aspects of this system were explored in collaboration with the Tantillo group from UC-Davis.

Thermodynamic and Kinetic Considerations

The following computational work was performed by Osvaldo Gutierrez and Dean Tantillo (UC-Davis) in a collaborative effort aimed at gaining a deeper insight into the mechanism and thermodynamics of this reaction. Results were obtained through density functional theory (DFT) calculations using the M06/6-31G(d) method with the SDD basis set for Au and a DCE solvent continuum (CPCM), as implemented in GAUSSIAN09.[75] While the Tantillo group performed these

calculations it is important to report the findings here for a thorough discussion of the energetics of this system.

The Tantillo group computationally explored the two potential mechanistic pathways that we proposed (see Figure 3.6). The results of these calculations are shown in Figure 3.23. Pathway **A** follows the originally envisioned Cope rearrangement pathway, via a tertiary carbocation (**A1**) to provide cyclooctene products (**A2**/**A3**). The barrier for this reaction is ca. 21 kcal/mol, relative to Au(I)-complexed **127a**. Initiation of a second Cope rearrangement at the endocyclic alkene (from **A3**) proceeds via **A3-TS** to tertiary carbocation **A4**. While the free energy of the transition state is lower **A3-TS** than **A4**, the electronic energy of **A4** is ~0.3 kcal/mol than **A3-TS**. Interestingly, the Tantillo group reported that a transition state could not be located for the direct ring expansion of the cyclopropane ring at this point. Instead, a confirmation change was found to be necessary in order to correctly orient the bonds and associated orbitals to allow facile ring expansion, resulting in formation of intermediate **A5**. Ring expansion (via **A5-TS**, the highest energy structure in the calculated mechanistic pathways) would then lead to structure **C**, which after deprotonation and protodemetallation provides [Au]-**135a**, calculated to be ca. 26 kcal/mol downhill. Gratifyingly, this is close to the value calculated using Mac Spartan ’10 for the uncoordinated structures (see Initial Explorations, p. 90).

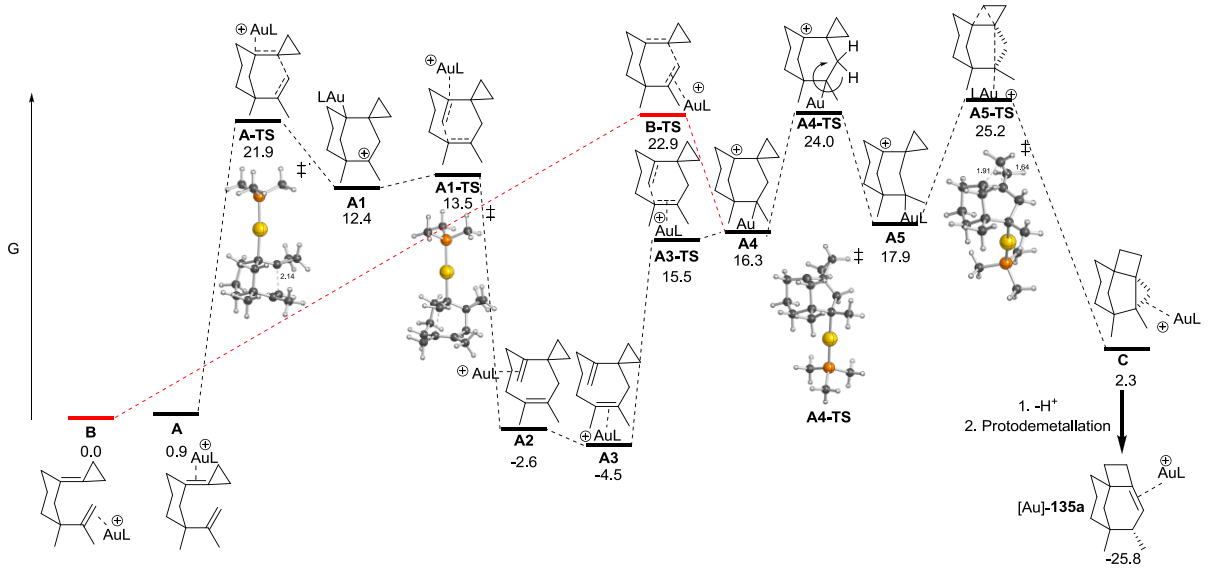

Figure 3.23. Calculated relative energies (kcal/mol) of structures involved in potential rearrangement pathways of 127a.

In pathway **B** the Cope rearrangement is initiated at the pendant alkene, and proceeds through a slightly higher energy transition state (ca. 23 kcal/mol) before converging with pathway **A** at structure **A4**. The computed difference in transition state energies (ca. 2 kcal/mol) is too small to definitively say which mechanistic pathway is active, but both pathways converge to provide a single product.

Also explored computationally was the failure of substrates **127c-127e** to undergo productive reactivity. The results of these calculations are shown in Table 3.2. It was found that the rearrangement of **127a** is exergonic by ca. 3 kcal/mol; notably this is nearly 6 kcal/mol less energetically favorable than indicated by the calculations performed in Mac Spartan '10 using the B3LYP routine.

Table 3.2. Thermodynamics of ring expansion of cyclohexyl substrates.

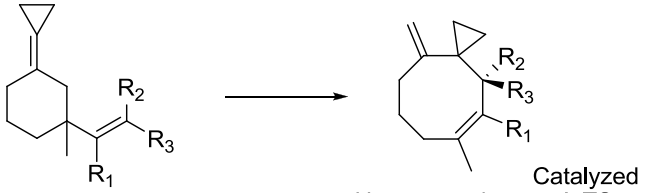

				Uncatalyzed		Catalyzed A-TS
Substrate	R_1	R_2	R_3	ΔH^a	ΔG	$\Delta G^{\ddagger}$
127a	Me	H	H	-1.8	-2.6	21.9
(*Z*)-**127c**	H	Me	H	4.7	6.1	N/A
(*E*)-**127c**	H	H	Me	-1.2	0.1	27.7
127d	Me	H	Me	-0.3	1.1	22.4
127e	H	Me	Me	4.4	5.9	N/A

[a] Calculated enthalpies and Gibbs free energies for formation of **A2**, along with computed relative energies for **A**-TS, in kcal/mol. [b] M06-2X/6-31G(d) (gas phase) calculations employed for uncatalyzed reaction and M06/SDD-6-31G(d) (DCE) for catalyzed.

For the other cyclohexyl substrates it was found that substitution at R_2 creates unfavorable steric interactions with the cyclohexane ring, leading to high energy transition states (**A-TS**) which prevent the Cope rearrangement from proceeding. This is reflected in the failure to locate transition states for compounds (*Z*)-**127c** and **127e**. Rearrangement of (*E*)-**127c** would proceed through a secondary carbocation, leading to the prohibitively high transition state energy (ca. 28 kcal/mol). While **127d** had a relatively low energy barrier, the analogous **A5-TS**, leading to ring expansion was calculated to be ca. 31 kcal/mol. This high energy appears to arise from a steric clash between methyl groups. As the cyclooctene product of **127d** is calculated to be uphill, it is anticipated that this reaction would be rapidly reversible. With computational work providing an energetic explanation for the limited substrate scope of this system and insight into the mechanism, an experimental probe of the mechanism was attempted.

Attempted Isolation of a Cyclooctene Product via Substrate Modification

It was hypothesized that it may be possible to design a substrate such that the cyclooctene intermediate, if it is part of the mechanistic pathway, would be stable enough to prohibit further rearrangement to the tricyclic product. Due to the strong thermodynamic driving force for rearrangement to the tricycle (see Figure 3.23), it was reasoned that it would not be possible to make

the cyclooctene the energetically favored product, but perhaps the reaction barrier (**A3-TS**) could be raised in energy to allow isolation of the 8-membered ring intermediate. With input from the Tantillo group, it was decided that the most likely structural variation to achieve this goal would be addition of a functional group to the substrate that would create conjugation in the cyclooctene not present in the starting material; rearrangement to the tricyclic compound would break this conjugation. For instance, it was envisioned that substrate **140** could rearrange, via **141**, to cyclooctene **142** (see Scheme 3.3). It was noted that steric interactions due to the increased bulk from the phenyl group might inhibit the Cope rearrangement (the same type of interactions prevent rearrangement of (*Z*)-**127c** and **127e**, which have bulky substituents at key positions on the pendant alkene, see Table 3.2), despite the geminal hydrogens on the terminal end of the pendant alkene. It was also observed that if the cyclooctene intermediate is formed in the rearrangement, substrate **127b** would have a styrene moiety in the 8-membered ring intermediate which does not prevent further rearrangement, despite removal of the conjugation upon formation of the tricyclic product (**135b**). This situation is slightly different, however, in that the styrene moiety is also present in the starting material. It was also postulated that if substrate **140** still rearranged to a tricyclic product, perhaps use of a pendant styrenyl moiety, such as in **143**, would allow isolation of the medium-sized ring product **144**. In this case, two styrene moieties would have to be transformed in order for the rearrangement to proceed.

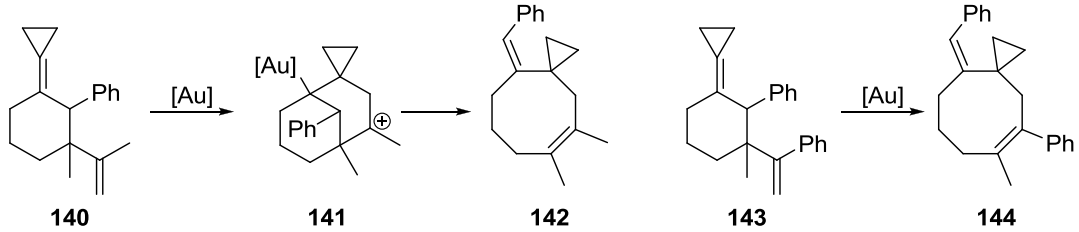

Scheme 3.3. Proposed substrate modification to allow isolation of cyclooctene intermediate.

The synthesis of substrates **140**/**143** began with addition of I_2 to 3-methyl-2-cyclohexen-1-one to provide halide **145** in moderate yield (Scheme 3.4). This compound could then be

transformed, via a Suzuki coupling, to the phenyl substituted enone **146** in good yield.[83] At this point, however, the synthesis ran into unexpected difficulties. The previously established method for conjugate addition to enones (see Scheme 3.1) did not work on compound **146**, instead giving a large mixture of product compounds using both the isopropenyl and styrenyl Grignard reagents.

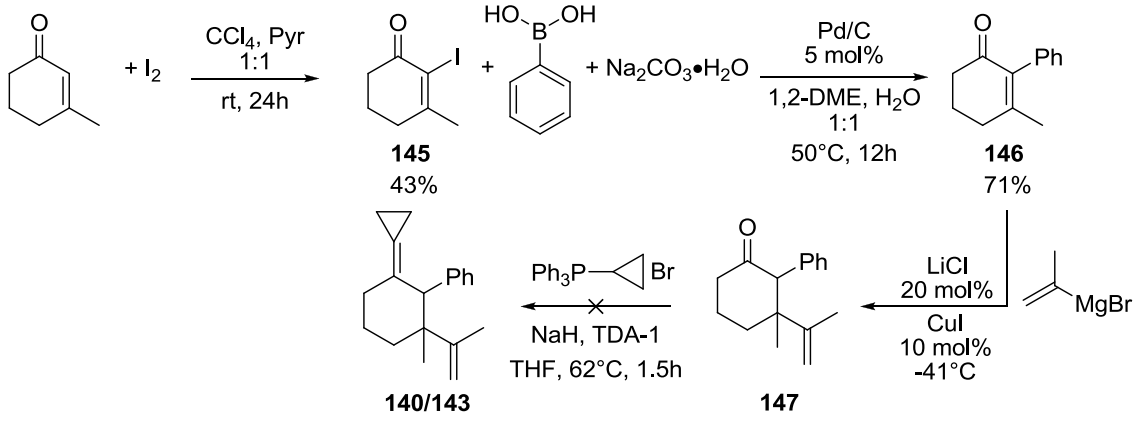

Scheme 3.4. Attempted synthesis of substrates 140/143.

Employing a lithium chloride/copper(I) iodide protocol simplified the reaction mixture using the isopropenyl Grignard reagent to allow isolation of a single product.[84] However, no carbonyl peak was observed in the ^{13}C NMR spectrum, indicating that this could be a 1,2-addition product instead of the desired 1,4-addition product (**147**). Taking this product on and subjecting it to the normal Wittig conditions gave no desired product (GC-MS). When the Grignard reagent prepared from α-bromostyrene was combined with **146** no reactivity was observed. The difficulty encountered preparing compound **147**, in combination with the problems that could arise from the acidic α-hydrogen (deprotonation should be facile as it would lead to an anion stabilized by conjugation with both the carbonyl and the aromatic ring) have prevented this synthetic route, and the subsequent attempts to probe the mechanism of this rearrangement, from being completed. Future exploration of these mechanistic aspects could provide important information relevant to our understanding of these Au(I) catalyzed rearrangements.

[83] Felpin, F.-X. *J. Org. Chem.* **2005**, *70*, 8575.
[84] Reetz, M. T.; Kindler, A. *J. Organomet. Chem.* **1995**, *502*, C5-C7.

Conclusions and Future Work

The Au(I)-catalyzed Cope rearrangement has been applied to cyclic substrates with pendant alkenes. In contrast to the predicted cyclooctene products, tricyclic compounds are formed with a bicyclo[4.2.0]oct-1-ene core, a structural motif present in several classes of natural products. The reaction proceeds at room temperature to provide the products in good isolated yields, but is limited in substrate scope to 2,2-disubstitution on the pendant alkene. DFT calculations predict that other substitution patterns experience prohibitively high reaction barriers or result in formation of the proposed cyclooctene intermediate being energetically uphill, and therefore reversible. This work demonstrates the potential of 1,5-dienes to undergo unique rearrangements, while also expanding our understanding of some of the limitations of the Au(I)-catalyzed rearrangement of methylenecyclopropanes.

There are many promising areas that this reactivity can be expanded into; for instance, Claisen and oxy-Cope rearrangements are an obvious extension of the system reported in Chapter 2. More interesting possibilities exist in harnessing the ring strain in the cyclopropylidene moiety to drive unique processes such as breaking conjugation and/or aromaticity, or ring expansions. Indeed, an interesting result has recently been discovered in the Gagné lab that indicates methylenecyclopropane 1,5-enynes can be transformed into bicyclic dienes. While the Au(I) catalyzed reactivity of 1,6-enynes has been explored,[85] the relative dearth of systems utilizing 1,5-diene MCPs leaves open a broad range of possibilities for discovering new, synthetically useful Au(I)-catalyzed rearrangements.

Experimental Section

General Information

All chemicals were reagent grade quality and used as received from Aldrich unless otherwise noted. Anhydrous THF (Stabilized, 99.9%, Acros Organics) and 1,2-Dichloroethane (99.8+%, extra pure)

[85] Sethofer, S. G.; Staben, S. T.; Hung, O. Y.; Toste, F. D. *Org. Lett.* **2008**, *10*, 4315.

were purchased from Fisher Scientific and used as received. Phosphorous ligands were purchased from Strem Chemicals, Inc. and used without further purification. All glassware was flame-dried under vacuum unless otherwise indicated. Anhydrous CH_2Cl_2, diethyl ether, and pentanes were passed through a column of alumina. Column chromatography was performed using SilaFlash P60 40-63 μm (230-400 mesh). All NMR spectra were recorded on either a Bruker Avance 600 MHz or 400 MHz spectrometer at STP. All deuterated solvents were used as received from Cambridge Isotope Laboratories, Inc. ^{1}H, and ^{13}C chemical shifts are reported in parts per million (ppm) relative to residual solvent resonances ($CDCl_3$ or CD_2Cl_2). GC-MS data was obtained using an Agilent G2570A GC/MSD system containing a 6850 GC equipped with an HP-5MS column (length 30 m,; I.D. 0.250 mm) connected to an Agilent 5983N MSD. High resolution mass spectra (HRMS) were obtained from the University of Illinois Mass Spectrometry lab (Dr. Furong Sun).

General Procedure A for Michael Addition Reactions. (For the preparation of *3-methyl-3-(prop-1-en-2-yl)cyclohexanone***)** To a flame-dried 100 mL round-bottom flask under N_2 was added CuI (3.45 g, 18.2 mmol, 2.00 eq.) then THF (18 mL). The reaction vessel was cooled to -41°C before the addition of the Grignard reagent, isopropenylmagnesium bromide (0.5 M THF, 36.3 mL, 18.2 mmol, 2.00 eq.) over 30 min. The reaction was stirred at -41°C for 30 min before transferring in 3-methyl-2-cyclohexen-1-one (1.03 mL, 9.08 mmol, 1.00 eq.) dissolved in THF (9 mL) via cannula. The reaction was then stirred 1.5 h at -41°C before quenching with saturated aqueous NH_4Cl (50 mL). The aqueous layer was separated and the organic layer was washed 2 additional times with saturated aqueous NH_4Cl. The combined aqueous washes were then extracted with Et_2O (2x). The combined organic layers were washed with brine until the aqueous layer was no longer blue-tinted. The organic layers were then dried over $MgSO_4$, filtered, and concentrated *in vacuo.* Purification by silica gel chromatography (15% EtOAc/Petroleum Ether) provided the product compound as a yellow oil (1.30 g, 94% yield).

General Procedure B for Wittig cyclopropylidination. (For preparation of *3-cyclopropylidene-1-methyl-1-(prop-1-en-2-yl)cyclohexane* (**127a**)) To a Schlenk flask loaded with a suspension of dry

NaH (0.102 g, 4.26 mmol, 1.30 eq.) in THF (25 mL) under N_2 atmosphere was added cyclopropyltriphenylphosphonium bromide (1.63 g, 4.26 mmol, 1.30 eq.) at rt. The reaction flask was then equipped with a condenser and heated to 62°C for 18 h. To the resulting orange suspension was then added the ketone (3-methyl-3-(prop-1-en-2-yl)cyclohexanone, 0.500 g, 3.28 mmol, 1.00 eq.) and tris[2-(2-methoxyethoxy)ethyl]amine (TDA-1) (0.105 mL, 0.328 mmol, 0.10 eq.) in THF (6 mL). The reaction was stirred for 5 h at 62°C before cooling to rt and quenching with saturated aqueous $NaHCO_3$. The reaction was diluted with deionized H_2O and Et_2O before separating the layers. The aqueous layer was extracted with Et_2O (2x) and the combined organic layers were then washed with brine (2x). The organic layer was then dried over $MgSO_4$, filtered, and concentrated *in vacuo*. Purification by silica gel chromatography (Hexanes) provided the product compound as a colorless oil (0.269 g, 47%). A small amount of CH_2Cl_2 was used to load the material onto the column.

General procedure C for preparation and use of (1-phenylvinyl)magnesium bromide: (For preparation of *3-methyl-3-(1-phenylvinyl)cyclohexanone*) To a flame-dried 100-mL 3-neck RBF equipped with a condenser under N_2 atmosphere was added Mg (0.467 g, 19.2 mmol, 2.12 eq) and THF (32.3 mL) and a few small crystals of I_2. Alpha-bromo-styrene (2.35 mL, 18.1 mmol, 2.00 eq) was dissolved in THF (4 mL) then added to the reaction mixture. The solution was heated to 70°C for 5-15 minutes until the consumption of Mg appeared to have stopped. After cooling to room temperature the Grignard solution (~0.5 M) was transferred via cannula to a suspension of CuI (3.45 g, 18.1 mmol, 1.00 eq) in THF (36 mL) at -41°C. The reaction was stirred at -41°C for 30 min before transferring in a solution of 3-methyl-2-cyclohexen-1-one (1.03 mL, 9.07 mmol, 1.00 eq.) dissolved in THF (9 mL) via cannula. The reaction was then stirred 1.5 h at -41°C before quenching with saturated aqueous NH_4Cl (50 mL). The aqueous layer was separated and the organic layer was washed 2 additional times with saturated aqueous NH_4Cl. The combined aqueous washes were then extracted with EtOAc (2x). The combined organic layers were washed with brine until the aqueous layer was no longer blue-tinted, and finally dried over $MgSO_4$, filtered, and concentrated *in vacuo.*

Purification by silica gel chromatography (15% EtOAc/Petroleum Ether) provided the product compound as a yellow oil as a mixture with styrene (1.32 g total, 0.971 g product, 50% yield).

General Procedure D for Au(I) Catalyzed Rearrangement: (For preparation of *6,7-dimethyltricyclo[5.3.1.0]undec-4-ene (***135a***)* To a 1-dram vial equipped with a stirbar was added $Ph_3PAuNTf_2$ (0.011 g, 0.0142 mmol, 0.10 eq) followed by DCM (0.5 mL). The reaction was stirred briefly before addition of **127a** (0.025g, 0.142 mmol, 1.00 eq). The reaction was then stirred for 12 h before concentrating *in vacuo*. A pipette column was then used for purification by silica gel chromatography (Hexanes) to provide the product compound as a colorless oil (0.019 g, 76%). A small amount of DCM was used to add the material to the column.

*3-methyl-3-(prop-1-en-2-yl)cyclohexanone***:** Yellow oil (1.30 g, 94% yield). ^{1}H NMR: (600 MHz, $CDCl_3$) δ 4.80 (s, 1H), 4.71 (s, 1H), 2.58 (d, *J* = 14.4 Hz, 1H), 2.28 (dt, *J* = 15.0, 5.7 Hz, 1H), 2.22-2.18 (m, 1H), 2.17 (d, *J* = 14.4 Hz, 1H), 1.91-1.87 (m, 1H), 1.84-1.77 (m, 1H), 1.71-1.67 (m, 1H), 1.69 (s, 3H), 1.56 (ddd, *J* = 13.2, 9.6, 3.6 Hz, 1H), 1.06 (s, 3H); ^{13}C-NMR: (150 MHz, $CDCl_3$) δ 211.9, 150.0, 112.0, 52.7, 43.9, 41.0, 35.0, 27.0, 22.0, 19.3. HRMS (EI+) calculated for $C_{10}H_{16}O$ 152.12012, found 152.12093.

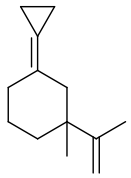

127a

3-cyclopropylidene-1-methyl-1-(prop-1-en-2-yl)cyclohexane **(127a):** Colorless oil (0.269 g, 47% yield). ^{1}H NMR: (600 MHz, $CDCl_3$) δ 4.74 (s, 1H), 4.73 (s, 1H), 2.41 (d, *J* = 13.2 Hz, 1H), 2.26-2.22 (m, 1H), 2.17-2.14 (m, 1H), 2.13 (d, *J* = 13.2 Hz, 1H), 1.71 (s, 3H), 1.71-1.68 (m, 1H), 1.55-1.50 (m, 2H), 1.47-1.44 (m, 1H), 0.99-0.96 (m, 4H), 0.94 (s, 3H); ^{13}C-NMR: (150 MHz, $CDCl_3$) δ 152.9, 126.1, 113.9, 109.4, 43.8, 41.0, 36.5, 33.2, 25.9, 23.4, 19.8, 2.13, 2.10. HRMS (EI+) calculated for $C_{13}H_{20}$ 176.15650, found 176.15722.

3-methyl-3-(1-phenylvinyl)cyclohexanone: Characterization data matched that previously reported.[86]

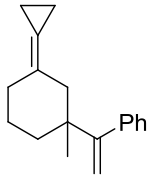

127b

(1-(3-cyclopropylidene-1-methylcyclohexyl)vinyl)benzene **(127b)**: Synthesized following general procedure **B** using 3-methyl-3-(1-phenyvinyl)cyclohexanone. Stirred 5 h at 62°C after addition of ketone in THF. Purified by silica gel chromatography (Hexanes) to give a colorless oil (0.281g, 36% yield). ^{1}H NMR: (400 MHz, CD_2Cl_2) δ 7.30-7.22 (m, 3H), 7.16-7.13 (m, 2H), 5.23 (d, *J* = 1.6 Hz, 1H), 4.82 (d, *J* = 1.6 Hz, 1H), 2.46 (d, *J* = 13.2 Hz, 1H), 2.31 (dt, *J* = 13.2, 5.2 Hz, 1H), 2.23 (d, *J* = 12.8 Hz, 1H), 2.15-2.09 (m, 1H), 1.75-1.69 (m, 1H), 1.68-1.60 (m, 1H), 1.59-1.46 (m, 2H), 1.06 (s, 3H), 1.02-0.89 (m, 4H); ^{13}C-NMR: (100 MHz, CD_2Cl_2) δ 159.6, 144.0, 129.7, 127.8, 126.8, 126.1, 114.5, 113.5, 44.5, 41.5, 37.2, 33.4, 25.9, 23.7, 2.21. HRMS (EI+) calculated for $C_{18}H_{22}$ 238.17215, found 238.17139.

3-methyl-3-(prop-1-enyl)cyclohexanone: Synthesized following general procedure **A** using 1-propenylmagnesium bromide solution (0.5 M THF). Purified by silica gel chromatography (15% EtOAc/Petroleum Ether) to give a yellow oil as a 1:1 inseperable mixture of *E*/*Z* isomers (0.981 g, 71% yield). Spectroscopic data reported is of the mixture of isomers. ^{1}H NMR: (600 MHz, CD_2Cl_2) δ 5.39 (ddt *J* = 12.0, 7.8, 7.2 Hz, 1H), 5.36-5.29 (m, 2H), 5.20 (dq, *J* = 11.7, 1.8 Hz, 1H), 2.45 (d, *J* = 13.2 Hz, 1H), 2.34 (dt, *J* = 13.8, 1.8 Hz, 1H), 2.22-2.16 (m, 5H), 2.10 (d, *J* = 13.8 Hz, 1H), 1.95-1.91 (m, 1H), 1.88-1.76 (m, 4H), 1.69 (dd, *J* = 7.2, 1.8 Hz, 3H), 1.64-1.55 (m, 3H), 1.62 (d, *J* = 4.8 Hz, 3H), 1.16 (s, 3H), 1.00 (s, 3H); ^{13}C-NMR: (150 MHz, CD_2Cl_2) δ 211.6, 211.5, 139.4, 137.0, 125.6, 123.4, 55.1, 52.8, 41.7, 41.4, 41.3, 38.1, 37.5, 28.2, 27.6, 23.1, 22.7, 18.4, 14.8. HRMS (EI+) calculated for $C_{10}H_{16}O$ 152.12012, found 152.12048.

[86] Müller, D.; Tissot, M.; Alexakis, A. *Org. Lett.* **2011**, *13*, 3040.

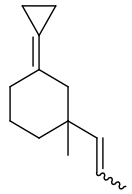

127c

3-cyclopropylidene-1-methyl-1-(prop-1-enyl)cyclohexane **(127c)**: Synthesized following general procedure **B** using 3-methyl-3-(prop-1-enyl)cyclohexanone. Stirred 2.5 h at 62°C after addition of ketone in THF. Purified by silica gel chromatography (Hexanes) to give a colorless oil as a 1:1 inseparable mixture of *E*/*Z* isomers (0.185 g, 32% yield). Spectroscopic data reported is of the mixture of isomers. ^{1}H NMR: (600 MHz, CD_2Cl_2) δ 5.43-5.36 (m, 1H), 5.35-5.29 (m, 2H), 5.23 (dq, *J* = 12.0, 1.8 Hz, 1H), 2.39 (d, *J* = 12.6 Hz, 1H), 2.29-2.23 (m, 1H), 2.21 (d, *J* = 13.2 Hz, 1H), 2.17-2.10 (m, 2H), 2.06 (d, *J* = 19.5 Hz, 1H), 2.04 (d, *J* = 19.8, 1H), 1.86-1.82 (m, 1H), 1.71 (dd, *J* = 7.2, 1.8 Hz, 3H), 1.63 (dd, *J* = 4.8, 1.2 Hz, 3H), 1.61-1.46 (m, 6H), 1.44-1.38 (m, 2H), 1.11 (s, 3H), 1.03-0.95 (m, 8H), 0.91 (s, 3H); ^{13}C-NMR: (150 MHz, CD_2Cl_2) δ 141.9, 139.3, 126.4, 126.2, 123.9, 121.1, 114.2, 114.0, 47.7, 45.4, 39.3, 39.0, 38.9, 38.3, 33.5, 33.4, 27.2, 26.5, 24.2, 23.7, 18.6, 15.0, 2.21, 2.17, 2.11. HRMS (EI+) calculated for $C_{13}H_{20}$ 176.15650, found 176.15742.

(E)-3-(but-2-en-2-yl)-3-methylcyclohexanone: Synthesized following general procedure **A** using 1-methyl-1-propenylmagnesium bromide solution (0.5 M THF). Stirred 2 h at -41°C after addition of ene-one. Purified by silica gel chromatography (15% EtOAc/Petroleum Ether) to give a yellow oil; 3:1 ratio of inseperable diastereomers (1.13 g, 75% yield). Spectroscopic data reported is of the mixture of isomers. ^{1}H NMR: (600 MHz, CD_2Cl_2) δ 5.31 (q, *J* = 7.8 Hz, 1H), 5.24 (q, *J* = 6.6 Hz, (1/3) = 1H, minor isomer), 2.69 (d, *J* = 13.8 Hz, 1H), 2.54 (d, *J* = 14.4 Hz, (1/3) = 1H, minor isomer), 2.29-2.20 (m, 2H), 2.18-2.12 (m, 2H), 1.93-1.74 (m, 2H), 1.70-1.67 (m, 6H), 1.56-1.55 (m, 1H), 1.14 (s, 3H), 1.03 (s, (1) = 3H, minor isomer); ^{13}C-NMR: (150 MHz, CD_2Cl_2) δ 211.9, 211.8, 140.9, 140.8, 121.7, 119.4, 54.1, 53.0, 44.7, 44.3, 41.4, 41.3, 36.3, 35.3, 27.2, 26.2, 24.2, 22.8, 22.4, 15.9, 14.0, 12.4. HRMS (EI+) calculated for $C_{11}H_{18}O$ 166.13577, found 166.13636.

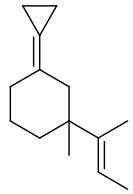

127d

(E)-1-(but-2-en-2-yl)-3-cyclopropylidene-1-methylcyclohexane **(127d)**: Synthesized following general procedure **B** using (*E*)-3-(but-2-en-2-yl)-3-methylcyclohexanone. Stirred 4.5 h at 62°C after addition of ketone in THF. Purified by silica gel chromatography (Hexanes) to give a colorless oil as an inseperable 3:1 ratio of diastereomers (0.106 g, 17% yield). Spectroscopic data reported is of the mixture of isomers. ^{1}H NMR: (600 MHz, CD_2Cl_2) δ 5.33-5.30 (m, (1/3) = 1H, minor isomer), 5.26-5.23 (m, 1H), 2.54 (d, *J* = 13.2 Hz, 1H), 2.37 (d, *J* = 12.6 Hz, (1/3) = 1H, minor isomer), 2.28-2.24 (m, 1H), 2.20-2.16 (m, 1H), 2.13 (d, *J* = 13.2 Hz, 1H), 2.01-1.97 (m, 1H), 1.69 (bs, 6H), 1.60-1.50 (m, 3H), 1.06 (s, 3H), 0.99 (bs, 4H), 0.91 (s, (1) = 3H, minor isomer); ^{13}C-NMR: (150 MHz, CD_2Cl_2) δ 143.23, 143.16, 126.9, 126.7, 120.3, 116.7, 114.1, 113.8, 45.4, 44.1, 41.64, 41.58, 37.6, 36.8, 33.6, 33.5, 25.5, 25.3, 24.03, 23.99, 23.7, 16.1, 14.0, 12.6, 2.4, 2.21, 2.19, 2.1. HRMS (EI+) calculated for $C_{14}H_{22}$ 190.17215, found 190.17239.

3-methyl-3-(2-methylprop-1-enyl)cyclohexanone: Synthesized following general procedure **A** using 2-methyl-1-propenylmagnesium bromide solution (0.5 M THF). Stirred 1.5 h at -41°C after addition of ene-one. Purified by silica gel chromatography (15% EtOAc/Petroleum Ether) to give a yellow oil (1.02 g, 68% yield). ^{1}H NMR: (600 MHz, CD_2Cl_2) δ 5.03 (s, 1H), 2.41 (d, *J* = 12.6 Hz, 1H), 2.21 (d, *J* = 4.8 Hz, 2H), 2.17 (d, *J* = 13.2 Hz, 1H), 1.93 (bs, 1H), 1.83 (bs, 2H), 1.71 (s, 3H), 1.67 (s, 3H), 1.60 (bs, 1H), 1.15 (s, 3H); ^{13}C-NMR: (150 MHz, CD_2Cl_2) δ 211.7, 133.6, 131.0, 55.6, 41.4, 40.9, 38.3, 28.3, 27.6, 23.1, 19.5. HRMS (EI+) calculated for $C_{11}H_{18}O$ 166.13577, found 166.13609.

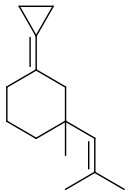

127e

3-cyclopropylidene-1-methyl-1-(2-methylprop-1-enyl)cyclohexane **(127e)**: Synthesized following general procedure **B** using 3-methyl-3-(2-methylprop-1-enyl)cyclohexanone. Stirred 3 h at 62°C after addition of ketone in THF. Purified by silica gel chromatography (Hexanes) to give a colorless oil (0.206 g, 33% yield). ^{1}H NMR: (600 MHz, CD_2Cl_2) δ 5.04 (s, 1H), 2.35 (d, *J* = 13.2 Hz, 1H), 2.26-2.24 (m, 1H), 2.12 (bs, 1H), 2.02 (d, *J* = 12.6 Hz, 1H) 1.82-1.79 (m, 1H), 1.70 (s, 3H), 1.64 (s, 3H) 1.57-1.54 (m, 1H), 1.51-1.45 (m, 1H), 1.42-1.38 (m, 1H), 1.08 (s, 3H), 1.03-0.98 (m, 4H); ^{13}C-NMR: (150 MHz, CD_2Cl_2) δ 133.5, 131.4, 126.6, 114.1, 48.0, 39.5, 38.0, 33.5, 28.3, 27.1, 24.2, 19.5, 2.2, 2.1. HRMS (EI+) calculated for $C_{14}H_{22}$ 190.17215, found 190.17146.

3-methyl-3-(prop-1-en-2-yl)cyclopentanone: Synthesized following general procedure **A** using isopropenylmagnesium bromide (0.5 M THF) and 3-methylcyclopent-2-enone. Stirred 1.5 h at -41°C after addition of ene-one. This material was sufficiently pure to be taken on without further purification as a yellow oil (0.991 g, 79% yield). ^{1}H NMR: (600 MHz, CD_2Cl_2) δ 4.78 (t, *J* = 1.8 Hz, 1H), 4.71 (s, 1H), 2.38 (d, *J* = 17.4 Hz, 1H), 2.28-2.24 (m, 2H), 2.09 (d, *J* = 17.4 Hz, 1H), 2.07-2.02 (m, 1H), 1.88-1.84 (m, 1H), 1.79 (s, 3H), 1.17 (s, 3H); ^{13}C-NMR: (150 MHz, CD_2Cl_2) δ 218.9, 151.6, 109.5, 51.6, 45.3, 37.1, 34.3, 25.9, 19.8. HRMS (EI+) calculated for $C_9H_{14}O$ 138.10447, found 138.10502.

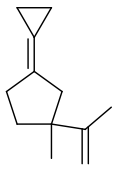

130a

3-cyclopropylidene-1-methyl-1-(prop-1-en-2-yl)cyclopentane **(130a)**: Synthesized following general procedure **B** using 3-methyl-3-(prop-1-en-2-yl)cyclopentanone. Stirred 5 h at 62°C after addition of ketone in THF. Purified by silica gel chromatography (Hexanes) to give a colorless oil

(0.096g, 18% yield). ^{1}H NMR: (600 MHz, $CDCl_3$) δ 4.70 (s, 1H), 4.68 (s, 1H), 2.47-2.41 (m, 3H), 2.23 (d, *J* = 15.0 Hz, 1H), 1.82-1.77 (m, 1H), 1.76 (s, 3H), 1.63-1.58 (m, 1H), 1.04 (s, 3H), 0.97-0.95 (m, 4H); ^{13}C-NMR: (150 MHz, $CDCl_3$) δ 153.1, 130.6, 111.4, 108.2, 47.7, 44.7, 37.2, 30.0, 25.4, 20.3, 2.5, 2.4. HRMS (EI+) calculated for $C_{12}H_{19}$ (M+1) 163.14868, found 163.14901.

3-methyl-3-(1-phenylvinyl)cyclopentanone: Synthesized following general procedure **C** using 3-methylcyclopent-2-enone. Stirred 4 h at -41°C after addition of ene-one. Purification by gradient silica gel chromatography (Petroleum Ether to 95:5 Pet. Ether:Et_2O to 90:5:5 Pet. Ether:Et_2O:EtOAc) provided the product compound as a yellow oil (0.327g, 18% yield) ^{1}H NMR: (600 MHz, $CDCl_3$) δ 7.31-7.26 (m, 3H), 7.15-7.14 (m, 2H), 5.17 (s, 1H), 4.96 (s, 1H), 2.50 (d, *J* = 17.4 Hz, 1H), 2.31-2.28 (m, 2H), 2.20-2.14 (m, 1H), 2.15 (dd, *J* = 17.4, 1.8 Hz, 1H), 1.86 (ddt, *J* = 9.6, 6.6, 1.8 Hz, 1H), 1.25 (s, 3H); ^{13}C-NMR: (150 MHz, $CDCl_3$) δ 218.8, 156.4, 142.3, 128.8, 128.0, 127.2, 113.8, 51.9, 45.2, 36.7, 34.5, 26.6. HRMS (EI+) calculated for $C_{14}H_{16}O$ 200.12012, found 200.11936.

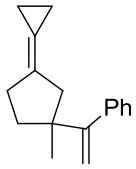

130b

(1-(3-cyclopropylidene-1-methylcyclopentyl)vinyl)benzene **(130b)**: Synthesized following general procedure **B** using 3-methyl-3-(1-phenylvinyl)cyclopentanone. Stirred 8.5 h at 62°C after addition of ketone in THF. Purified by silica gel chromatography (Hexanes) to give a colorless oil (0.221 g, 30% yield). ^{1}H NMR: (600 MHz, $CDCl_3$) δ 7.29-7.24 (m, 3H), 7.20-7.18 (m, 2H), 5.17 (d, *J* = 1.2 Hz, 1H), 4.87 (d, *J* = 1.2 Hz, 1H), 2.57 (d, *J* = 15.6 Hz, 1H), 2.44 (bs, 2H), 2.26 (d, *J* = 15.6 Hz, 1H), 1.97-1.92 (m, 1H), 1.66-1.62 (m, 1H), 1.13 (s, 3H), 0.96-0.94 (m, 4H); ^{13}C-NMR: (150 MHz, $CDCl_3$) δ 158.4, 143.7, 130.3, 128.8, 127.7, 126.7, 112.6, 111.7, 47.8, 45.4, 37.8, 29.8, 26.2, 2.5, 2.4. HRMS (EI+) calculated for $C_{17}H_{20}$ 224.15650, found 224.15584.

3-(1-phenylvinyl)cycloheptanone: Synthesized following general procedure **C** using 2-cyclohepten-1-one. Stirred 1.5 h at -41°C after addition of ene-one. Purification by gradient silica gel

chromatography (Petroleum Ether to 95:5 Pet. Ether:Et_2O to 90:5:5 Pet. Ether:Et_2O:EtOAc) provided the product compound as a pale yellow oil (1.13 g, 58% yield). ^{1}H NMR: (400 MHz, $CDCl_3$) δ 7.32-7.31 (m, 4H), 7.29-7.26 (m, 1H), 5.19 (s, 1H), 5.02 (s, 1H), 2.82 (t, *J* = 10.4 Hz, 1H), 2.70-2.61 (m, 1H), 2.69 (t, *J* = 14.4 Hz, 1H), 2.55-2.51 (m, 2H), 2.07-2.03 (m, 1H), 1.99-1.90 (m, 2H), 1.69-1.59 (m, 1H), 1.52-1.35 (m, 2H); ^{13}C-NMR: (100 MHz, $CDCl_3$) δ 214.1, 154.0, 142.0, 128.6, 127.7, 126.8, 111.7, 49.7, 44.2, 41.0, 37.3, 29.3, 24.4. HRMS (EI+) calculated for $C_{15}H_{18}O$ 214.13577, found 214.13519.

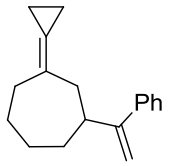

134

1-cyclopropylidene-3-(1-phenylvinyl)cycloheptane **(134)**: Synthesized following general procedure **B** using 3-(1-phenylvinyl)cycloheptanone. Stirred 3.5 h at 62°C after addition of ketone in THF. Purified by silica gel chromatography (Hexanes) to give a colorless oil (0.367 g, 47% yield). ^{1}H NMR: (400 MHz, $CDCl_3$) δ 7.39-7.37 (m, 2H), 7.33-7.29 (m, 2H), 7.27- 7.25 (m, 1H), 5.19 (s, 1H), 5.06 (s, 1H), 2.71 (d, *J* = 14.0 Hz, 1H), 2.64 (t, *J* = 10.4 Hz, 1H), 2.52 (d, *J* = 14.8 Hz, 1H), 2.42-2.36 (m, 1H), 2.28 (t, *J* = 12.4 Hz, 1H), 1.94-1.91 (m, 1H), 1.85-1.79 (m, 2H), 1.56-1.49 (m, 1H), 1.44-1.30 (m, 2H), 0.99-0.93 (m, 4H); ^{13}C-NMR: (100 MHz, $CDCl_3$) δ 155.7, 143.0, 128.9, 128.4, 127.3, 126.8, 116.8, 110.6, 44.9, 41.0, 36.7, 34.6, 28.5, 27.8, 2.35. HRMS (EI+) calculated for $C_{18}H_{22}$ 238.17215, found 238.17115.

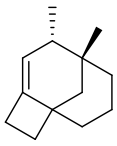

135a

6,7-dimethyltricyclo[5.3.1.0]undec-4-ene (**135a**): Colorless oil (0.019 g, 76%). ^{1}H NMR: (600 MHz, $CDCl_3$) δ.5.17 (s, 1H), 2.82-2.75 (m, 1H), 2.50-2.46 (m, 1H), 2.01 (bs, 1H), 1.74-1.70 (m, 3H), 1.63 (dd, *J* = 13.8, 2.4 Hz, 1H), 1.50-1.40 (m, 3H), 1.32 (dt, *J* = 12.3, 4.2 Hz, 1H), 1.26 (d, *J* = 11.4 Hz, 1H), 0.94 (d, *J* = 7.2 Hz, 3H), 0.87 (dt, *J* = 13.8, 5.4 Hz, 1H), 0.84 (s, 3H); ^{13}C-NMR: (150 MHz,

$CDCl_3$) δ 143.1, 121.7, 48.9, 46.5, 42.2, 35.8, 34.9, 33.4, 32.5, 30.8, 28.9, 22.2, 14.7. HRMS (EI+) calculated for $C_{13}H_{20}$ 176.15650, found 176.15578.

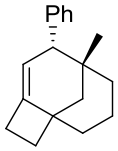

135b

7-methyl-6-phenyltricyclo[5.3.1.0]undec-4-ene (**135b**): Synthesized following general procedure **D** using compound **127b**. Purified by silica gel chromatography (Hexanes) to give a colorless oil (0.022 g, 88% yield). ^{1}H NMR: (600 MHz, $CDCl_3$) δ 7.31-7.26 (m, 4H), 7.22-7.20 (m, 1H), 5.37 (s, 1H), 3.35 (s, 1H), 2.95-2.88 (m, 1H), 2.59 (dt, *J* = 13.8, 5.4 Hz, 1H), 1.91-1.88 (m, 1H), 1.84-1.76 (m, 3H), 1.70 (d, *J* = 10.8 Hz, 1H), 1.45-1.41 (m, 3H), 1.07-1.04 (m, 1H), 0.97 (s, 3H), 0.79 (dt, *J* = 13.8 5.4 Hz, 1H); ^{13}C-NMR: (150 MHz, $CDCl_3$) δ 145.2, 142.7, 130.0, 127.8, 126.2, 119.4, 55.4, 49.7, 46.4, 36.3, 35.4, 33.7, 32.6, 31.4, 29.3, 22.5. HRMS (EI+) calculated for $C_{18}H_{22}$ 238.17215, found 238.17229.

Chapter 4 – Theoretical Exploration of 5-Exo Versus 6-Endo Ring Closures in Transition Metal Catalyzed Cyclizations

Ring Closure Modes

The creation of cyclic compounds from acyclic precursors are affected primarily by three factors: 1) ring size, 2) hybridization of carbon at site of ring closure, and 3) whether the reacting bond is endocyclic or exocyclic to forming ring.[24] Thermodynamic considerations of ring size were discussed briefly in Chapter 3 (see Medium-Sized Rings). A set of rules have been developed to relate these three factors to transition state geometry and are known collectively as Baldwin's rules.[87] A number of the rules formalized by Baldwin and co-workers are summarized in Table 4.1. The abbreviations fav and unfav refer to the closure mode being either favorable or unfavorable, respectively.

Table 4.1. Baldwin's rules for 4-6 membered rings.

	Exocyclic bonds			Endocyclic bonds	
Ring Size	sp (*dig*)	sp^2 (*trig*)	sp^3 (*tet*)	sp (*dig*)	sp^2 (*trig*)
4	unfav	fav	fav	fav	unfav
5	fav	fav	fav	fav	unfav
6	fav	fav	fav	fav	fav

These rules are not concrete and many examples of exceptions to them exist in the literature, but they are useful for thinking about the nature of the transition state of the ring closure reaction. The reactions are classified by the hybridization of the electrophilic atom in the ring closure (Figure 4.1a) and whether the reacting bond, the bond to the leaving group, is outside (exocyclic) or inside

[87] a) Baldwin, J. E. *J. Chem. Soc., Chem. Comm.* **1976**, 734. b) Baldwin, J. E.; Cutting, J.; Dupont, W.; Kruse, L.; Silberman, L.; Thomas, R. C. *J. Chem. Soc., Chem. Comm.* **1976**, 736.

(endocyclic) the forming ring (Figure 4.1b). For instance, the displacement of bromide by a tethered oxygen nucleophile to form tetrahydrofuran (Figure 4.1c), would be classified as a 5-*exo-tet* cyclization due to the formation of a 5-membered ring with the bond to the leaving group being outside the formed ring, and a sp^3 hybridized electrophilic carbon. Figure 4.1d shows an example of a 6-*endo-trig* cyclization.

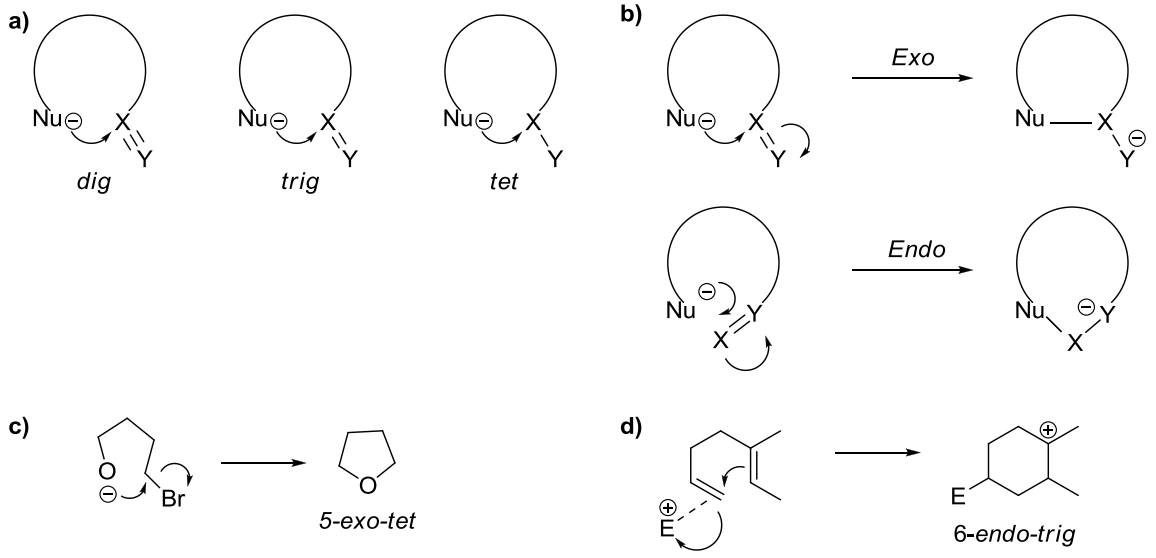

Figure 4.1. Examples of Baldwin's rules terminology.

The rules summarized in Table 4.1 denote each reaction type as either favorable or unfavorable. This is based qualitatively on the transition state geometry that needs to be assumed for each closure mode to proceed. For instance, for a 5-*endo-trig* cyclization, such as that shown in Figure 4.2a, the nucleophile must approach the electrophilic carbon in the plane of the π*-bond. This means a transition state such as **148** is impossible and instead the nucleophile must attack from above or below the nodal plane (**149**). This results in a large distortion of the 5-membered ring geometry and leads to a higher energy transition state, making this closure mode unfavorable. In contrast, a 5-*endo-dig* cyclization is a favorable ring closure mode (Figure 4.2b). Due to the perpendicular π-bonds of the triple bond, a π* orbital is oriented to allow approach of the nucleophile without a large distortion of the normal ring geometry (**150**), making this a more favorable process than the 5-*endo-trig* cyclization.

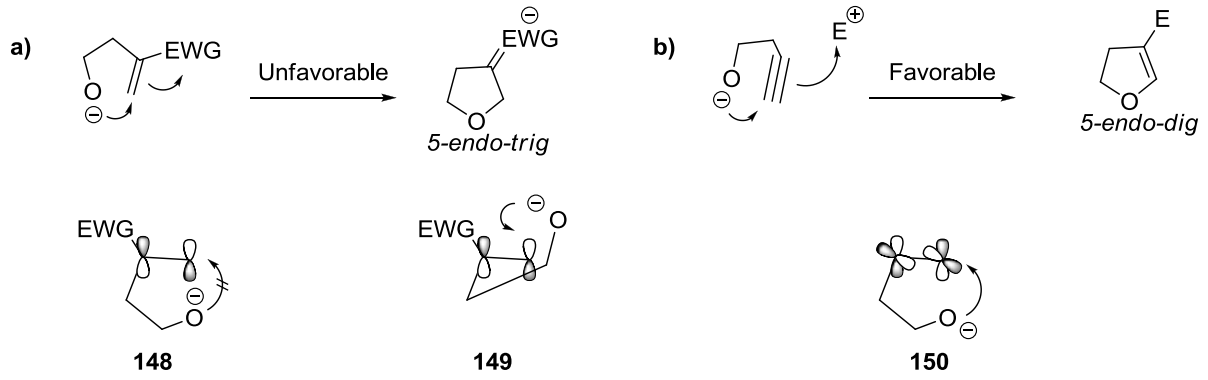

Figure 4.2. Comparison of 5-*endo-trig* and 5-*endo-dig* closure modes.

In transition metal mediated electrophilic activations of alkenes two ring closure modes are often possible, 5-*exo-trig* and 6-*endo-trig*, both of which are considered favorable pathways by Baldwin's rules (Figure 4.3). In practice, however, a large preference is often seen for one pathway over the other based on the nature of the nucleophile; when the nucleophile is a heteroatom/lone pair 5-*exo* cyclization occurs preferentially and when the adding fragment is a π-bond nucleophile different selectivity is observed. A rationale for the cyclization selectivity demonstrated by π-nucleophiles, based on a proposed nontraditional-carbocation-like bicyclic transition state, has been developed from analysis of the Gagné Pt(II)-systems and is the focus of this chapter.

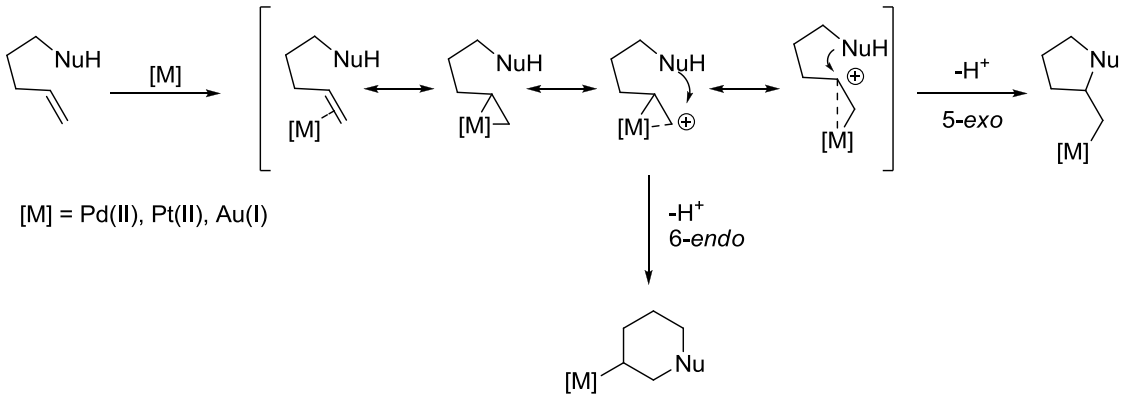

Figure 4.3. 6-*endo-trig* and 5-*exo-trig* closure modes mediated by transition metals.

5-Exo Cyclizations

In addition to the Gagné group the research groups of Ross Widenhoefer and Forrest Michael have also conducted extensive research utilizing transition metals for the electrophilic activation of

alkenes. In contrast to the cyclization chemistry favored by the Gagné group, these latter groups explore hydrofunctionalization reactions (see Figure 1.4) using heteroatom and carbon nucleophiles.

In an early study focused on the hydroamination of alkenes the Widenhoefer group employed the Pt(II) catalyst dimer, $[PtCl_2(CH_2{=}CH)]_2$, to transform amine **151** to the product compound (**152**) in good yield (Scheme 4.1).[88] This reaction could be applied to a variety of alkenyl amines to provide the products in moderate to high yields, but in all cases only 5-*exo* ring closure was observed.

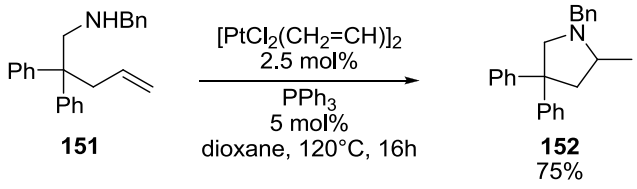

Scheme 4.1. Hydroamination reaction catalyzed by $[PtCl_2(CH_2{=}CH)]_2$.

The lone pair nucleophile (nitrogen) in this system preferentially attacks the internal carbon of the olefin to give 5-*exo* cyclization. This could reflect an energetic preference for formation of the intermediate with the least unfavorable steric interactions between the ring structure and the Pt(II) center (Figure 4.4). For instance, the proposed intermediate, **153**, separates the metal center from the 5-membered ring by one methylene, whereas the intermediate resulting from 6-*endo* cyclization (**154**) would result in the direct bonding of the metal center to the ring. The latter situation would almost certainly result in greater steric strain due to the closer proximity of the bulky Pt(II) complex to the other substituents on the ring.

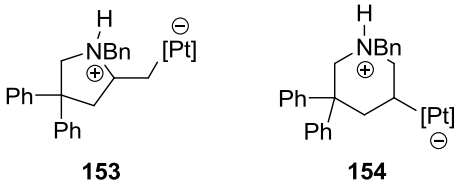

Figure 4.4. Potential intermediates for 5-*exo* and 6-*endo* cyclizations of compound 151.

The preference for 5-*exo* cyclization has been observed in similar systems with different transition metals as well. Utilizing $(PNP)PdCl_2$, the Michael group was able to synthesize a number

[88] Bender, C. F.; Widenhoefer, R. A. *J. Am. Chem. Soc.* **2005**, *127*, 1070.

of cyclic amines (**156**) in high yields from the acyclic starting material (**155**, Scheme 4.2).[89] Similar to the Widenhoefer Pt(II) system, no 6-*endo* cyclization was observed. The reaction is proposed to proceed through an intermediate analogous to **153**.

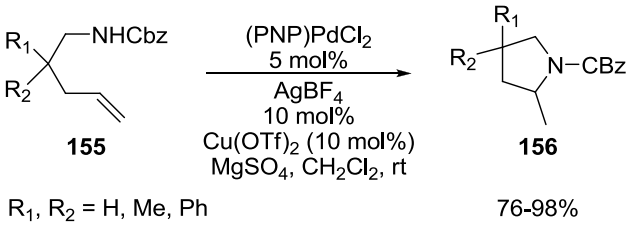

Scheme 4.2. Hydroamination of alkenes catalyzed by (PNP)Pd(II).

In a subsequent study reacting Pd(II) catalysts, an additive alcohol, and *N*-fluorobenzenesulfonimide with compound **155**, the Michael group observed both 5-*exo* (**157**) and 6-*endo* (**158**) cyclization products (Scheme 4.3).[90] It was observed that utilizing $Pd(TFA)_2$ (TFA = trifluoroacetate) as the catalyst provided only **157**, while adding halide salts or using $PdCl_2(MeCN)_2$ increased the amount of **158** observed. More polar solvents were also found to increase the amount of the 6-*endo* product. Experimental observations led to proposal of a common intermediate (**159**) for formation of both products. 5-*exo* products could be produced directly from **159** by nucleophilic displacement of the Pd(IV) center by the alcohol. It was hypothesized that under highly polar conditions an intramolecular reaction occurs, with the nitrogen displacing the Pd(IV), leading to a bicyclo[3.1.0]aziridinium intermediate, which could ring open to **158** with attack of the alcohol.

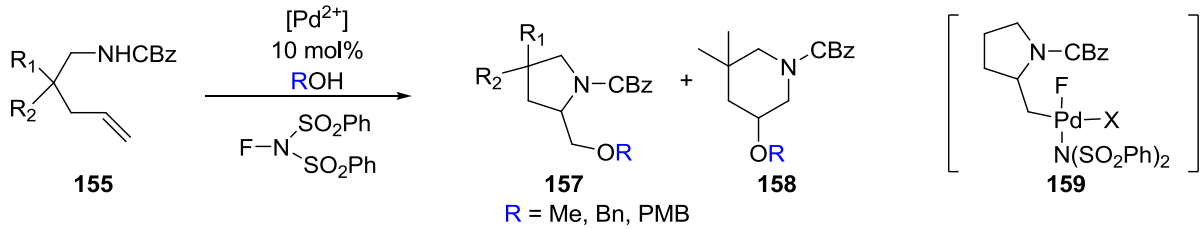

Scheme 4.3. Alkoxyamination of 155.

[89] Michael, F. E.; Cochran, B. M. *J. Am. Chem. Soc.* **2006**, *128*, 4246.
[90] Liskin, D. V.; Sibbald, P. A.; Rosewall, C. F.; Michael, F. E. *J. Org. Chem.* **2010**, *75*, 6294.

Similar results were seen in the aminotrifluoroacetoxylation of alkenes using iodobenzene diacetate ($PhI(OAc)_2$).[91] In this system different products were observed based on the substitution pattern on the starting material amine, **160** (Figure 4.5). The observed stereochemistry and the manner in which starting material substitution affected the formation of the products led to proposal of common intermediate **163** leading to both 5-*exo* (**161**) and 6-*endo* (**162**) products. It was proposed that for more reactive styrenyl substrates, **163** would be rapidly trapped by the trifluoroacetate counterion, leading to formation of the 5-*exo* product. For less reactive substrates it was proposed that the nitrogen atom displaces the halide, resulting in formation of a bicyclic intermediate that could then be ring-opened by the trifluoroacetate counterion, thus providing the 6-*endo* type products.

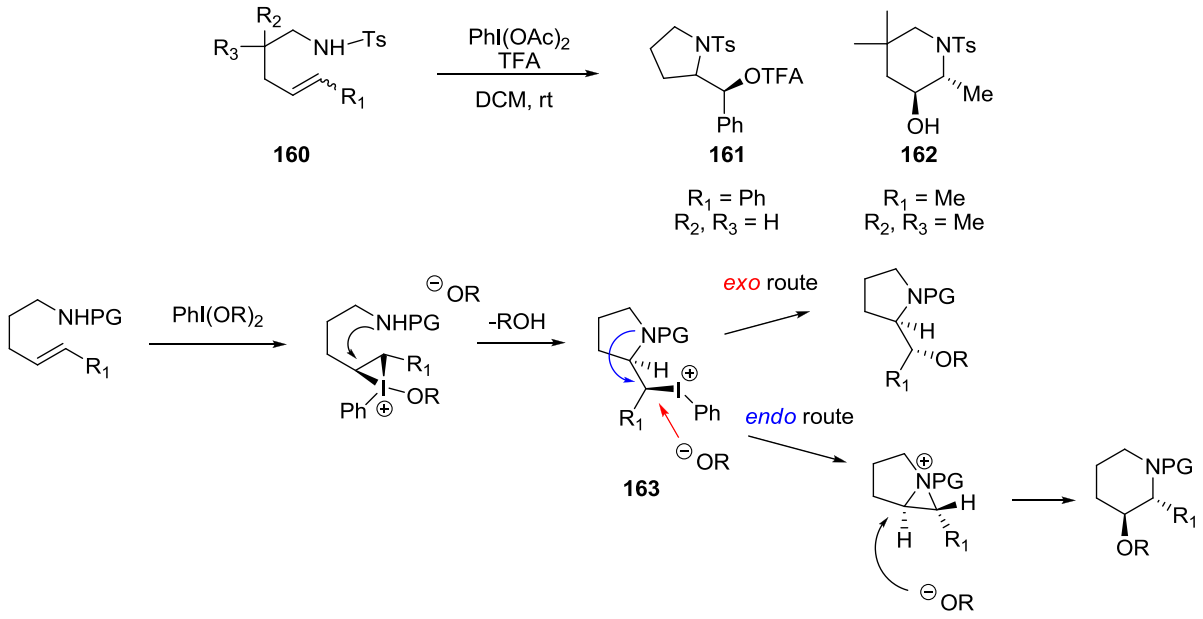

Figure 4.5. Aminotrifluoroacetoxylation of alkenes using $PhI(OAc)_2$.

A final example of the preference for 5-*exo* ring closure demonstrated by lone pair nucleophiles is a Pd(II)-catalyzed system developed by the Widenhoefer group for furan synthesis (Scheme 4.4).[92] In this system it was proposed that Pd(II) activates the pendant olefin, promoting attack of the enol form (**166**) of the diketone **164**. This leads to formation of intermediate **167** which,

[91] Lovick, H. M.; Michael, F. E. *J. Am. Chem. Soc.* **2010**, *132*, 1249.
[92] Han, X.; Widenhoefer, R. A. *J. Org. Chem.* **2004**, *69*, 1738.

after undergoing β-hydride elimination and alkene isomerization, provides **165** in good yield. All of these results create a consistent picture of lone pair nucleophiles preferring to add to electrophilically activated alkenes via exocyclic ring closure pathways. This is in contrast to the selectivity displayed by π-nucleophiles, as will be shown in the next section.

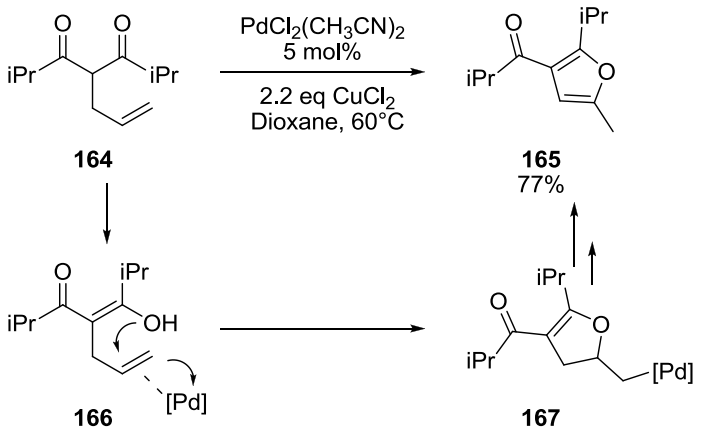

Scheme 4.4. Pd(II)-catalyzed furan synthesis via 5-*exo* cyclization.

6-Endo Cyclizations

The system shown in Scheme 4.4 differs significantly from earlier studies conducted by the Widenhoefer group.[93] When a linear substrate, such as **168** or **170**, was employed instead of a branched substrate, such as **164**, 6-*endo* ring closure was observed (Scheme 4.5). While the addition still proceeds via the enol form of the ketone (**172**), it is the alkene moiety that is adding in these reactions, in contrast to the hydroxyl group in the branched substrates (**166**). No 5-*exo* addition was seen in these reactions, an important example of the different reactivity of π-nucleophiles versus lone-pair nucleophiles. A potential explanation for this behavior will be presented in the next section.

[93] a) Qian, H.; Widenhoefer, R. A. *J. Am. Chem. Soc.* **2003**, *125*, 2056. b) Wang, X.; Pei, T.; Han, X.; Widenhoefer, R. A. *Org. Lett.* **2003**, *5*, 2699.

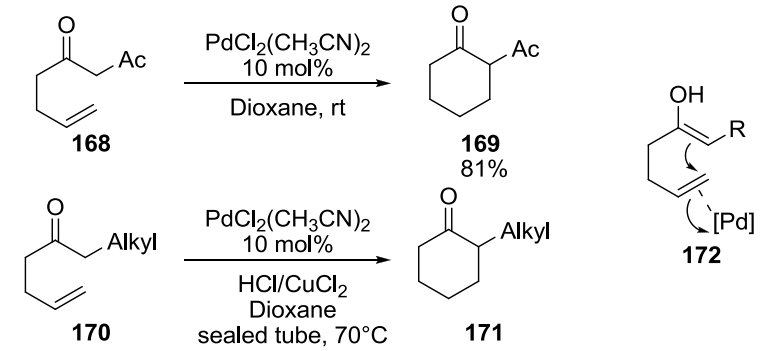

Scheme 4.5. Pd(II)-catalyzed 6-*endo* ring closure of alkenyl ketones.

In all the cyclization chemistry of 1,5-dienes explored by the Gagné group 6-*endo* ring closure is seen exclusively (see Table 1.3, Table 1.4).[48-50] All these systems involve a π-nucleophile adding to an electrophilically activated olefin and each can theoretically close by either 5-*exo* or 6-*endo* modes (Figure 4.6). It is worth noting that the carbocationic species shown are not intermediates; previous studies have determined that these cyclization reactions are concerted processes in the presence of an additive base. Based on steric considerations (see 5-Exo Cyclizations, above), it might be assumed that 5-*exo* would be the preferred closure mode due to the bulky Pt(II) center being situated further away from the cyclic backbone. However, in these systems no 5-*exo* closure is observed and all product compounds contain a 6-membered A ring.

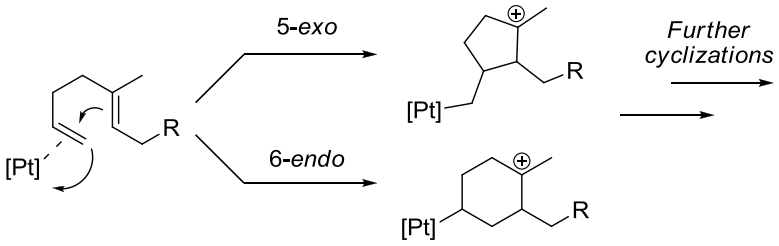

Figure 4.6. Closure modes available to Pt(II)-mediated cyclizations of 1,5-dienes.

The situation is different for the Pt(II) initiated cyclization of 1,6-dienes.[42] In the cyclization of substrate **48** both 5-*exo* and 6-*endo* closure modes are active (Scheme 1.14, reproduced below). While both closure modes lead to the same product (**49**), trapping experiments with benzyl alcohol provided evidence for formation of product via both **51a** and **51b**.

The difference in cyclization selectivity is proposed to arise from the nature of the transition state for these ring closure modes. For lone pair nucleophiles the traditional Baldwin's rules apply, with a single atom attacking the electrophilic carbon. With π-nucleophiles, however, it is proposed that the attacking olefin adopts nonclassical-carbocation-like character in the transition state in order to better stabilize the developing positive charge. This leads to a transition state featuring a large amount of bicyclic character; the strain associated with these structures is the source of the selectivity observed with π-nucleophiles.

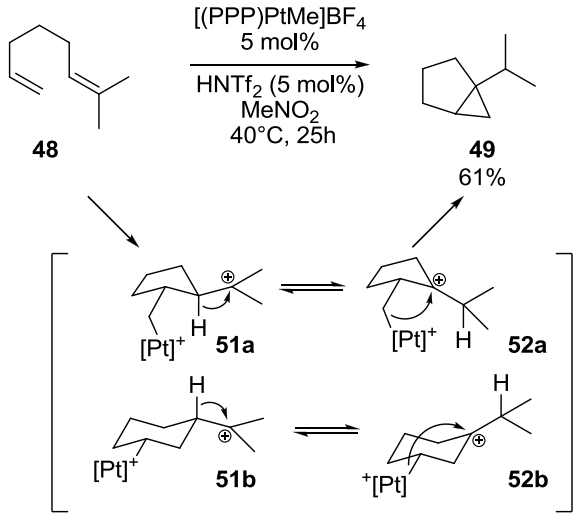

Scheme 1.14. Cyclopropanation reaction catalyzed by an *in situ* activated Pt(II) complex.

Nonclassical-Carbocation Transition States

A nonclassical carbocation is a carbocation that is stabilized by a three-center-two-electron bonding arrangement. The two electrons can come from either a σ-bond ("σ-bridging"), such as in the norbornyl cation (**173**), or from a π-bond (**174**).[94] Extensive research has shown that this electron arrangement has an overall stabilizing effect on the molecule, particularly when a secondary "classical" carbocation is involved (Figure 4.7).

[94] a) Olah, G. A.; Prakash, G. K. S.; Saunders, M. *Acc. Chem. Res.* **1983**, *16*, 440. b) Walling, C. *Acc. Chem. Res.* **1983**, *16*, 448. c) Grob, C. A. *Acc. Chem. Res.* **1983**, *16*, 426.

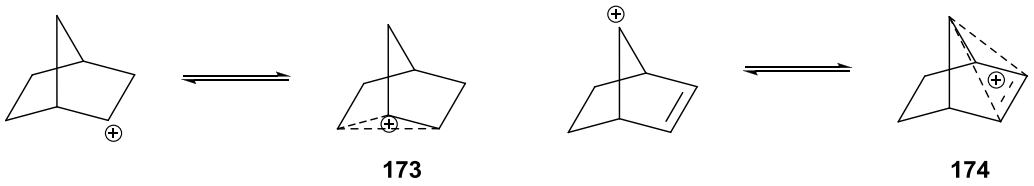

Figure 4.7. Nonclassical carbocations involving σ- and π-bonds.

It is proposed that in the electrophilic cyclization of dienes mediated by transition metals, the transition state resembles such a three-center-two-electron structure (Figure 4.8). This nonclassical-cation-like species could lower the energy of the transition state by spreading the developing positive charge, induced by the transition metal, across three carbons, mitigating the penalty of localizing a charge on a single atom.

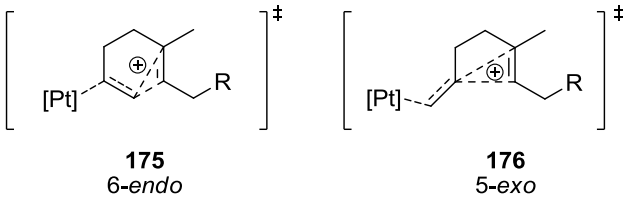

Figure 4.8. Proposed nonclassical-carbocation-like transition states.

In stabilizing the carbocation through a nonclassical-cation bonding arrangement, the transition states develop bicyclic character, leading to the energy difference that determines ring closure selectivity (Figure 4.9). Closure of a 1,5-diene through a 6-*endo* mode leads to formation of a bicyclo[3.1.0]-like transition state (**175**), while closure through a 5-*exo* mode produces a bicyclo[2.1.0] transition state (**176**). The ground state structures of these two bicyclic compounds (**177** and **178**) are calculated to have significantly different strain energies.[95] Indeed, the strain energy (SE) of the bicyclo[2.1.0]pentane (**178**) is predicted to be approximately 24 kcal/mol higher than the bicyclo[3.1.0]hexane (**177**). It is postulated that some portion of this ground state energy difference is reflected in the transition state of these transition metal mediated ring closures, resulting in the less strained bicyclic closure mode being favored for π-nucleophiles (**175**, 6-*endo* for 1,5-dienes).

[95] Borst, M. L. G.; Ehlers, A. W.; Lammertsma, K. *J. Org. Chem.* **2005**, *70*, 8110.

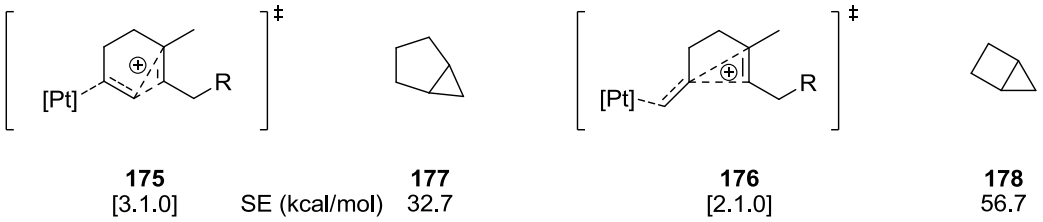

Figure 4.9. Bicyclic-like character of nonclassical transition states.

In collaboration with the Tantillo group once again, it was explored computationally whether these transition states do, in fact, resemble bicyclic, nonclassical-cation structures.[96] Utilizing M06-2X/6-31G(d) for organic structures and M06 for organometallic systems with the 6-31G(d) basis for main group atoms and the SDD basis set for Pt and Pd, as implemented in GAUSSIAN*09*,[75] the Tantillo group determined that the transition states do resemble nonclassical carbocations. Table 4.2 shows the calculated free energies of a number of transition states and cationic species relevant to Pt(II)-mediated cyclizations. It is clear from this data that the 6-*endo* ring closure mode is kinetically favored, in all cases being the lower energy cyclization pathway. In the most relevant case, the all methyl substituted substrate, the 6-*endo* transition state is favored by nearly 5 kcal/mol. This leads to preferential cyclization to the cyclohexyl product, despite the cyclopentyl product being thermodynamically favored. The largest component of this energy difference is believed to be a residue of the ground state strain energy of the bicyclo[*n*.1.0]alkanes.

Table 4.2. Transition states and cationic species relevant to Pt(II) mediated cyclization of 1,5-dienes.

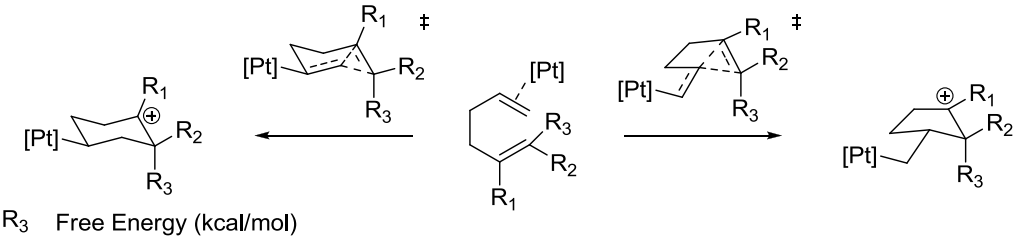

R_1, R_2, R_3	Free Energy (kcal/mol)				
Me, Me, Me	0.0	6.8	0.0	11.2	-2.7
Me, H, Me	-3.3	6.5	0.0	10.6	-1.6
Me, Me, H	-1.3	7.5	0.0	13.4	-0.1

[96] Gutierrez, O.; Harrison, J. G.; Felix, R. J.; Guzman, F. C.; Gagné, M. R.; Tantillo, D. J. *Manuscript in preparation* **2013**.

Using this framework to analyze the Gagné Pt(II) cyclization systems, the exclusive observation of 6-*endo* ring closure of 1,5-dienes can now be explained. Closure to produce 6-membered rings proceeds through a lower energy bicyclo[3.1.0]-like transition state, whereas for production of 5-membered A rings the closure would need to proceed through a higher energy bicyclo[2.1.0]-like transition state. This prohibits the 5-*exo* closure mode.

This analysis can also be used to explain other results from the literature, such as the ring closure modes observed by Widenhoefer (Scheme 4.4, Scheme 4.5).[92,93] With the linear substrates **168** and **170**, a π-nucleophile is attacking the electrophilically activated olefin. Cyclization can proceed from the enol form of the substrate through either a bicyclo[3.1.0]-like transition state, leading to products derived from intermediate **179**, or through a bicyclo[2.1.0]-like transition state leading to intermediate **180**, which would eventually yield cyclopentanone derivatives (Figure 4.10a). Experimentally, only products derived from proposed intermediate **179** are observed, reflecting the preference for the lower energy [3.1.0]-like transition state.

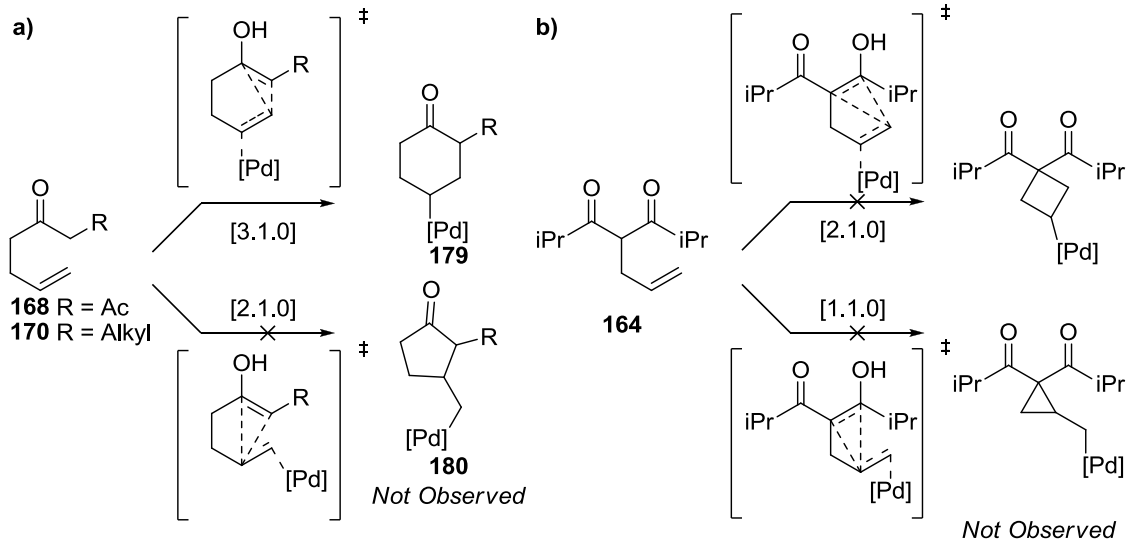

Figure 4.10. Proposed transition states leading to observed ring closure selectivity for Widenhoefer Pd(II) systems.

Branched substrate **164**, however, shows only nucleophilic addition of the oxygen to the activated alkene, and follows the 5-*exo* closure mode preferred by lone pair nucleophiles, despite also being proposed to react from the enol form of the compound. The difference in this system is that the

enol form of the substrate is a 1,4-diene instead of a 1,5-diene. For nucleophilic attack of the π-bond to occur the cyclization would have to proceed through either a high energy bicyclo[2.1.0]-like transition state or an even higher energy bicyclo[1.1.0]-like transition state (Figure 4.10b). In the absence of a relatively low energy cyclization pathway for the π-nucleophile, the ring closure proceeds via attack of the heteroatom on the electrophilically activated olefin.

An explanation for the observed cyclization of 1,6-dienes through both 5-*exo* and 6-*endo* closure modes (Scheme 1.14) can now be offered. In contrast to the bicyclo[3.1.0] and [2.1.0] transition states available to 1,5-dienes, the analogous transition states in 1,6-dienes are bicyclo[3.1.0]- (**181**) and [4.1.0]-like (**182**) structures (Figure 4.11). The predicted strain energy of the ground state structures of these two bicyclo[*n*.1.0]alkanes differs by less than 1 kcal/mol.[95] As it seems only a portion of the ring strain of the parent bicycle is reflected in the transition state of these cyclizations, the 5-*exo* and 6-*endo* ring closure transition states would not feature a large difference in energy based on this principle, allowing both cyclization modes to be active, consistent with experimental results.

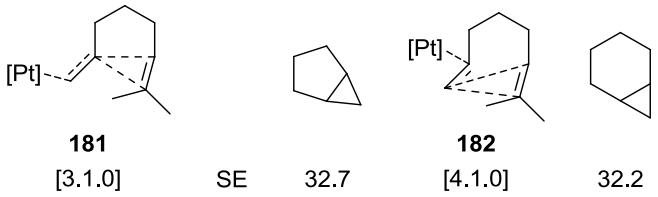

Figure 4.11. Bicyclo[*n*.1.0]-like transition states for cyclization of 1,6-dienes.

Conclusions

An explanation for the cyclization mode selectivity observed in the electrophilic activation of 1,5-dienes by Pt(II) complexes has been proposed. The ring closure mode can be rationalized by considering the transition state as a nonclassical-carbocation-like structure, with a significant amount of bicyclo[*n*.1.0]alkane character. A portion of the ring strain present in the ground state bicyclic alkane is reflected in these transition states, leading to preferential cyclization via the least strained bicyclic-like transition state; for 1,5-dienes this provides 6-*endo* closure exclusively. Density

functional theory calculations performed by the Tantillo group support the notion of a nonclassical-cation-like transition state. These results can also be used to explain other systems from the literature in which alkene π-nucleophiles add to electrophilically activated olefins, rationalizing the ring closure selectivity seen in those systems as well.

The analysis presented in this chapter also delineates a fundamental difference between the reactivity of lone-pair nucleophiles and π-nucleophiles in ring closure selectivity. Lone-pair nucleophiles do not proceed through a transition state with bicyclic character, and so are subject to the traditional Baldwin's rules criteria. The bicyclic nature of the transition state with π-nucleophiles, however, necessitates consideration of the ring strain present in the parent ground state bicyclic species. It is hoped that this analysis of ring closure selectivity in transition metal mediated cyclization reactions will help predict and rationalize the reactivity of future systems.

Appendix A – ^{31}P NMR Shifts and Pt-P Coupling Constants

^{31}P NMR shifts are referenced to 85% phosphoric acid in D_2O (set to 0 ppm). Tables A.2 and A.3 are data composed of data collected by Nikki Cochrane.

Table A.1. ^{31}P NMR data for $(PPP)Pt^{2+}$ complexes.

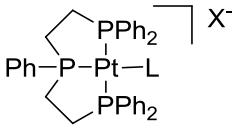

L	X^-	δ ^{31}P *trans* (ppm)	*Trans* coupling constant (Hz)	δ ^{31}P *cis* (ppm)	*Cis* coupling constant (Hz)	Solvent
NCC_6F_5	$(BF_4)_2$	86.1	3329	49.3	2352	CD_3NO_2
NCC_6F_5	$(BF_4)_2$	86	3329	49.0	2359	$EtNO_2$
NCC_6F_5	$(BF_4)_2$	84.7	3344	48.5	2352	CH_2Cl_2
MeOH	$(BF_4)_2$	86	2923	46.3	2419	CD_3NO_2
MeOH	$(BF_4)_2$	86	2921	46.0	2421	$EtNO_2$
MeOH	$(BF_4)_2$	85.2	2924	45.3	2417	CH_2Cl_2
1-Butanol	$(BF_4)_2$	85.1	2911	44.5	2422	CH_2Cl_2
$^-$OMe	$(BF_4)_2$	73.8	2665	40.9	2686	CH_2Cl_2
$^-CH_2NO_2$	$(BF_4)_2$	93.6	1940	45.7	2557	CD_3NO_2
Acetone	$(BF_4)_2$	80.4	3469	51.3	2446	Acetone-D6
Acetone	$(BF_4)_2$	79.1	3510	50.4	2436	CD_3NO_2
I	I	92.2	2886	42.4	2421	$CDCl_3$
Cl	Cl	86.3	3028	42.3	2484	CH_2Cl_2
1-Hexene	$(BF_4)_2$	106.4	2959	50.2	2265	CH_2Cl_2

Table A.2. ^{31}P NMR data for P_2PtI_2 complexes.

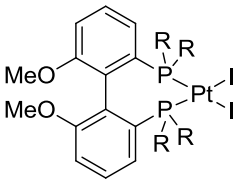

R	δ ^{31}P (ppm)	Coupling Constant (Hz)	Solvent	R	δ ^{31}P (ppm)	Coupling Constant (Hz)	Solvent
	21.24	3476	CD_2Cl_2		-31.5[a]	3648[a]	CD_2Cl_2
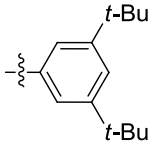	6.94	3498	CD_2Cl_2	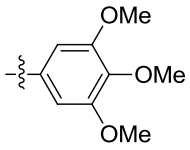	6.52[a]	3523[a]	CD_2Cl_2
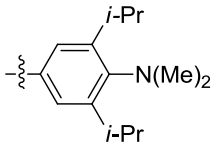	2.96	3497	CD_2Cl_2	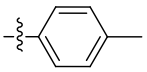	2.0[a]	3480[a]	CD_2Cl_2
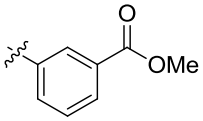	2.98	3440	CD_2Cl_2	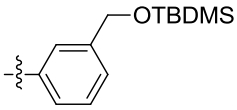	Not soluble in NMR solvents		
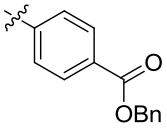	2.19	3430	CD_2Cl_2	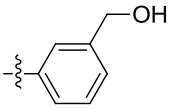	Not soluble in NMR solvents		
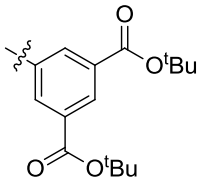	2.06	3446	CD_2Cl_2	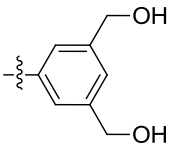	Not soluble in any NMR solvents		
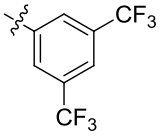	5.64	3364	CD_2Cl_2				

a) Perez-Powell, I. *Platinum Catalysed Wacker-Type Reactions* **2011**, Honours degree of MSci Chemistry Thesis.

Table A.3. ^{31}P NMR data for additional P_2PtI_2 complexes.

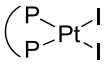

P,P	δ ^{31}P (ppm)	Coupling Constant (Hz)	Solvent	P,P	δ ^{31}P (ppm)	Coupling Constant (Hz)	Solvent
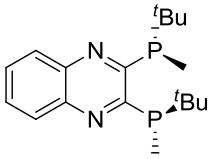	32.0	3248	CD_2Cl_2	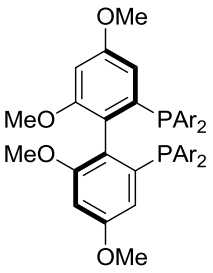	3.0	3486	CD_2Cl_2
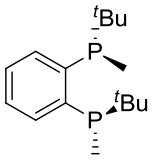	50.0	3366	CD_2Cl_2	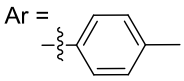			
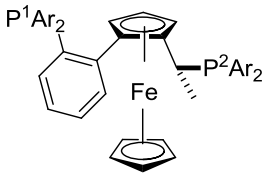 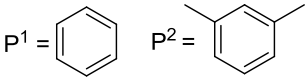	22.4 2.97	3413 3515	CD_2Cl_2	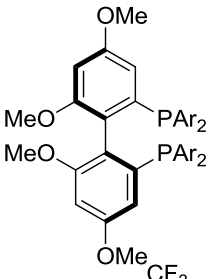	5.0	3366	CD_2Cl_2
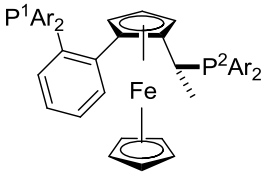 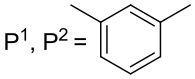	22 2.92	3423 3498	CD_2Cl_2	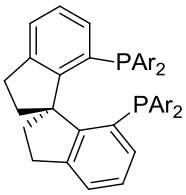	12.8	3424	CD_2Cl_2
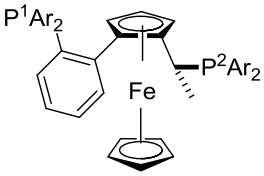 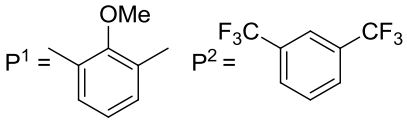	20.3 1.71	3444 3364	CD_2Cl_2	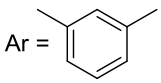			

Appendix B – Catalytic Turnover via β-Methoxy Elimination

An early study I initiated in the Gagné group was aimed at increasing the atom economy of the catalytic cycle (see Figure 1.13) by modifying the substrate to allow for β-methoxy elimination to occur from the cyclized Pt(II)-alkyl species. For example, upon reacting substrate **183** with a Pt(II) complex, cyclization could occur to give the Pt-alkyl **184** (Figure B.1). In the presence of a $P_2Pt(II)$ species, β-methoxy elimination could occur to give diene **185** and an acid labile Pt-OMe compound. Protonolysis could then turn over the catalytic cycle, eliminating the need to employ trityl cation.

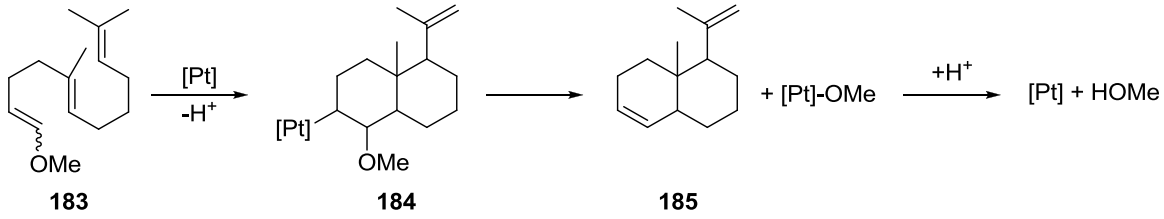

Figure B.1. Potential catalytic turnover via β-hydride elimination.

Substrate **183** was prepared by Wittig reaction of compound **78** (for synthesis, see Scheme 2.2) with methoxymethyltriphenylphosphonium chloride to provide the product compound in moderate yield (Scheme B.1). Unfortunately, in reacting substrate **183** with the Pt(II) species obtained by halide abstraction from either $(PPP)PtI_2$ or (*rac*)-$(BINAP)PtI_2$ with $AgBF_4$, no cyclization was observed, regardless of the solvent or base employed. When the reaction was run in a nitroalkane solvent ($MeNO_2$ or $EtNO_2$) formation of the Pt(II)-enolate, a sideproduct of solvent deprotonation (e.g. $[(PPP)Pt(CH_2NO_2)][BF_4]$) was observed.

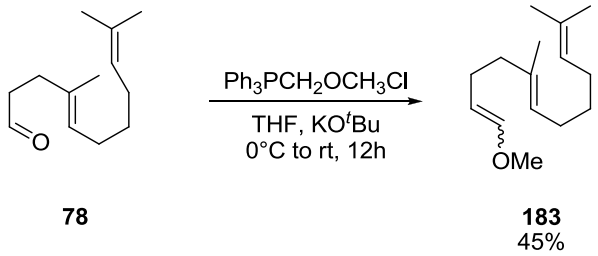

Scheme B.1. Synthesis of substrate 183.

Through extensive testing with various solvents, bases, and control reactions with strong acids (HBF_4, HCl), it was determined that the vinyl ether functionality was too sensitive to survive

the Pt(II)-mediated reactions conditions. Observations also indicated that **183** was itself a poor ligand for the Pt(II) complexes employed. In light of this, compound **183** was further modified to synthesize four additional substrates to investigate alternatives to β-hydride elimination (Scheme B.2).

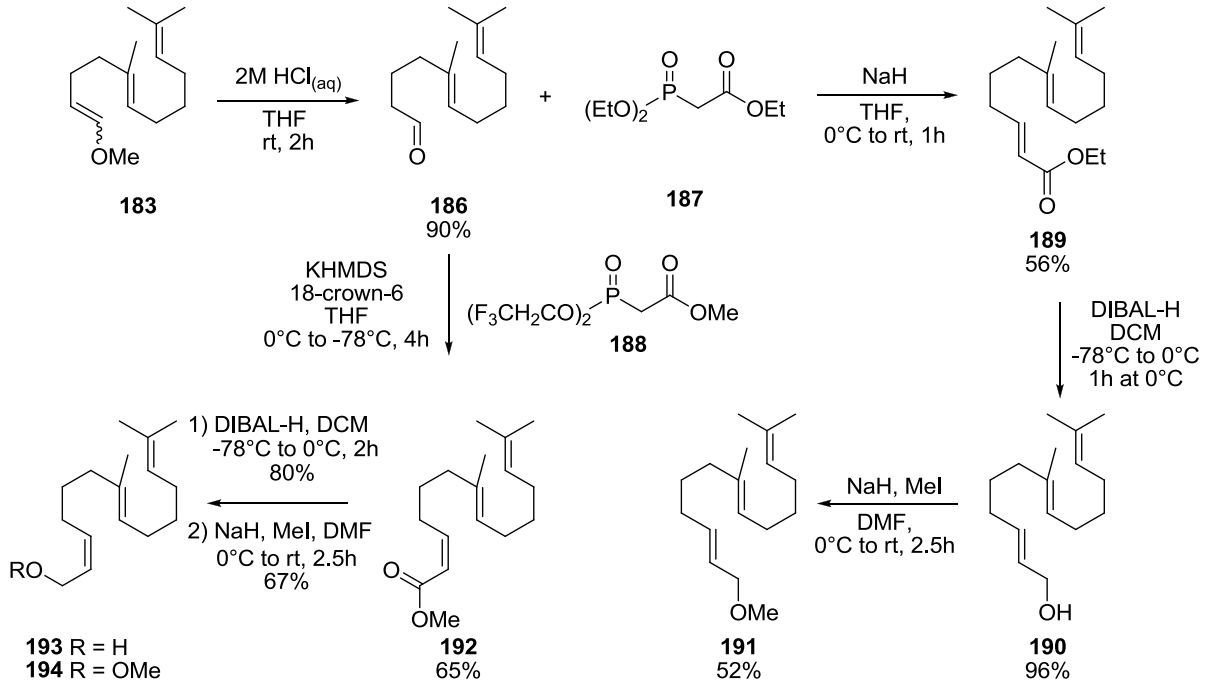

Scheme B.2. Synthesis of substrates 190, 191, 193, and 194.

Homologation of **183** with aqueous HCl in THF was provided aldehyde **186** in high yield. Horner-Wadworths-Emmons reaction of **186** with **187** and NaH provided the (*E*)-alkene **189** in moderate yield. Alternatively, the (*Z*)-alkene **192** could be obtained in slightly higher yield by reacting **186** with **188** and KHMDS in the presence of 18-crown-6. Reduction of esters **189**/**192** with DIBAL-H provided alcohols **190**/**193** (respectively) in good yields. The alcohols could then be methylated to provide ethereal substrates **191**/**194** in moderate yields.

The alcohols **190** and **193** were explored as potential substrates, reasoning that perhaps β-hydroxy elimination could also be an alternative pathway for catalyst turnover. Employing $AgBF_4$ with either (PPP)PtI_2 or (*rac*)-(BINAP)PtI_2, substrate **190** did not undergo cyclization and instead reaction monitoring by ^{31}P NMR indicated the formation of Pt(II)-alcohol species, coordinated through the oxygen atom. This result was not surprising as it had been previously noted that (*E*)-

alkenes are less efficient substrates than (*Z*)-alkenes.[50] In addition, the (*E*)-alkene in this substrate has reduced nucleophilicity due to the inductively deactivating allylic oxygen atom. Thus, it was also not surprising when substrate **191** also failed to cyclize.

It was hoped that (*Z*)-alkene **193** would successfully cyclize; unfortunately, reaction monitoring by GC-MS indicated substrate decomposition. Reacting methoxy substrate **194** with (PPP)PtI_2 and monitoring by ^{31}P NMR led only to formation of the [(PPP)Pt(NCC_6F_5)][BF_4]$_2$ and the Pt(II)-enolate. Reacting substrate **194** with a stoichiometric amount of (*rac*)-(BINAP)PtI_2, however, led to the β-methoxy elimination product **195** (Scheme B.3) and an unidentified Pt(II) species. Unfortunately, attempts to make this reaction catalytic failed, even with different P_2 ligands (e.g. dppe, xylyl-PHANEPHOS).

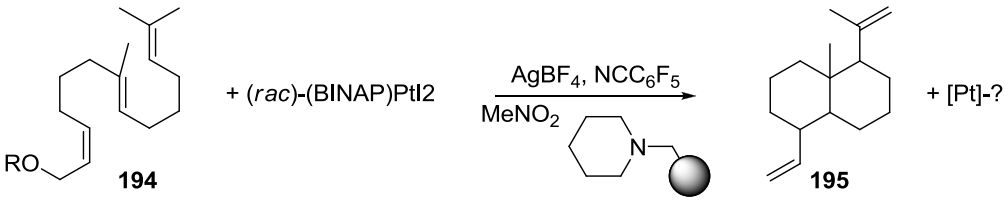

Scheme B.3. β-methoxy elimination from a P_2Pt-alkyl.

With the difficulties of this project and the long and inefficient substrate syntheses this study was discontinued. It was only near the very end of this project, however, that I began investigating the acidity of nitromethane and the facile formation of the Pt-enolate, a common sideproduct observed when reactions are conducted in nitromethane and, to a lesser extent, nitroethane. Methoxide is a strong enough base to deprotonate nitromethane, potentially explaining why attempts to make this reaction catalytic were unsuccessful. The one successful cyclization event, however, showed that β-methoxy elimination seemingly occurs preferentially to β-hydride elimination. If a more efficient synthetic route were developed to provide the applicable substrates, it may be worth reinvestigating this area in nonacidic solvents such as DCM or nitrobenzene.

Appendix C – Attempted Cyclization of Tetraene Substrates

Another area I investigated in the Gagné lab was the question of how far from the Pt(II) metal center could control over the outcome of the cyclization be extended. The idea derived from a computational study performed by the Tantillo group, in which they explored the mechanistic pathways by which a number of natural products could be formed from a single intermediate (Figure C.1).[32a] It is known that enzymes are capable of transforming geranylgeranyl diphosphate (**196**) into a variety of natural products such as *ent*-beyerene (**199**), *ent*-atiserene (**200**), and *ent*-trachylobane (**201**). These structures are all believed to arise from a common, tertiary-carbocationic intermediate (**197**). It was believed that the product formed would be determined by the enzymatic fate of putative secondary carbocation **198**, but in this study, adding to previous computational studies, it was determined that the intermediacy of secondary carbocations is avoided by elaborate σ-shifts (hydrogen, methyl, alkyl).

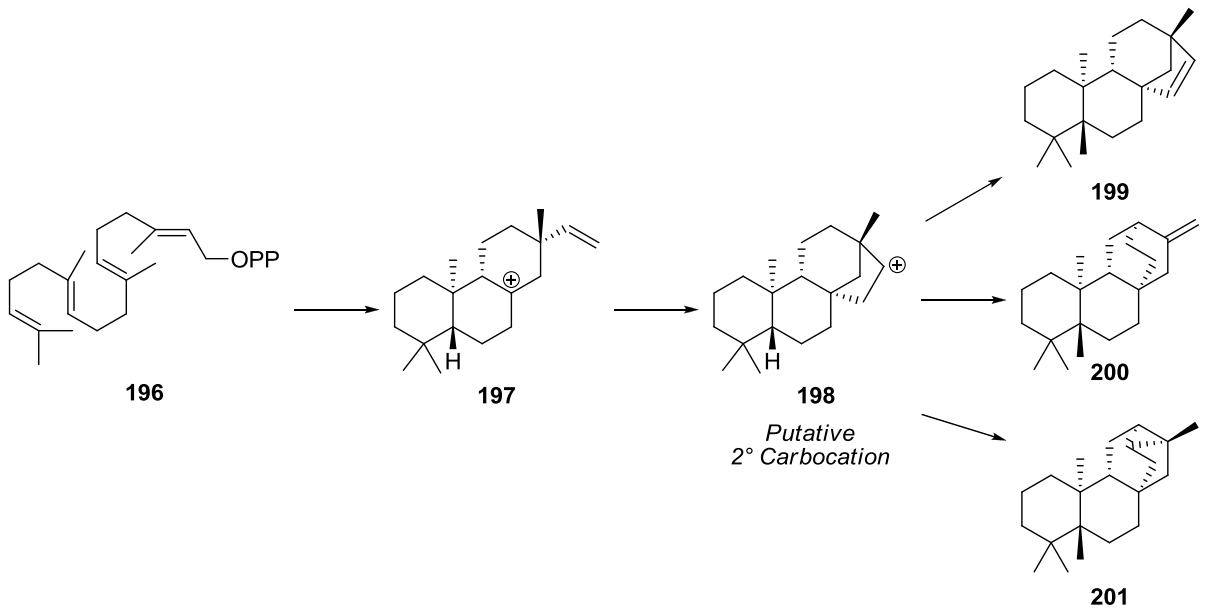

Figure C.1. Selected natural products derived from geranylgeranyl diphopshate.

The work reported in this Appendix focused on synthesizing substrates (**202a-c**) which could theoretically cyclize to an intermediate analogous to **197**. This would allow us to study the ultimate

fate of this carbocation outside of the uniquely stabilizing environments of cyclase enzymes (Figure C.2).

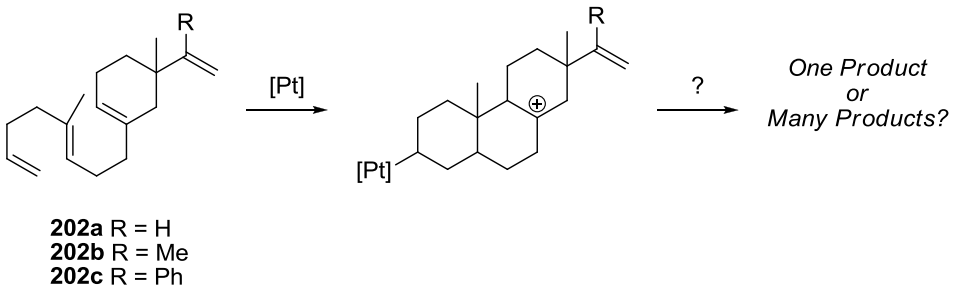

Figure C.2. Proposed cyclization of substrate 202.

Substrates **202a-c** could be synthesized in 5 linear steps starting from 3-methyl-2-cyclohexen-1-one (Scheme C.1). Copper(I)-catalyzed conjugate addition, followed by selective deprotonation and trifluoromethanesulfonylation at low temperature provided the triflates **203a-c** in moderate yield. These triflates could then be transformed under Suzuki conditions to provide epoxides, which after oxidation with $NaIO_4$, provided aldehydes **206a-c** in low yield. Unfortunately, the triflates were poor coupling partners in these reactions and attempts to optimize the reaction conditions failed to give higher yields.[97] This greatly reduced the efficiency of the overall synthesis. A simple Wittig reaction of compounds **206a-c** was capable of providing the desired substrates, **202a-c**, in moderate to good yields.

[97] a) Nicolaou, K. C.; Bulger, P. G.; Sarlah, D. *Angew. Chem. Int. Ed.* **2005**, *44*, 4442. b) Ritter, K. *Synthesis* **1993**, *8*, 735.

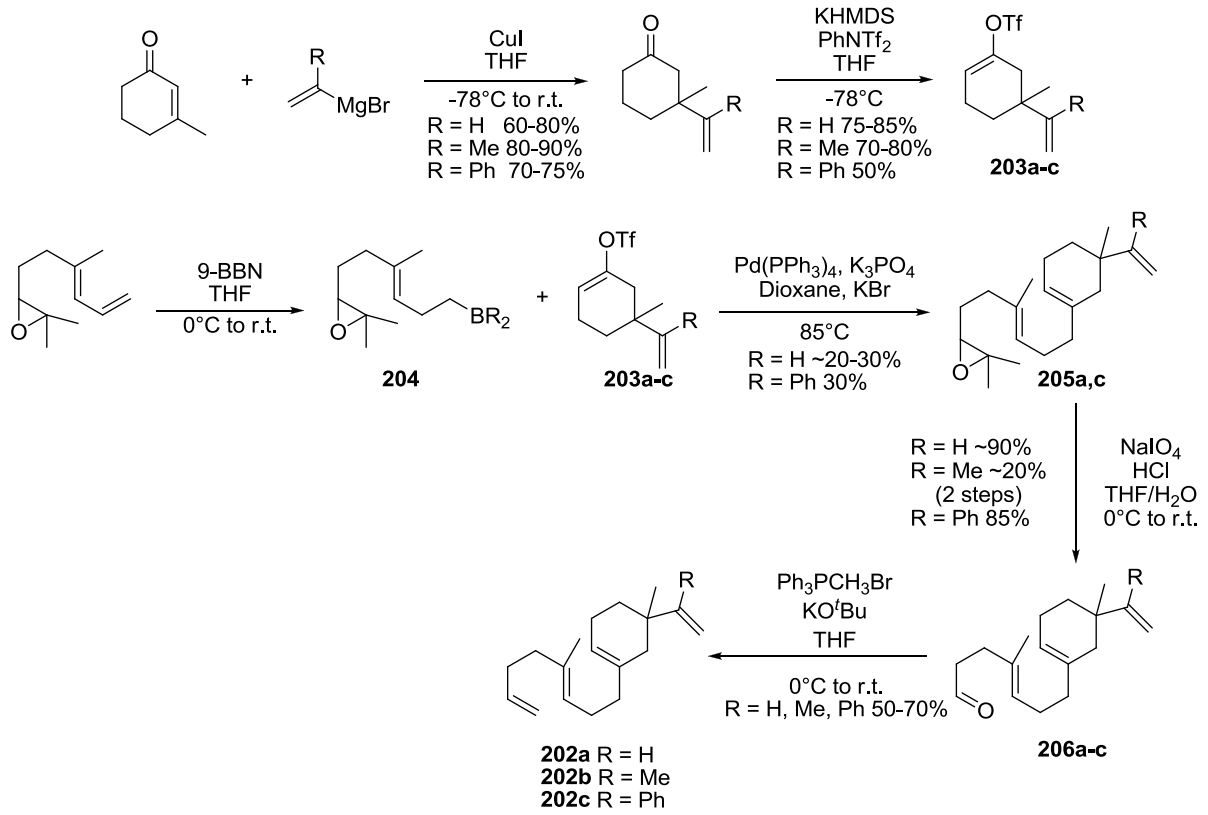

Scheme C.1. Synthesis of substrates 202a-c.

All of the substrates were reacted with (PPP)PtI_2/$AgBF_4$ in the presence of NCC_6F_5. Interestingly, while complexation of **202a** was observed by a *trans*-Pt-P coupling characteristic of Pt(II)-alkenes (see Appendix A), no cyclization was observed. Two possible explanations for this lack of reactivity are shown in Figure C.3 Substrate **202a** actually features two monosubstituted olefins that can serve as sites for Pt(II) coordination. Coordination via **A** was the originally envisioned cyclization pathway, which would lead to secondary carbocation **208**. It is possible this species is too high in energy to form, due to both the presence of a secondary carbocation and the bridging, bicyclic ring structure. However, this doesn't account for why bicyclization products derived from deprotonation of **207** are not observed; the reason for this absence is unknown. If coordination at the opposite end of the molecule occurs preferentially (not expected due to the neopentyl-like nature of this olefin) this could explain the lack of reactivity. Cyclization via **B** would give a strained, sterically congested bicyclic species (**209**). For cyclization to proceed further, it

would have to proceed through a high energy bicyclo[2.1.0]-like transition state (see Nonclassical-Carbocation Transition States). It is therefore postulated that initiation of reactivity at this olefin would be reversible back to **202a**.

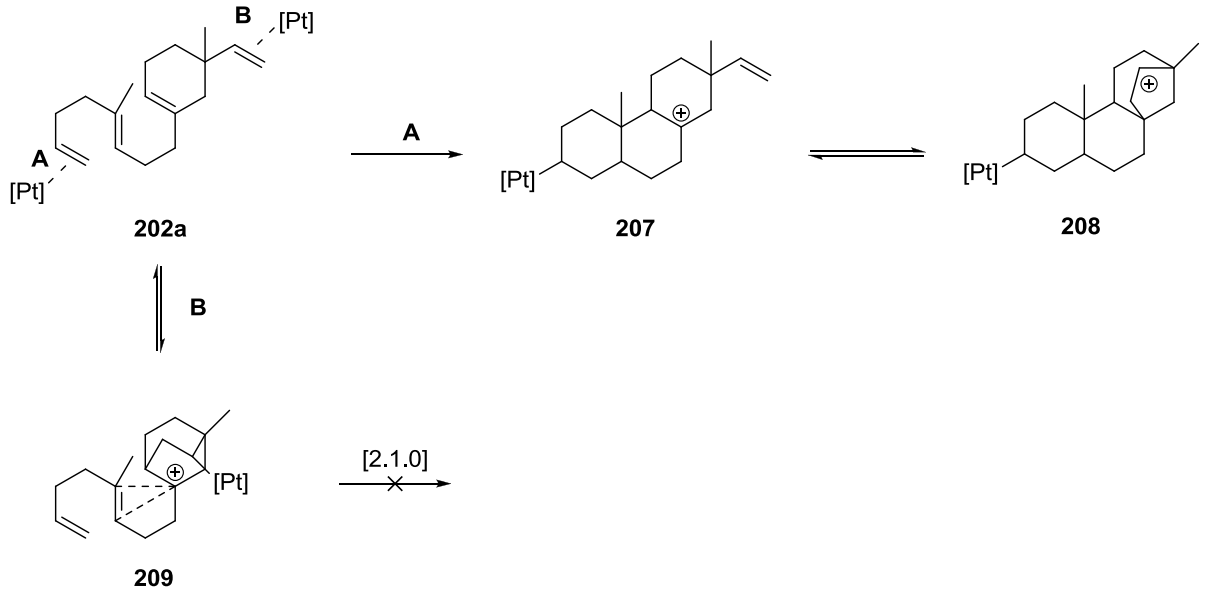

Figure C.3. Potential explanations for observed failure of 202a to cyclize.

Reaction of the methyl substituted compound **202b** was found to be slow, but cyclization did proceed. This compound has two distinct advantages over **202a**: the methyl group will disfavor coordination of the Pt(II)-complex at one of the terminal alkenes and, if cyclization occurs via pathway A (Figure C.3), will result in formation of a tertiary carbocation instead of a secondary. At short reaction times (12-24 hours) two Pt-alkyls would be observed in the ^{31}P NMR spectrum. If the reaction was extended (24-72 hours) more Pt-alkyl peaks would begin to grow in. It is unknown whether these resulted from alkene isomerization side reactions or reversibility effects leading to thermodynamically more favorable Pt-alkyl products. ^{1}H and ^{13}C NMR analysis of the two initially formed Pt-alkyl species was inconclusive but the four most likely structures, based on the spectroscopic data, are show in Figure C.4.

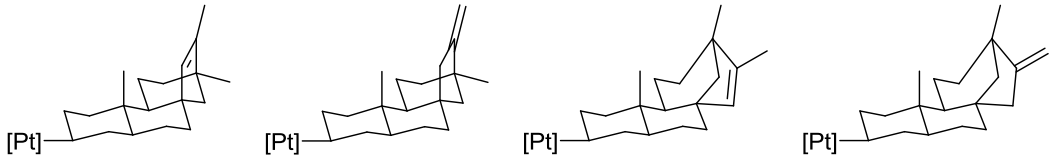

210a **210b** **211a** **211b**

Figure C.4. Potential products from cyclization of substrate 202b.

It was hoped that the aromatic ring in substrate **202c** would provide a handle by which more information could be discerned from the NMR spectra of the cyclized product and possibly assist in crystallization of the Pt(II)-alkyl as well. Only two reactions were conducted with this substrate but they each showed formation of two Pt-alkyl species. Unfortunately, at the same time this substrate was beginning to be investigated the research into methylenecyclopropane substrates was occurring, and with the success of that project this exploration became a secondary priority and was not resumed. If this project were to be resumed I think there is potential with substrate **202c** to either crystallize the Pt-alkyl or begin to establish structural features by NMR spectroscopy.

Sources Cited

Abraham, W.-R. *Curr. Med. Chem* **2001**, *8*, 583.

Allin, S. M.; Baird, R. D. *Curr. Org. Chem.* **2001**, *5*, 395.

Allinger, N. L.; Tribble, M. T.; Miller, M. A.; Wertz, D. H. *J. Am. Chem. Soc.* **1971**, *93*, 1637.

Alonso, I.; Trillo, B.; López, F.; Montserrat, G.; Ujaque, L.; Castedo, A.; Lledós, J. L.; Mascarenhas, C. *J. Am. Chem. Soc.* **2009**, *131*, 13020.

Anderson, C. E.; Overman, L. E. *J. Am. Chem. Soc.* **2003**, *125*, 12412.

Bach, R. D.; Dmitrenko, O. *J. Am. Chem. Soc.* **2004**, *126*, 4444.

Baldwin, J. E. *J. Chem. Soc., Chem. Comm.* **1976**, 734.

Baldwin, J. E.; Cutting, J.; Dupont, W.; Kruse, L.; Silberman, L.; Thomas, R. C. *J. Chem. Soc., Chem. Comm.* **1976**, 736.

Barone, V.; Cossi, M. *J. Phys. Chem. A* **1998**, *102*, 1995.

Bender, C. F.; Widenhoefer, R. A. *J. Am. Chem. Soc.* **2005**, *127*, 1070.

Borst, M. L. G.; Ehlers, A. W.; Lammertsma, K. *J. Org. Chem.* **2005**, *70*, 8110.

Carey, F. A.; Sundberg, R. J. *Advanced Organic Chemistry*; 4th ed.; Spring: New York, N.Y., 2000.

Chatani, N.; Morimoto, T.; Muto, T.; Murai, S. *Organometallics* **1996**, *15*, 901.

Chatt, J.; Duncanson, L. A. *J. Chem. Soc.* **1953**, 2939.

Chianese, A. R.; Lee, S. J.; Gagné, M. R. *Angew. Chem. Int. Ed.* **2007**, *46*, 4042.

Christianson, D. W. *Chem. Rev.* **2006**, *106*, 3412.

Cohen, D. T.; Scheidt, K. A. *Chem. Sci.* **2012**, *3*, 53-57.

Cope, A. C.; Hardy, E. M. *J. Am. Chem. Soc.* **1940**, *62*, 441.

Dedieu, A. *Chem. Rev.* **2000**, *100*, 543.

Derien, S.; Jan, D.; Dixneuf, P. H. *Tetrahedron* **1996**, *52*, 5511.

Dewar, M. J. S. *Bull. Soc. Chim. Fr.* **1951**, *18*, C71.

El-Hachach, N.; Gerke, R.; Noltemeyer, M.; Fitjer, L. *Tetrahedron* **2009**, *65*, 1040.

Eschenmoser, A.; Arigoni, D. *Helv. Chim. Acta* **2005**, *88*, 3011.

Fanning, K. N.; Jamieson, A. G.; Sutherland, A. *Curr. Org. Chem.* **2006**, *10*, 1007.

Feducia, J. A.; Campbell, A. N.; Doherty, M. Q.; Gagné, M. R. *J. Am. Chem. Soc.* **2006**, *128*, 13290.

Feducia, J. A.; Gagné, M. R. *J. Am. Chem. Soc.* **2008**, *130*, 592.

Felix, R. J.; Weber, D.; Gutierrez, O.; Tantillo, D. J.; Gagné, M. R. *Nature Chem.* **2012**, *4*, 405.

Felpin, F.-X. *J. Org. Chem.* **2005**, *70*, 8575.

Frenking, G.; Frohlich, N. *Chem. Rev.* **2000**, *100*, 717.

Fürstner, A. *Chem. Soc. Rev.* **2009**, *38*, 3208.

Fürstner, A.; Aissa, C. *J. Am. Chem. Soc.* **2006**, *128*, 6306.

Fürstner, A.; Davies, P. W. *Angew. Chem. Int. Ed.* **2007**, *46*, 3410.

Gaussian 09, Revision B.01, M. J. Frisch, G. W. Trucks, H. B. Schlegel, G. E. Scuseria, M. A. Robb, J. R. Cheeseman, G. Scalmani, V. Barone, B. Mennucci, G. A. Petersson, H. Nakatsuji, M. Caricato, X. Li, H. P. Hratchian, A. F. Izmaylov, J. Bloino, G. Zheng, J. L. Sonnenberg, M. Hada, M. Ehara, K. Toyota, R. Fukuda, J. Hasegawa, M. Ishida, T. Nakajima, Y. Honda, O. Kitao, H. Nakai, T. Vreven, J. A. Montgomery, Jr., J. E. Peralta, F. Ogliaro, M. Bearpark, J. J. Heyd, E. Brothers, K. N. Kudin, V. N. Staroverov, T. Keith, R. Kobayashi, J. Normand, K. Raghavachari, A. Rendell, J. C. Burant, S. S. Iyengar, J. Tomasi, M. Cossi, N. Rega, J. M. Millam, M. Klene, J. E. Knox, J. B. Cross, V. Bakken, C. Adamo, J. Jaramillo, R. Gomperts, R. E. Stratmann, O. Yazyev, A. J. Austin, R. Cammi, C. Pomelli, J. W. Ochterski, R. L. Martin, K. Morokuma, V. G. Zakrzewski, G. A. Voth, P. Salvador, J. J. Dannenberg, S. Dapprich, A. D. Daniels, O. Farkas, J. B. Foresman, J. V. Ortiz, J. Cioslowski, and D. J. Fox, Gaussian, Inc., Wallingford CT, 2010.

Gorin, D. J.; Toste, F. D. *Nature* **2007**, *446*, 395.

Grob, C. A. *Acc. Chem. Res.* **1983**, *16*, 426.

Gutierrez, O.; Harrison, J. G.; Felix, R. J.; Guzman, F. C.; Gagné, M. R.; Tantillo, D. J. *Manuscript in preparation* **2013**.

Hahn, C. *Chem. Eur. J.* **2004**, *10*, 5888.

Hahn, C.; Morvillo, P.; Vitagliano, A. *Eur. J. Inorg. Chem.* **2001**, 419.

Hahn, C.; Vitagliano, A.; Giordano, F.; Taube, R. *Organometallics* **1998**, *17*, 2060.

Hamel, C.; Prusov, E. V.; Gertsch, J.; Schweizer, B.; Altmann, K.-H. *Angew. Chem. Int. Ed.* **2008**, *47*, 10081.

Hamilton, G. L.; Kang, E. J.; Mba, M.; Toste, F. D. *Science* **2007**, *317*, 496-499.

Han, X.; Widenhoefer, R. A. *J. Org. Chem.* **2004**, *69*, 1738.

Hansen, J. H.; Gregg, T. M.; Ovalles, S. R.; Lian, Y.; Autschbach, J.; Davies, H. M. L. *J. Am. Chem. Soc.* **2011**, *133*, 5076.

Hess, B. A., Jr. *Org. Lett.* **2003**, *5*, 165.

Hess, B. A., Jr.; Smentek, L. *Org. Lett.* **2004**, *6*, 1717.

Hoffman, R.; Stohrer, W.-D. *J. Am. Chem. Soc.* **1971**, *93*, 6941.

Hong, Y. J.; Tantillo, D. J. *J. Am. Chem. Soc.* **2010**, *132*, 5375.

Illuminati, G.; Mandolini, L. *Acc. Chem. Res.* **1981**, *14*, 95.

Ishibashi, H.; Ishihara, K.; Yamamoto, H. *Chem. Rec.* **2002**, *2*, 177.

Ishihara, K.; Nakamura, S.; Yamamoto, H. *J. Am. Chem. Soc.* **1999**, *121*, 4906.

Ito, Y.; Sawamura, M.; Hayashi, T. *J. Am. Chem. Soc.* **1986**, *108*, 6405.

Johansson, M. J.; Gorin, D. J.; Stabe, S. T.; Toste, F. D. *J. Am. Chem. Soc.* **2005**, *127*, 18002.

Johnson, W. S.; Bailey, D. M.; Owyang, R.; Bell, R. A.; Jacques, B.; Crandall, J. K. *J. Am. Chem. Soc.* **1964**, *86*, 1959.

Johnson, W. T. G.; Borden, W. T. *J. Am. Chem. Soc.* **1997**, *119*, 5930.

Kawada, A.; Mitamura, S.; Kobayashi, S. *Chem. Commun.* **1996**, 183.

Keck, G. E.; Abbott, D. E.; Boden, E. P.; Enholm, E. J. *Tetrahedron Lett.* **1984**, *25*, 3927.

Kerber, W. D.; Gagné, M. R. *Org. Lett.* **2005**, *7*, 3379.

Kerber, W. D.; Koh, J. H.; Gagné, M. R. *Org. Lett.* **2004**, *6*, 3013.

Kessar, S. V.; Singh, P. *Chemical Reviews* **1997**, *97*, 721.

Khoury, P. R.; Goddard, J. D.; Tam, W. *Tetrahedron* **2004**, *60*, 8103.

Kleinbeck, F.; Toste, F. D. *J. Am. Chem. Soc.* **2009**, *131*, 9178.

Kobayashi, S. *Synlett* **1994**, 689.

Kobayashi, S.; Manabe, K. *Acc. Chem. Res.* **2002**, *35*, 209.

Koh, J. H.; Gagné, M. R. *Angew. Chem. Int. Ed.* **2004**, *43*, 3459.

Koh, J. H.; Mascarenhas, C.; Gagné, M. R. *Tetrahedron* **2004**, 7405.

Kol, M.; Rozen, S. *Chem. Soc., Chem. Commun.* **1991**, *0*, 567.

Komoto, I.; Matsuo, J.; Kobayashi, S. *Top. Catal.* **2002**, *19*, 43.

Koreeda, M.; Tanaka, Y. *Tetrahedron Lett.* **1987**, *28*, 143.

Korotchenko, V. N.; Gagné, M. R. *J. Org. Chem.* **2007**, *72*, 4877.

Kumazawa, K.; Ishihara, K.; Yamamoto, H. *Org. Lett.* **2004**, *6*, 2551.

Leemans, E.; D'hooghe, M.; De Kimpe, N. *Chem. Rev.* **2011**, *111*, 3268.

Lewis, G. N. *Valence and the Structure of Atoms and Molecules*; The Chemical Catalog Co.: New York, N.Y., 1923.

Lian, Y.; Davies, H. M. L. *J. Am. Chem. Soc.* **2011**, *133*, 11940.

Liskin, D. V.; Sibbald, P. A.; Rosewall, C. F.; Michael, F. E. *J. Org. Chem.* **2010**, *75*, 6294.

Liu, C.; Bender, C. F.; Han, X.; Widenhoefer, R. A. *Chem. Commun.* **2007**, 3607.

Liu, F.; Yu, Y.; Zhang, J. *Angew. Chem. Int. Ed.* **2009**, *48*, 5505.

Lodewyk, M. W.; Gutta, P.; Tantillo, D. J. *J. Org. Chem.* **2008**, *73*, 6570.

Lovick, H. M.; Michael, F. E. *J. Am. Chem. Soc.* **2010**, *132*, 1249.

Lu, B.-L.; Dai, L.; Shi, M. *Chem. Soc. Rev.* **2012**, *41*, 3318.

Ma, Y.; Qian, C. *Tetrahedron Lett.* **2000**, *41*, 945.

Mac Spartan '10, Wavefunction, Inc.: Irvine, CA, 2011.

Maercker, A.; Daub, V. E. E. *Tetrahedron* **1994**, *50*, 2439.

Martín-Matute, B.; Cárdenas, D. J.; Echavarren, A. M. *Angew. Chem. Int. Ed.* **2001**, *40*, 4754.

Matsubara, S.; Wakamatsu, K.; Morizawa, Y.; Tsuboniwa, N.; Oshima, K.; Nozaki, H. *Bull. Chem. Soc. Jpn.* **1985**, *58*, 1196.

Matsuda, S. P. T.; Wilson, W. K.; Xiong, Q. *Org. Biomol. Chem.* **2006**, *4*, 530.

Mauleon, P.; Krinsky, J. L.; Toste, F. D. *J. Am. Chem. Soc.* **2009**, *131*, 4513.

Mehta, G.; Singh, V. *Chem. Rev.* **1999**, *99*, 881.

Melhado, A. D.; Luparia, M.; Toste, F. D. *J. Am. Chem. Soc.* **2007**, *129*, 12638.

Mézailles, N.; Ricard, L.; Gagosz, F. *Org. Lett.* **2005**, *7*, 4133.

Michael, F. E.; Cochran, B. M. *J. Am. Chem. Soc.* **2006**, *128*, 4246.

Michelet, V.; Toullec, P. Y.; Genet, J.-P. *Angew. Chem. Int. Ed.* **2008**, *47*, 4268.

Moss, T. A.; Fenwick, D. R.; Dixon, D. J. *J. Am. Chem. Soc.* **2008**, *130*, 10076.

Mullen, C. A.; Campbell, A. N.; Gagné, M. R. *Angew. Chem. Int. Ed.* **2008**, *47*, 6011.

Mullen, C. A.; Gagné, M. R. *J. Am. Chem. Soc.* **2007**, *129*, 11880.

Müller, D.; Tissot, M.; Alexakis, A. *Org. Lett.* **2011**, *13*, 3040.

Munoz, M. P.; Adrio, J.; Carretero, J. C.; Echavarren, A. M. *Organometallics* **2005**, *24*, 1293.

Nakamura, H.; Iwama, H.; Ito, M.; Yamamoto, Y. *J. Am. Chem. Soc.* **1999**, *121*, 10850.

Nakanishi, W.; Yamanaka, M.; Nakamura, E. *J. Am. Chem. Soc.* **2005**, *127*, 1446.

Namba, K.; Yamamoto, H.; Sasaki, I.; Mori, K.; Imagawa, H.; Nishizawa, M. *Org. Lett.* **2008**, *10*, 1767.

Nechaev, M. S.; Rayon, V. M.; Frenking, G. *J. Phys. Chem. A* **2004**, *108*, 3134.

Nicolaou, K. C.; Bulger, P. G.; Sarlah, D. *Angew. Chem. Int. Ed.* **2005**, *44*, 4442.

Nieto-Oberhuber, C.; Paz Munoz, M.; Lopez, S.; Jimenez-Nunez, E.; Nevado, C.; Herrero-Gomez, E.; Raducan, M.; Echavarren, A. M. *Chem. Eur. J.* **2006**, *12*, 1677.

Nishigaichi, Y.; Takuwa, A.; Naruta, Y.; Maruyama, K. *Tetrahedron* **1993**, *49*, 7395.

Nishizawa, M.; Takenaka, H.; Nishide, H.; Hayashi, Y. *Tetrahedron Lett.* **1983**, *24*, 2581.

Nowicki, J. *Molecules* **2000**, *5*, 1033.

Nowroozi-Isfahani, T.; Musaev, D. G.; Morokuma, K.; Gagné, M. R. *Organometallics* **2007**, *26*, 2540.

Nubbemeyer, U. *Synthesis* **2003**, 961.

Olah, G. A.; Prakash, G. K. S.; Saunders, M. *Acc. Chem. Res.* **1983**, *16*, 440.

Ooi, T.; Taniguchi, M.; Kameda, M.; Maruoka, K. *Angew. Chem. Int. Ed.* **2002**, *41*, 4542.

Overman, L. E.; Knoll, F. M. *J. Am. Chem. Soc.* **1980**, *102*, 865.

Overman, L. E.; Renaldo, A. F. *J. Am. Chem. Soc.* **1990**, *112*, 3945.

Pangborn, A. B.; Giardello, M. A.; Grubbs, R. H.; Rosen, R. K.; Timmers, F. J. *Organometallics* **1996**, *15*, 1518.

Paquette, L. A.; Doherty, A. M.; Rayner, C. M. *J. Am. Chem. Soc.* **1992**, *114*, 3910.

Parr, R. G.; Pearson, R. G. *J. Am. Chem. Soc.* **1983**, *105*, 7512.

Pearson, R. G. *J. Am. Chem. Soc.* **1963**, *85*, 3533.

Pearson, R. G. *J. Chem. Educ.* **1987**, *64*, 561.

Petasis, N. A.; Patane, M. A. *Tetrahedron* **1992**, *48*, 5757.

Plietker, B.; Padron, J. I.; Martin, V. In *Iron Catalysis*; Springer Berlin Heidelberg, 2011; Vol. 33; pp 1-26.

Poulter, C. D.; King, C. R. *J. Am. Chem. Soc.* **1982**, *104*, 1422.

Prakash, G. K. S.; Mathew, T.; Olah, G. A. *Acc. Chem. Res.* **2012**, *45*, 565.

Prakash, G. K. S.; Yan, P.; Bela Torok, P. Y.; Bucsi, I.; Tanaka, M.; Olah, G. A. *Catal. Lett.* **2003**, *85*, 1.

Prunet, J. *Eur. J. Org. Chem.* **2011**, 3634.

Qian, H.; Widenhoefer, R. A. *J. Am. Chem. Soc.* **2003**, *125*, 2056.

Raup, D. E. A.; Cardinal-David, B.; Holte, D.; Scheidt, K. A. *Nature Chem.* **2010**, *2*, 766.

Razzak, M.; De Brabander, J. K. *Nat. Chem. Biol.* **2011**, *7*, 865.

Reetz, M. T.; Kindler, A. *J. Organomet. Chem.* **1995**, *502*, C5-C7.

Ritter, K. *Synthesis* **1993**, *8*, 735.

Seiser, T.; Cramer, N. *Org. Biomol. Chem.* **2009**, *7*, 2835.

Seiser, T.; Saget, T.; Tran, D. N.; Cramer, N. *Angew. Chem. Int. Ed.* **2011**, *50*, 7740.

Sengupta, S.; Shi, X. *ChemCatChem* **2010**, *2*, 609.

Sethofer, S. G.; Mayer, T.; Toste, F. D. *J. Am. Chem. Soc.* **2010**, *132*, 8276.

Sethofer, S. G.; Staben, S. T.; Hung, O. Y.; Toste, F. D. *Org. Lett.* **2008**, *10*, 4315.

Siebert, M. R.; Tantillo, D. J. *J. Am. Chem. Soc.* **2007**, *129*, 8686.

Siengalewicz, P.; Mulzer, J.; Rinner, U. *Eur. J. Org. Chem.* **2011**, *35*, 7041.

Smentek, L.; Hess, B. A., Jr. *J. Am. Chem. Soc.* **2010**, *132*, 17111.

Sokol, J. G.; Korapala, C. S.; White, P. S.; Becker, J. J.; Gagné, M. R. *Angew. Chem. Int. Ed.* **2011**, *50*, 5658.

Stafford, J. A.; McMurry, J. E. *Tetrahedron Lett.* **1988**, *29*, 2531.

Surendra, K.; Qiu, W.; Corey, E. J. *J. Am. Chem. Soc.* **2011**, *133*, 9724.

Tantillo, D. J. *J. Phys. Org. Chem.* **2008**, *21*, 561.

Tantillo, D. J. *Nat. Prod. Rep.* **2011**, *28*, 1035.

Tarselli, M. A.; Chianese, A. R.; Lee, S. J.; Gagné, M. R. *Angew. Chem. Int. Ed.* **2007**, *46*, 6670.

Tschumimoto, T.; Tobita, K.; Hiyama, T.; Fukuzawa, S. *J. Org. Chem.* **1997**, *62*, 6997.

Walling, C. *Acc. Chem. Res.* **1983**, *16*, 448.

Wang, X.; Pei, T.; Han, X.; Widenhoefer, R. A. *Org. Lett.* **2003**, *5*, 2699.

Watson, M. P.; Overman, L. E.; Bergman, R. G. *J. Am. Chem. Soc.* **2007**, *129*, 5031.

Wendt, K. U.; Schulz, G. E.; Corey, E. J.; Liu, D. R. *Angew. Chem. Int. Ed.* **2000**, *39*, 2812.

Werner, T. *Adv. Synth. Catal.* **2009**, *351*, 1469.

Widenhoefer, R. A. *Chem. Eur. J.* **2008**, *14*, 5382.

Williams, D. R.; Pinchman, J. R. *Can. J. Chem.* **2013**, *91*, 21.

Womack, G. B.; Angeles, J. G.; Fanelli, V. E.; Heyer, C. A. *J. Org. Chem.* **2007**, *72*, 7046.

Yadav, J. S.; Antony, A.; Rao, T. S.; Subba Reddy, B. V. *J. Organomet. Chem.* **2011**, *696*, 16.

Yoder, R. A.; Johnston, J. N. *Chem. Rev.* **2005**, *105*, 4730.

Zhang, Z.; Bender, C. F.; Widenhoefer, R. A. *J. Am. Chem. Soc.* **2007**, *129*, 14148.

Zhao, J.-F.; Loh, T.-P. *Angew. Chem. Int. Ed.* **2009**, *48*, 7232.

Zu, L.; Xu, M.; Lodewyk, M. W.; Cane, D. E.; Peters, R. J.; Tantillo, D. J. *J. Am. Chem. Soc.* **2012**, *134*, 11369.